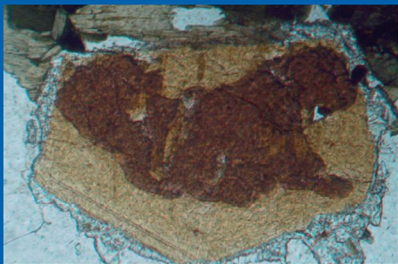


Energy Dispersive Spectrometry of Common Rock Forming Minerals

Kenneth P. Severin



KLUWER ACADEMIC PUBLISHERS

ENERGY DISPERSIVE SPECTROMETRY OF COMMON ROCK
FORMING MINERALS

Energy Dispersive Spectrometry of Common Rock Forming Minerals

By

Kenneth P. Severin

*Department of Geology and Geophysics,
University of Alaska Fairbanks,
U.S.A.*



KLUWER ACADEMIC PUBLISHERS

DORDRECHT / BOSTON / LONDON

A C.I.P. Catalogue record for this book is available from the Library of Congress.

ISBN 1-4020-2840-7 (HB)
ISBN 1-4020-2841-5 (e-book)

Published by Kluwer Academic Publishers,
P.O. Box 17, 3300 AA Dordrecht, The Netherlands.

Sold and distributed in North, Central and South America
by Kluwer Academic Publishers,
101 Philip Drive, Norwell, MA 02061, U.S.A.

In all other countries, sold and distributed
by Kluwer Academic Publishers,
P.O. Box 322, 3300 AH Dordrecht, The Netherlands.

Cover illustration:
Zoned allanite surrounded by epidote in granodiorite.
Gilmore Dome pluton, Fairbanks, Alaska. Field of view approximately 1 mm.

Printed on acid-free paper

All Rights Reserved
© 2004 Kluwer Academic Publishers

No part of this work may be reproduced, stored in a retrieval system, or transmitted in any form or by any means, electronic, mechanical, photocopying, microfilming, recording or otherwise, without written permission from the Publisher, with the exception of any material supplied specifically for the purpose of being entered and executed on a computer system, for exclusive use by the purchaser of the work.

Printed in the Netherlands.

Contents

Acknowledgments	vii
Preface	ix
Energy Dispersive Spectrometry	1
Samples and Spectra	15
The Key	25
The Spectra	37
References	221
Index to Spectra, Minerals, and Mineral Groups	223

Acknowledgments

Many thanks to Rainer Newberry and Mary Keskinen (both at the University of Alaska Fairbanks) for help in obtaining the vast majority of the specimens used for the spectra. Peter Schiffman (University of California Davis) and John Fournelle (University of Wisconsin, Madison) also provided help in filling some of the holes in the spectra. Drs. Jeffrey Post and Glenn MacPherson, and Pete Dunn of The Department of Mineral Sciences at the Smithsonian Institution's Department of Mineral Sciences kindly provided the following specimens: Analcite (NMNH 136544), Bustamite (NMNH 83929-2), Danalite (NMNH 133036), Gibbsite (NMNH 114108-2), Kalsilite (NMNH 136447), Knebelite (NMNH C2818), Maghemite (NMNH 105868), Magnesiochromite (NMNH 137679), Magnesioferrite (NMNH C1591), Merwinite (NMNH 94418), Mullite (NMNH 137062), Nosean (NMNH 138751), Paragonite (NMNH B16888), Petalite (NMNH 117282-14), Rankinite (NMNH 122131), Sapphirine (NMNH 148879), Spurrite (NMNH 159071), Tilleyite (NMNH 115214-2), Trevorite (NMNH 1440467), Uvarovite (NMNH 106829), and Zinnwaldite (NMNH R4437-1). Thanks also go to Eugene Jarosewich (Smithsonian National Museum of Natural History) for providing the various "Smithsonian Standards." Most of these standards still are available from the Smithsonian.

Thanks also to Fairbanks friends Kim DeRuyter, Diana Solie, Brian Joy and my electron microprobe students for help in various ways. S.J.B. Reed (Cambridge University) kindly commented on an early version of the manuscript. This project benefited greatly from the help, advice, and patience of all these good people, any errors that remain are mine.

Preface

This book came about because of my poor memory. It is amazing how quickly and easily an experienced electron microscopist/mineralogist can identify minerals with an Energy Dispersive Spectrometer (EDS). It is also amazing how long it takes someone who is not good at mineralogy to search through a mineralogy text, trying to match the peaks on their unknown spectrum with the chemical formula of some mineral. After the mineral is finally identified, it is easy to identify other specimens of similar composition as EDS spectra have very distinctive patterns. For me, however, as I move between projects, it is easy to forget the patterns. After several episodes of having to relearn the spectra of some all too common rock forming minerals, I decided that a book of EDS "flashcards" would be useful. Instead of looking in a mineralogy text, looking at chemical formulæ, trying to guess how they translated into spectral peaks, why not make a catalogue of the minerals that are commonly found in rocks? In addition, why not make a key? On more than one occasion I would find myself saying "I know I've seen this pattern before. No aluminium, lots of silicon, magnesium, and iron. Oh yes, must be some kind of olivine." Nothing at all surprising to a good mineralogist or geologist, but something that is not readily apparent from a mineralogy text. I hope that the key will save a fair amount of time for those who are less experienced mineralogists, but, for whatever reason, use an Energy Dispersive Spectrometer to identify minerals.

The question of just what minerals to include was not an easy one, and I'm sure that most mineralogists will be upset because I have omitted their "favourite" mineral. Rather than trying to include spectra of every mineral found in the teaching collections at the University of Alaska Fairbanks (to say nothing of trying to include an example of even a small portion of the minerals from a collection at a place such as the Smithsonian Institution!), I chose to select the major minerals found in "An Introduction to the Rock Forming Minerals" by W.A. Deer, R.A. Howie, and J. Zussman, with a few others as suggested by colleagues. This made the task of collecting samples and spectra at least somewhat manageable, and I hope, the product useful to the majority of readers. Suggestions of minerals to be included in future editions (should they occur) are welcomed.

Chapter 1

ENERGY DISPERSIVE SPECTROMETRY

An Overview

1. WHY USE ENERGY DISPERSIVE X-RAY SPECTROMETRY?

There is no doubt that minerals can be identified quickly and relatively cheaply using the traditional tools of polarised light and optical microscopy. However, this method requires an optical thin section, a petrographic microscope, and some skill in optical mineralogy. Grains smaller than about 20 microns are difficult to identify optically. In cases where it is not feasible to make an optical thin section, where mineral grains are small, or there is no optical mineralogist available, rapid identification often can be made using a Scanning Electron Microscope (SEM) equipped with an Energy Dispersive X-ray Spectrometer (EDS) (Figure 1.1).

SEMs have become fairly common laboratory instruments, and over half of them are equipped with an EDS (Goldstein et al., 2003). The reasons are simple: An EDS can, within a few seconds, produce an X-ray spectrum that ranges from zero to many tens of kilo electron-volts (keV), and it can produce that spectrum from a micron-sized sample that has had only minimal preparation. Modern software makes interpreting the spectra fairly simple and investigators can obtain a qualitative, or even semi-quantitative elemental analysis of their sample in short order. Elements present in abundances of one weight per cent and even less are readily detectable.

There are, however, several common pitfalls which can prevent the acquisition of good EDS spectra as well as several ways in which EDS spectra can be misinterpreted. For these reasons the investigator should have a basic understanding of the generation of X-rays in an SEM, and how those X-rays are detected by the EDS. Complete descriptions of these processes are beyond the scope of this brief introduction; detailed

discussions are found in Goldstein et al. (2003), Potts (1987), Williams (1987), or Reed (1996).

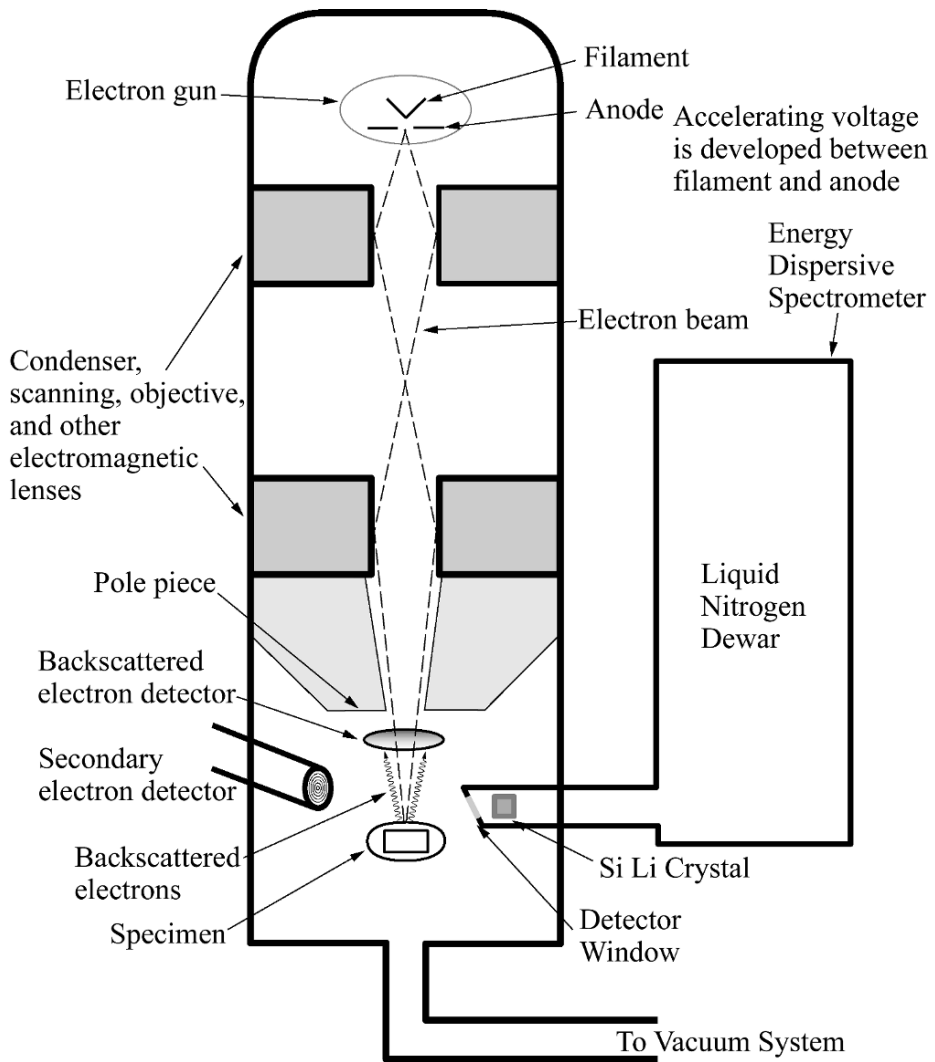


Figure 1.1. Scanning Electron Microscope equipped with an Energy Dispersive X-ray Spectrometer

2. X-RAY GENERATION

In an SEM the sample is bombarded with electrons. A beam is formed from electrons that are produced at an electron source such as a heated tungsten filament, accelerated through a potential of 2 to 30 or more kilovolts (kV), and focused to a fine point by a series of electromagnetic lenses. The potential that accelerates the electrons is known as the accelerating voltage, and is held constant. All electrons in the beam have approximately the same energy, equal to the accelerating voltage. Conveniently, an electron accelerated through a potential of X kilovolts has an energy of X kilo-electron volts (keV), so if the SEM is being operated at 25 kV, then the beam electrons have energies of 25 keV. Workers performing EDS analysis typically use accelerating voltages of 15 to 25 kV. Under typical conditions some 6×10^9 electrons (at a 1 nano ampere [nA] beam current)¹ interact with the sample each second. The beam current can be varied from a few pico amperes to several hundred nA, with typical values being about 0.1 – 1 nA.

The beam electrons interact with the sample in a variety of ways. Two kinds of inelastic interactions are the most important for X-ray generation. In the first type of interaction the beam electrons simply decelerate as they pass atoms in the sample. As the electrons are slowed they lose some or all of their energy. This energy is given up as a photon with energy equivalent to that lost during decelerations and can range between just above 0 keV to the energy of the accelerating voltage of the electron beam. Most of these photons fall into the energy range that is called X-rays (between about 100 eV and 1,000 keV). The X-rays produced by this slowing are called braking radiation or Bremsstrahlung. The intensity of the Bremsstrahlung spectrum was described by Kramers (1923) as

$$I(E)dE = k \cdot i \cdot Z \cdot \left[\frac{E_{\max} \cdot E}{E} \right] \cdot dE$$

where $I(E)$ is the intensity of the spectrum at a given energy,

k is a constant,

i is the beam current,

Z is the atomic number of the specimen

and

E_{\max} is the energy of the electron beam causing the Bremsstrahlung. For spectra generated in an SEM, E_{\max} is equal to the accelerating voltage.

For a given accelerating voltage, the shape of the Bremsstrahlung spectrum is fixed; its intensity varies only as a function of the atomic number of the specimen and beam current, i.e., the number of electrons in the beam. Bremsstrahlung will be present in all spectra produced by an electron beam. It will range in energy from 0 keV to E_{\max} keV. It forms the major portion of the background that can complicate the identification and

¹One nano ampere is 1×10^{-9} coulombs second⁻¹; a coulomb is the charge on 6.24×10^{18} electrons.

quantification of the X-rays produced by the second kind of inelastic interaction: characteristic X-rays.

Characteristic X-rays are produced when the beam electrons interact with the inner shell electrons of the atoms in the specimen (Figure 1.2). Under certain conditions a beam electron can cause an inner shell electron to be ejected from the target atom, leaving the atom in an energized state. The atom returns to a lower energy state when one of its outer shell electrons fills the vacant space in the lower energy shell. During this reaction a photon with the energy equal to that of the difference of the energy levels of the two shells may be produced.² The majority of these photons are in the X-ray energy range. Quantum mechanics describes several characteristics of the energy levels of electrons surrounding an atom as well the manner in which electrons can move from one level to another. The energy levels of the electron shells may have only certain discrete values and these values are determined mainly by the atomic number of the nucleus. This means that the energy levels of the electron shells are different for different elements. Electrons can transit only between certain shells. The combination of energy levels of electron shells being different for different elements along with the fact that not all transitions are allowable means that the X-ray photons emitted from atoms that have undergone inner shell ionization are, to a large extent, diagnostic of the atomic number of the target atom and thus, are termed characteristic X-rays.

After inner shell ionization, there is usually more than one outer shell electron that is allowed to transit to the vacant inner shell site. If these outer shell electrons have different energies, then each will emit a different energy X-ray when it fills the inner shell vacancy. When two or more transitions are allowed it is impossible to predict which one will occur in any particular atom, but it is possible to assign a probability for each event. As there are several million inner shell ionisations and subsequent decays every second in the SEM, the probabilities for the various transitions can be used to predict the percentage of each particular transition across all the atoms quite accurately. The result is a "family" of X-ray energies emitted from the sample, with each corresponding to a transition between one of several outer shells and one particular inner shell, the shell that was originally ionised. If the family is the result of the ionization of the innermost shell, the X-rays are known as K X-rays. If it is the result of a second shell ionization the X-rays are known as L X-rays. If it is the result of a third shell ionization the X-rays are known as M X-rays. Within a given family of X-rays, the most probable transition will occur most often and will produce the largest number of X-rays in a given amount of time. This is the same as saying that it will be the most intense or brightest X-ray line. The second most probable transition will produce the second largest number of X-rays per unit time, and so on. The most common transition is generally known as the α line, the next most common is known as the β line, the third is known as the γ line, and so on. The names for these lines came from early spectroscopy.

²Other actions, such as the production of Auger electrons, also occur. Consult Williams (1987) or Goldstein et al. (2003) for more information).

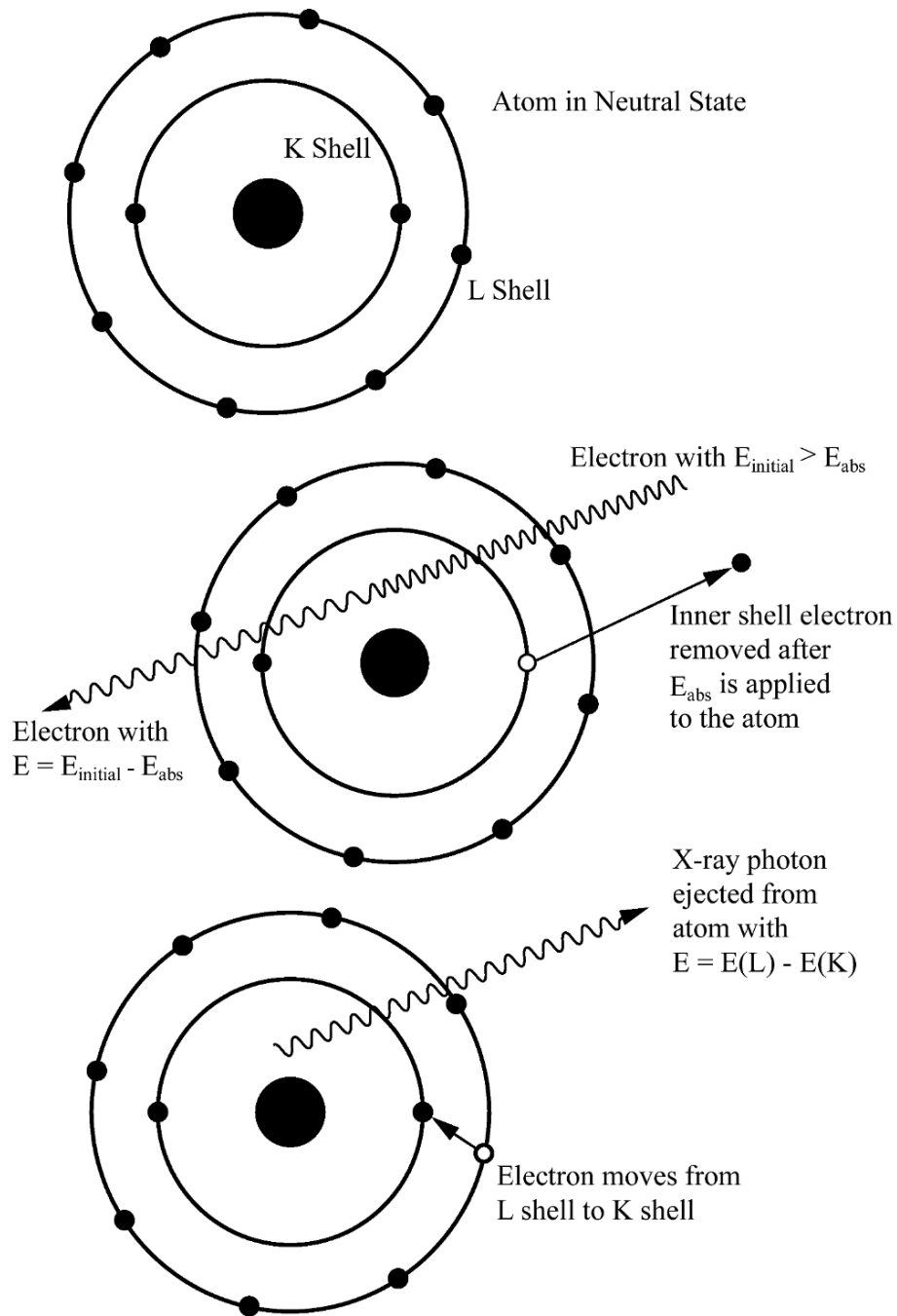


Figure 1.2. Generation of X-ray after electron excitation.

pists who based their terminology on observed brightness. The nomenclature does not always correspond well with the nomenclature based on shell transitions used by quantum physicists.

The amount of energy needed to remove an inner shell electron is known as the critical or absorption energy for a particular ionization and is usually denoted as E_{crit} , E_{abs} , or E_{edge} . E is often replaced by the shell designator of interest. As an example, for the Fe K series of lines, $K_{\text{abs}} = 7.111$ keV. It takes more energy to remove an inner shell electron completely from an atom than is released by moving an electron between an outer and an inner shell. In all cases the energy of emitted X-rays is less than the energy that it takes to ionise the atom. Continuing with the Fe example, the energies of the emitted lines in the K series are $K\alpha = 6.404$ keV and $K\beta = 7.057$ keV. Thus, if an accelerating voltage of 7.000 keV were used on an iron-bearing sample, no iron K series X-rays would be generated, even though the energy of Fe $K\alpha$ X-rays is 6.404 keV. To generate K series iron X-rays the accelerating voltage must be greater than the iron K_{abs} of 7.111 keV.³

Moseley (1913, 1914) discovered that the energy level of a given electron shell, say the K shell, increases with atomic number. Put another way, E_{abs} is larger for higher atomic number elements than for lower atomic number elements. Thus, K_{abs} for aluminium (atomic number 13) is 1.6 keV, K_{abs} for iron (atomic number 26) is 7.1 keV, and K_{abs} for gold (atomic number 79) is 80.7 keV. Energies of the emitted X-rays increase similarly with Al $K\alpha = 1.5$ keV, Fe $K\alpha = 6.4$ keV, and Au $K\alpha = 70.0$ keV. SEM work is rarely done with accelerating voltages much more than about 30 keV, meaning few microscopists will generate Au $K\alpha$ X-rays. However, less energy is required to remove an electron from the L shell than from the K shell (and also from the M shell than from the L shell), so the radiation from these transitions can be observed instead. Using gold as an example, $K_{\text{abs}} = 80.7$ keV, $L_{\text{I abs}} = 14.3$ keV, and $M_{\text{IV abs}} = 2.3$ keV. Unless the SEM is operated with an accelerating voltage less than about 5 keV, at least one K, L, or M shell of any element will be abundantly ionised, and X-rays will be available for analysis by EDS.

³There is fine structure in the X-ray spectrum that is beyond the resolution of the EDS spectrometer. Thus the α and β lines are often designated as α_1 , α_2 , β_1 , β_2 , and so on. Additionally, there are slightly different ionization levels within the L and M shells. These levels are noted as $L_{\text{I abs}}$, $L_{\text{II abs}}$, $M_{\text{IV abs}}$, $M_{\text{V abs}}$ and so on. This fine structure is rarely of any import when using EDS.

3. X-RAY DETECTION IN AN ENERGY DISPERSIVE SPECTROMETER

X-rays produced in the SEM have energies that range from just above 0 keV to equal to the beam energy. The energy dispersive spectrometer delivers quantitative information of how many X-rays of any given energy are produced.

The heart of an ED detector is a single crystal of silicon (or, less commonly, germanium) which should be intrinsically pure. Since this is impossible, the crystal is "drifted" with lithium (hence the name Si(Li) detector) to compensate for impurities in the silicon lattice and to allow it to act like an intrinsically pure crystal. In this state, electrons of the silicon atoms can be moved from the valence band to the conduction band with an energy of 3.8 eV. In most cases, an X-ray with E electron volts of energy will produce a pulse of $(E/3.8)$ electrons when it is absorbed by the Si(Li) crystal. These electrons can be collected by putting an electric field across the crystal. It is easy to imagine that one could count the number of electrons collected and multiply that number by 3.8 to get the energy (in eV) of the X-ray that hit the detector. The device that detects the pulse of electrons and measures its size is called a Pulse Height Analyser (PHA). The pulses are sorted according to size, then recorded and stored in a device that keeps track of the number pulses of each size that have been generated at the detector. This device is known as a Multi-Channel Analyser (MCA). Typical MCAs sort pulses into 1024 categories, or channels. If each channel is capable of recording pulses that represent a 0.01 KeV range of X-ray energy, then the entire MCA could record X-rays over a 10.24 KeV range. The range of the MCA is typically software selectable.

The complete process of converting the X-ray to a count in the MCA takes several steps and presents several practical problems. The process of collecting and counting the electrons in the Si(Li) crystal takes a finite time, typically in the range of 10 microseconds. During that time it is possible for a second X-ray to impinge on the crystal, produce more electrons, and cause confusion. Manufacturers have developed "Pileup rejection" circuitry, which essentially turns off the detection process for a short time after an X-ray interacts with the crystal. While this circuitry is quite good at preventing two closely spaced X-rays from getting measured, it cannot prevent the measurement of two X-rays that arrive at exactly the same time. If the two X-rays were Ca $K\alpha$ ($E=3690$ eV) then they would produce $(2 \cdot 3691)/3.8 = 1942$ electrons, which would be interpreted as a X-ray with $E=1942 \cdot 3.8 = 7380$ eV, the sum of the two X-rays. Thus a spectrum of calcite (CaCO_3) will contain a peak at 7380 eV, the sum of Ca $K\alpha$ plus Ca $K\alpha$, a smaller peak at 7702 eV, the sum of Ca $K\alpha$ plus Ca $k\beta$, and even a peak at 8024 eV, the sum of Ca $K\beta$ plus Ca $K\beta$. These sum peaks will occur whenever two X-rays of any energy impinge on the Si(Li) crystal at the same time. They are typically only noticeable as the product of an intense peak or pair of peaks (See fluorite, pages 214-215).

While the simultaneous arrival of two X-rays at the detector is an unlikely event, it is not at all uncommon for an X-ray to arrive at the detector during the 10 or so microseconds that the detector is busy processing a previous X-ray. Although the counting part of the detector circuitry can ignore the second X-ray, the X-ray will have moved valence electrons to the conduction band in the Si(Li) crystal, creating a confused situation for counting the number conduction electrons generated. The counting circuitry will not resume counting until X-rays have not interacted with the Si(Li) crystal for a fixed amount of time, a time long enough the crystal to recover and have all the conduction band electrons removed. The practical consequence of this is that if there are too many X-rays generated in the SEM, then the Si(Li) crystal will never have enough time to recover and no X-rays will be detected. The time that the detector is shut off is known as “dead time,” and the percentage of dead to live time is usually displayed by the EDS software. Most software can acquire spectra for a fixed amount of live time, ensuring that spectra are collected for equal intervals. Manufacturers generally recommend operating the detector at about 20–40% dead time for the best count rate in terms of clock time.

When an X-ray generated in the SEM crystal has $E > K_{\text{abs}} \text{ Si} = 1838 \text{ eV}$ it may cause a K shell ionization of a silicon atom in the Si(Li) detector. If it does, then the silicon atom may emit a characteristic Si $K\alpha$ X-ray. In most cases the X-ray will be absorbed within the Si(Li) crystal where it will move valence electrons to the conduction band, and the observer who is counting conduction band electrons will be none the wiser. If, however, the silicon X-ray exits the crystal, then the number of electrons produced by the original X-ray will be reduced by $1740/3.8 = 458$ electrons. For the case of where calcium $K\alpha$ X-rays ($E=3690 \text{ eV}$) are being measured, the “shifted” X-ray would appear at

$$3.8 \cdot \left[\left(\frac{3690}{3.8} \right) - \left(\frac{1740}{3.8} \right) \right] = 1950 \text{ eV}$$

These peaks are known as escape peaks. Most software will indicate where an escape peak should be expected for any given characteristic peak.

The Si(Li) crystal must be kept cold (usually with liquid nitrogen) both to prevent the lithium from migrating in the crystal as well as to reduce thermal noise. This means that it would act as a “cold finger” if it were mounted openly in the SEM sample chamber. If the chamber were vented to exchange specimens water vapour would condense onto the crystal. If the chamber were evacuated use any hydrocarbons and other contaminants present in the chamber would collect on the cooled crystal. Finally, the crystal would react to visible light, a problem if the sample fluoresced under the electron beam. While some windowless detectors have been manufactured they were never very popular because of their delicate nature. In most spectrometers the Si(Li) crystal is mounted behind an isolating window. The ideal window would be transparent to X-rays as well as strong enough to withstand atmospheric pressure when the chamber

is vented (the volume between the window and the detector must be under vacuum to prevent the absorption of X-rays). Unfortunately there is no ideal window, those that are

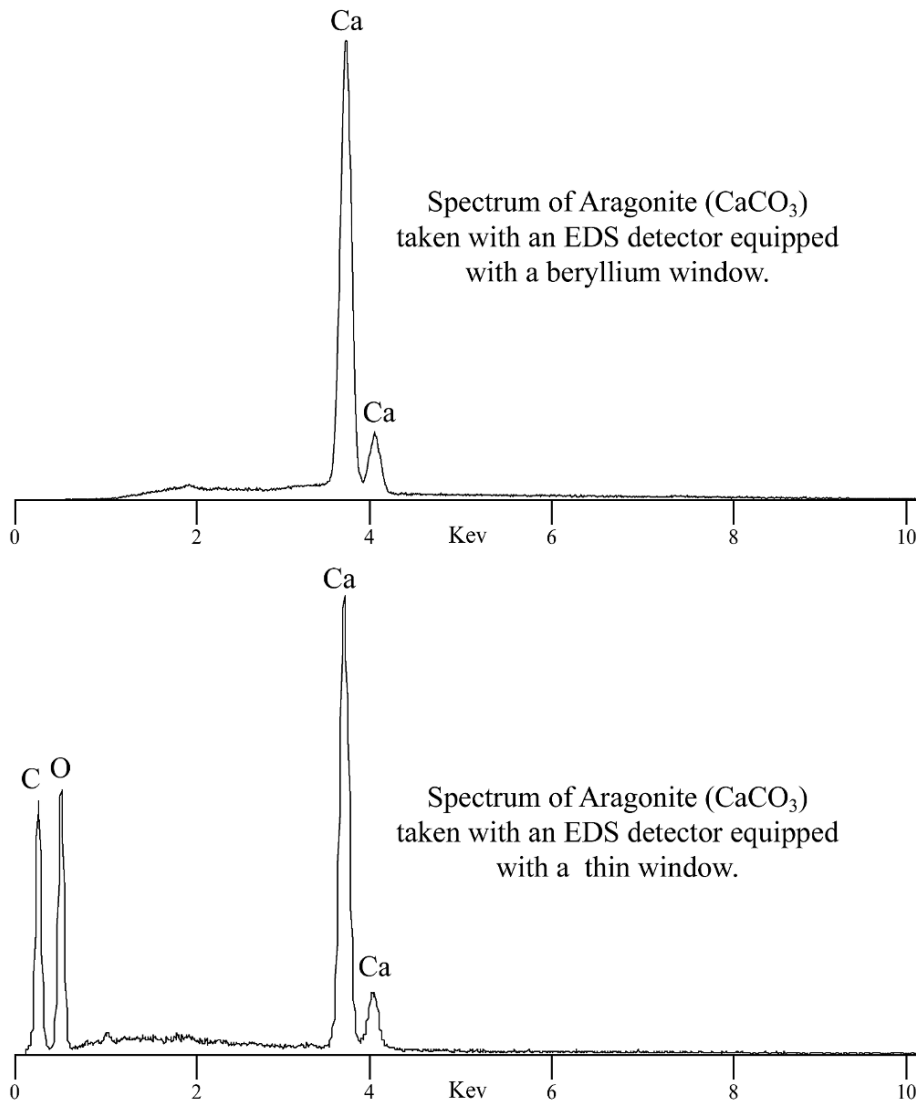


Figure 1.3. Comparison of spectra obtained with detectors equipped with beryllium and thin windows. The thin window detector detects carbon and oxygen.

rugged enough to withstand the pressure difference created when the chamber is vented tend to absorb lower energy X-rays while those that are thinner (and more transparent to X-rays) tend to be more fragile. The most commonly used material for windows is

beryllium. These windows absorb virtually all X-rays from elements lighter than sodium. Windows made of various polymers are becoming more common, and can allow the detection of elements as light as beryllium. These “thin” windows have almost completely replaced “windowless” detectors. The microscopist must be aware of the

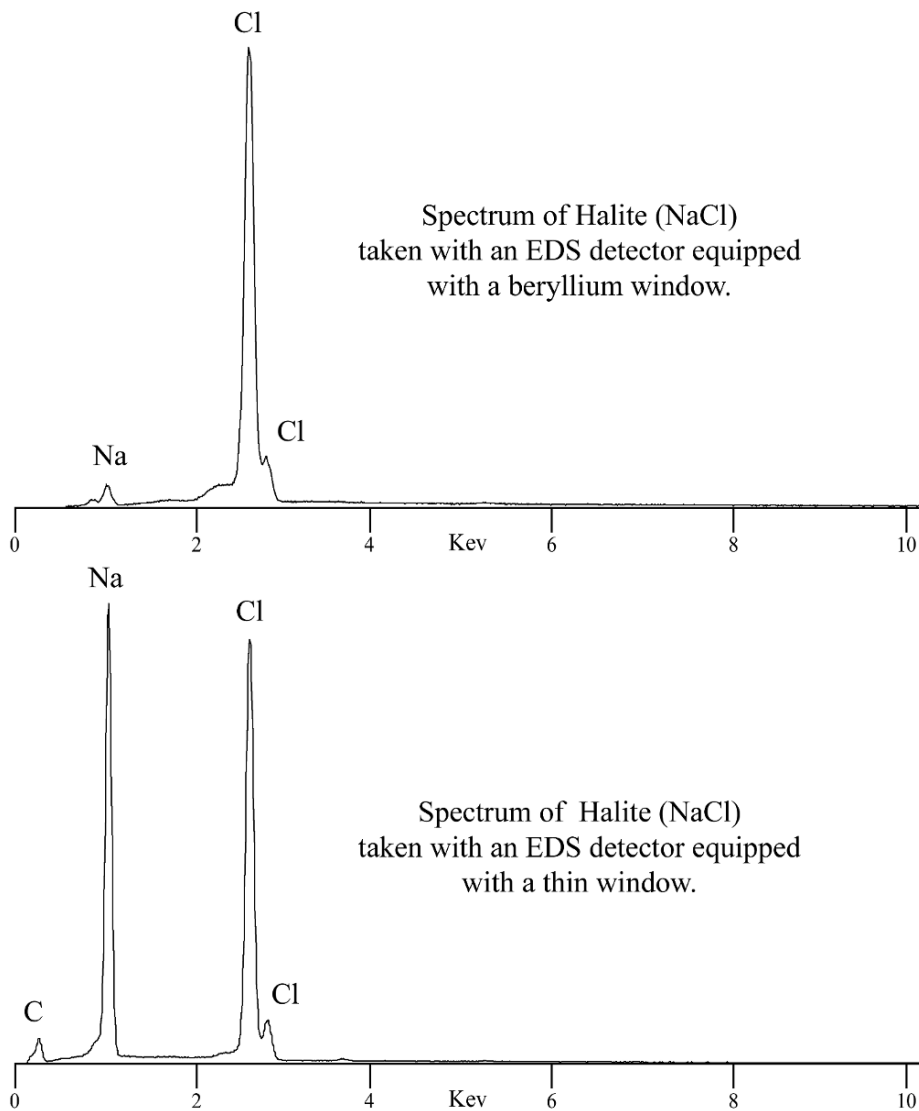


Figure 1.4. Comparison of spectra obtained with detectors equipped with beryllium and thin windows. The thin window detector is much more sensitive to sodium and also reveals the carbon from the coating.

kind of window on the EDS as it will put a lower limit on the energies (and thus the elements) that can be detected. The majority of the spectra in this book were collected with an EDS equipped with a beryllium window. As a result peaks from elements such as carbon and oxygen are not present in the spectra (Figure 1.3) and sodium is under-represented due to absorption of the Na $K\alpha$ X-rays by the beryllium window (Figure 1.4).

4. BEAM INTERACTION IN THE SPECIMEN

The beam in a scanning electron microscope can be smaller 20 Angstroms, and the resolution of an image produced by secondary electrons can be similar. X-rays, however are produced from a much larger volume in the specimen because the electron beam spreads in three dimensions when it interacts with the specimen. The volume of interaction can be approximated by:

$$y = 0.077 \cdot \frac{E_0^{1.5} - E_C^{1.5}}{\rho} \quad \text{and} \quad z = 0.01 \cdot \frac{E_0^{1.5} - E_C^{1.5}}{\rho}$$

where ρ is the density of the specimen in $\text{g}\cdot\text{cm}^{-3}$, E_0 , the accelerating voltage, and E_C , the critical excitation voltage, are in keV, and z (=depth) and y (=width) are in μm . (Figure 1.5, formulae modified from Potts, 1987). A good selection of software for modeling these interactions is available in Goldstein et al., 2003. For typical silicates and accelerating voltages, the interaction volume is roughly pear shaped and approximately 2 microns across and 2 microns deep. Thus, it is impossible to get a pure X-ray spectrum from a specimen that is smaller than 2 microns in diameter as the beam will spread into the surrounding material. In the case of a particle less than 2 microns thick sitting on a substrate, the beam will penetrate through the particle and generate X-rays in the substrate. The spectrum will then be a combination of X-rays from the particle and the substrate. A common example of this is the spectrum of a gold coated specimen: The characteristic X-rays of the specimen are readily visible in addition to the characteristic X-rays generated by the gold coating (Figure 1.6).

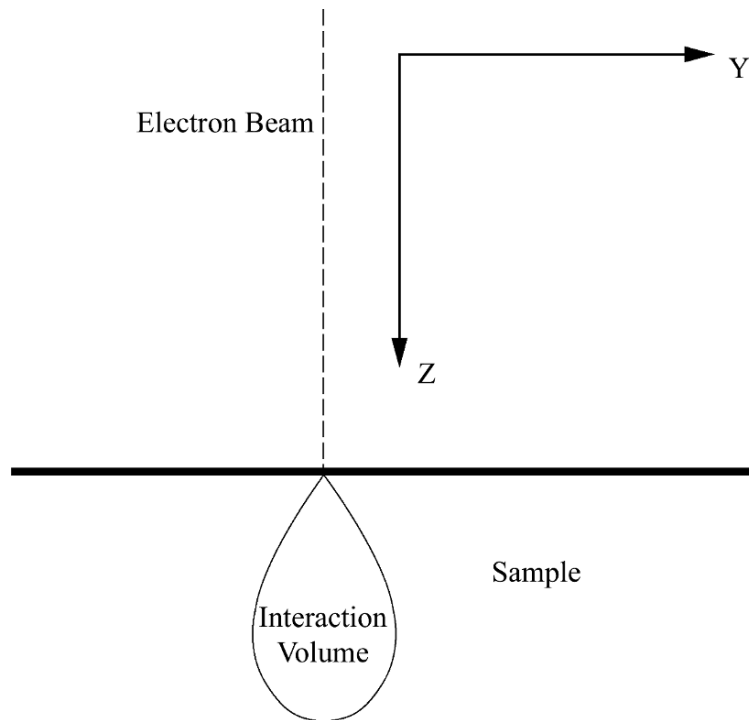


Figure 1.5. The electron beam penetrates the specimen and X-rays are generated beneath the specimen surface.

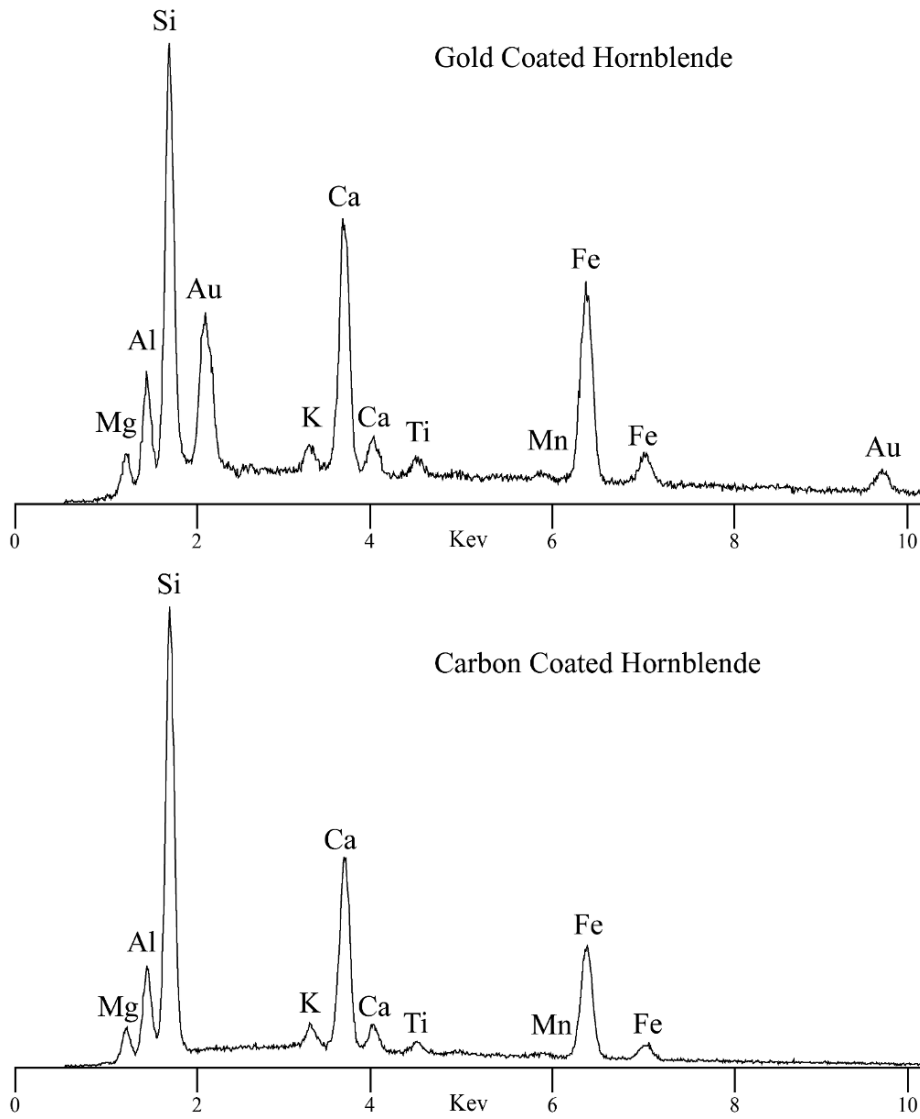


Figure 1.6. Comparison of spectra from gold and carbon coated specimens.

Chapter 2

SAMPLES AND SPECTRA

Preparation, Acquisition, and Interpretation

1. SAMPLE REQUIREMENTS AND PREPARATION

One of the great advantages of analysis by EDS in the SEM is the ease with which a wide variety of samples can be easily examined. Samples can range from a few microns to several inches across, depending on the size of the stage on the SEM. There are, however, two major requirements for the specimens: they must be dry and they must be conductive. Because the SEM operates with a vacuum in the range of 10^{-5} – 10^{-6} Torr, specimens must be dry. This is not a particular limitation for most geologic samples as they can be dried gently in an oven at 50–75 °C without distortion, although some clays may be affected by the procedure. More sophisticated techniques such as critical point or freeze drying are needed for delicate and water rich biological structures (Bozzola and Russell, 1999).

Specimens must be conductive so there is some means for the beam electrons to leave the sample after they interact with it. If the sample were non-conductive then the first electrons down the column would accumulate on the specimen, creating a static charge on it. This charge would remain on the specimen, as it could not bleed off through the vacuum or across the non-conductive specimen. Subsequent beam electrons would be deflected from the sample by the static charge, producing a distorted image and reducing the number of generated X-rays. If the sample is conductive (i.e. a metal) then making a conductive connection between the sample and the grounded stage is all that is necessary. In most instruments this connection is automatic. If the sample is non- or poorly conductive then it must be coated with a thin layer of a conductive substance. For imaging, a 200 Angstrom gold or a gold–palladium alloy are the coatings of choice as they enhance the production of secondary electrons, but they are not ideal for the production of X-ray spectra for two reasons. First, the coatings will produce

characteristic peaks that may mask peaks of interest (Figure 1.6). Second, the metallic coating will absorb X-rays that are generated in the sample. The absorption is greater for low energy X-rays such as sodium or oxygen. In spite of these problems gold or gold alloy coatings are tough and easy to make. As long as the microscopist is aware of the effects of metallic coatings, the problems associated with them are not serious for qualitative EDS work.

A coating that has less of an affect on the X-rays generated in the sample is carbon. Carbon coats are typically 300 Angstroms thick. Carbon absorbs few of the X-rays produced in the specimen, and, with few exceptions, the characteristic peak generated by the carbon (at 0.282 keV) can be ignored. Carbon coats, however, are fairly fragile and specimens that are carbon coated often need to be re-coated if they have not been examined for some time, particularly if they have been subjected to vibration. Finally, carbon is not a very good source of secondary electrons, so it is less than ideal for imaging. In some instances, samples are coated with carbon, examined for composition with the EDS, and then gold coated for imaging.

Most SEMs require samples mounted on disks or plugs that have a top surface about 1–2 cm in diameter, although many other sizes are available. Samples such as loose sand grains can be attached to the disks with double sided sticky tape or white glue that is almost dry. Especially delicate specimens can be mounted successfully by applying white glue to the mounting disk, letting the glue dry completely, placing the specimen on the stub, and then re-wetting the glue by holding the stub over a steaming cup of tea. Larger specimens can be mounted on stubs with conductive paint or tape. After coating with the conductive material of choice, the specimen is ready for examination.

Mounting stubs generally are made from aluminium. They can generate X-rays if the beam penetrates the specimen or if backscattered electrons interact with them. For this reason carbon stubs, which will produce low energy carbon X-rays are often used. However, if the samples are more than 10 microns thick and the beam is kept on the specimen, X-ray production from the stub itself is not a major worry.

Sample geometry should be considered when mounting the specimen. X-rays travel in a straight line from the sample to the ED detector. Figure 2.1 shows how a sample can shadow itself, with the result being low to minimal X-ray detection.

Another problem associated with sample geometry is the production of X-rays in the sample. It is obvious that the more electrons stay in the sample, the more X-rays will be

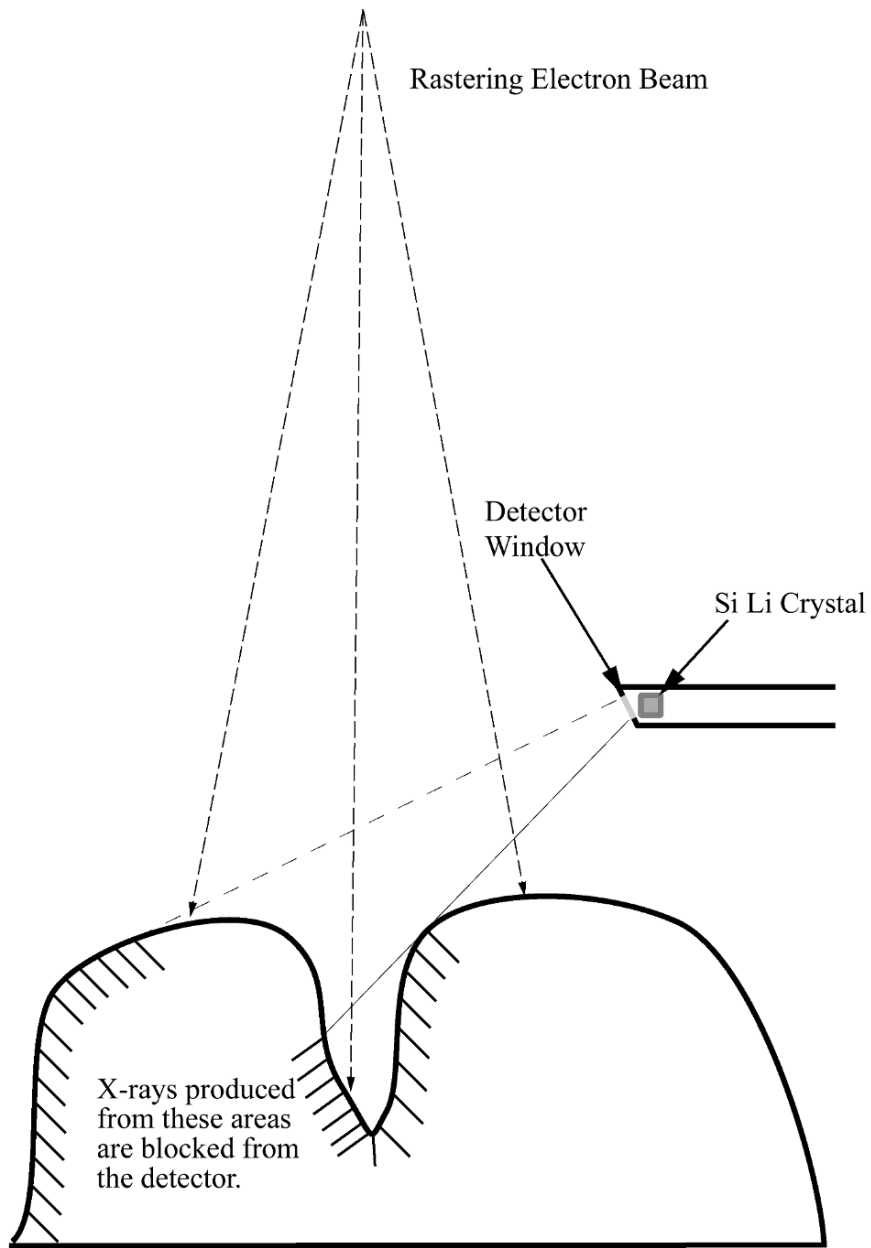


Figure 2.1. Self-shadowing of X-rays by an irregularly shaped specimen.

produced in the sample. The maximum number of electrons stays in the sample when the beam is perpendicular to the sample surface. At any other angle there is fore-

scattering which allows electrons to escape the sample rather than generating X-rays. This effect becomes greater as the angle increases.

2. OPERATION FOR GOOD EDS SPECTRA

The ideal EDS spectrum would contain obvious characteristic peaks for all elements in the sample. This ideal is modified by limitations of the detector. As an example, a detector with a beryllium window will not show oxygen, which comprises approximately 50 weight per cent of typical silicate minerals. The microscopist has no control over the detection of the lighter elements that are absorbed by the detector, but can control the maximum energy of generated X-rays. No X-rays with an energy greater than E_{\max} will be generated from the specimen, and E_{\max} must be greater than E_{abs} for whatever spectral series the microscopist wished to observe. As a rule of thumb, E_{\max} should be roughly twice E_{abs} for efficient X-ray generation. This is well illustrated in the spectra of galena (PbS) on pages 189-191.

The spectrum that was collected with $E_{\max} = 15$ keV has a large peak at about 2.3 keV. There are no X-rays in the Bremsstrahlung with an energy greater than 15keV, as expected because $E_{\max} = 15$ keV. Examination of X-ray tables reveals the S $K\alpha$ peak has an energy of 2.308 keV and that the Pb- $M\alpha$ line has an energy of 2.346 keV. These energies are close enough that EDS cannot differentiate them. Based on this peak alone it is not possible to say whether the specimen is pure S, pure Pb, or a combination of the two. Further examination of the spectrum reveals a small peak at about 10.5 keV. This small peak is the Pb $L\alpha$ peak which has an energy of 10.549 keV. Examining X-ray tables further reveals that E_{abs} for the Pb LIII series is 13.044 keV (and is more than 15.000 keV for the Pb LI and LII series). Even though the specimen is being stimulated with an E_{\max} of 15 keV, an energy that is greater than E_{abs} for the Pb LIII series, Pb LIII series X-rays are not being generated very efficiently. Increasing E_{\max} to 25 keV (almost twice E_{abs} for the Pb LIII series) greatly increases the number of Pb La X-rays generated and also allows the generation of the Pb LI and LII series.

At this point the microscopist can conclude that Pb is present in the specimen. It is impossible, however, to determine whether the sample is Pb or PbS (or possibly contains Mo, $L\alpha = 2.293$ KeV) based on the EDS spectrum alone. Other evidence (such as a Wavelength dispersive spectrometry, X-ray diffraction or examination of the sample's crystal morphology) would be needed for complete identification. Often the microscopist will be aware of the general geologic setting for the specimen and be able to produce a "best guess" based on that evidence.

A question frequently asked by EDS users is "how long do I need to collect a spectrum" or "how many counts does it take to make a good spectrum?" There is no simple answer to this question as demonstrated by the spectra of a chrome-rich augite shown in Figure 2.2. The first series of spectra were acquired with a beam current of 1 nA. As the counting time is increased the background becomes smoother and the peaks

become better defined. The Si (23.6 Wt%) and Ca (12.4 Wt%) peaks are identifiable after counting for only 1 second. A counting time of 4 to 8 seconds allows the identification of Mg (10.5 Wt%), Al (4.2 Wt%), and possibly Fe (3.6Wt%). Cr (0.6Wt%) starts to become identifiable at about 16 seconds, and Ti (0.3Wt%) becomes identifiable somewhere around 256–512 seconds. Thus, it takes more X-rays to identify elements that are present in lower concentrations.

Within limits, increasing the beam current has the same effect as increasing the counting time, as it increases the number of electrons that interact with the sample and produce X-rays. As more X-rays are produced and detected, it is possible to differentiate the peaks produced by characteristic X-rays from Bremsstrahlung X-rays with more confidence, even when those peaks are small. The second series of spectra in Figure 2.2 were collected with a 10 nA beam current. The spectra are approximately the same as if they had been collected for 10 times as long with a tenth as much beam current.

Increasing the beam current has some limitations. First, spatial resolution suffers as beam current increases. While this is not a significant problem for the generation of X-rays, it may be a problem for imaging with secondary electrons. Second, if too many X-rays are generated the detector can be flooded with so many X-rays that the dead time of the EDS system becomes significant and the detector is off for more time than it is on. Most manufacturers suggest operating the system with a dead time of 20–40% for the best throughput of X-rays in real time. When operating in these ranges doubling the beam current will approximately double the dead time, and halving it will approximately half the dead time.

Moving the detector toward or away from the sample also will affect the dead time. As the detector is moved closer to the sample allows the detector to capture a larger proportion of the X-rays generated from the sample and will increase the dead time. It also changes the beam–sample–detector geometry, altering X-ray absorption through the specimen. The effect will be greatest on lower energy X-rays, but it is rarely a problem in qualitative work. If the detector is moved toward the specimen, it should be done with extreme care. On most scanning electron microscopes it is possible to move

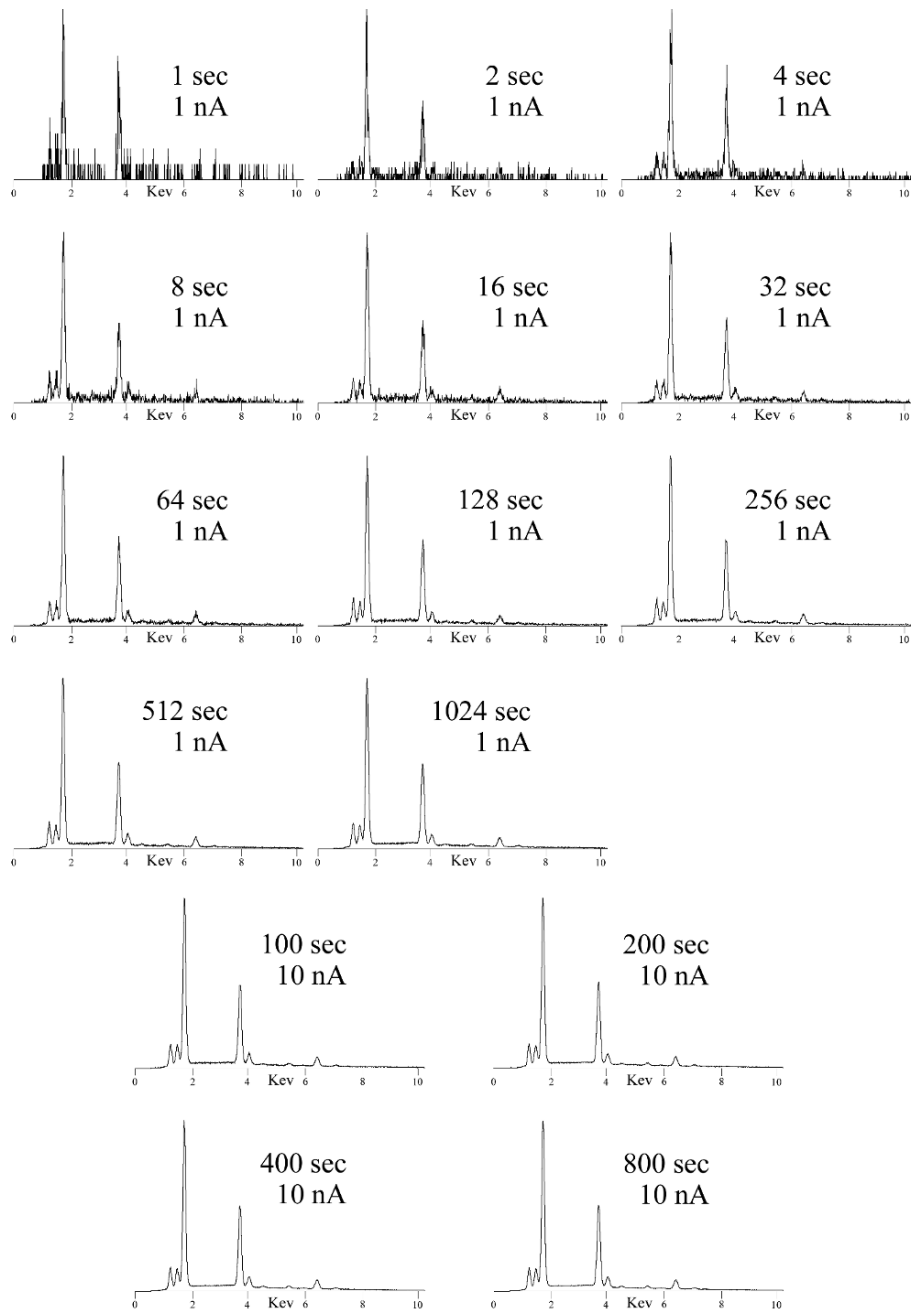


Figure 2.2. Effect of counting time and beam current on EDS spectra.

the detector close enough to the stage so that an odd shaped specimen can touch or even puncture the detector window. A puncture will cost the user several thousand dollars, and should be avoided at all costs.

There is no absolute set of correct machine settings for all samples, and it is not necessary to operate the EDS at maximum efficiency when collecting qualitative spectra. The accelerating voltage should be high enough so that all lines of interest are energised. The typical rule of thumb is to make the accelerating voltage about twice the energy needed to generate the highest energy characteristic X-rays of interest. Higher accelerating voltages will result in better spatial resolution with the secondary electrons in the microscope, but will also result in deeper penetration of the beam into the sample, increasing the possibility that the spectrum is collected from more than one material and decreasing the X-ray spatial resolution. The EDS detector must also be set up so that it can detect and/or display these higher energy X-rays. This is typically done through software. A higher beam current will result in the generation of more X-rays from the sample, but will also increase the "spot size" of the microscope, thus decreasing spatial resolution of the secondary electrons. On most scanning electron microscopes the control for Beam Current may be labelled Spot Size, Beam Current, or Condenser Lens Current. Dead time should be monitored as beam current is increased, as too much beam current can generate enough X-rays to flood the detector and decrease overall collection efficiency.

3. SPECTRAL INTERPRETATION

Before beginning the interpretation of a spectrum, make sure that there are enough counts so the characteristic peaks can easily be separated from the background formed by the Bremsstrahlung. There is no exact number of counts or amount of time that can be defined as "enough," but a good rule of thumb is to examine the spectrum as it is being collected. If possible, set up the software so that the spectrum is displayed in an "auto vertical scale" mode. In this mode the spectrum is scaled such that the channel with the greatest number of X-rays fills the maximum vertical scale on the screen. This is how most of the spectra in this book are displayed. If the relative heights of the peaks are not changing and the spectrum appears stable, then the spectrum probably has "enough" counts for interpretation. Experienced users examining specimens that are of only three or four possible compositions can identify the composition with relatively few counts, while more counts are needed to confidently identify minor constituents or specimens about which less is known.

The next step is to identify the characteristic peaks in the spectrum. While most modern software packages have some form of automatic peak identification, this feature should be used only as a guideline. More than one EDS user (and manufacturer!) has referred to it a "Automatic Peak Misidentification!" Automatic peak identification software expects peaks at certain positions and if the EDS detector is slightly

miscalibrated then it will produce erroneous identifications. Additionally, this software can be set up to identify peaks that are merely statistical aberrations of the background. It is a good idea to experiment with the auto ID software on samples of known composition to see what results it produces. Finally, auto ID software is not capable of differentiating peaks such as the S $K\alpha$ and the Pb- $M\alpha$ lines which differ in energy by only 0.03 keV.

When identifying the characteristic peaks, take advantage of the fact that most elements generate families of X-rays, and that those peaks will appear in fixed ratios. If a line is identified as the β or the γ line of an element, then the α line should also be present, and should be larger. Approximate relative peak heights are found in Table 2.1. Modern EDS software can display marker lines for any element, and some manufacturers use some version of Table 2.1 to scale all the markers to the α line, which is scaled to the height of the spectrum. If the markers only match for unreasonable elements, consider the possibility of miscalibration of the EDS detector. Calibration can be checked on two widely separated lines such as Al $K\alpha$ and Cu $K\alpha$. In cases where it is impossible to distinguish a K line from a light element such as S from an M line a heavy element such as Pb, look for the L or K lines of the heavier element. This may require adjusting the accelerating voltage of the SEM and the EDS acquisition software so that the higher energy X-rays can be generated and detected.

After identifying the characteristic peaks, eliminate spurious ones from further consideration. Au peaks from the specimen coating are common. If these are a problem then another coating material should be used. A less obvious source of spurious peaks is X-rays generated in places other than the specimen. Some of the beam electrons that interact with the specimen undergo Rutherford scattering, that is they interact with the nuclei of the target atoms and reverse their path. These electrons, known as backscattered electrons, have essentially E_{\max} energy and can generate characteristic X-rays. Because of their path (Figure 1.1) they are likely to collide with either the bottom of the column or walls the sample chamber. If E_{\max} is greater than about 10 keV they can generate Cu, Fe, Ni, or Cr X-rays. In addition to X-ray generation caused by the backscattered electrons, the X-rays generated in the sample can interact with the chamber and cause fluorescence. Tilting the specimen may eliminate these peaks as the distribution of the backscattered electrons will change. On occasion sum peaks may be present, although this is not common. Escape peaks may also be present — modern software often includes markers for these along with the α , β , and γ lines.

Table 2.1. . Relative weights (heights) of X-ray lines. Modified from Goldstein et al. (2003).

Family	Weight
K	$K\alpha=1$, $K\beta=0.1$
L	$L\alpha=1$, $L\beta_1=0.7$, $L\beta_2=0.2$, $L\gamma_1=0.08$, $L\gamma_2=0.03$, $L\gamma_3=0.03$, $L\eta=0.04$, $L\zeta=0.01$
M	$M\alpha=1$, $M\beta=0.6$, $M\zeta=0.06$, $M\gamma=0.05$

Identifying the peaks generated by elements present at abundances greater than a few weight per cent is generally easy (assuming no peak overlaps such as with the Pb $M\alpha$ and S $K\alpha$) but it is more difficult to identify the peaks generated by elements present at abundances less than about 0.5 weight per cent. This is because the Bremsstrahlung, which forms the background, can have the same energy as a characteristic X-ray, and there is no way to differentiate between the two. An X-ray of 1.740 keV could have been produced by a Si $K\alpha$ transition, or by a 15 keV electron that was suddenly slowed to 13.260 keV. A discussion of the methods used to differentiate between small peaks and the background can be found in Goldstein et al. (2003) or Reed (1993). For qualitative analysis it is sufficient to say that if a peak is visible after a reasonable amount of counting time with a reasonable beam current, then the element is present in the spectrum. If the microscopist wishes to be certain it is probably better to switch to a wavelength dispersive spectrometer if possible.

After determining which elements are in the specimen, determine the approximate relative concentrations of the elements. The number of characteristic X-rays is, to a first order, related to the number of atoms of a particular element in the sample provided that the X-rays are in the same family. Clearly, no characteristic calcium X-rays will be produced in a sample that does not contain calcium, while many will be produced in a calcium rich sample. For elements that are relatively close in atomic number the number of characteristic X-rays from each can be used to approximate the relative abundances of those elements provided that X-rays from the same families are used. Comparison between families of lines (e.g. K lines to L or M lines) will not be successful because the ionization efficiencies for three shells are very different. Comparison of lines from the same family for elements that differ greatly in atomic number (e.g. Na and Fe) will also be inexact because of differences in detector and X-ray generation efficiency. With practice and comparison to samples of known composition the microscopist will get a good feel for these differences.

Account for any elements that are not detectable by the EDS. When using an EDS with a beryllium window, elements lower in atomic number than Na will not be detected. This will make the spectra of, e.g. periclase (MgO) and magnesite ($MgCO_3$) appear identical, with only the Mg $K\alpha$ peak being detected. An EDS with a thin window, on the other hand, would show a much larger C $K\alpha$ peak on magnesite than on periclase. In most cases the microscopist will be able to differentiate between the two based on other evidence.

Remember that EDS spectra ultimately provide elemental, not structural data. Calcium carbonate ($CaCO_3$) is commonly found as both calcite and aragonite. In their pure forms they have identical compositions, and thus will have identical spectra. They can, however, often be differentiated based on morphology, and can readily be distinguished using X-ray diffraction.

Most X-rays are produced beneath the surface of the specimen, and those X-rays must travel through the specimen before they are detected by the EDS (Figure 2.3). X-rays that are produced anywhere except at the surface of the specimen are subject to

absorption as they travel through the specimen and, possibly, through the surrounding matrix. The amount of absorption, as well as the energy of the X-rays absorbed, will depend on the composition of the specimen and the length of the path that they travel as they leave the specimen. As an additional complication, the absorbed X-rays may generate other X-rays in the specimen in a phenomenon known as fluorescence.

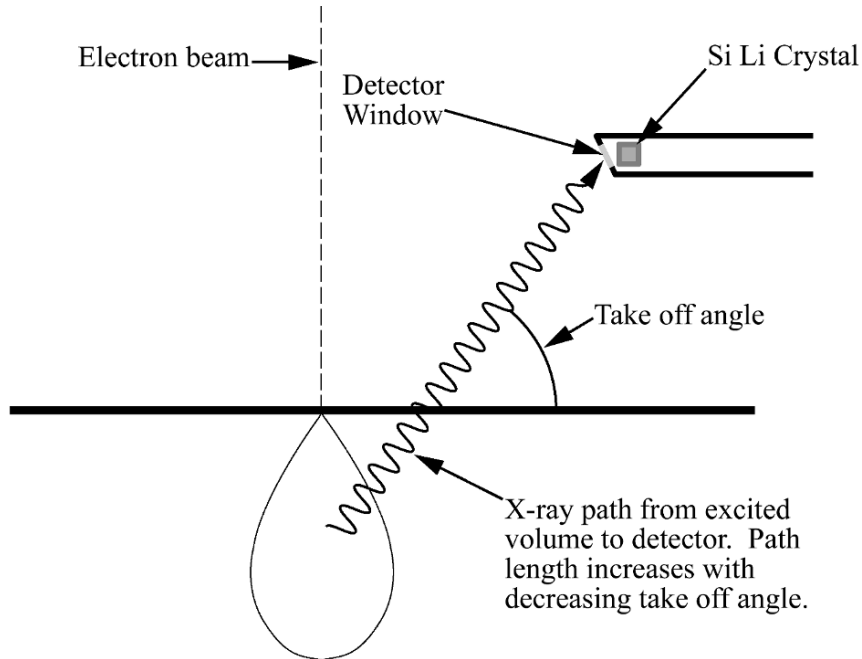


Figure 2.3. X-ray path length through specimen and take off angle.

The microscopist has some control over the length of the path that the X-rays travel as they exit the specimen before they enter the detector. By keeping the take-off angle (Figure 2.3) as large as possible, the path length through the specimen will be as small as possible. The short path length means that absorption and fluorescence effects will be small compared to what they would be if the path length were longer. In addition, a smaller specimen may be analysed with fewer complications from the surrounding matrix. The take-off angle can be changed by adjusting the height of the specimen relative to the EDS detector, by moving the detector toward or away from the specimen, and by tilting the specimen. Most manufacturers provide a table that can be used to calculate the take-off angle for a specimen in various positions, but because typically SEM specimens have irregular surfaces the value from the table should be regarded as an estimate. Highly accurate quantitative compositional analysis requires knowing the take off angle so that absorption and fluorescence effects can be accurately calculated. For qualitative analysis it is less important.

Chapter 3

THE KEY

1. HOW TO USE THE KEY

After acquiring a spectrum, identify the elements in it. If a line is identified as a β or γ line in a series then the α line from that series must be present. The height of each peak from a single element will be present in approximately the ratios listed in Table 2.1. If the beam energy is sufficient, look for K lines in addition to the lower energy L lines, or L lines in addition to the M lines. As an example, the gold $M\alpha$ peak at 2.123 keV is difficult to distinguish from the lead $M\alpha$ peak at 2.345 keV, particularly as M peaks are rather broad. However, the gold $L\alpha$ peak at 9.712 keV is easily differentiated from the lead $L\alpha$ peak at 10.550 keV. If necessary increase the accelerating voltage to generate the higher energy lines. Use automatic peak identification for suggestions, but make sure that the elements make geologic sense. After identifying the characteristic peaks, determine which elements are spurious and eliminate them from further consideration.

Determine if there are likely to be any elements not detected by the EDS. In particular, when using a detector with a beryllium window, carbon and oxygen will not be detected, leading to similar spectra from different minerals. Methods such as X-ray diffraction or examination of crystal morphology (see Welton, 1984) may be needed if these minerals must be precisely differentiated.

After determining which elements are present in the spectrum and accounting for probable undetected elements, estimate relative elemental abundance by comparing peak heights. Only comparisons within the same family of lines (i.e., comparing $K\alpha$ to $K\alpha$ or $L\alpha$ to $L\alpha$, but not $K\alpha$ to $L\alpha$) are valid. The estimate of relative abundance will be approximate even within a single family of lines because of differences in X-ray generation and detector efficiency at different energies. Specimen tilt will also affect the

relative heights of the peaks, having the greatest effect on the lighter elements at lower takeoff angles.

The key is arranged in binary fashion with two major sections, one for silicates (numbered choices) and one for non-silicates (lettered choices). The first step is to decide whether silicon is the dominant element in the sample. If it is, use the key where choices are designated by numbers. If not use the key where the choices are designated by letters. At each step choose between two options. Proceed through the selected choices until a mineral is indicated, then compare the unknown spectrum to the spectrum suggested by the key. Minor differences between the collected spectrum and those here are to be expected as the spectra were obtained naturally formed minerals. This is particularly true for minerals such as the plagioclase feldspars that form a solid solution series.

2. KEY FOR IDENTIFYING MINERALS USING EDS

Minerals marked N/A do not have spectra but should be considered as possibilities

Is Silicon a major component?

Yes: Go to Section I, **Silicates**

No: **Go To Section II - Non Silicates** (Oxides, sulphides, carbonates, phosphates, spinels, halides)

Section I, Silicates

1) Is there an Aluminum peak?

Yes: 2

No: 3

2) Only Aluminum and Silicon peaks

Yes:

Sillimanite Al_2SiO_5 **Page 56**

Mullite $3\text{Al}_2\text{O}_3 \cdot 2\text{SiO}_2$ **Page 57**

Andalusite Al_2SiO_5 **Page 58**

Kyanite Al_2SiO_5 **Page 59**

Topaz $\text{Al}_2[\text{SiO}_4](\text{OH},\text{F})_2$ **Page 60**

Beryl $\text{Be}_3\text{Al}_2[\text{Si}_6\text{O}_{10}]$ **Page 81**

Spodumene $\text{LiAl}[\text{Si}_2\text{O}_6]$ **Page 95**

Pyrophyllite $\text{Al}_4[\text{Si}_8\text{O}_{20}](\text{OH})_4$ **Page 122**

Kaolinite group (Kandites) $\text{Al}_4[\text{Si}_4\text{O}_{10}](\text{OH})_8$ **Page 126**

Petalite $\text{Li}[\text{AlSi}_4\text{O}_{10}]$ **Page 146**

No: 4

3) Has only Si

Yes:

Silica Minerals: Quartz, Tridymite, or Cristobalite SiO_2 **Pages 142, 143**

No: 18

4) Contains Chlorine or Sulphur

Yes:

Sodalite Group:

Sodalite $\text{Na}_8[\text{Al}_6\text{Si}_6\text{O}_{24}]\text{Cl}_2$ **Page 148**

Nosean $\text{Na}_8[\text{Al}_6\text{Si}_6\text{O}_{24}]\text{SO}_4$ **Page 149**

Häüyne $(\text{Na,Ca})_{4-8}[\text{Al}_6\text{Si}_6\text{O}_{24}](\text{SO}_4,\text{S})_{1-2}$ **Page 149**

Cancrinite-Vishnevite $(\text{Na,Ca,K})_{6-8}[\text{Al}_6\text{Si}_6\text{O}_{24}](\text{CO}_3,\text{SO}_4,\text{Cl})_{1-2} \cdot 1-5\text{H}_2\text{O}$ **N/A**

Scapolite $(\text{Na,Ca,K})_4[\text{Al}_3(\text{Al,Si})_3\text{Si}_6\text{O}_{24}](\text{Cl,CO}_3,\text{SO}_4,\text{OH})$ **Page 151**

No: 5

5) Peak for element $Z > 26$ (Iron)

Yes:

Allanite $(\text{Ca,Ce})_2(\text{Fe}^{+2},\text{Fe}^{+3})\text{Al}_2\text{O} \cdot \text{OH}[\text{Si}_2\text{O}_7][\text{SiO}_4]$ **Pages 74,75**

Barium Feldspars:

Celsian $\text{Ba}[\text{Al}_2\text{Si}_2\text{O}_8]$ **Page 140**

Hyalophane $(\text{K,Na,Ba})[(\text{Al,Si})_4\text{O}_8]$ **Page 141**

Zeolite Group $(\text{Na}_2,\text{K}_2,\text{Ca,Ba})[(\text{Al,Si})_2\text{O}_2]_n \cdot x\text{H}_2\text{O}$ **Page 153-159**

No: 6

6) Has Sodium or Potassium peak

Yes: 7

No: 10

7) Contains Iron, Manganese, or Titanium

Yes: 8

No: 14

8) Contains Calcium

Yes: 9

No: 17

9) Contains Potassium

Yes:

Hornblende $(\text{Na}, \text{K})_{0-1} \text{Ca}_2 (\text{Mg}, \text{Fe}^{+2}, \text{Fe}^{+3}, \text{Al})_5 [\text{Si}_{6-7} \text{Al}_{2-1} \text{O}_{22}] (\text{OH}, \text{F})_2$ **Pages 108, 109**

Kaersutite $\text{Ca}_2 (\text{Na}, \text{K}) (\text{Mg}, \text{Fe}^{+2}, \text{Fe}^{+3})_4 \text{Ti} [\text{Si}_6 \text{Al}_2 \text{O}_{22}] (\text{O}, \text{OH}, \text{F})_2$ **Page 110**

Barkevikite $\text{Ca}_2 (\text{Na}, \text{K}) (\text{Fe}^{+2}, \text{Mg}, \text{Fe}^{+3}, \text{Mn})_5 [\text{Si}_{6.5} \text{Al}_{1.5} \text{O}_{22}] (\text{OH})_2$ **N/A**

Glauconite

$(\text{K}, \text{Na}, \text{Ca})_{1.2-2.0} (\text{Fe}^{+3}, \text{Al}, \text{Fe}^{+2}, \text{Mg})_{4.0} [\text{Si}_{7-7.6} \text{Al}_{1-0.4} \text{O}_{20}] (\text{OH})_4 \cdot n (\text{H}_2\text{O})$ **Page 114**

No:

Melilite $(\text{Ca}, \text{Na})_2 [(\text{Mg}, \text{Fe}^{+2}, \text{Al}, \text{Si})_3 \text{O}_7]$ **Page 78**

Augite-Ferroaugite $(\text{Ca}, \text{Na}, \text{Mg}, \text{Fe}^{+2}, \text{Mn}, \text{Fe}^{+3}, \text{Al}, \text{Ti})_2 [(\text{Si}, \text{Al})_2 \text{O}_6]$ **Page 91**

Hornblende

$(\text{Na}, \text{K})_{0-1} \text{Ca}_2 (\text{Mg}, \text{Fe}^{+2}, \text{Fe}^{+3}, \text{Al})_5 [\text{Si}_{6-7} \text{Al}_{2-1} \text{O}_{22}] (\text{OH}, \text{F})_2$ **Pages 108, 109**

Basaltic Hornblende $(\text{Ca}, \text{Na})_{2-3} (\text{Mg}, \text{Fe}^{+2})_{3-2} (\text{Fe}^{+3}, \text{Al})_{2-3} \text{O}_2 [\text{Si}_6 \text{Al}_2 \text{O}_{22}]$ **N/A**

Magnesiokatophorite-Katophorite $\text{Na}_2 \text{Ca} (\text{Mg}, \text{Fe}^{+2})_4 \text{Fe}^{+3} [\text{Si}_7 \text{AlO}_{22}] (\text{OH}, \text{F})_2$ **N/A**

Stilpnomelane

$(\text{K}, \text{Na}, \text{Ca})_{0-1.4} (\text{Fe}^{+3}, \text{Fe}^{+2}, \text{Mg}, \text{Al}, \text{Mn})_{5.9-8.2} [\text{Si}_8 \text{O}_{20}] (\text{OH})_4 (\text{O}, \text{OH}, \text{H}_2\text{O})_{3.6-8.5}$

Page 121

Montmorillonite Group:

(Smectites)

$^{1/2} (\text{Ca}, \text{Na})_{0.7} (\text{Al}, \text{Mg}, \text{Fe})_4 [(\text{Si}, \text{Al})_8 \text{O}_{20}] (\text{OH})_4 \cdot n \text{H}_2\text{O}$ **Page 128**

10) Large amount of Chrome

Yes:

Garnet, Uvarovite $\text{Ca}_3 \text{Cr}_2 \text{Si}_3 \text{O}_{12}$ **Page 54**

No: 11

11) Has Manganese peak

Yes

Garnet, Spessartine $\text{Mn}_3 \text{Al}_2 \text{Si}_3 \text{O}_{12}$ **Page 51**

Chloritoid $(\text{Fe}^{+2}, \text{Mg}, \text{Mn})_2 (\text{Al}, \text{Fe}^{+3}) \text{Al}_3 \text{O}_2 [\text{SiO}_4]_2 (\text{OH})_4$ **Page 62**

Piemontite $\text{Ca}_2 (\text{Mn}, \text{Fe}^{+3}, \text{Al})_2 \text{AlO} \cdot \text{OH} [\text{Si}_2 \text{O}_7] [\text{SiO}_4]$ **Pages 72, 73**

Axinite $(\text{Ca}, \text{Mn}, \text{Fe}^{+2})_3 \text{Al}_2 \text{BO}_3 [\text{Si}_4 \text{O}_{12}] \text{OH}$ **Page 85**

No: 12

12) Has Magnesium peak

Yes:

Garnet, Pyrope $\text{Mg}_3\text{Al}_2\text{Si}_3\text{O}_{12}$ **Page 49**
 Vesuvianite (Idocrase) $\text{Ca}_{10}(\text{Mg,Fe})_2\text{Al}_4[\text{Si}_2\text{O}_7]_2[\text{SiO}_4]_5(\text{OH,F})_4$ **Page 55**
 Staurolite $(\text{Fe}^{+2},\text{Mg})_2(\text{Al,Fe}^{+3})_9\text{O}_6[\text{SiO}_4]_4(\text{O,OH})_2$ **Page 61**
 Sapphirine $(\text{Mg,Fe})_2\text{Al}_4\text{O}_6[\text{SiO}_4]$ **Page 64**
 Pumpellyite $\text{Ca}_4(\text{Mg,Fe}^{+2})(\text{Al,Fe}^{+3})_5\text{O}(\text{OH})_3[\text{Si}_2\text{O}_7]_2[\text{SiO}_4]_2 \cdot 2\text{H}_2\text{O}$ **Page 77**
 Cordierite $\text{Al}_3(\text{Mg,Fe}^{+2})_2[\text{Si}_5\text{AlO}_{18}]$ **Page 82**
 Gedrite $(\text{Mg,Fe}^{+2})_5\text{Al}_2[\text{Si}_6\text{Al}_2\text{O}_{22}](\text{OH,F})_2$ **N/A**
 Clintonite $\text{Ca}_2(\text{Mg,Fe})_{4,6}\text{Al}_{1,4}[\text{Si}_{2,5}\text{Al}_{5,5}\text{O}_{20}](\text{OH}_4)$ **N/A**
 Xanthophyllite $\text{Ca}_2(\text{Mg,Fe})_{4,6}\text{Al}_{1,4}[\text{Si}_{2,5}\text{Al}_{5,5}\text{O}_{20}](\text{OH}_4)$ **Page 120**
 Chlorite $(\text{Mg,Al,Fe})_{12}[(\text{Si,Al})_8\text{O}_{20}](\text{OH})_{16}$ **Page 124**
 Septochlorites $\text{Y}_6[\text{Z}_4\text{O}_{10}](\text{OH})_8$ **N/A**
 Clay Minerals such as:
 Vermiculite
 $(\text{Mg,Ca})_{0,7}(\text{Mg,Fe}^{+3},\text{Al})_{6,0}[(\text{Al,Si})_8\text{O}_{20}](\text{OH}_4 \cdot 8\text{H}_2\text{O})$ **Pages 129, 130**

No: 13

13) Large Iron Peak?

Yes:

Garnets:

Almandine $\text{Fe}_3^{+2}\text{Al}_2\text{Si}_3\text{O}_{12}$ **Page 50**

Andradite $\text{Ca}_3(\text{Fe}^{+3},\text{Ti})_2\text{Si}_3\text{O}_{12}$ **Page 53**

Epidotes $\text{CaFe}^{+3}\text{Al}_2\text{O} \cdot \text{OH}[\text{Si}_2\text{O}_7][\text{SiO}_4]$ **Pages 69-75**

No:

Garnets:

Grossular $\text{Ca}_3\text{Al}_2\text{Si}_3\text{O}_{12}$ **Page 52**

Hydrogrossular $\text{Ca}_3\text{Al}_2\text{Si}_2\text{O}_8(\text{SiO}_4)_{1-m}(\text{OH})_{4m}$ **N/A**

Epidotes:

Zoisite $\text{Ca}_2\text{Al} \cdot \text{Al}_2\text{O} \cdot \text{OH}[\text{Si}_2\text{O}_7][\text{SiO}_4]$ **Page 69**

Clinozoisite $\text{Ca}_2\text{Al} \cdot \text{Al}_2\text{O} \cdot \text{OH}[\text{Si}_2\text{O}_7][\text{SiO}_4]$ **Page 70**

Lawsonite $\text{CaAl}_2(\text{OH})_2[\text{Si}_2\text{O}_7]\text{H}_2\text{O}$ **Page 76**

Melilite **Page 78**

Gehlenite $\text{Ca}_2[\text{Al}_2\text{SiO}_7]$ **N/A**

Pyroxenes **Page 86-96**

Amphiboles **Page 102-111**

Margarite $\text{Ca}_2\text{Al}_4[\text{Si}_4\text{Al}_4\text{O}_{20}](\text{OH})_4$ **Page 119**

Prehnite $\text{Ca}_2\text{Al}[\text{AlSi}_3\text{O}_{10}](\text{OH})_2$ **Page 132**

14) Contains Magnesium

Yes:

Glaucofanite $\text{Na}_2\text{Mg}_3\text{Al}_2[\text{Si}_8\text{O}_{22}](\text{OH})_2$ **Page 111**

No: 15

15) Is Potassium >> Sodium?

Yes:

Mica, Muscovite $K_2Al_4[Si_6Al_2O_{20}](OH,F)_4$ **Page 112**

Lepidolite $K_2(Li,Al)_{5-6}[Si_{6-7}Al_{2-1}O_{20}](OH,F)_4$ **Page 117**

Clay, Illite $K_{1-1.5}Al_4[Si_{7-6.5}Al_{1-1.5}O_{20}](OH)_4$ **Page 127**

Alkali Feldspar (K,Na)[AlSi₃O₈] **Page 133-135**

Kalsilite K[AlSiO₄] **Page 145**

Leucite K[AlSi₂O₆] **Page 147**

No: 16

16) Contains some Calcium

Yes:

Feldspar, Plagioclase (not pure Albite)Na[AlSi₃O₈]-Ca[Al₂Si₂O₈] **Page 137-139**

No:

Feldspar, (pure Albite)Na[AlSi₃O₈] **Page 136**

Jadeite NaAl[Si₂O₆] **Page 96**

Mica, such as Paragonite $Na_2Al_4[Si_6Al_2O_{20}](OH)_4$ **Page 113**

Nepheline $Na_3(Na,K)[Al_4Si_4O_{16}]$ **Page 144**

Analcite Na[AlSi₂O₆]•H₂O **Page 152**

Zeolites (Na₂,K₂,Ca,Ba)[(Al,Si)O₂]_n•xH₂O **Page 153-159**

17)Contains Potassium

Yes:

Phlogopite $K_2(Mg,Fe^{+2})_6[Si_6Al_2O_{20}](OH,F)_4$ **Page 115**

Biotite $K_2(Mg,Fe^{+2})_{6-4}(Fe^{+3},Al,Ti)_{0-2}[Si_{6-5}Al_{2-3}O_{20}](OH,F)_4$ **Page 116**

Zinnwaldite $K_2(Fe^{+2}_{2-1},Li_{2-3}Al_2)[Si_{6-7}Al_{2-1}O_{20}](F,OH)_4$ **Page 118**

No:

Tourmaline Na(Mg,Fe,Mn,Li,Al)₃Al₆[Si₆O₁₈](BO₃)₃(OH,F)₄ **Pages 83, 84**

Eckermannite-Arfvedsonite Na₃(Mg,Fe⁺²)₄Al[Si₈O₂₂](OH,F)₂ **N/A**

18) Contains Sulfur

Yes:

Helvite Mn₄[Be₃Si₃O₁₂]S **Page 150**

Danalite Fe₄[Be₃Si₃O₁₂]S **Page 150**

Genthelvite Zn₄[Be₃Si₃O₁₂]S **Page 150**

No: 19

19) Contains Zirconium

Yes:

Zircon $Zr[SiO_4]$ **Pages 46, 47**

Eudialyte (Eucolite) $(Na, Ca, Fe)_6Zr[(Si_3O_9)_2](OH, F, Cl)$ **Page 67**

Rosenbuschite $(Ca, Na, Mn)_3(Zr, Ti, Fe^{+3})[SiO_4]_2(F, OH)$ **Page 68**

Låvenite $(Na, Ca, Mn, Fe^{+2})_3(Zr, Nb, Ti)[Si_2O_7](OH, F)$ **N/A**

Catapleiite $(Na, Ca)_2Zr[Si_3O_9] \cdot 2H_2O$ **N/A**

No: 20

20) Contains Titanium

Yes:

Sphene $Ca Ti[SiO_4](O, OH, F)$ **Page 48**

Aenigmatite $Na_2Fe_5^{+2}TiSi_6O_{20}$ **N/A**

Astrophyllite $(K, Na)_3(Fe, Mn)_7Ti_2[Si_4O_{12}]_2(O, OH, F)_7$ **N/A**

No: 21

21) Contains Potassium

Yes:

Apophyllite $KFCa_4[Si_8O_{20}]8H_2O$ **Page 131**

No: 22

22) Contains Sodium

Yes:

Aegirine (Acmite) $NaFe^{+3}[Si_2O_6]$ **Page 93**

Aegirine-augite $(Na, Ca)(Fe^{+3}, Fe^{+2}, Mg)[Si_2O_6]$ **Page 94**

Riebeckite $Na_2Fe_3^{+2}Fe_2^{+3}[Si_8O_{22}](OH)_2$ **N/A**

Richterite-Ferrorichterite $Na_2Ca(Mg, Fe^{+3}, Fe^{+2}, Mn)_5[Si_8O_{22}](OH, F)_2$ **N/A**

Pectolite $Ca_2NaH[SiO_3]_3$ **Page 98**

No: 23

23) Contains Calcium

Yes: 24

No: 25

24) Contains Magnesium or Iron

Yes:

Monticellite $\text{CaMg}[\text{SiO}_4]$ **Page 43**

Merwinite $\text{Ca}_3\text{Mg}[\text{Si}_2\text{O}_8]$ **Page 65**

Åkermanite $\text{Ca}_2[\text{MgSi}_2\text{O}_7]$ **N/A**

Pyroxenes:

Diopside-Hedenbergite $\text{Ca}(\text{Mg,Fe})[\text{Si}_2\text{O}_6]$ **Pages 88, 89**

Johannsenite $\text{Ca}(\text{Mn,Fe})[\text{Si}_2\text{O}_6]$ **Page 90**

Pigeonite $(\text{Mg,Fe}^{+2},\text{Ca})(\text{Mg,Fe}^{+2})[\text{Si}_2\text{O}_6]$ **Page 92**

Rhodonite $(\text{Mn,Ca,Fe})[\text{SiO}_3]$ **Page 99**

Bustamite $(\text{Mn,Ca,Fe})[\text{SiO}_3]$ **Page 100**

Tremolite-Ferroactinolite $\text{Ca}_2(\text{Mg,Fe}^{+2})_5[\text{Si}_8\text{O}_{22}](\text{OH,F})_2$ **Pages 105-107**

No:

Datolite $\text{CaB}[\text{SiO}_4](\text{OH})$ **Page 63**

Larnite $\text{Ca}_2[\text{SiO}_4]$ **N/A**

Spurrite $2\text{Ca}_2[\text{SiO}_4]\cdot\text{CaCO}_3$ **Page 66**

Rankinite $\text{Ca}_3[\text{Si}_2\text{O}_7]$ **Page 79**

Tilleyite $\text{Ca}_3[\text{Si}_2\text{O}_7]\cdot 2\text{CaCO}_3$ **Page 80**

Wollastonite $\text{Ca}[\text{SiO}_3]$ **Page 97**

25) Contains only Magnesium and Silicon

Yes:

Forsterite Mg_2SiO_4 **Page 38,40**

Humite Group:

Humite $\text{Mg}(\text{OH,F})\cdot 3\text{Mg}_2\text{SiO}_4$ **N/A**

Clinohumite $\text{Mg}(\text{OH,F})_2\cdot 4\text{Mg}_2\text{SiO}_4$ **N/A**

Norbergite $\text{Mg}(\text{OH,F})_2\cdot \text{Mg}_2\text{SiO}_4$ **Page 44**

Chondrodite $\text{Mg}(\text{OH,F})_2\cdot 2\text{Mg}_2\text{SiO}_4$ **Page 454**

Talc $\text{Mg}_6[\text{Si}_8\text{O}_{20}](\text{OH})_4$ **Page 123**

Serpentine $\text{Mg}_3[\text{Si}_2\text{O}_5](\text{OH})_4$ **Page 125**

No: 26

26) Contains Manganese

Yes:

Tephroite $\text{Mn}_2[\text{SiO}_4]$ **Page 41**

Knebelite $(\text{Mn,Fe})_2[\text{SiO}_4]$ **Page 42**

Pyroxmangite $(\text{Mn,Fe})[\text{SiO}_3]$ **Page 101**

No:

Olivine: Fayalite Fe_2SiO_4 **Page 39**

Pyroxenes:

Enstatite-Orthoferrosilite $(\text{Mg,Fe}^{+2})[\text{SiO}_3]$
see Bronzite or Hypersthene Pages 86, 87

Amphiboles:

Anthophyllite $(\text{Mg,Fe}^{+2})_7[\text{Si}_8\text{O}_{22}](\text{OH,F})_2$ **Page 102**

Cumingtonite $(\text{Mg,Fe}^{+2})_7[\text{Si}_8\text{O}_{22}](\text{OH})_2$ **Page 103**

Grunerite $(\text{Fe}^{+2},\text{Mg})_7[\text{Si}_8\text{O}_{22}](\text{OH})_2$ **Page 104**

SECTION II NON SILICATES

A) Is there more than one Peak?

Yes: B (sulfide, sulfate, some oxides or carbonates, phosphates, halides)

No: C (Oxides, some carbonates or sulphide with overlapping peak)

B) Is there at major Sulphur Peak?

Yes: D (Sulfides and Sulfates)

No: E (Oxides, carbonate, phosphate, spinels, halide)

C) Oxides:

Periclase MgO **Pages 160, 161**

Cassiterite SnO_2 **Page 162**

Corundum $\alpha\text{-Al}_2\text{O}_3$ **Page 163**

Hæmatite $\alpha\text{-Fe}_2\text{O}_3$ **Pages 164, 165**

Anatase, Brookite or Rutile TiO_2 **Page 167**

Magnetite $\text{Fe}^{+2}\text{Fe}^{+3}_2\text{O}_4$ **Page 173**

Maghemite $\gamma\text{-Fe}^{+3}_2\text{O}_3$ **Page 174**

Hydroxides:

Brucite $\text{Mg}(\text{OH})_2$ **Page 179**

Gibbsite $\text{Al}(\text{OH})_3$ **Page 180**

Diaspore $\alpha\text{-AlO}(\text{OH})$ or Boehmite $\gamma\text{-AlO}(\text{OH})$ **Page 181**

Goethite $\alpha\text{-FeO}\cdot\text{OH}$ or Lepidocrocite $\gamma\text{-FeO}\cdot\text{OH}$ **Page 182**

Limonite $\text{FeO}\cdot\text{OH}\cdot n\text{H}_2\text{O}$ **Page 183**

Carbonates:

Calcite or Aragonite CaCO_3 **Pages 199, 200, and 208**

Magnesite MgCO_3 **Pages 201, 202**

Rhodochrosite MnCO_3 **Page 203**

Siderite FeCO_3 **Pages 204, 205**

Strontianite SrCO_3 **Page 210**

Witherite BaCO_3 **Page 211**

Halide: Fluorite CaF_2 **Pages 215, 216**

D) Is there an Iron Peak?

Yes:

Sulfides:

Pyrite FeS_2 **Page 184**

Pyrrhotite $\text{Fe}_7\text{S}_8\text{-FeS}$ **Page 185**

Chalcopyrite CuFeS_2 **Page 186**

Arsenopyrite FeAsS **Page 187**

No:

Sulfides:

Sphalerite ZnS **Pages 188, 189**

Galena PbS **Pages 190-192**

Sulphates:

Barytes BaSO_4 **Page 193**

Celestine SrSO_4 **Pages 194-196**

Gypsum $\text{CaSO}_4 \cdot 2\text{H}_2\text{O}$ **Page 197**

Anhydrite CaSO_4 **Page 198**

E) Is there a major phosphorus peak?

Yes:

Phosphates:

Apatite $\text{Ca}_5(\text{PO}_4)_3(\text{OH},\text{F},\text{Cl})$ **Pages 212, 213**

Monazite $(\text{Ce},\text{La},\text{Th})\text{PO}_4$ **Page 214**

No: F (Oxides, carbonate, spinels, halides)

F) Is there an Aluminum peak?

Yes:

Spinel:

Spinel MgAl_2O_4 **Page 170**

Hercynite $\text{Fe}^{+2}\text{Al}_2\text{O}_4$ **N/A**

Gahnite ZnAl_2O_4 **Page 171**

Galaxite MnAl_2O_4 **N/A**

No: G

G) Is there a Chromium peak?

Yes:

Magnesiochromite MgCr_2O_4 **Page 177**

Chromite $\text{Fe}^{+2}\text{Cr}_2\text{O}_4$ **Page 178**

No: H

H) Is there a Calcium peak?

Yes:

Dolomite $\text{CaMg}(\text{CO}_3)_2$ **Page 206**

Ankerite $\text{Ca}(\text{Mg}, \text{Fe}^{+2}, \text{Mn})(\text{CO}_3)_2$ **Page 207**

Huntite $\text{Mg}_3\text{Ca}(\text{CO}_3)_4$ **N/A**

No: I

I) Is there a Titanium peak?

Yes:

Perovskite $(\text{Ca}, \text{Na}, \text{Fe}^{+2}, \text{Ce})(\text{Ti}, \text{Nb})\text{O}_3$ **Page 169**

Ulvöspinel $\text{Fe}^{+2}_2\text{TiO}_4$ **N/A**

No: J

J) Is there an Iron peak?

Yes:

Magnesioferrite $\text{MgFe}^{+3}_2\text{O}_4$ **Page 172**

Franklinite $\text{ZnFe}^{+3}_2\text{O}_4$ **Page 175**

Jacobsite $\text{MnFe}^{+3}_2\text{O}_4$ **N/A**

Tevorite $\text{NiFe}^{+3}_2\text{O}_4$ **Page 176**

No:

Halides:

NaCl **Pages 217, 218**

Sylvite KCl **Page 219**

Chapter 4

THE SPECTRA

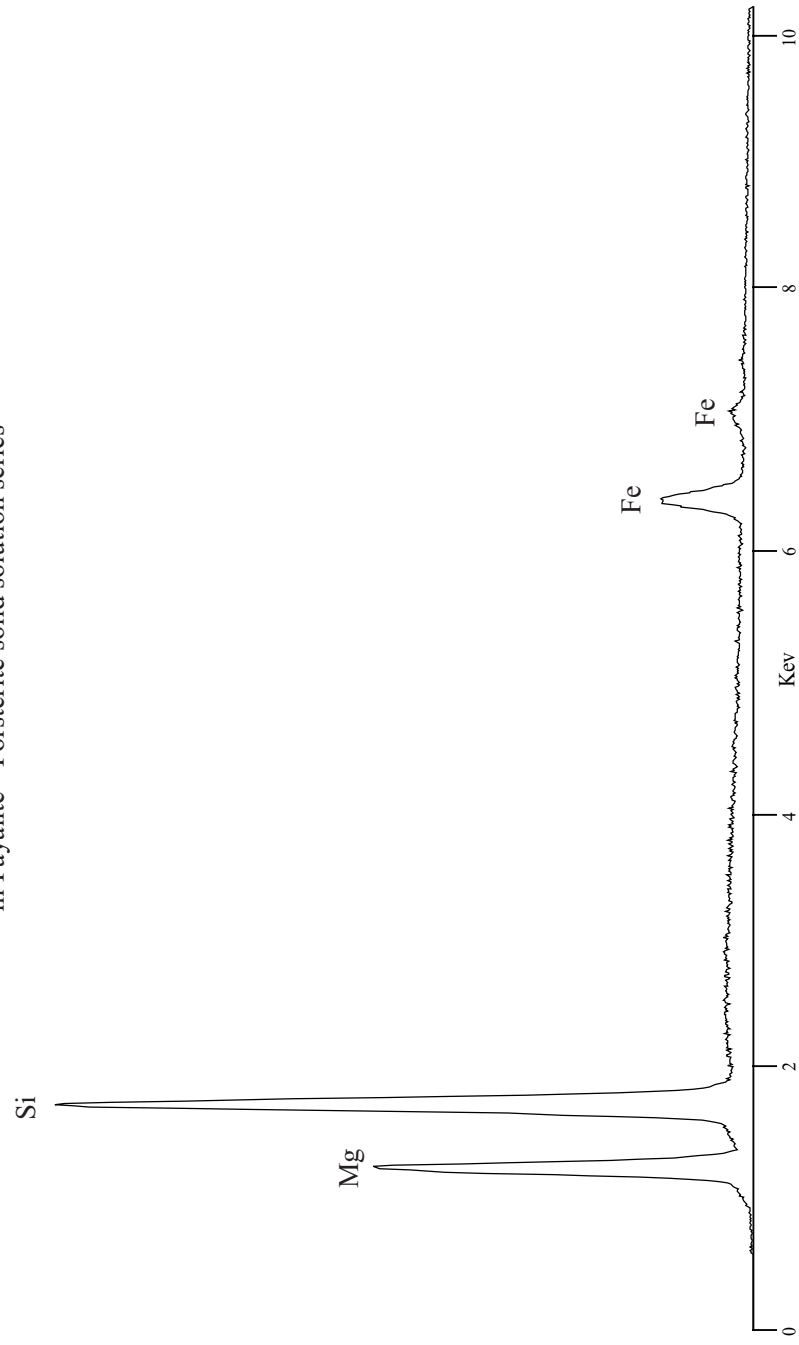
Most of the spectra were obtained from naturally occurring minerals and as a result often show elements that are not present in their chemical formulæ. In cases where the mineral is a member of a solid solution series the spectrum is labeled as being "end member rich," e.g. Pyrope rich Garnet (page 49) although the end member formula is given. The microscopist can estimate the approximate pyrope percentage based on relative Mg, Ca, and Fe peak heights.

Because of the difference in sensitivities between EDS detectors, it may be useful to compare spectra taken from known samples such as the Smithsonian Institution's mineral standards. Unless otherwise noted spectra were collected using a 15 keV accelerating voltage.

Most of these spectra were obtained using a detector with a beryllium window, so no carbon or oxygen peaks were recorded. In cases where several different minerals produce the same spectra, this is noted.

Olivine $(\text{Mg,Fe})_2[\text{SiO}_4]$

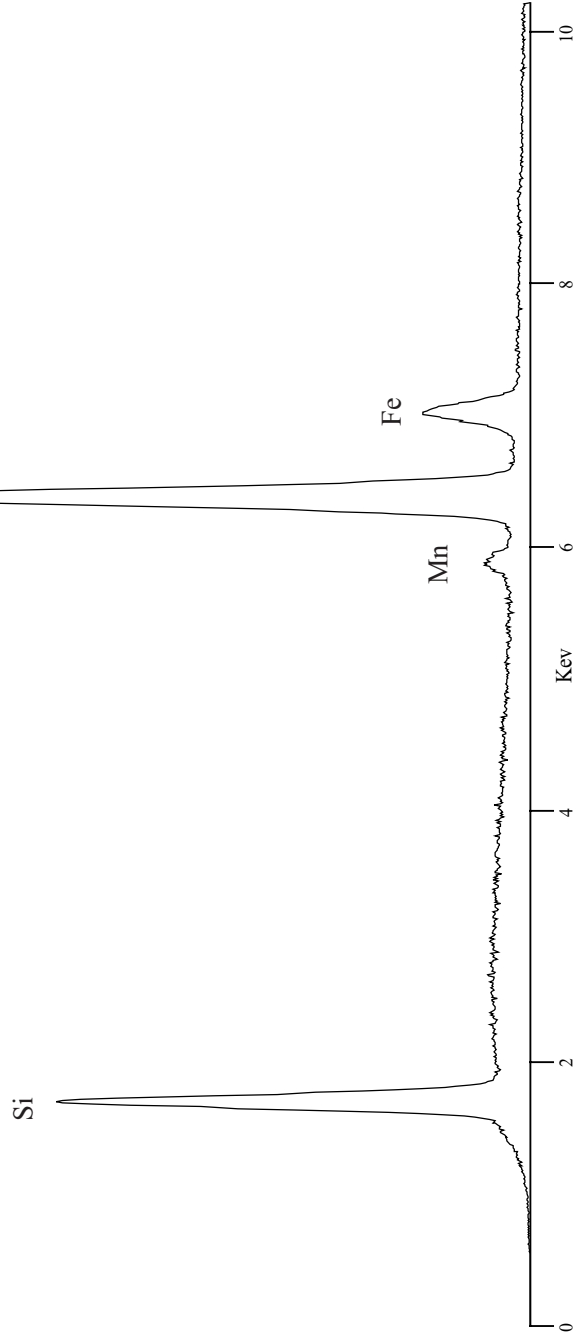
in Fayalite - Forsterite solid solution series



Smithsonian Standard
USNM 2566
Composition
SiO₂ 29.22
TiO₂ 0.04
MnO 2.14
FeO 67.53

Fayalite Fe₂[SiO₄]

Olivine in Fayalite - Forsterite solid solution series

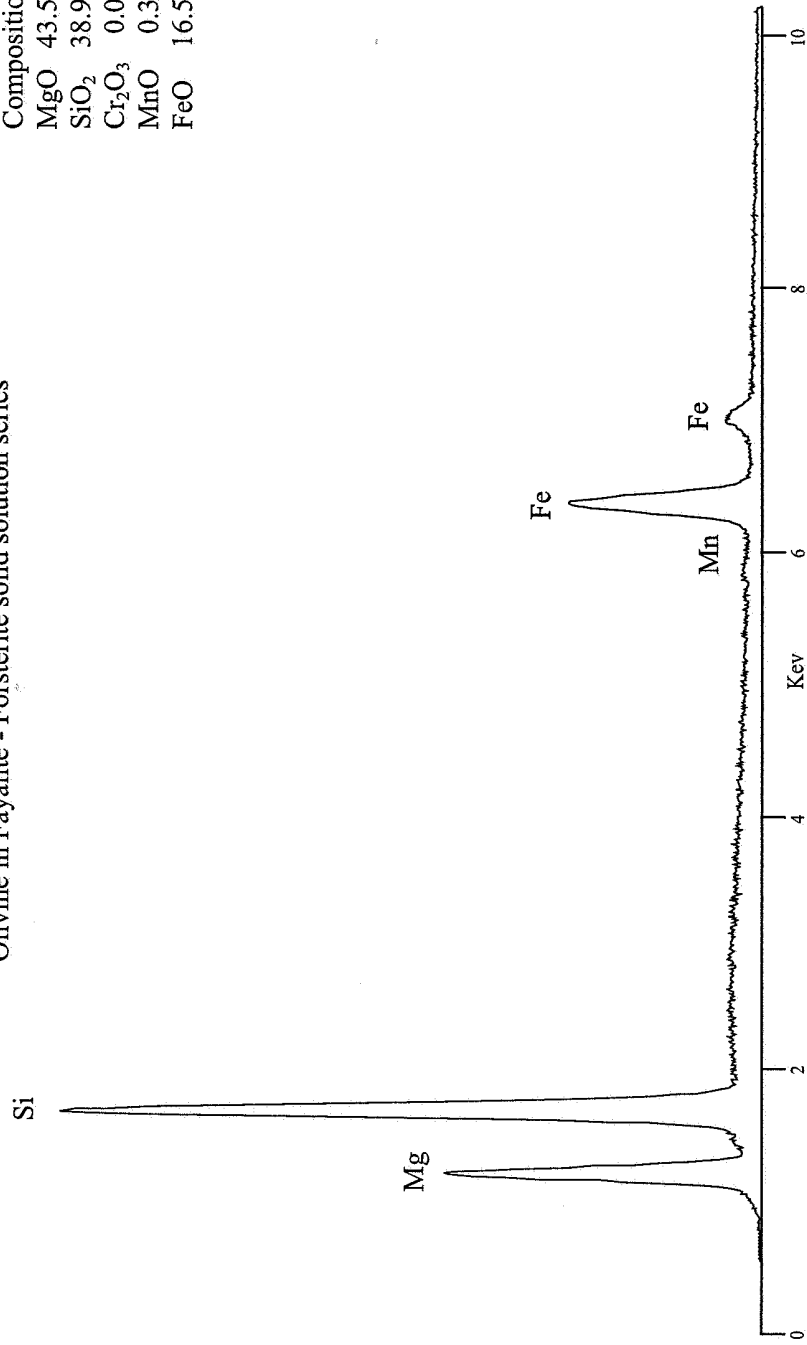


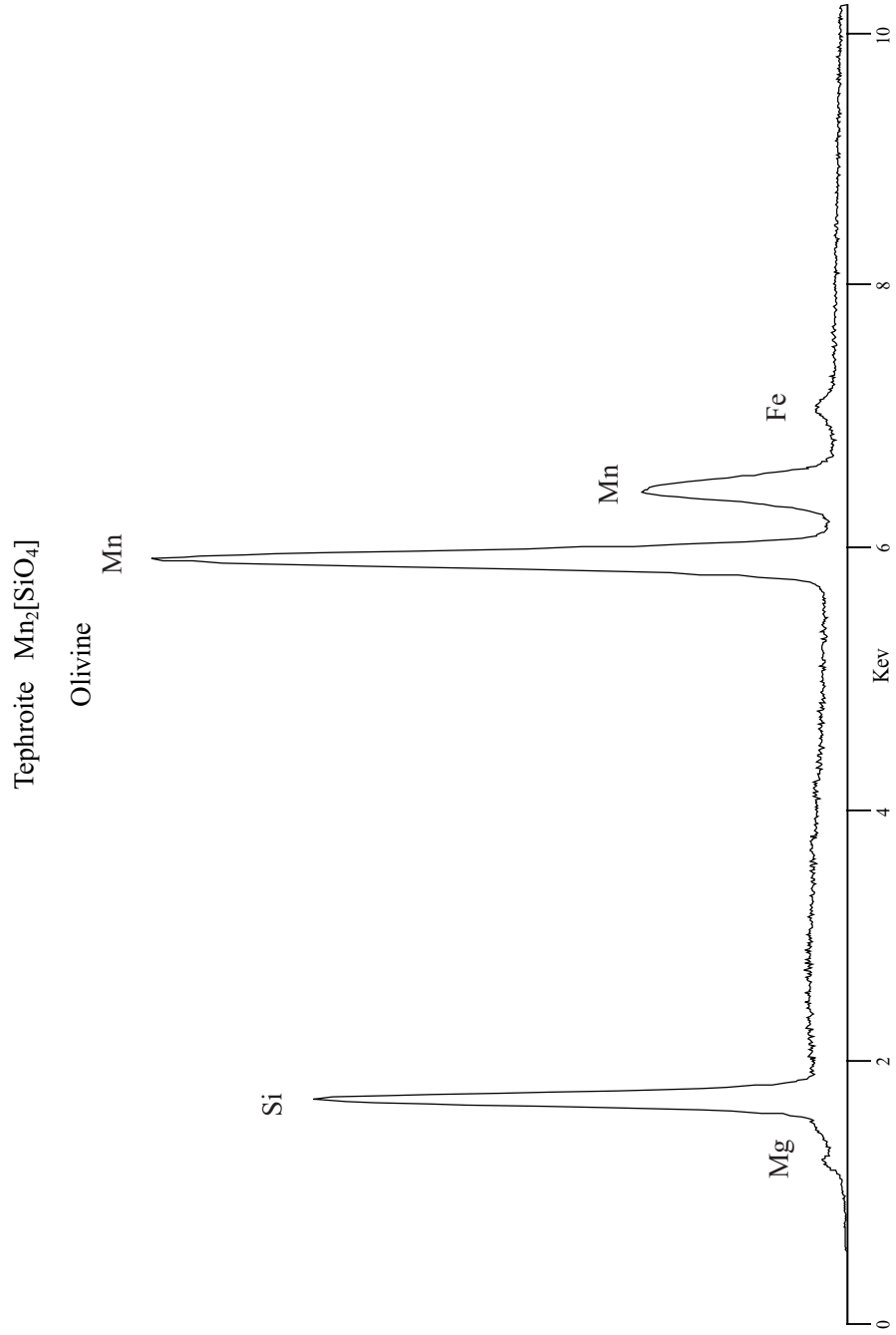
Smithsonian Standard
USNM 2566

Composition
MgO 43.58
SiO₂ 38.95
Cr₂O₃ 0.02
MnO 0.30
FeO 16.52

Forsterite (Fo₈₃) (Mg,Fe)₂[SiO₄]

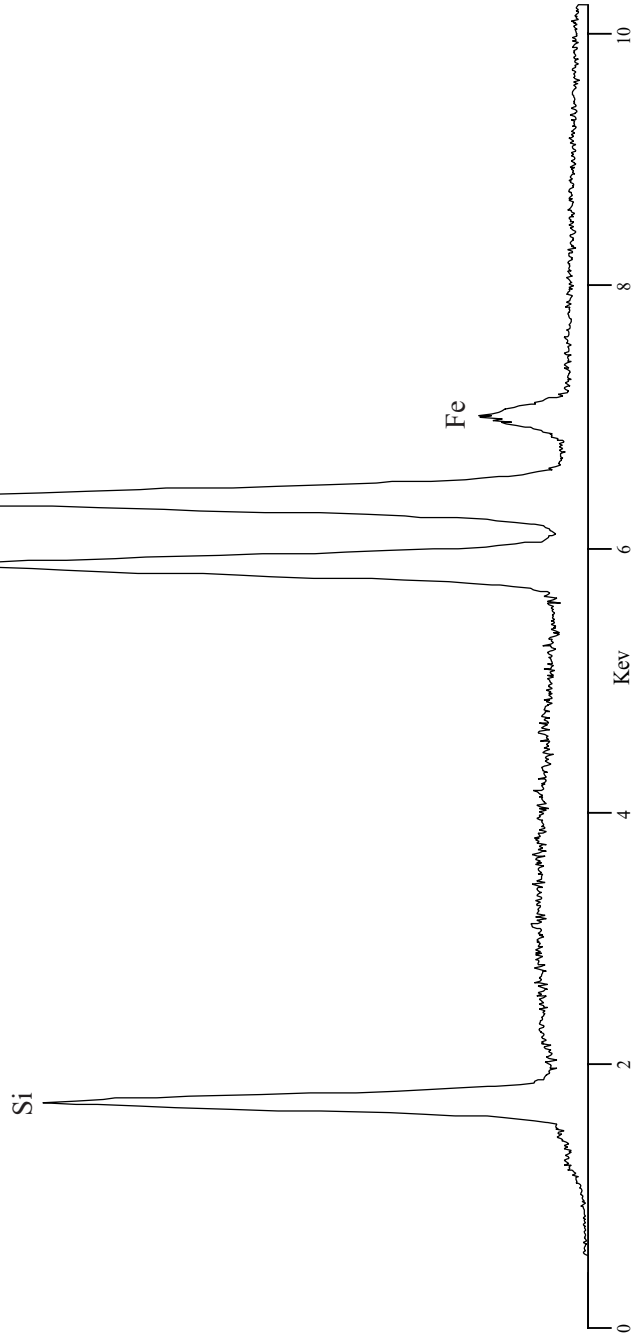
Olivine in Fayalite - Forsterite solid solution series



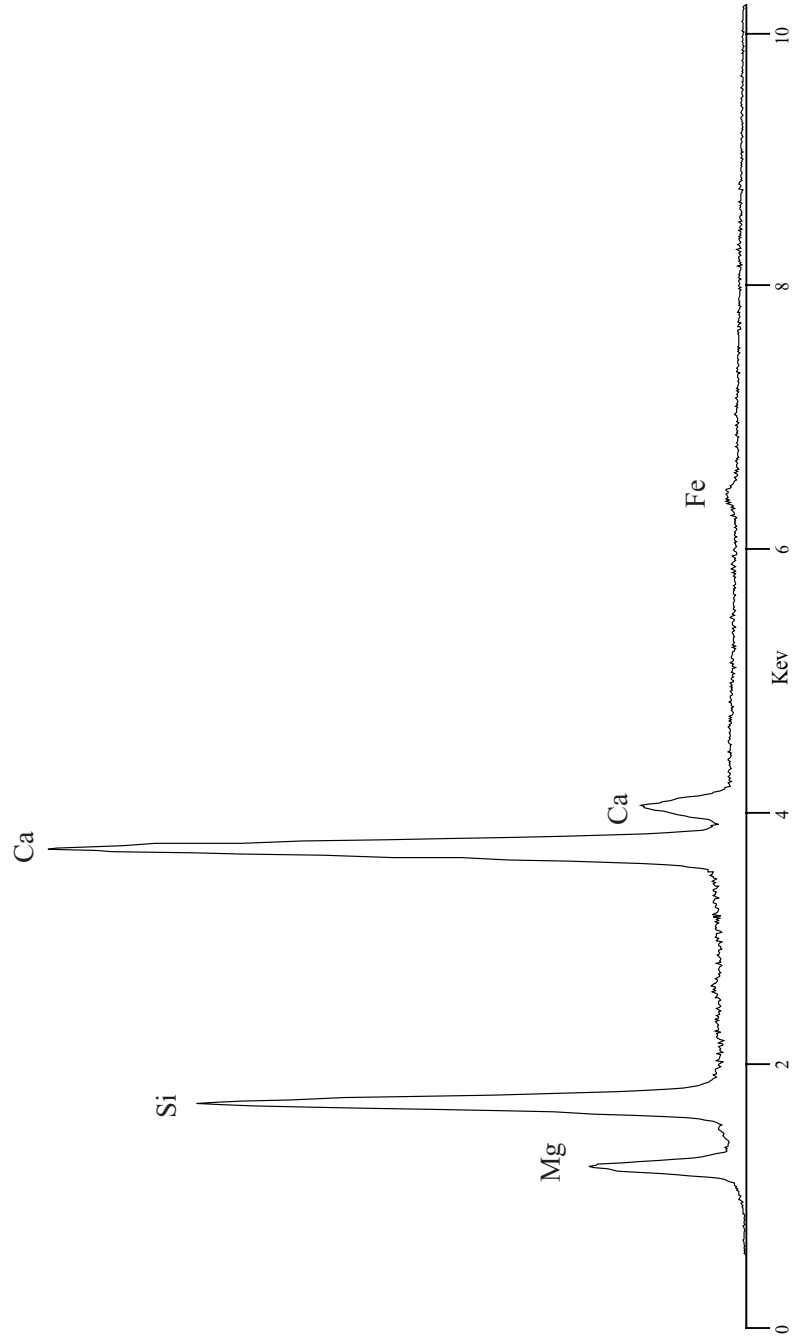


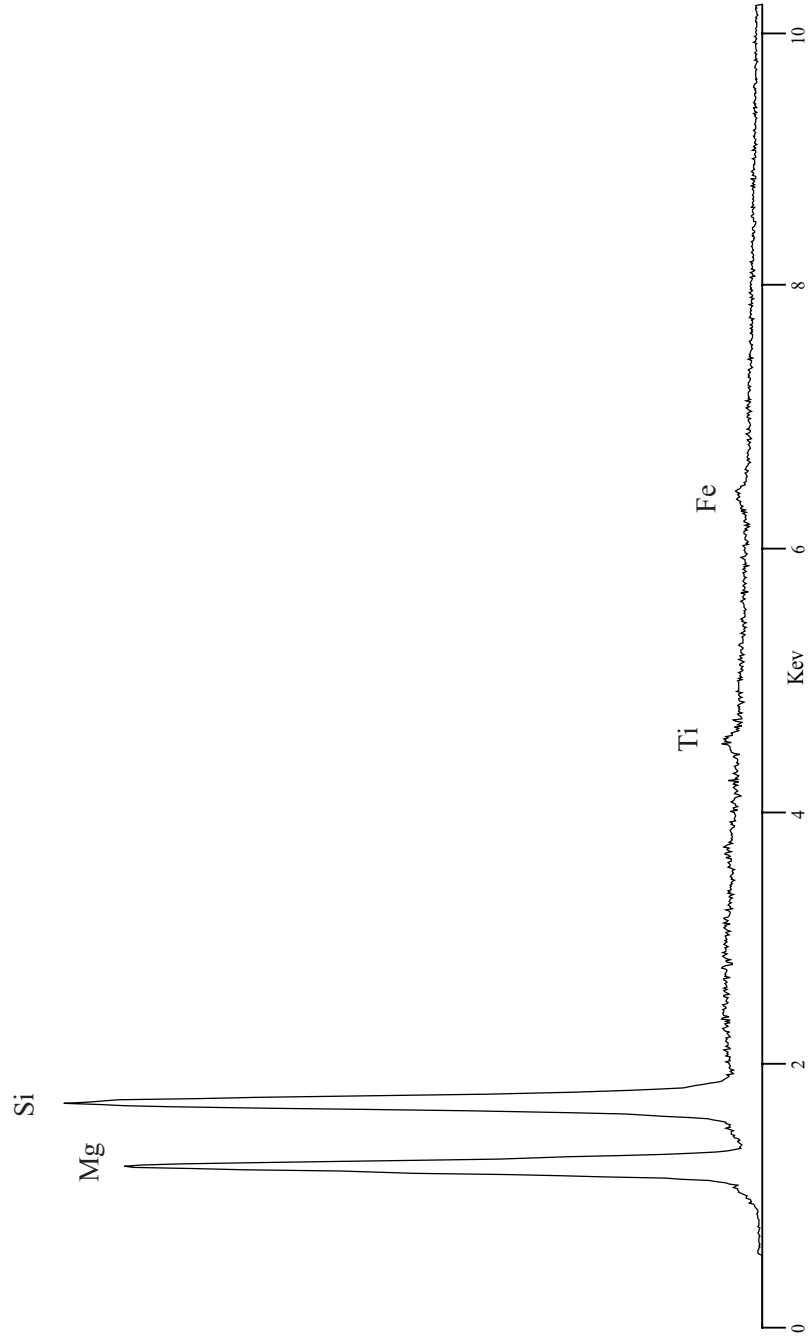
Knebelite $(\text{Mn,Fe})_2[\text{SiO}_4]$

Olivine

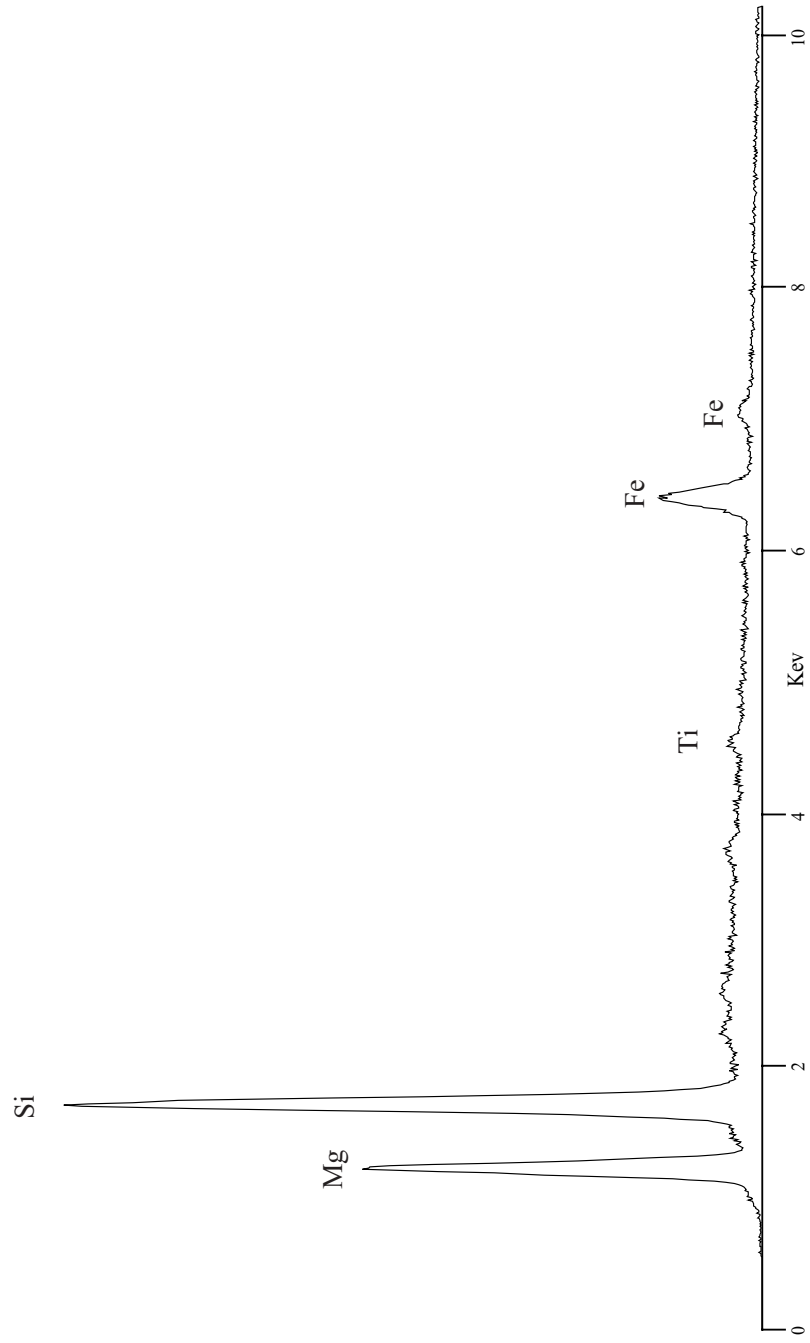


Monticellite $\text{CaMg}[\text{SiO}_4]$

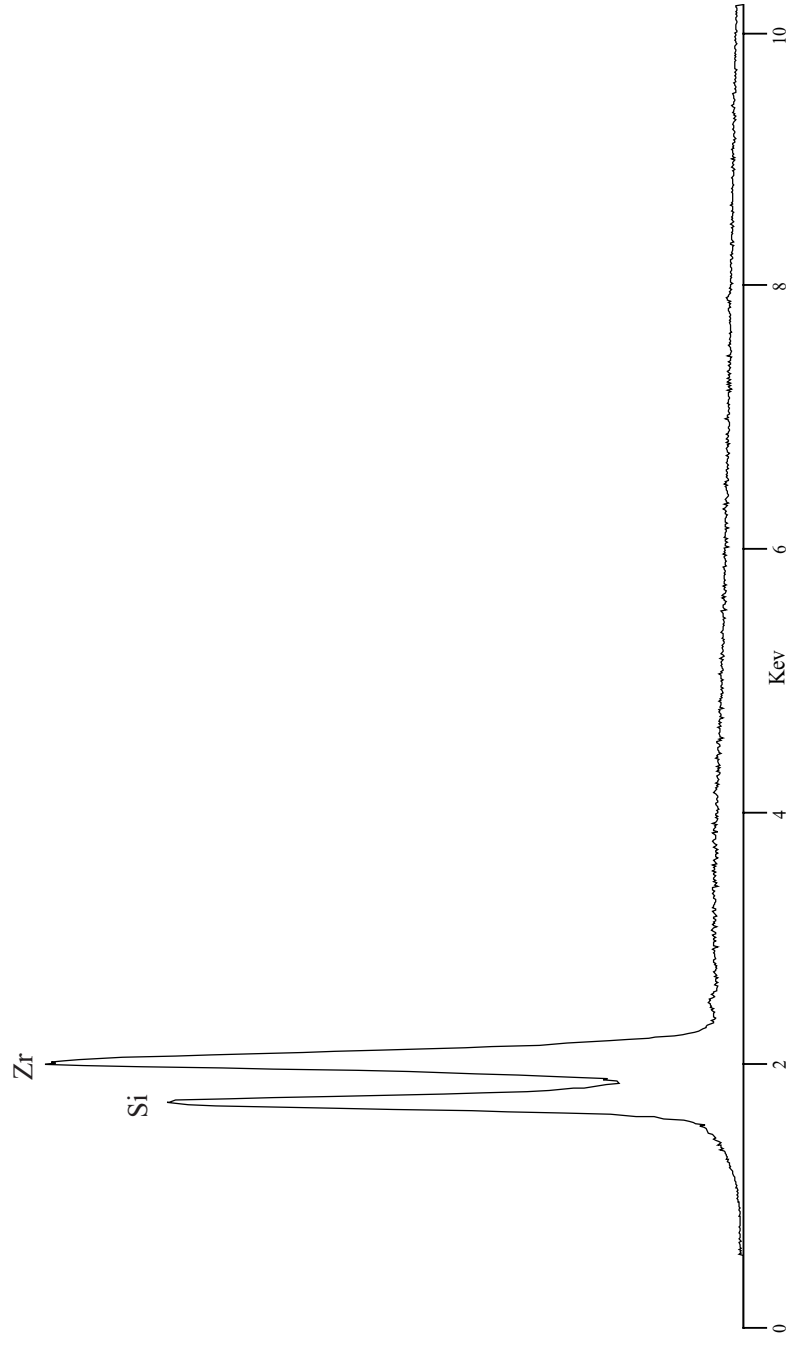


Norbergite $\text{Mg}(\text{OH},\text{F})_2 \cdot \text{Mg}_2\text{SiO}_4$ 

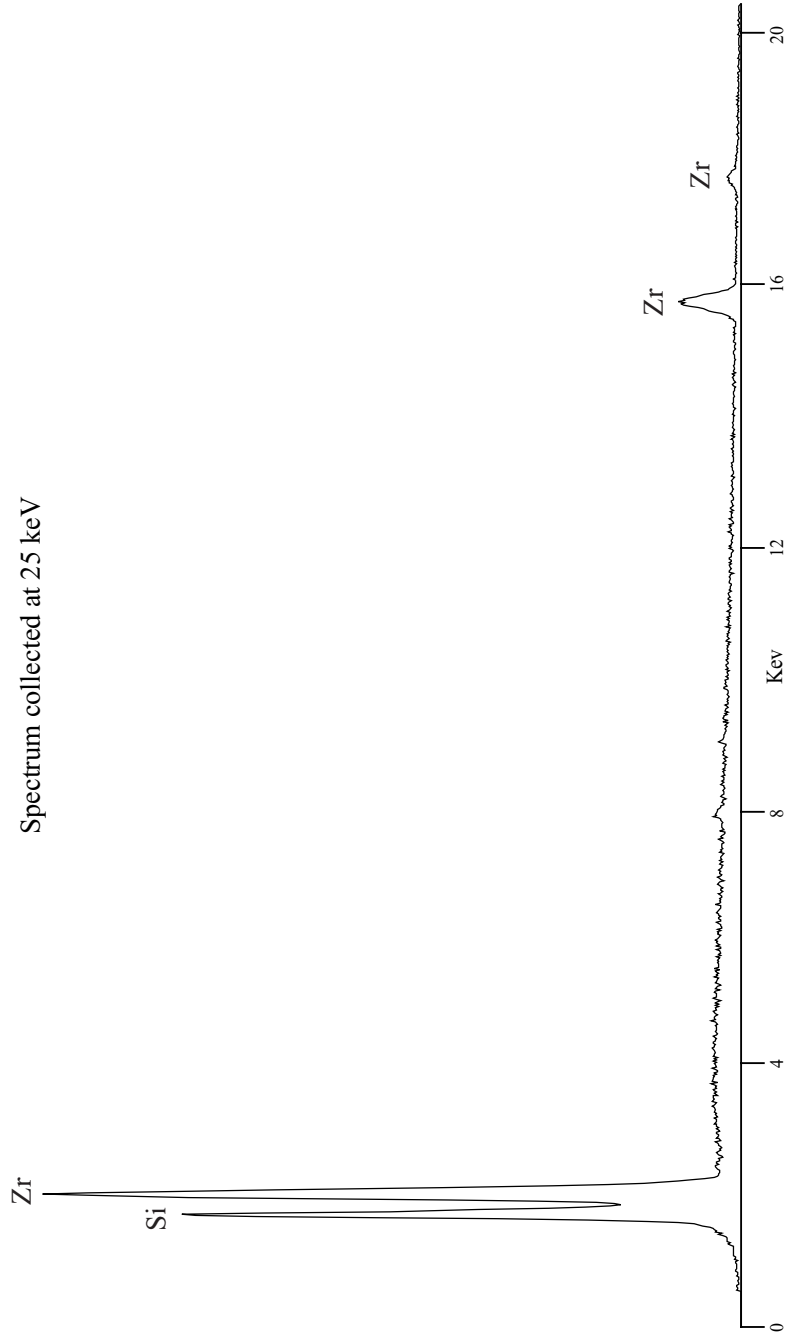
Chondrodite $\text{Mg}(\text{OH},\text{F})_2 \cdot 2\text{Mg}_2\text{SiO}_4$

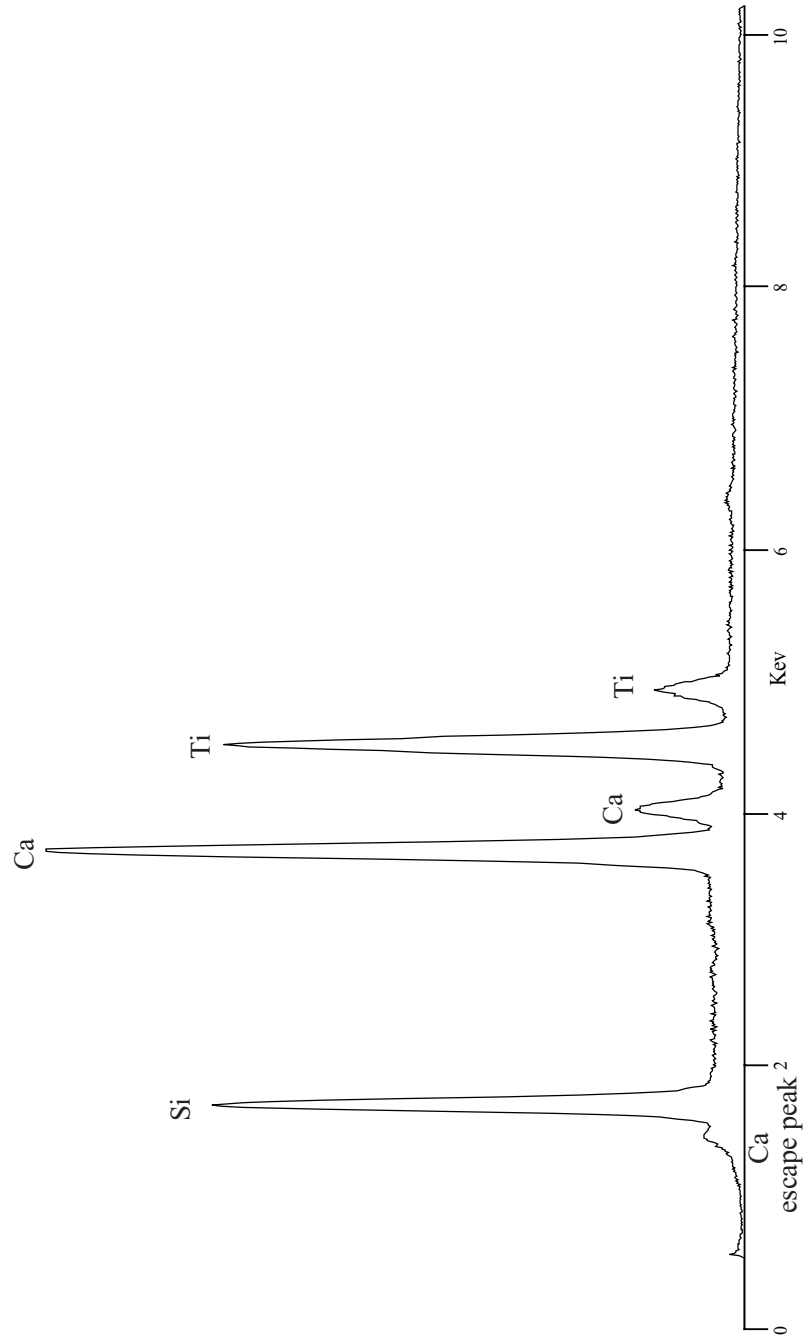


Zircon $Zr[SiO_4]$



Zircon $Zr[SiO_4]$
Spectrum collected at 25 keV



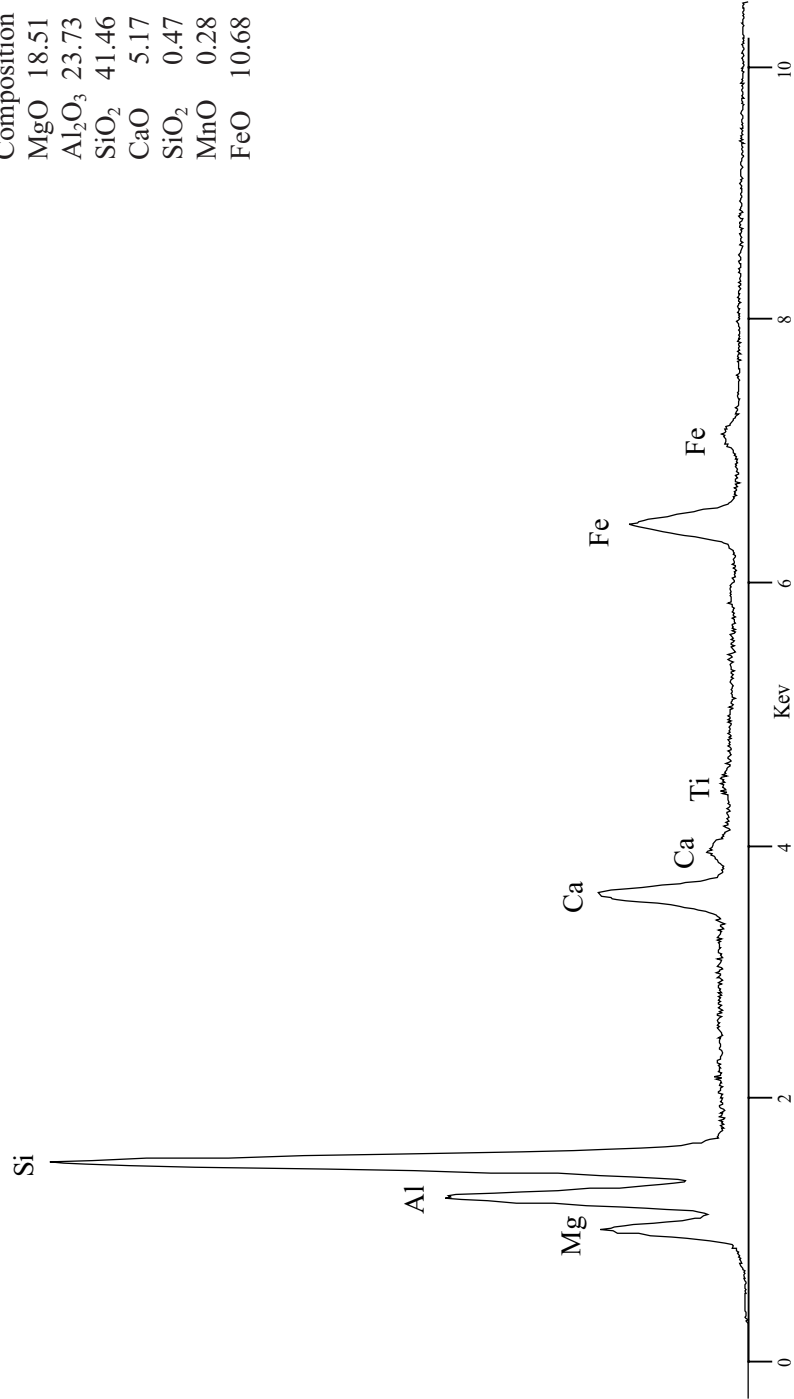
Sphene $\text{CaTi}[\text{SiO}_4](\text{O},\text{OH},\text{F})$ 

Pyrope Garnet $Mg_3Al_2Si_3O_{12}$

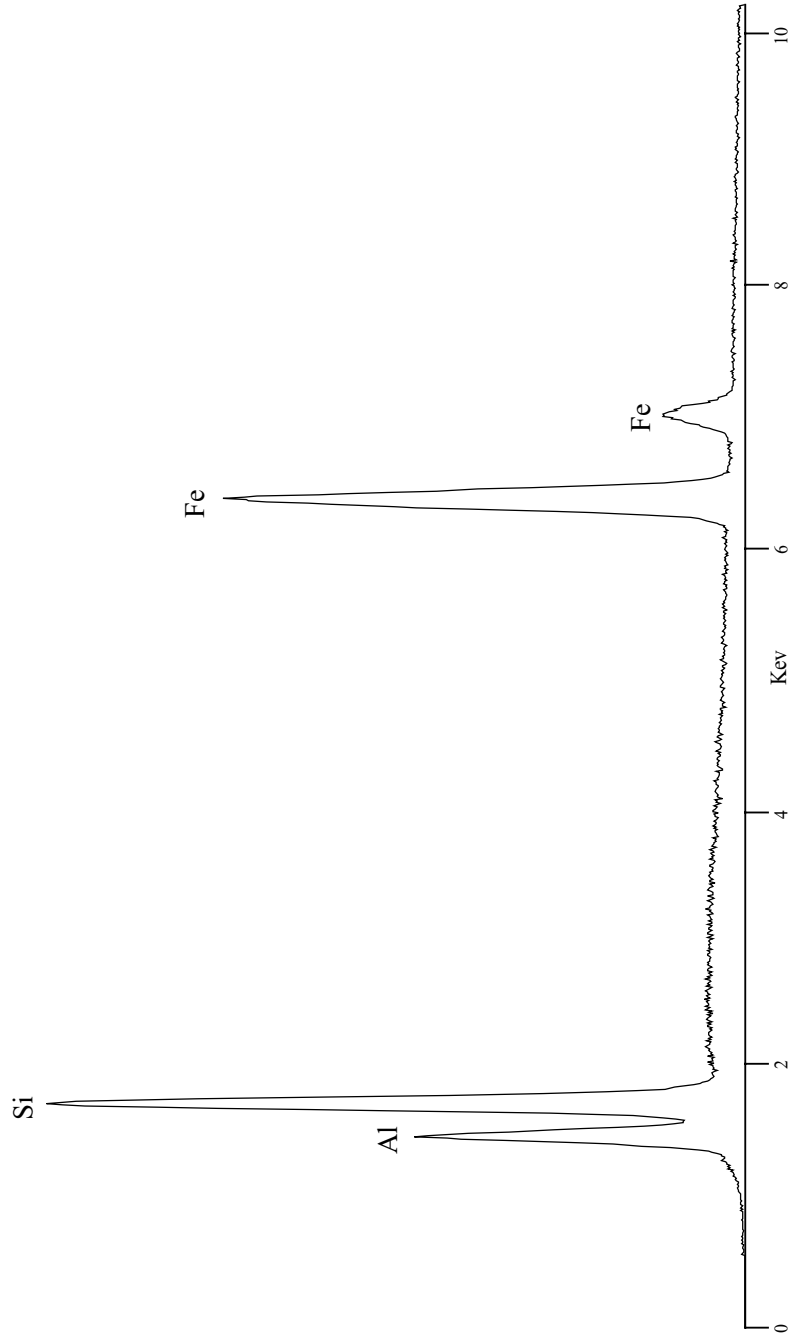
Smithsonian Standard
USNM 143968

Composition

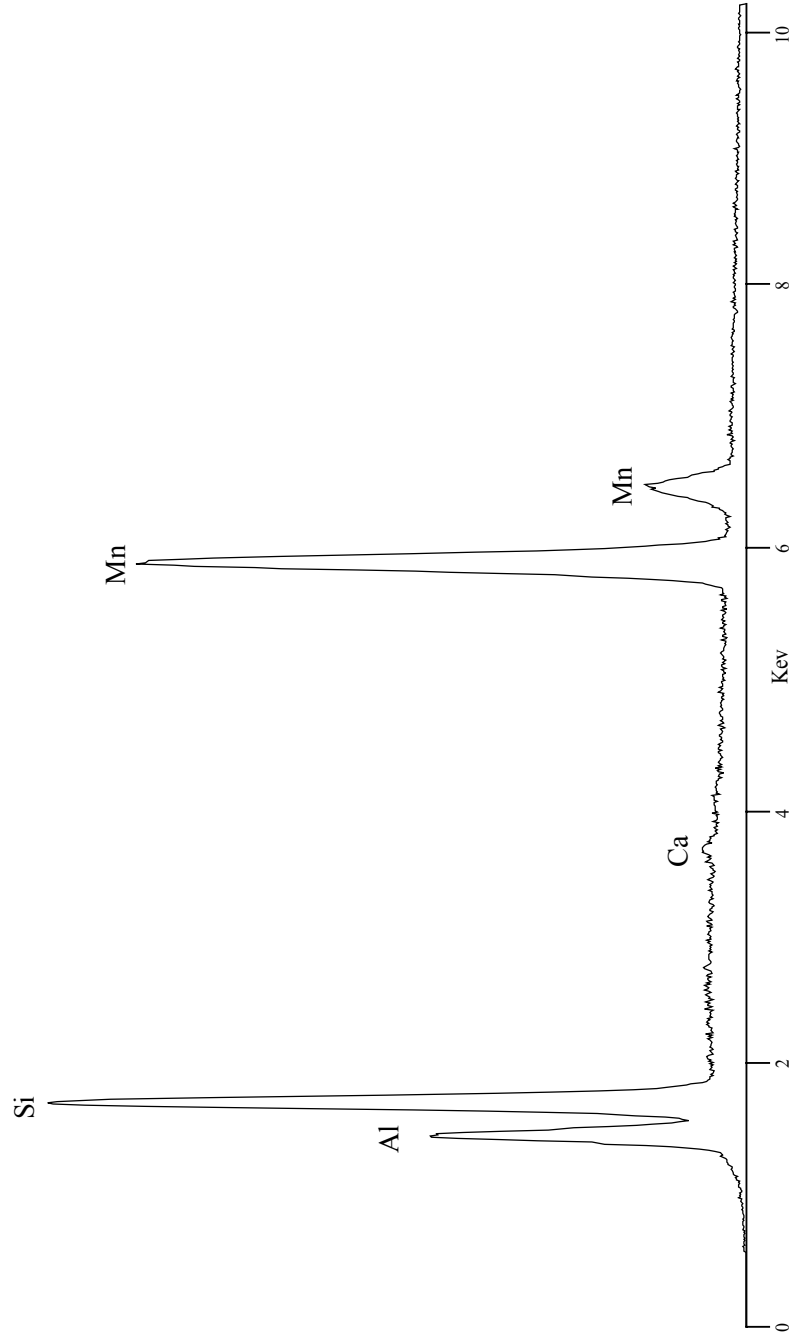
MgO	18.51
Al ₂ O ₃	23.73
SiO ₂	41.46
CaO	5.17
SiO ₂	0.47
MnO	0.28
FeO	10.68

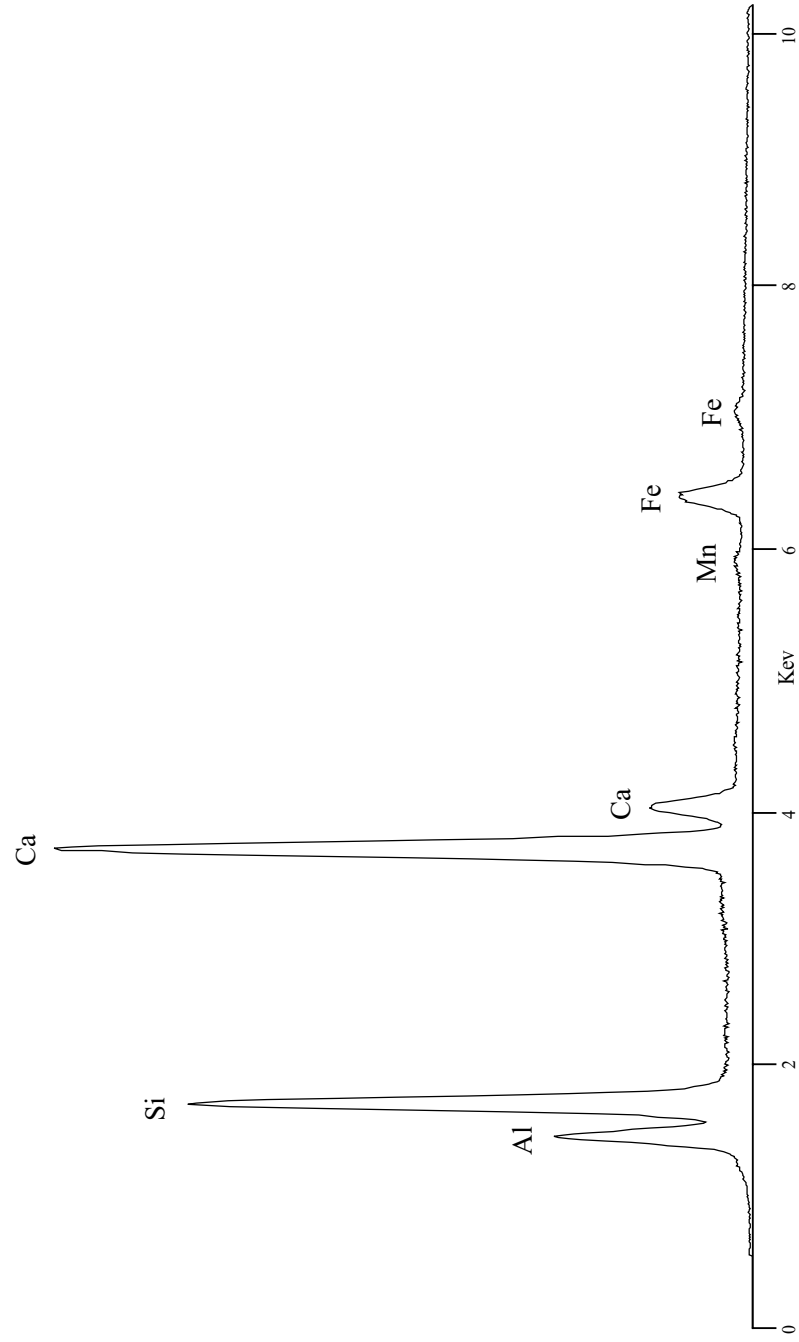


Almandine Garnet $\text{Fe}_3^{+2}\text{Al}_2\text{Si}_3\text{O}_{12}$

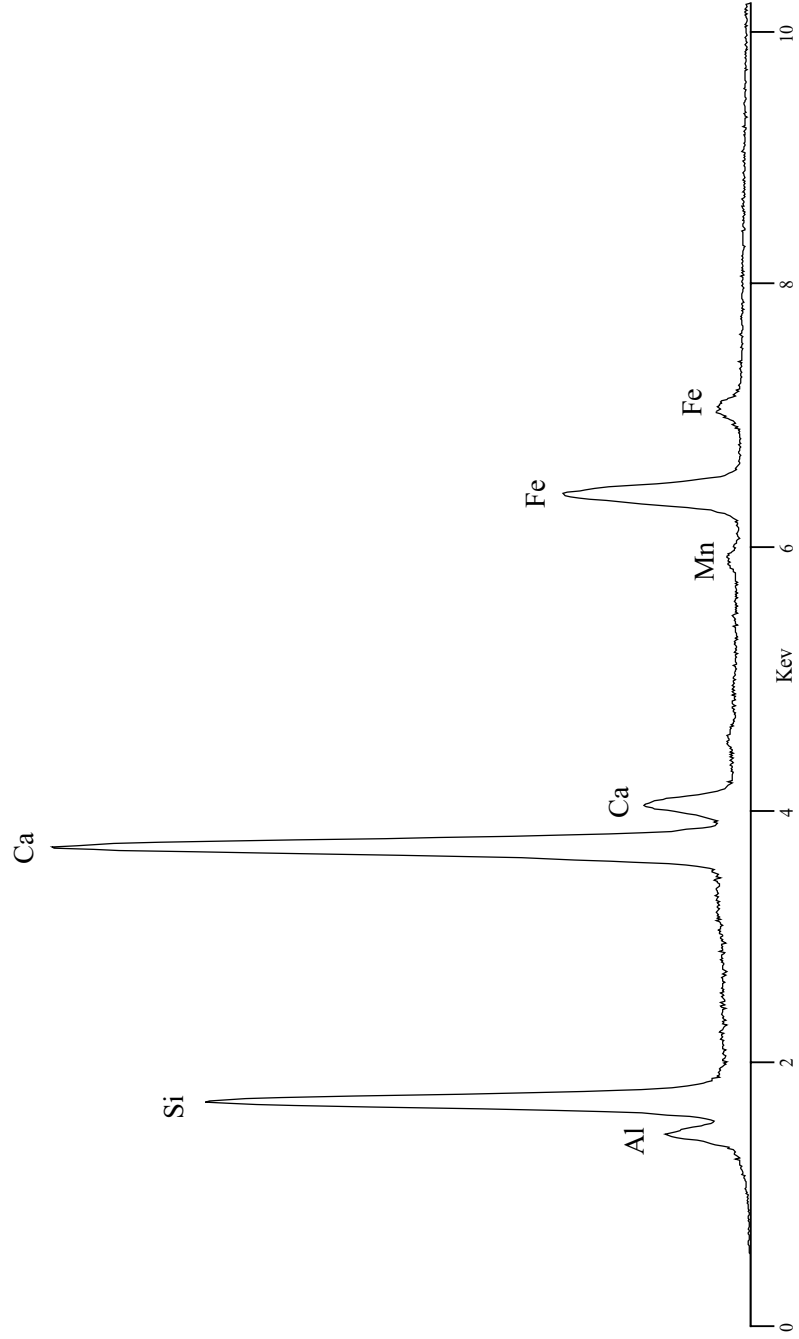


Spessartine Garnet $\text{Mn}_3\text{Al}_2\text{Si}_3\text{O}_{12}$

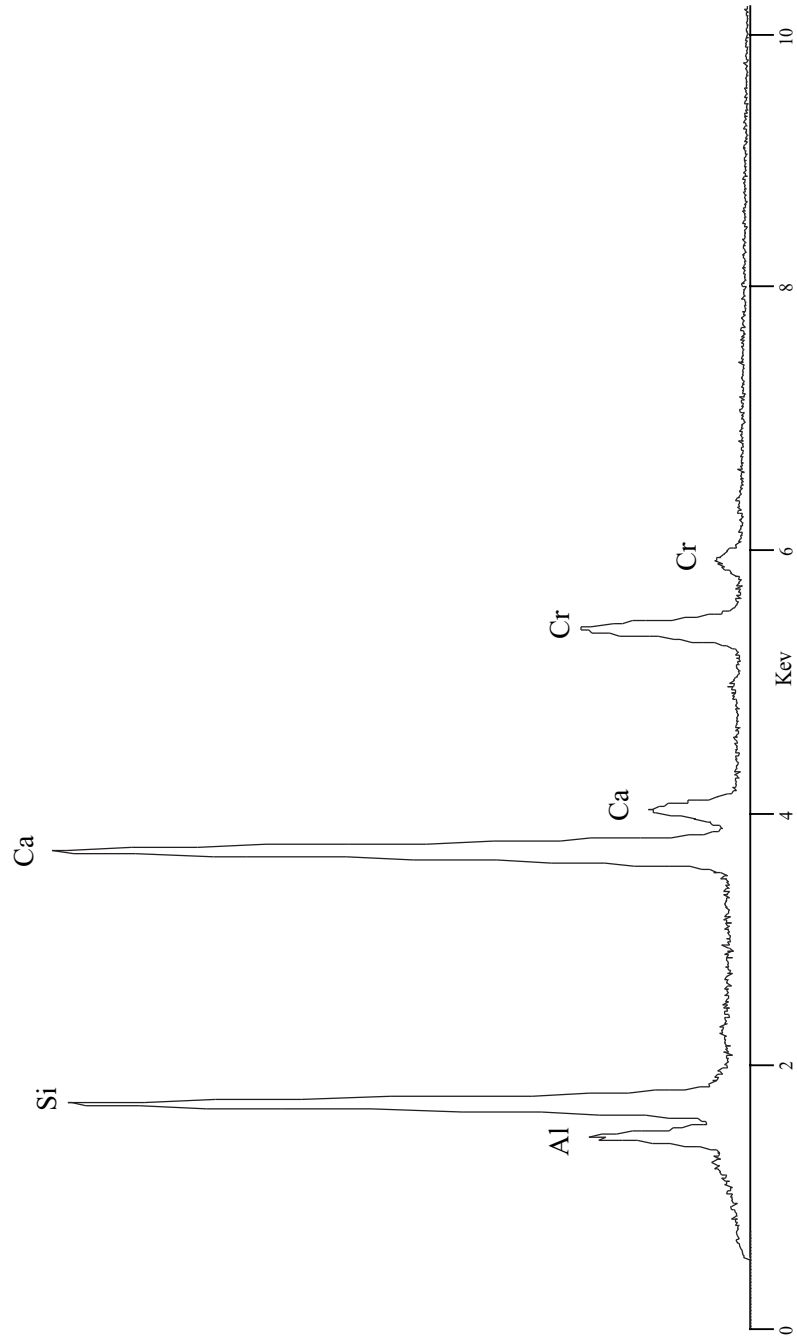


Grossular Garnet $\text{Ca}_3\text{Al}_2\text{Si}_3\text{O}_{12}$ 

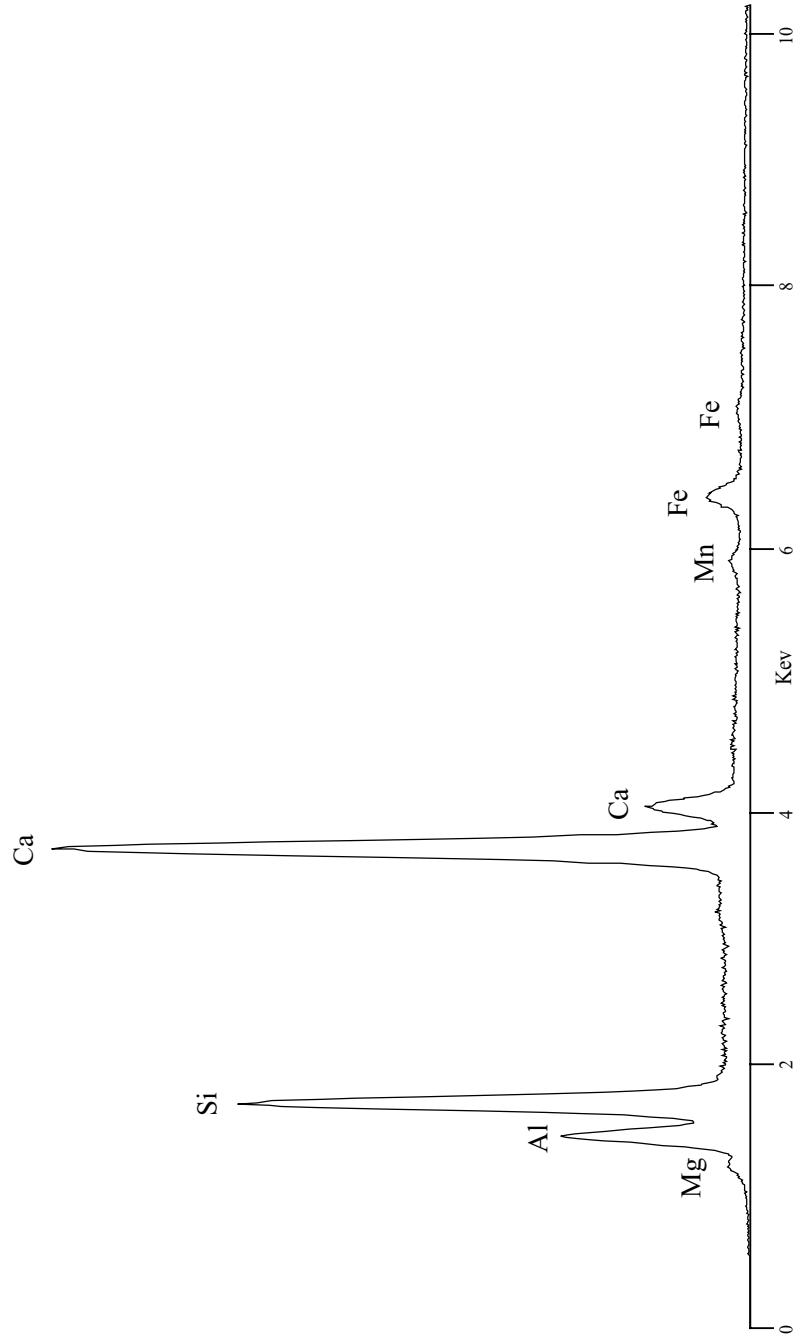
Andradite Garnet $\text{Ca}_3(\text{Fe}^{+3}, \text{Ti})_2\text{Si}_3\text{O}_{12}$



Uvarovite Garnet $\text{Ca}_3\text{Cr}_2\text{Si}_3\text{O}_{12}$

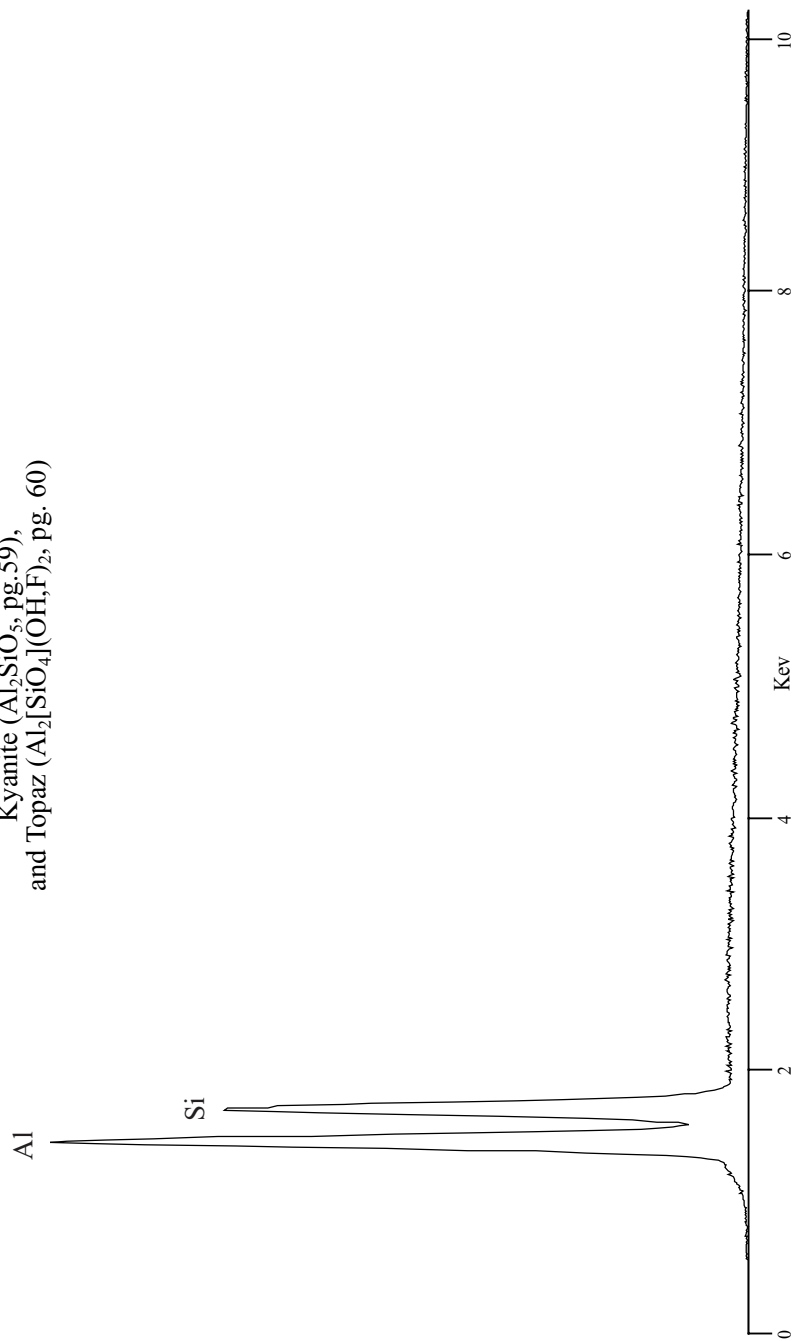


Vesuvianite (Idocrase) $\text{Ca}_{10}(\text{Mg,Fe})_2\text{Al}_4[\text{Si}_2\text{O}_7]_2[\text{SiO}_4]_5(\text{OH,F})_4$

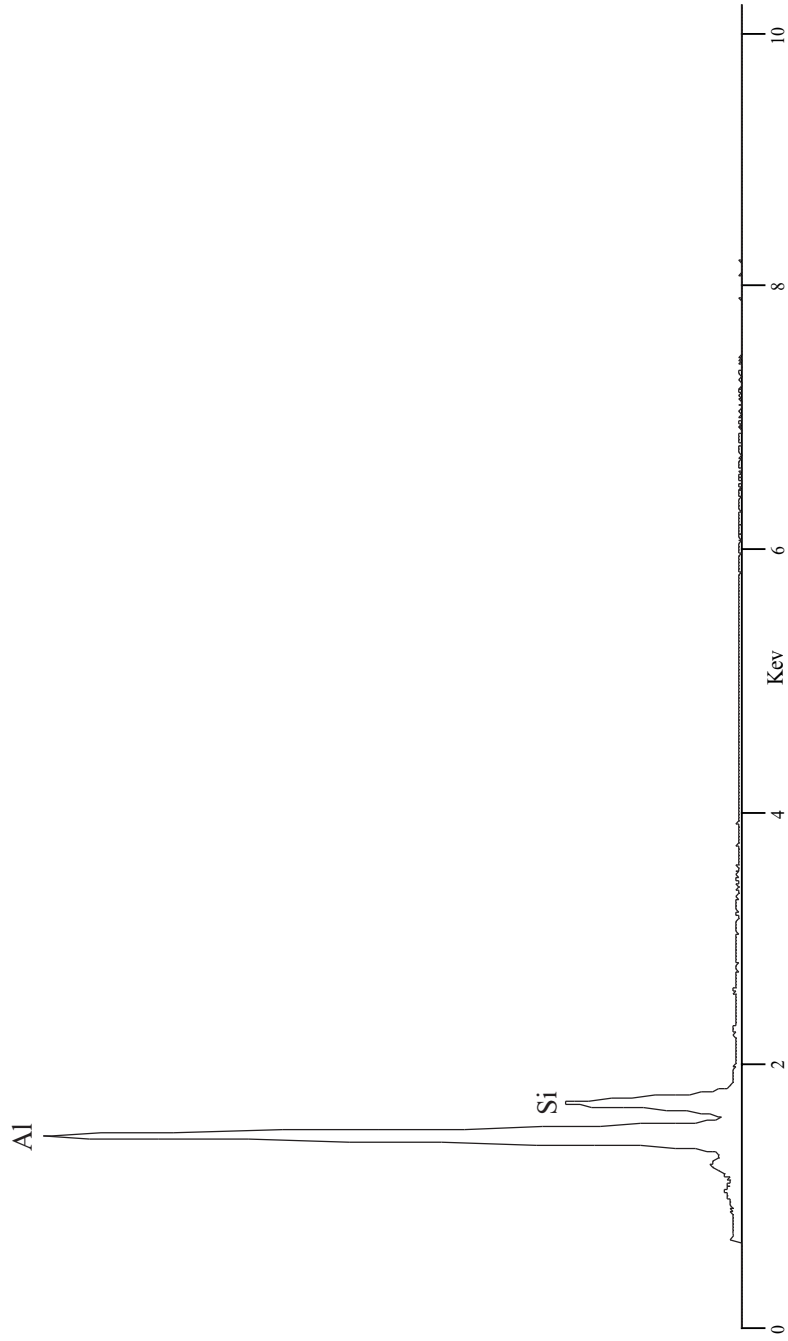


Sillimanite Al_2SiO_5

see also Andalusite (Al_2SiO_5 , pg. 58),
Kyanite (Al_2SiO_5 , pg. 59),
and Topaz ($\text{Al}_2[\text{SiO}_4](\text{OH},\text{F})_2$, pg. 60)

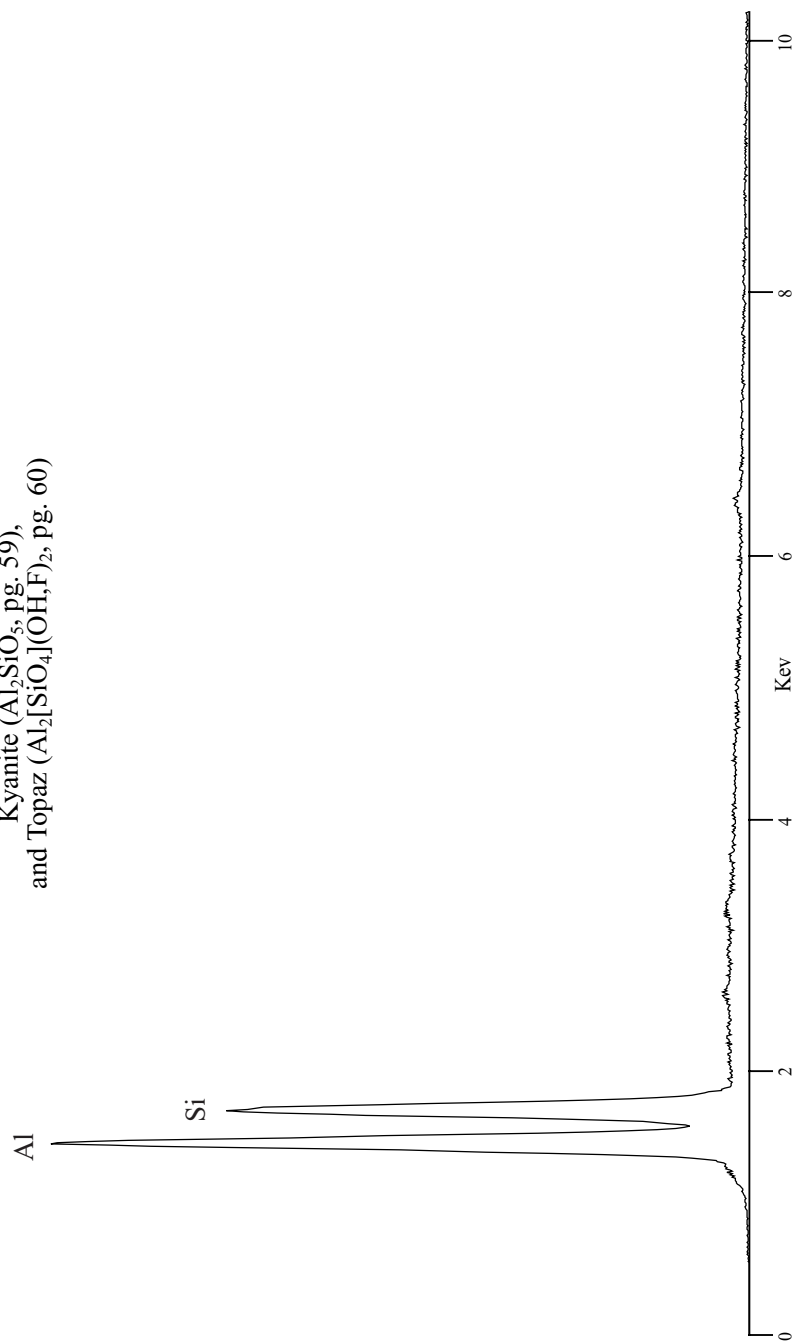


Mullite $3\text{Al}_2\text{O}_3 \cdot 2\text{SiO}_2$



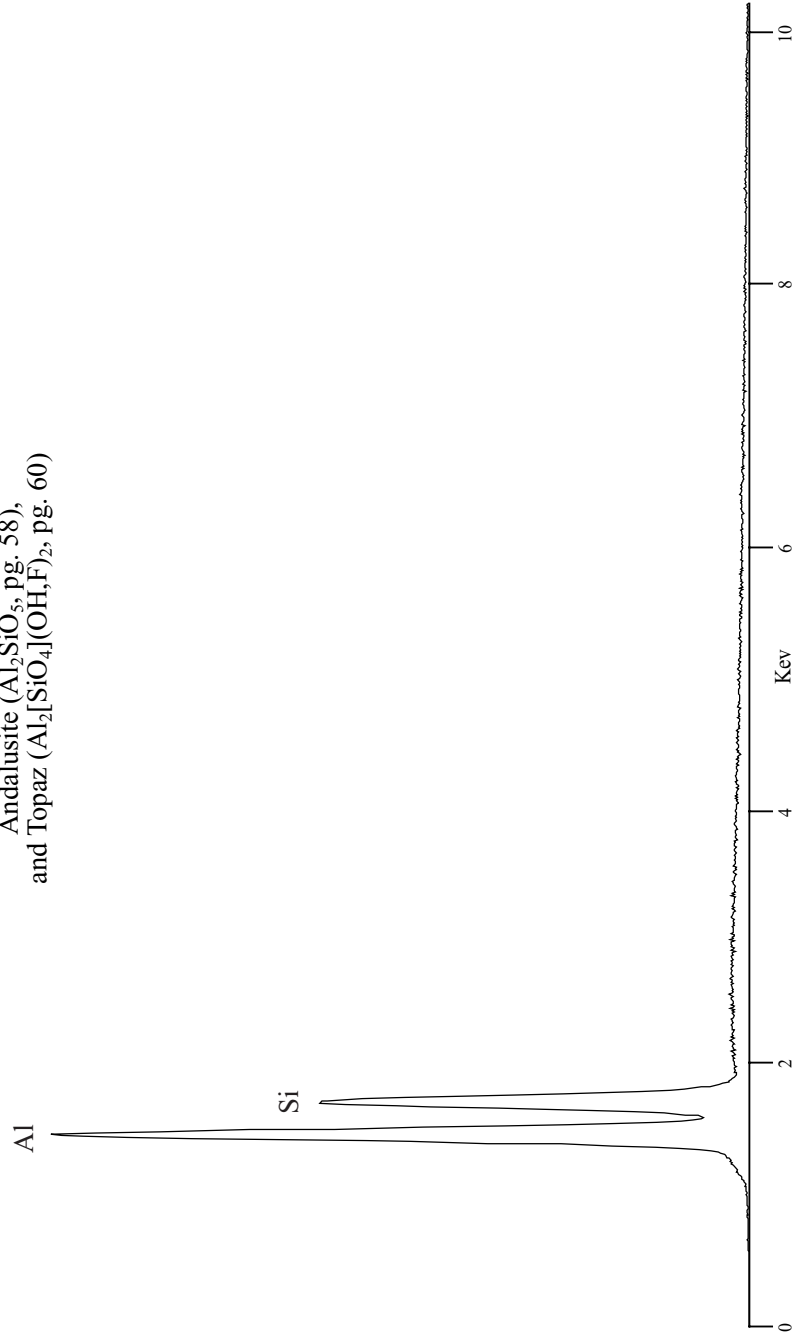
Andalusite Al_2SiO_5

see also Sillimanite (Al_2SiO_5 , pg. 56),
Kyanite (Al_2SiO_5 , pg. 59),
and Topaz ($\text{Al}_2[\text{SiO}_4](\text{OH},\text{F})_2$, pg. 60)



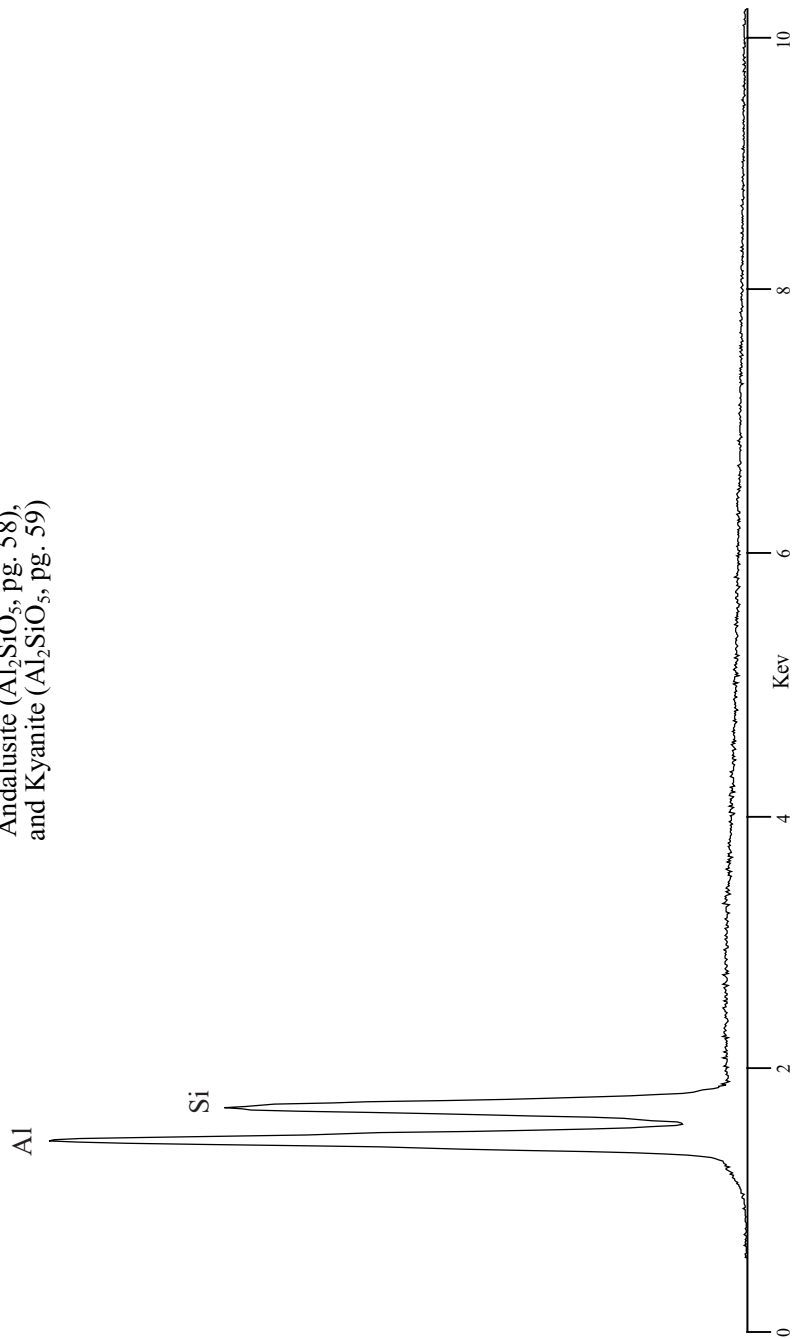
Kyanite Al_2SiO_5

see also Sillimanite (Al_2SiO_5 , pg. 56),
Andalusite (Al_2SiO_5 , pg. 58),
and Topaz ($\text{Al}_2[\text{SiO}_4](\text{OH},\text{F})_2$, pg. 60)

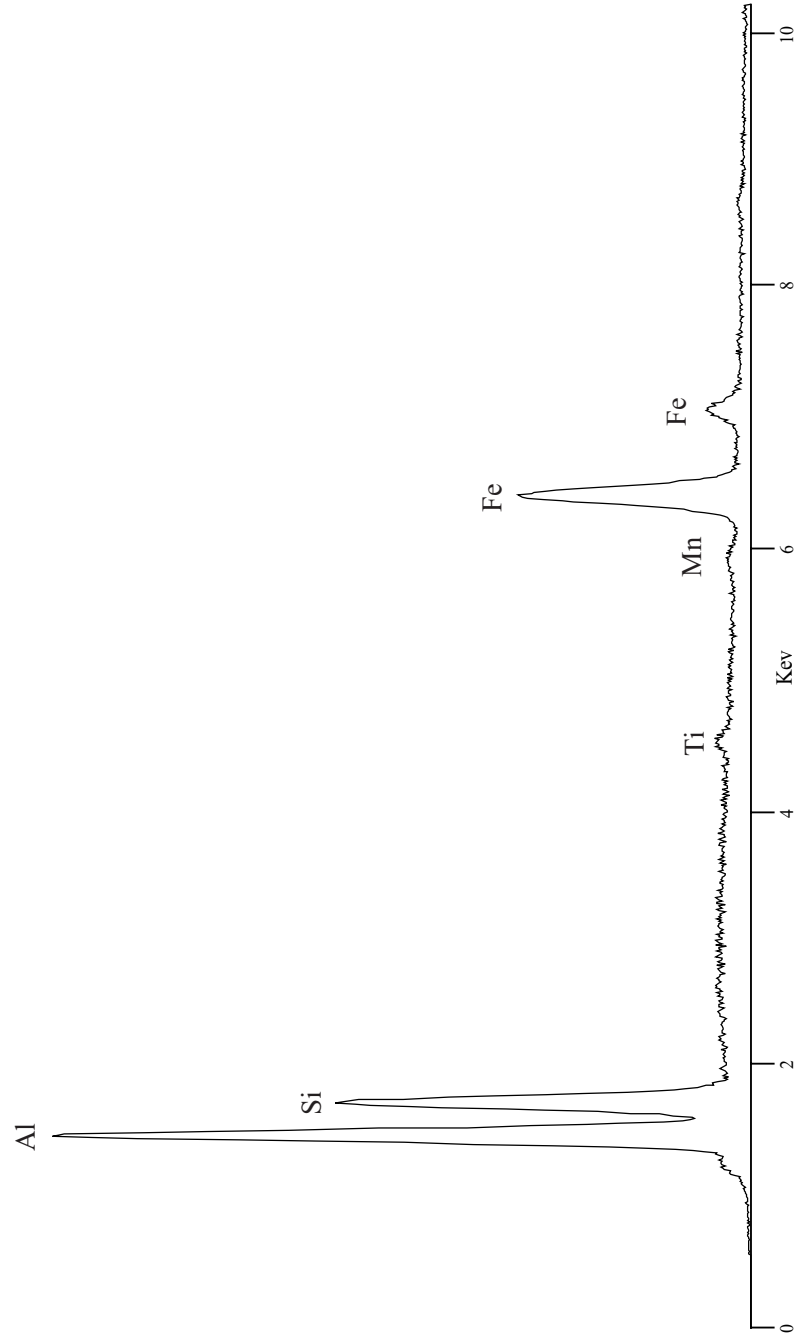


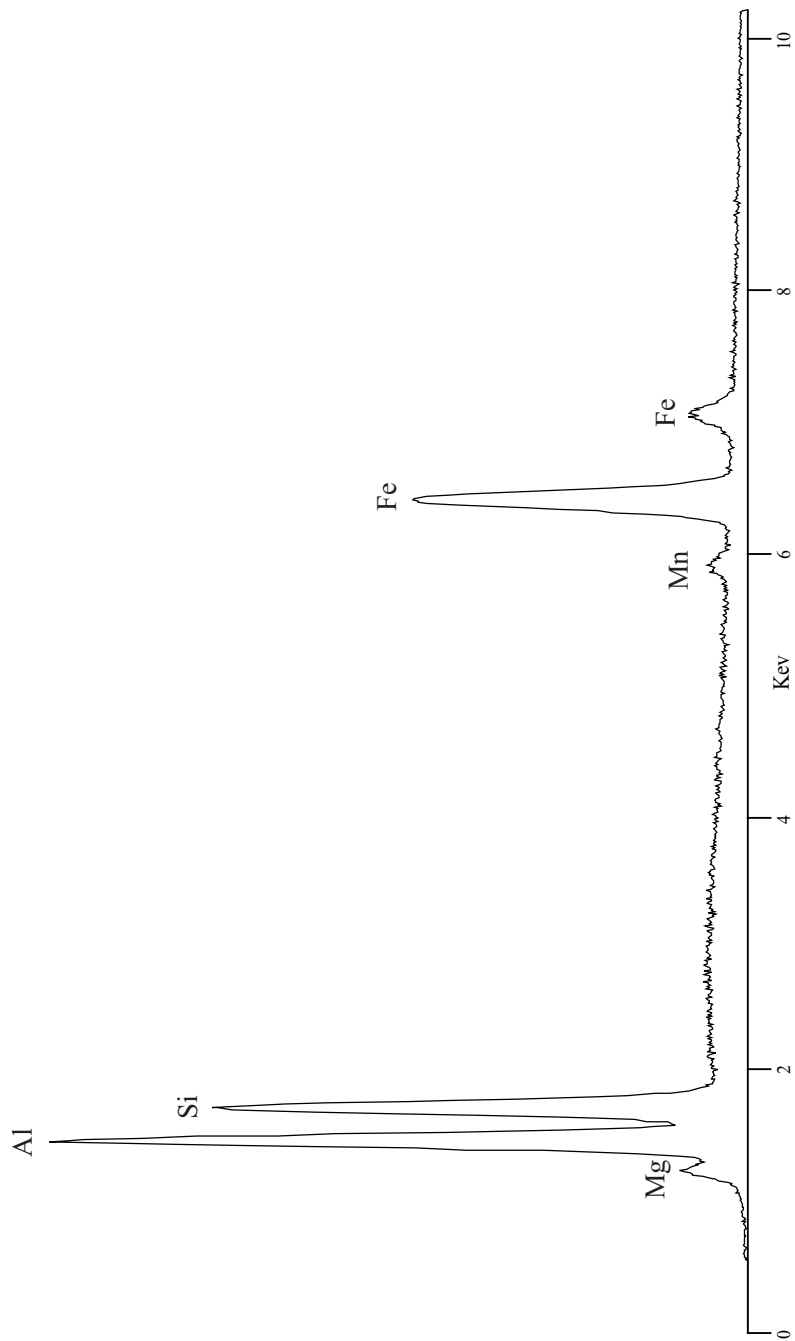
Topaz $\text{Al}_2[\text{SiO}_4](\text{OH},\text{F})_2$

see also Sillimanite (Al_2SiO_5 , pg. 56),
Andalusite (Al_2SiO_5 , pg. 58),
and Kyanite (Al_2SiO_5 , pg. 59)

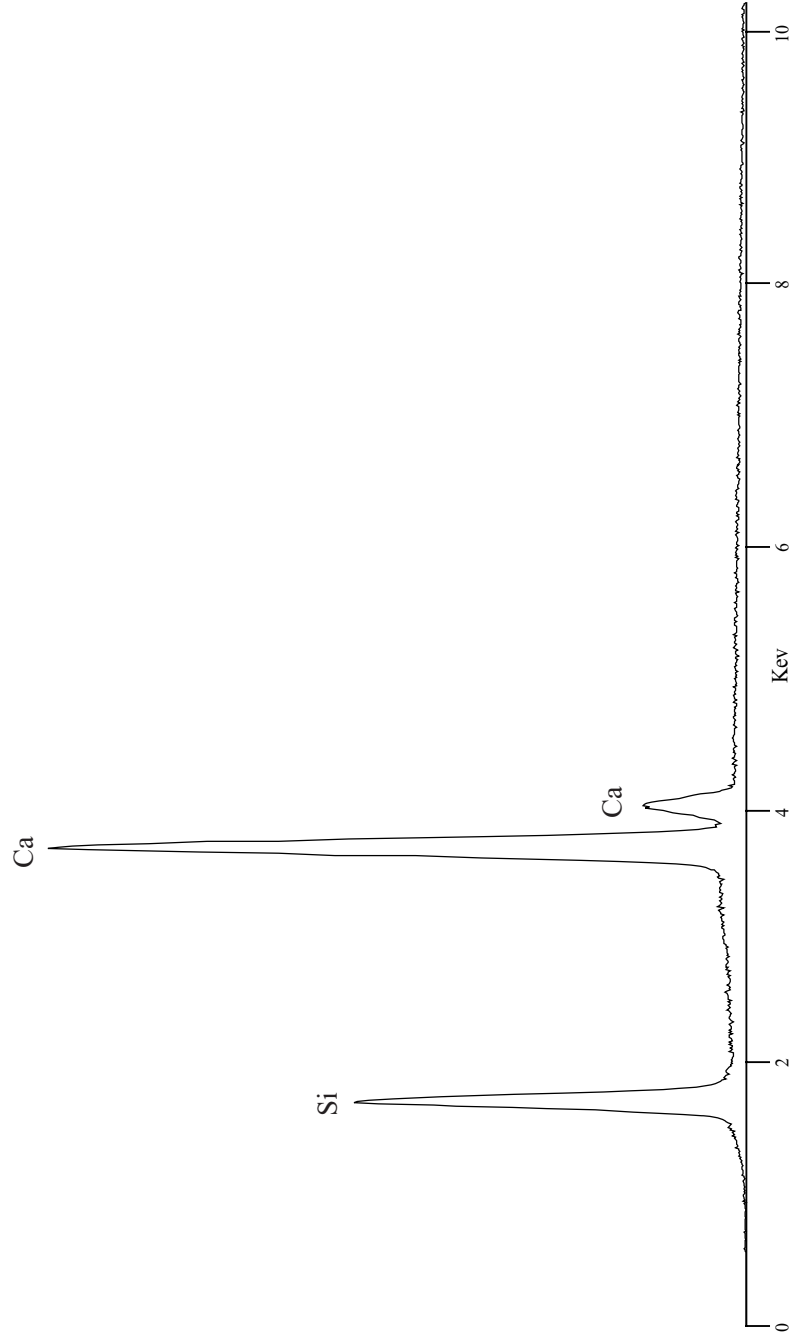


Staurolite $(\text{Fe}^{+2}, \text{Mg})_2[(\text{Al}, \text{Fe}^{+3})_9\text{O}_6[\text{SiO}_4](\text{O}, \text{OH})_2]$

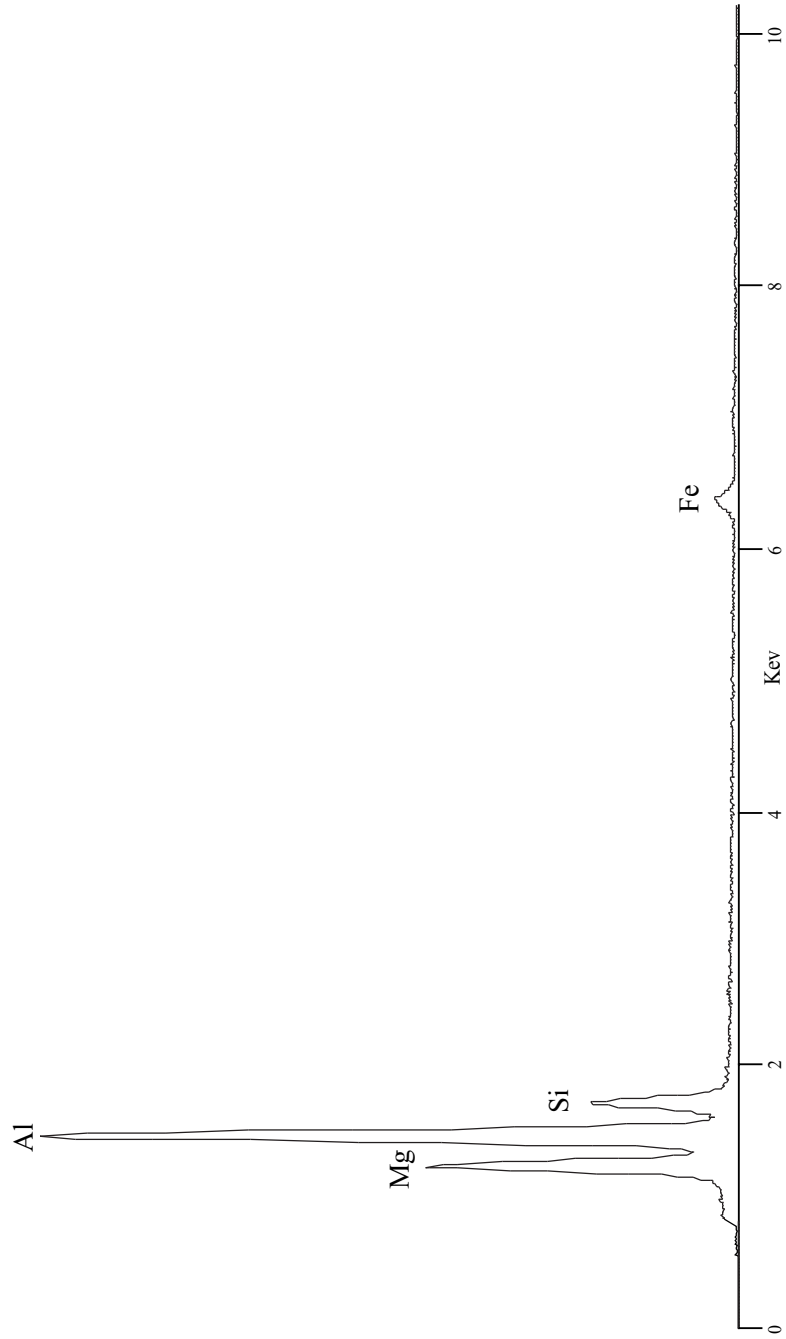


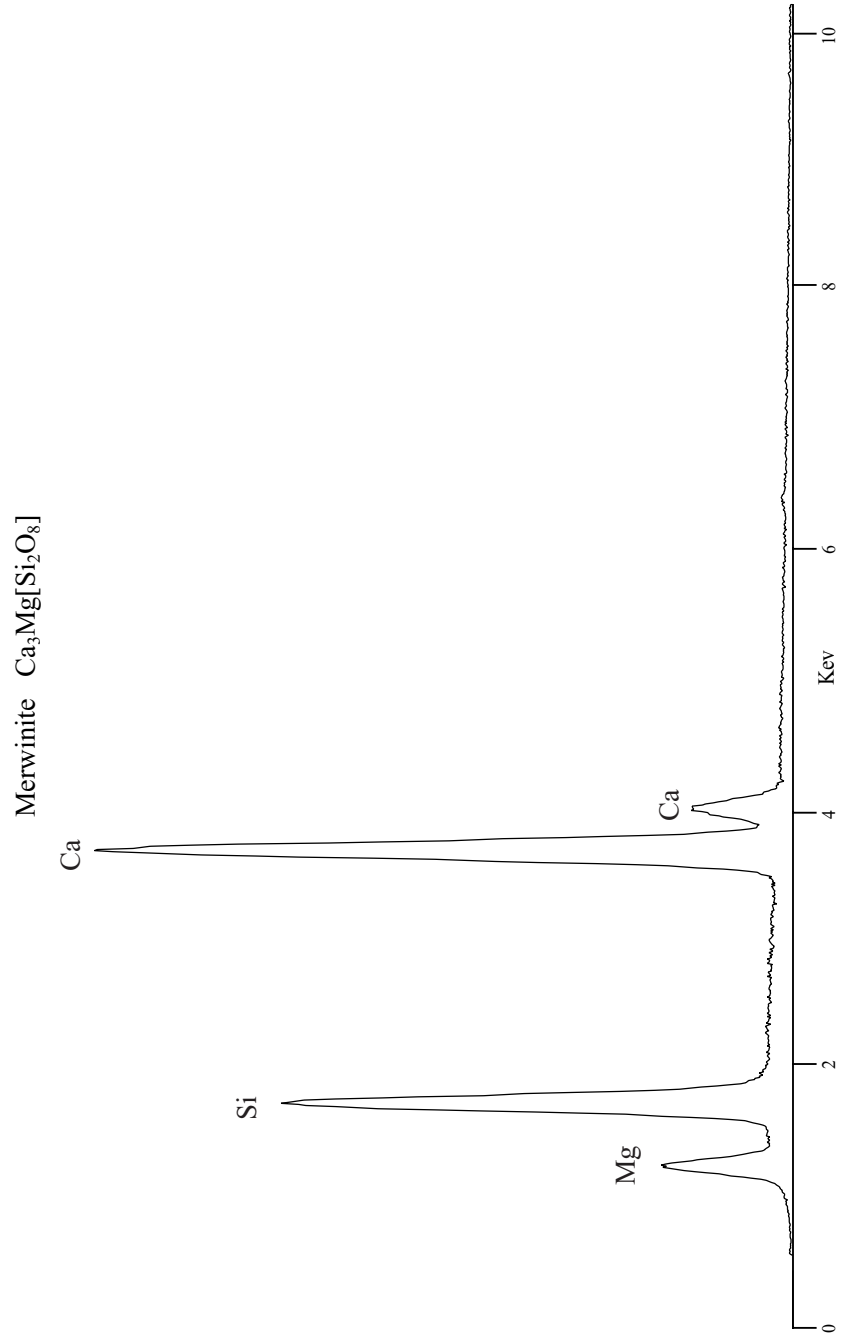
Chloritoid $(\text{Fe}^{+2}, \text{Mg}, \text{Mn})_2(\text{Al}, \text{Fe}^{+3})\text{Al}_3\text{O}_2[\text{SiO}_4]_2(\text{OH})_4$ 

Datolite $\text{CaB}[\text{SiO}_4](\text{OH})$



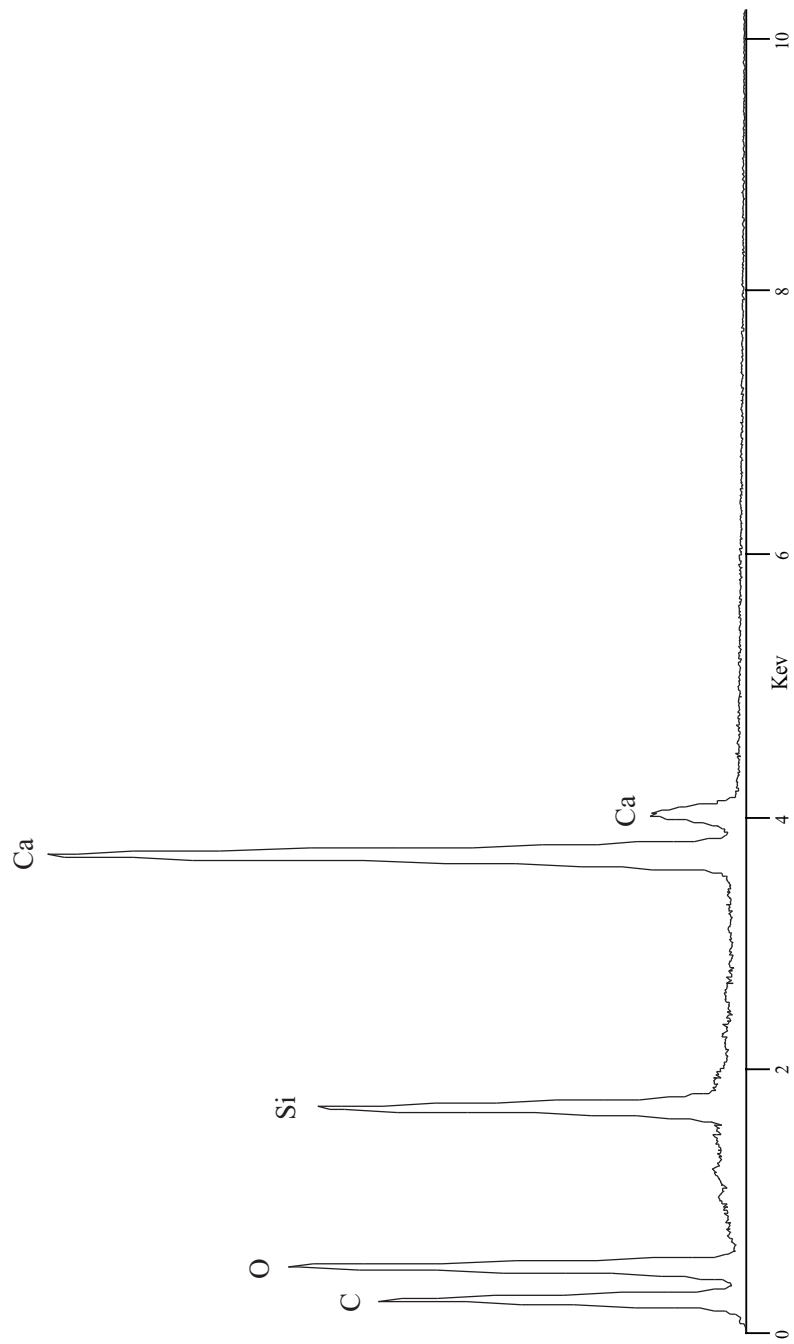
Sapphirine $(\text{Mg,Fe})_2\text{Al}_4\text{O}_6[\text{SiO}_4]$



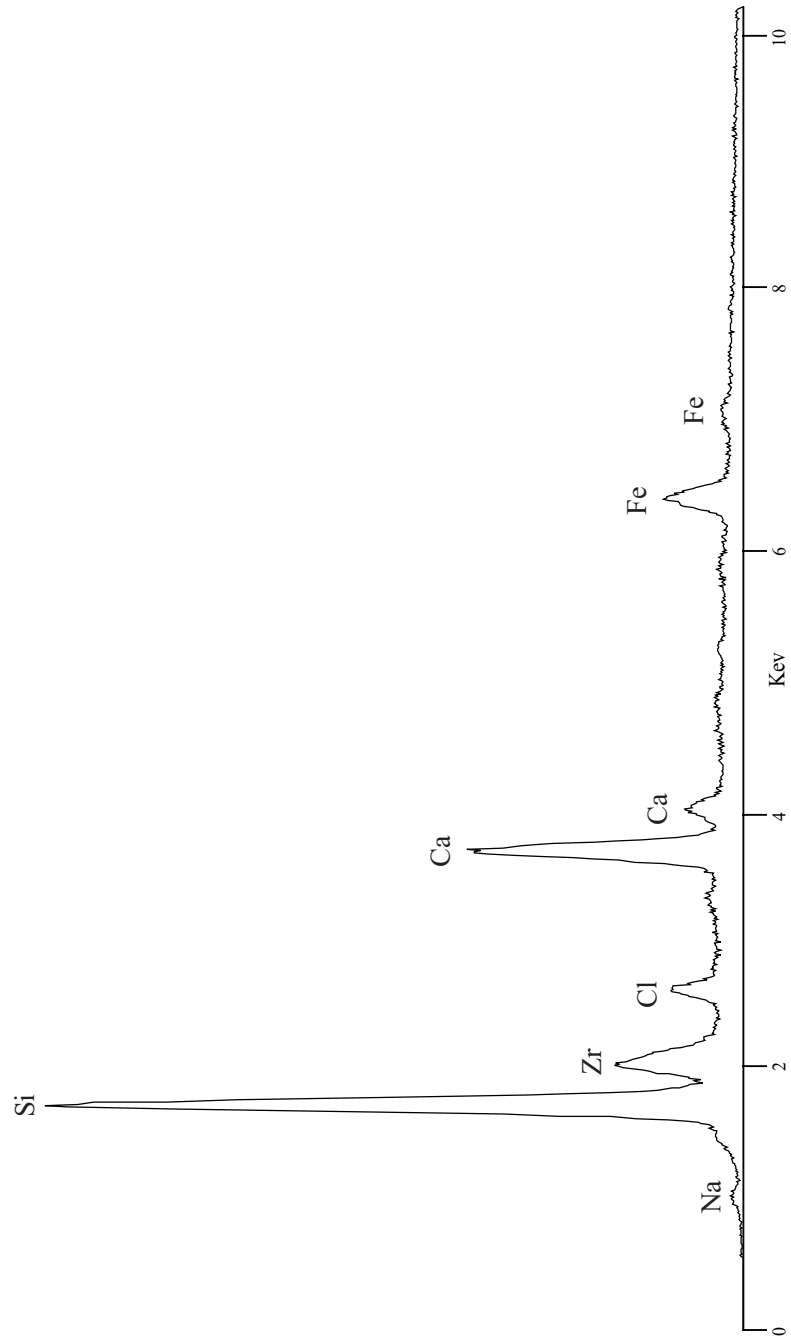


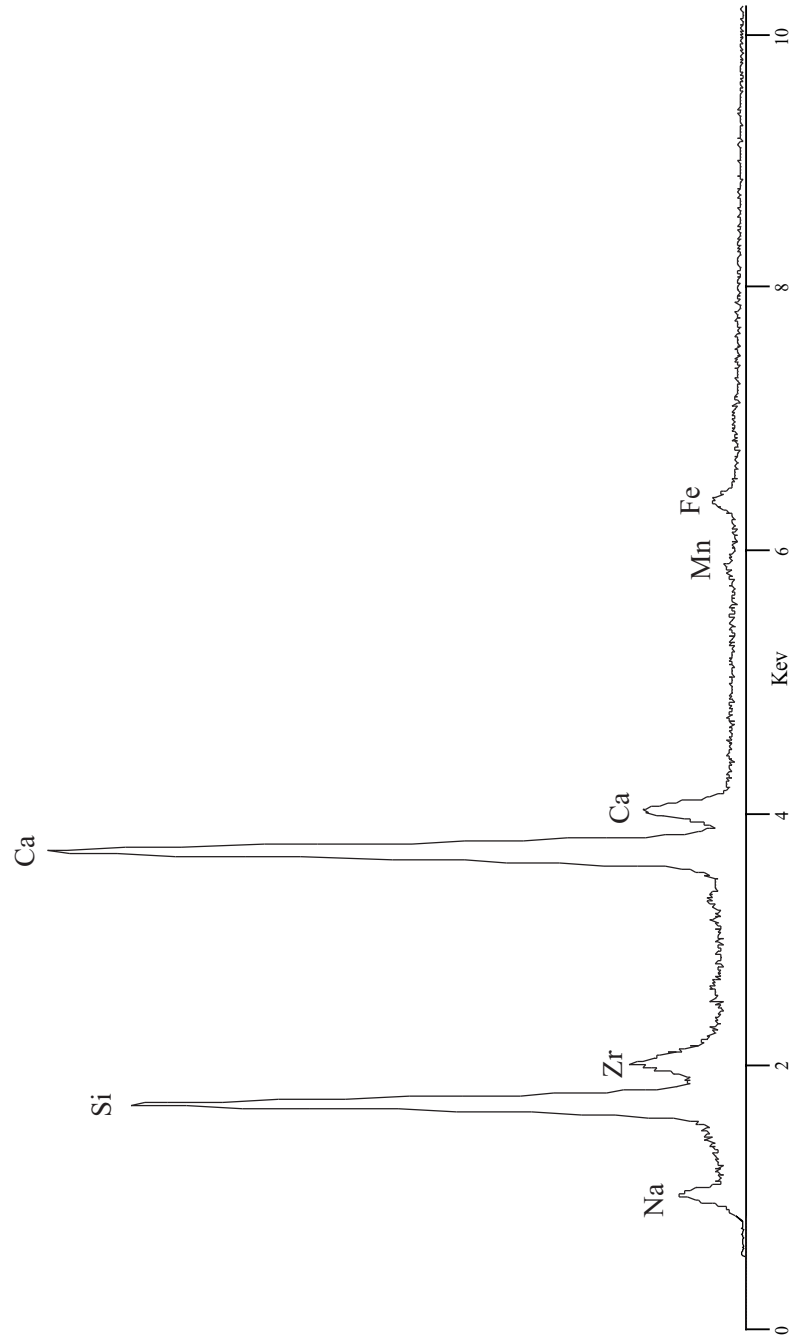
Spurrite $2\text{Ca}_2[\text{SiO}_4]\cdot\text{CaCO}_3$

Spectrum collected with thin window detector



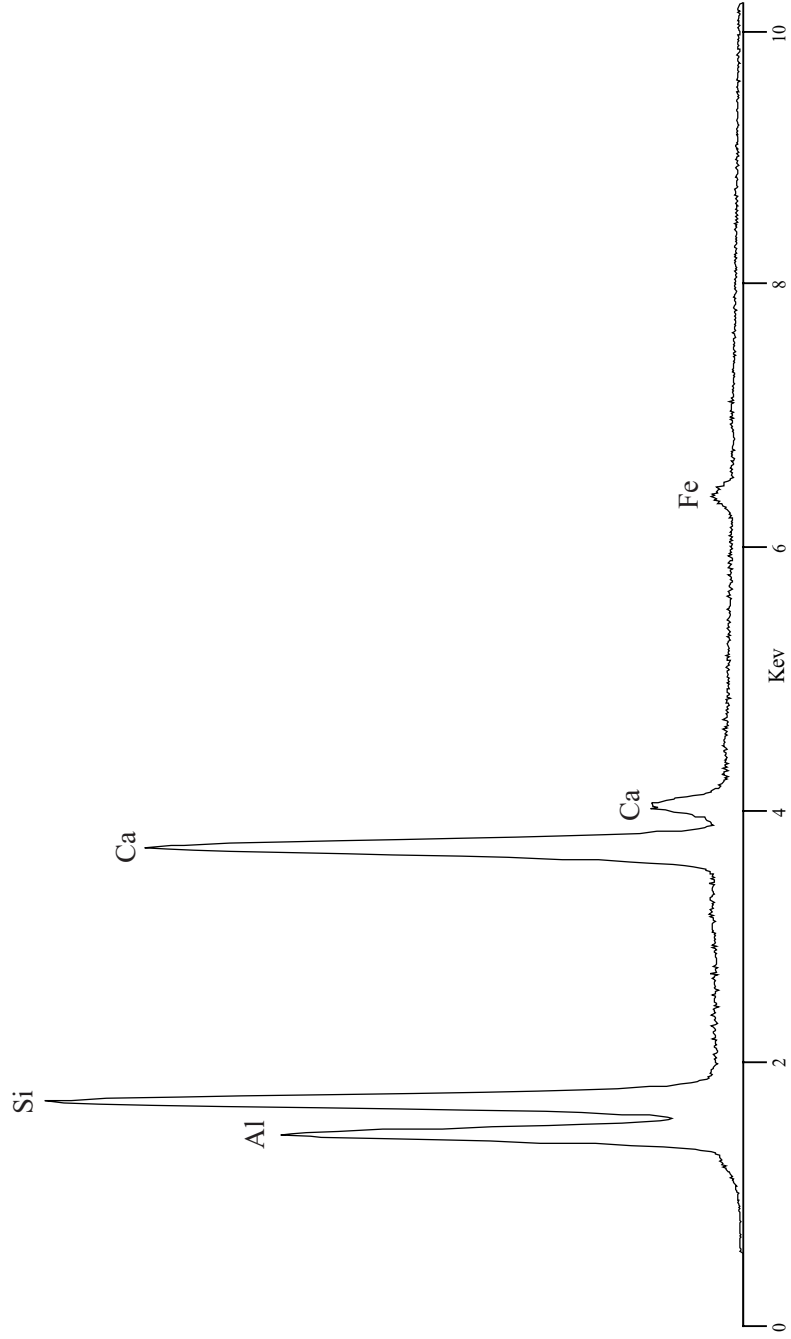
Eudialyte (Eucolite) $(\text{Na,Ca,Fe})_6\text{Zr}[(\text{Si}_3\text{O}_9)_2](\text{OH,F,Cl})$



Rosenbuschite $(\text{Ca,Na,Mn})_3(\text{Zr,Ti,Fe}^{+3})_2[\text{SiO}_4]_2(\text{F,OH})$ 

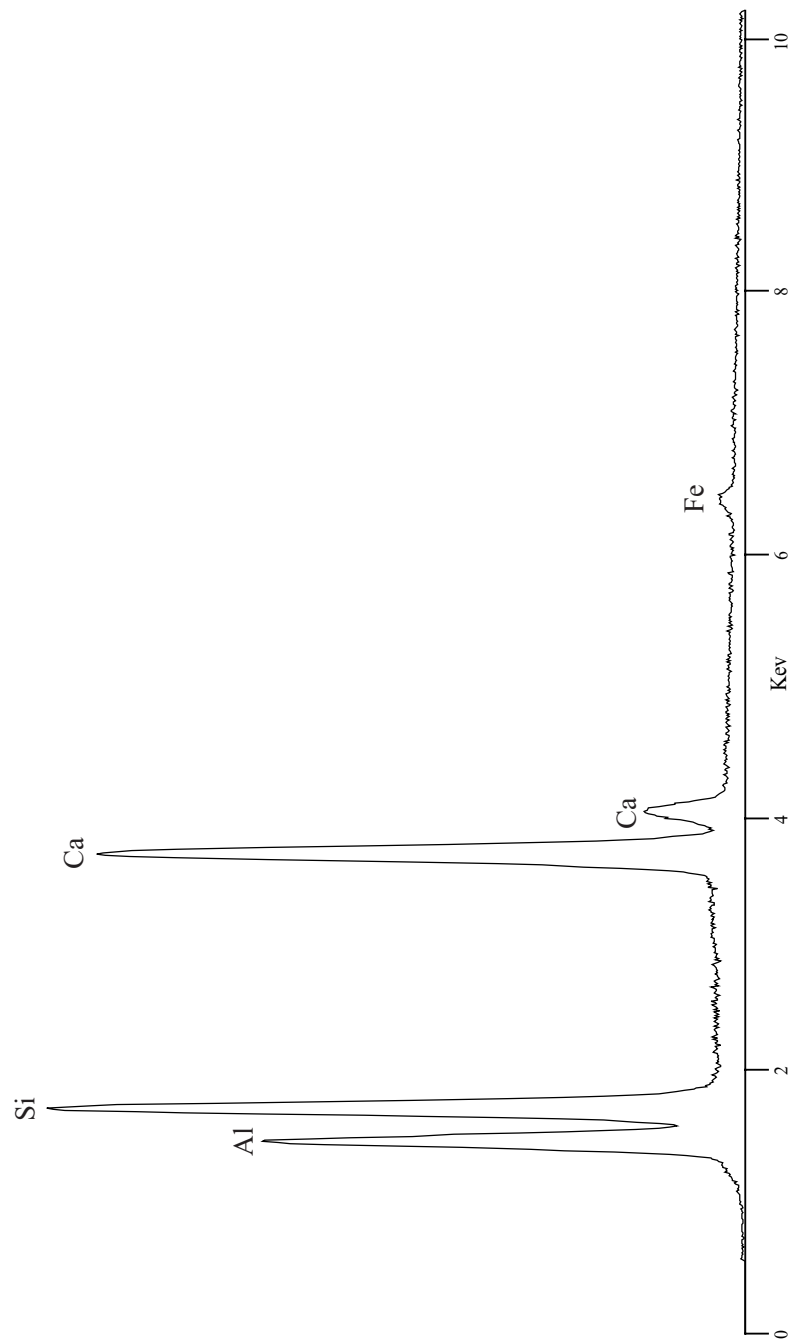
Zoisite $\text{Ca}_2\text{Al} \cdot \text{Al}_2\text{O} \cdot \text{OH}[\text{Si}_2\text{O}_7][\text{SiO}_4]$

Epidote



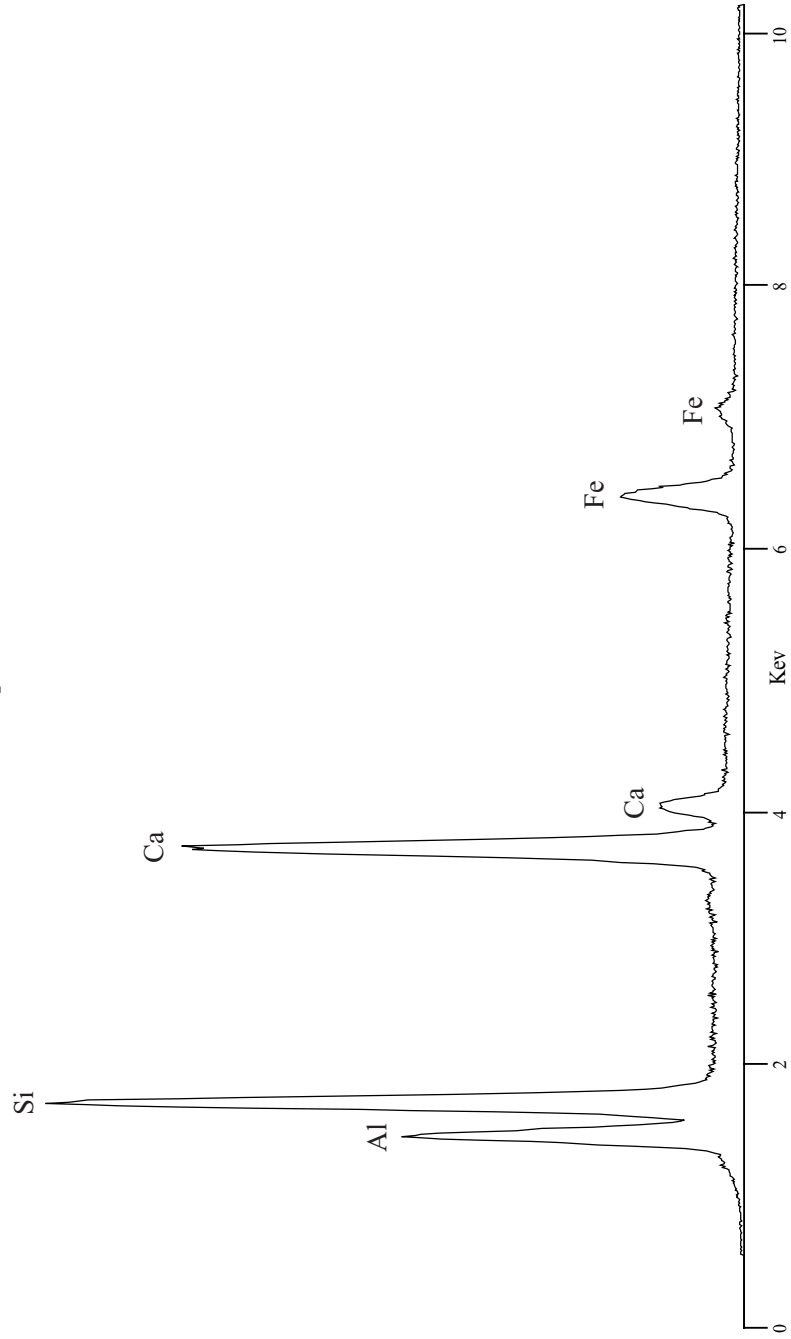
Clinzoisite $\text{Ca}_2\text{Al} \cdot \text{Al}_2\text{O} \cdot \text{OH}[\text{Si}_2\text{O}_7][\text{SiO}_4]$

Epidote



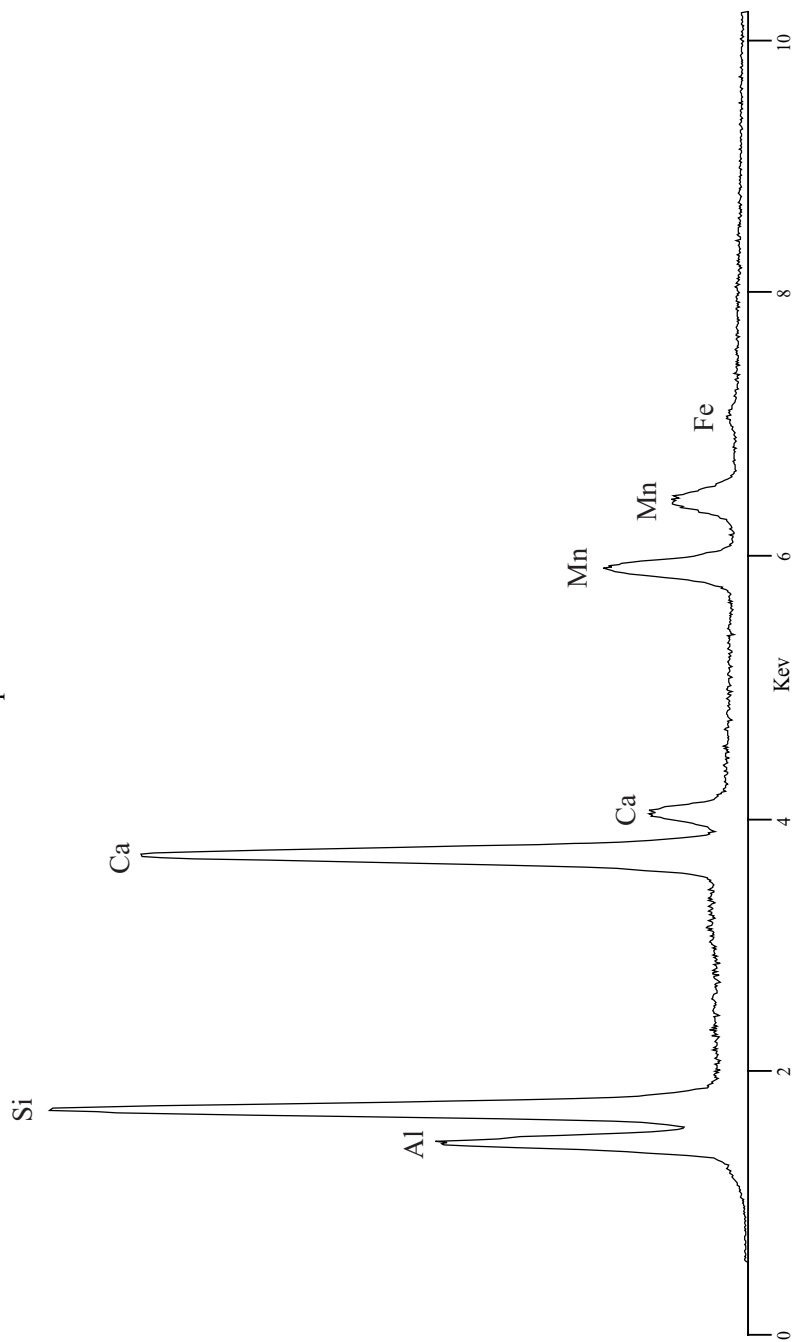
Epidote $\text{CaFe}^{+3}\text{Al}_2\text{O}\cdot\text{OH}[\text{Si}_2\text{O}_7][\text{SiO}_4]$

Epidote



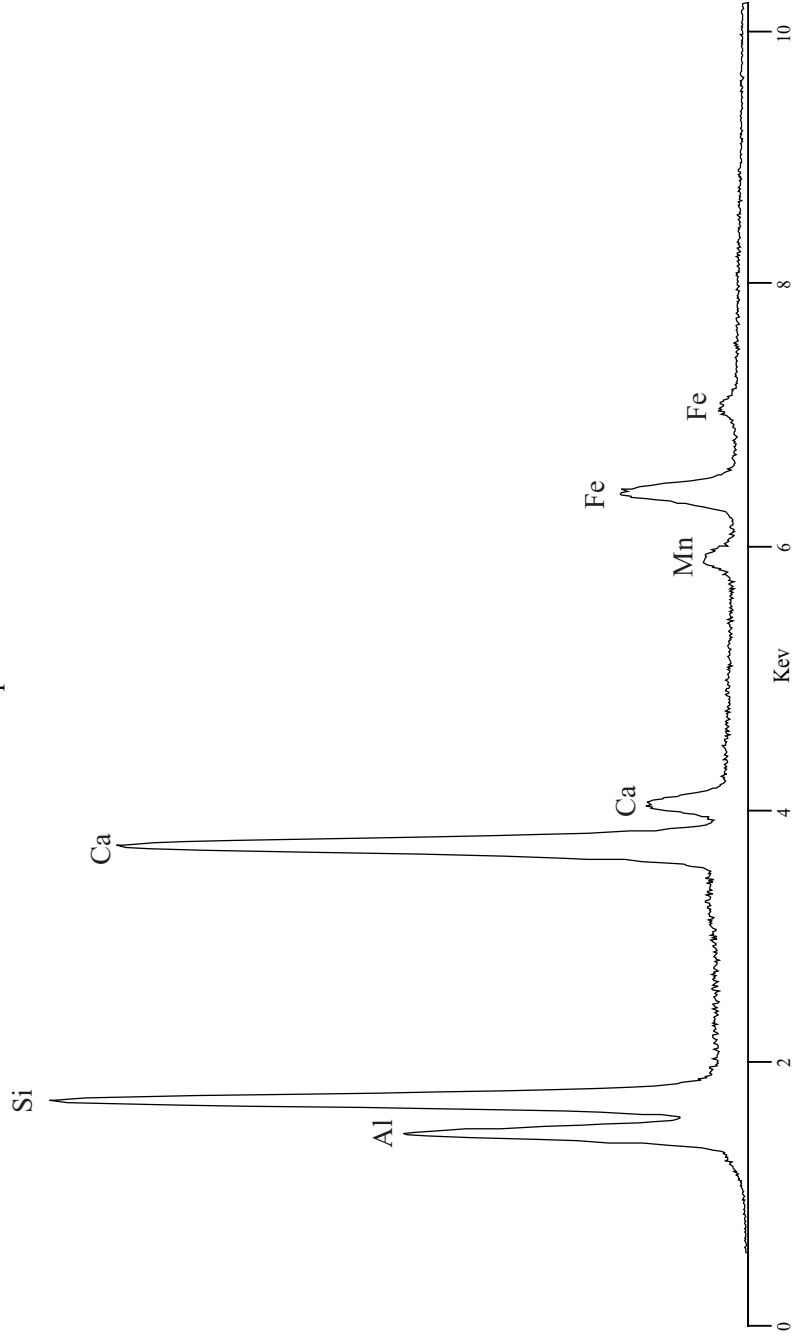
Piemontite $\text{Ca}_2(\text{Mn}, \text{Fe}^{3+}, \text{Al})_2\text{Al}_2\text{O} \cdot \text{OH}[\text{Si}_2\text{O}_7][\text{SiO}_4]$

Epidote



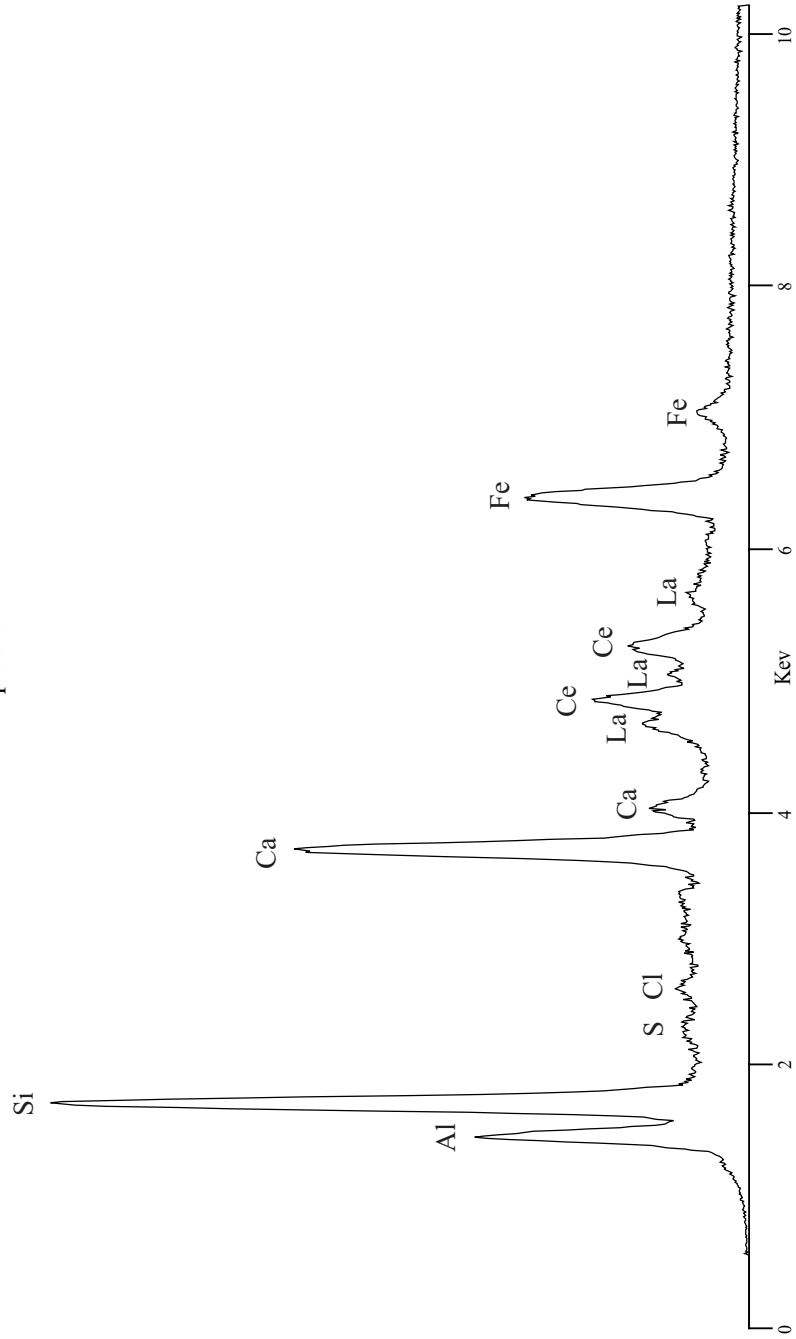
Piemontite $\text{Ca}_2(\text{Mn}, \text{Fe}^{3+}, \text{Al})_2\text{Al}_2\text{O} \cdot \text{OH}[\text{Si}_2\text{O}_7][\text{SiO}_4]$

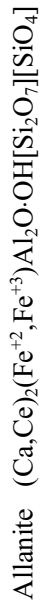
Epidote



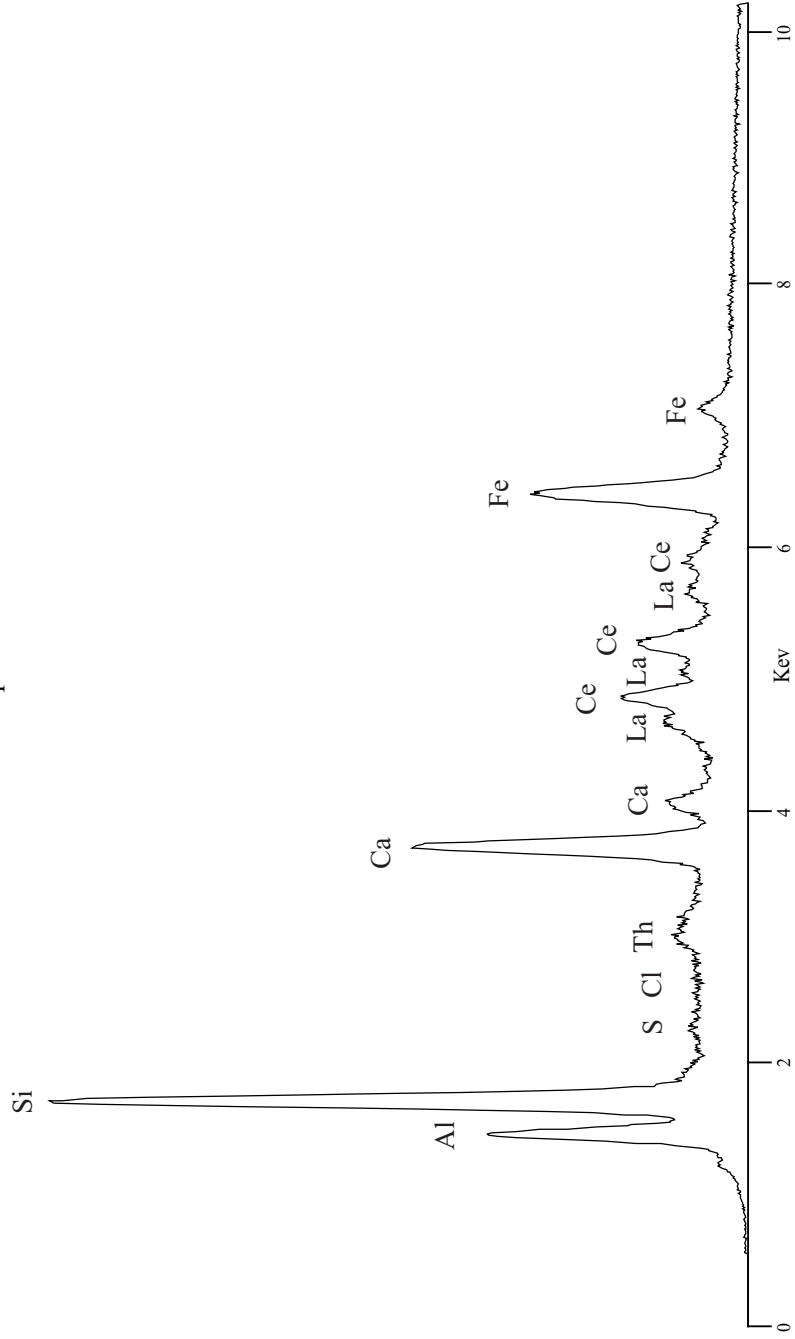
Allanite $(\text{Ca,Ce})_2(\text{Fe}^{+2}, \text{Fe}^{+3})\text{Al}_2\text{O} \cdot \text{OH}[\text{Si}_2\text{O}_7][\text{SiO}_4]$

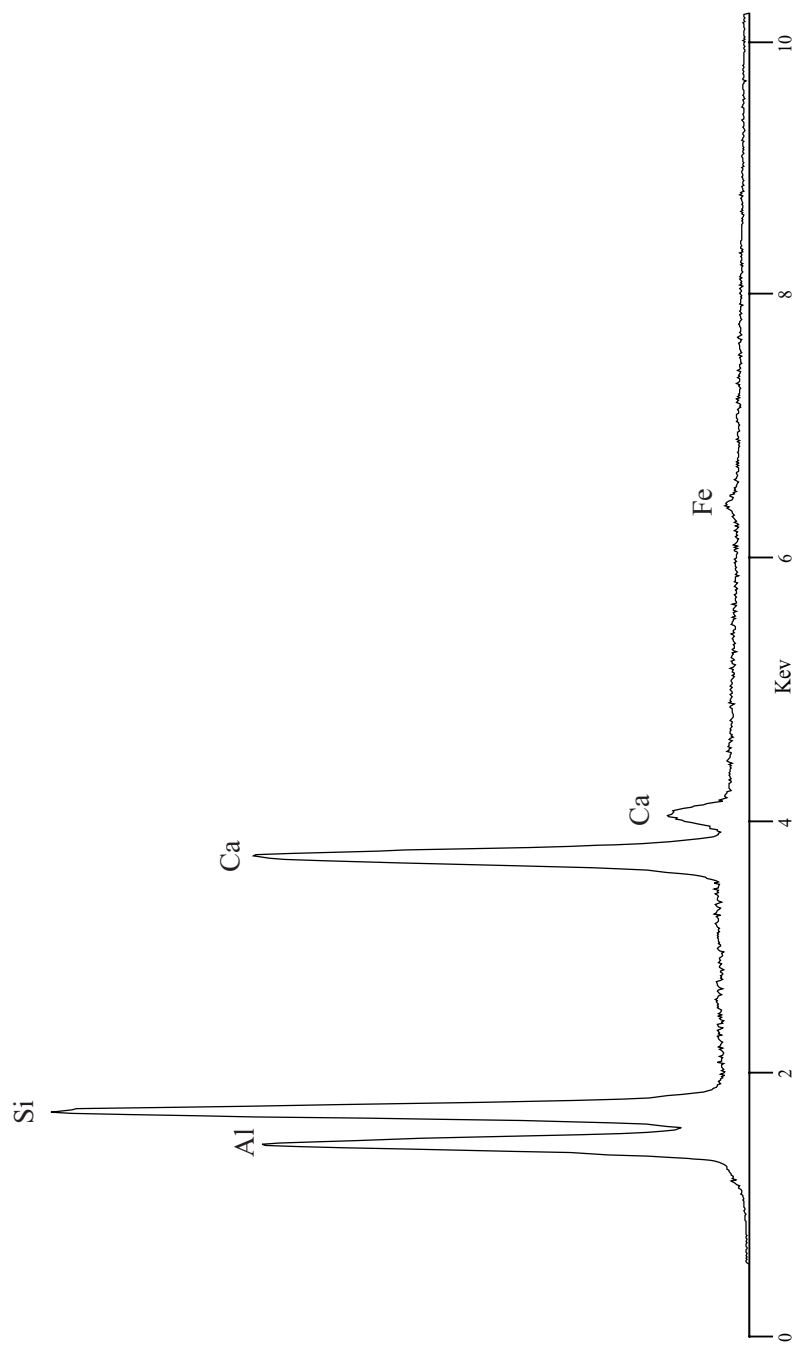
Epidote



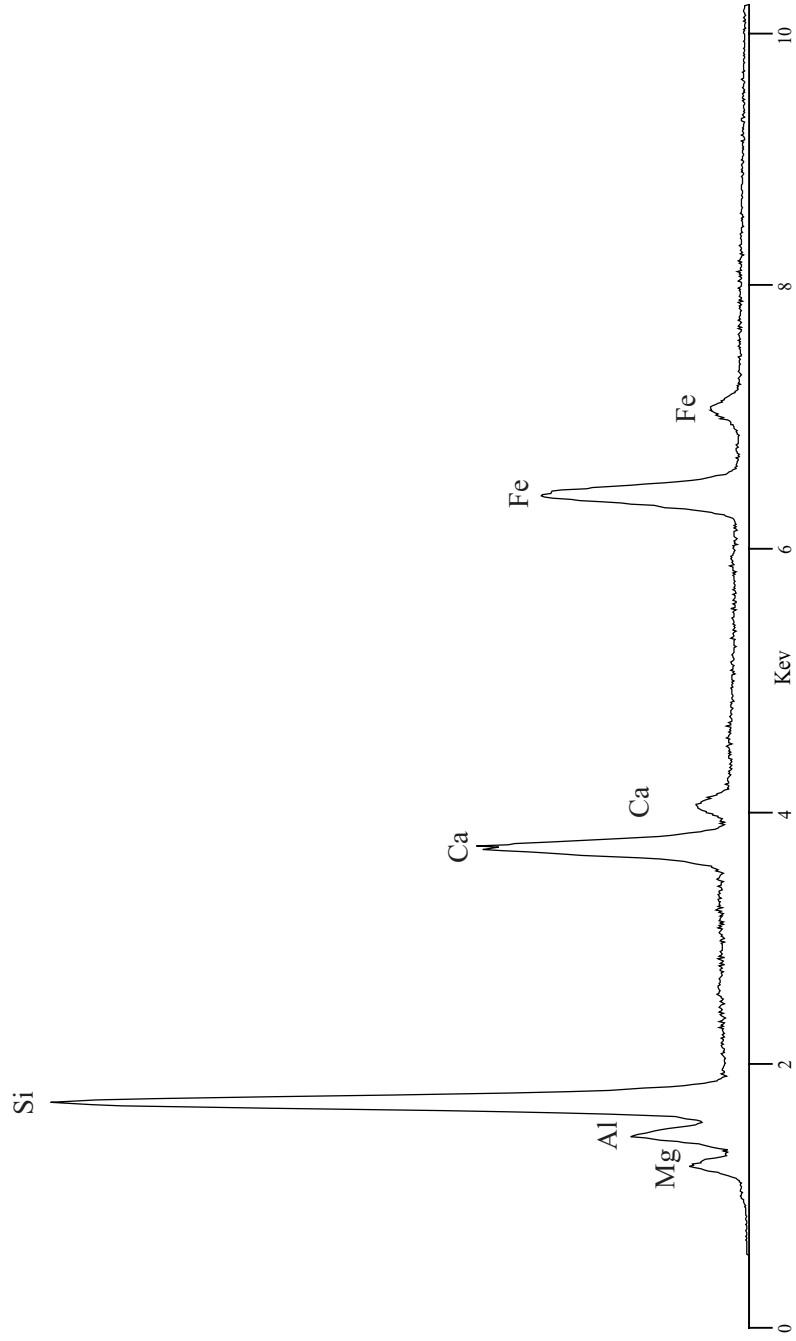


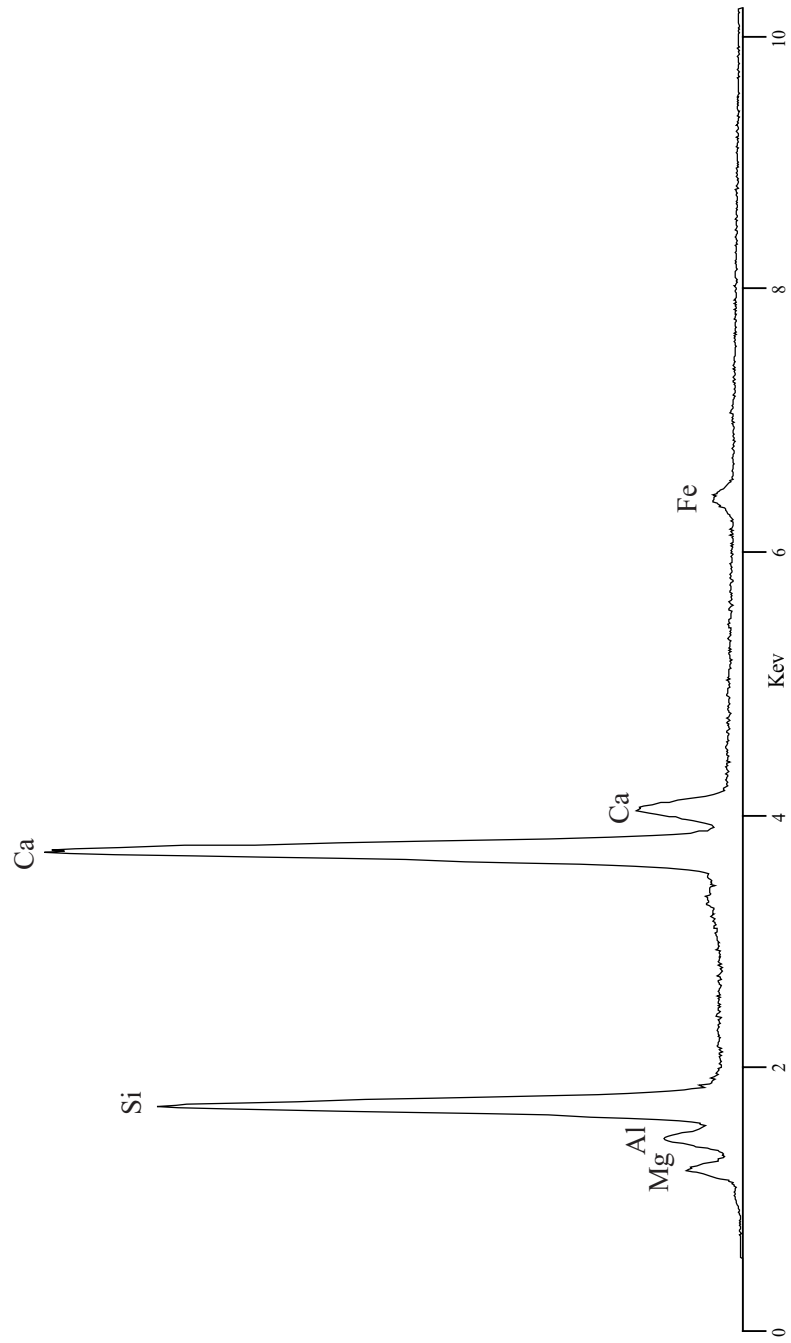
Epidote



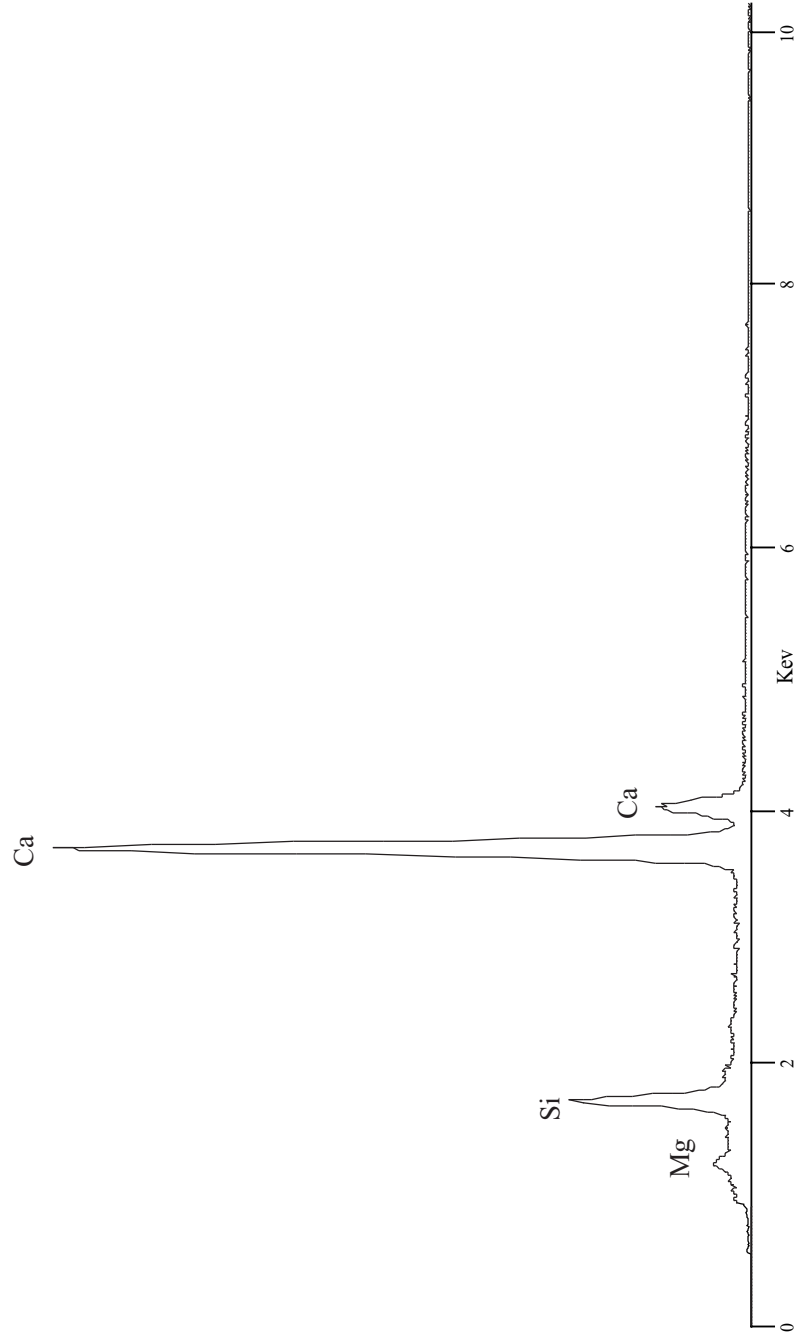
Lawsonite $\text{CaAl}_2(\text{OH})_2[\text{Si}_2\text{O}_7]\text{H}_2\text{O}$ 

Pumpellyite $\text{Ca}_4(\text{Mg,Fe}^{+2})(\text{Al,Fe}^{+3})_5\text{O}(\text{OH})_3[\text{Si}_2\text{O}_7]_3[\text{SiO}_4]_2 \cdot 2\text{H}_2\text{O}$

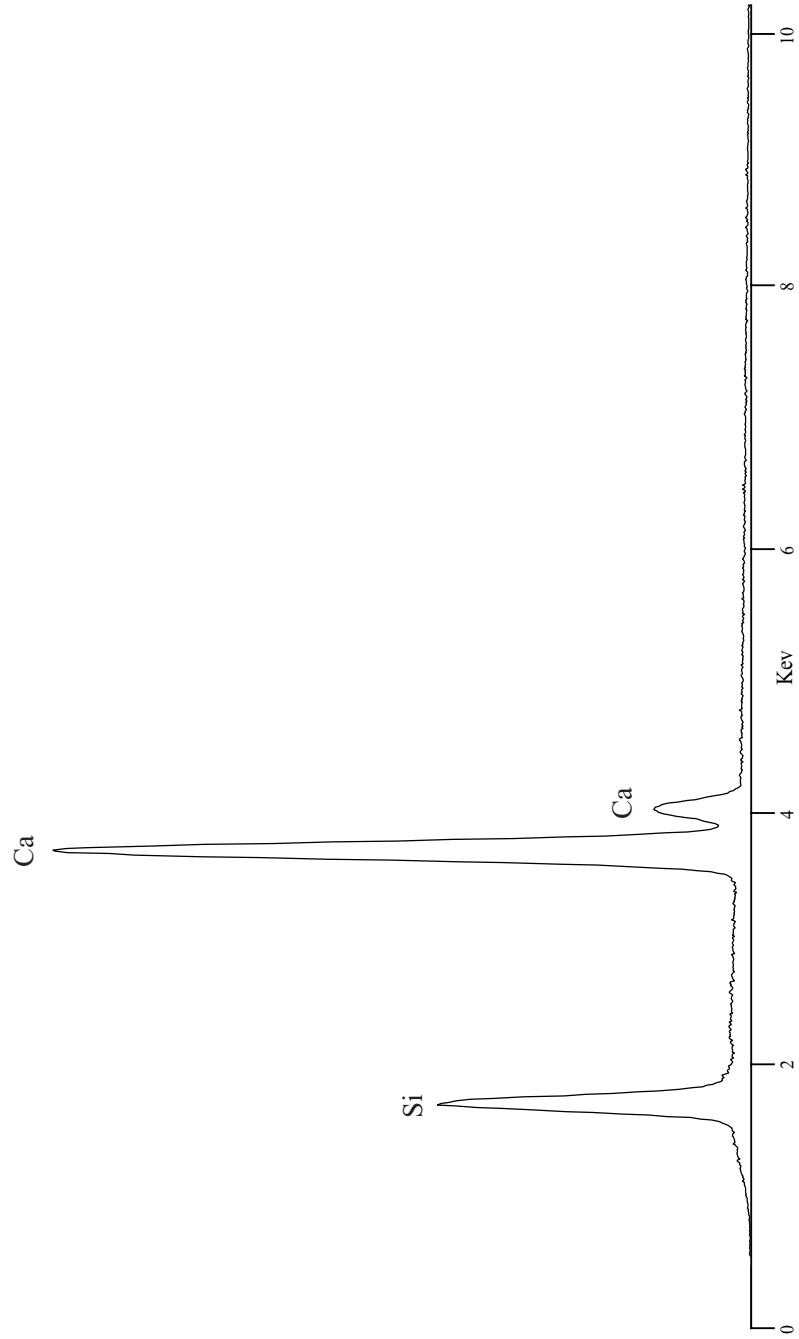


Melilite $(\text{Ca,Na})_2[(\text{Mg,Fe}^{+2},\text{Al,Si})_3\text{O}_7]$ 

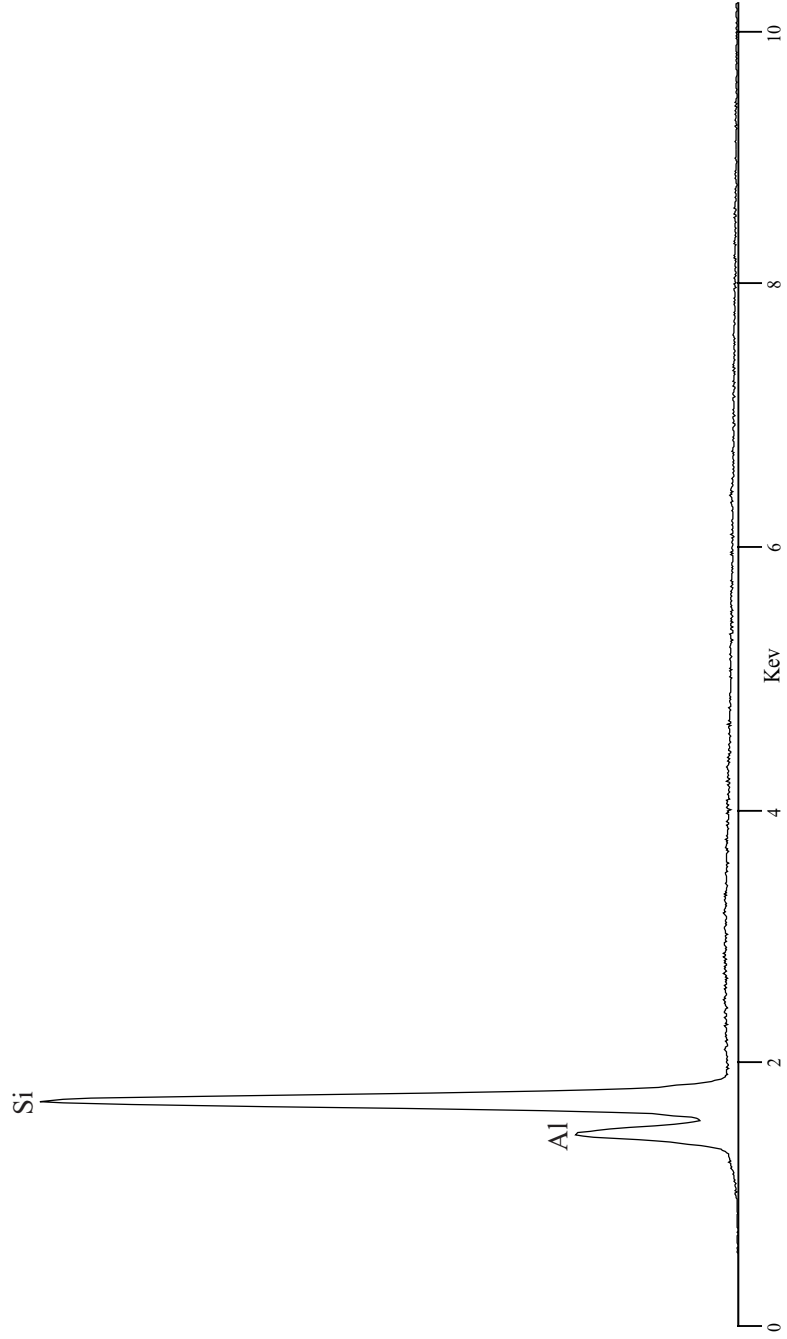
Rankinite $\text{Ca}_3[\text{Si}_2\text{O}_7]$



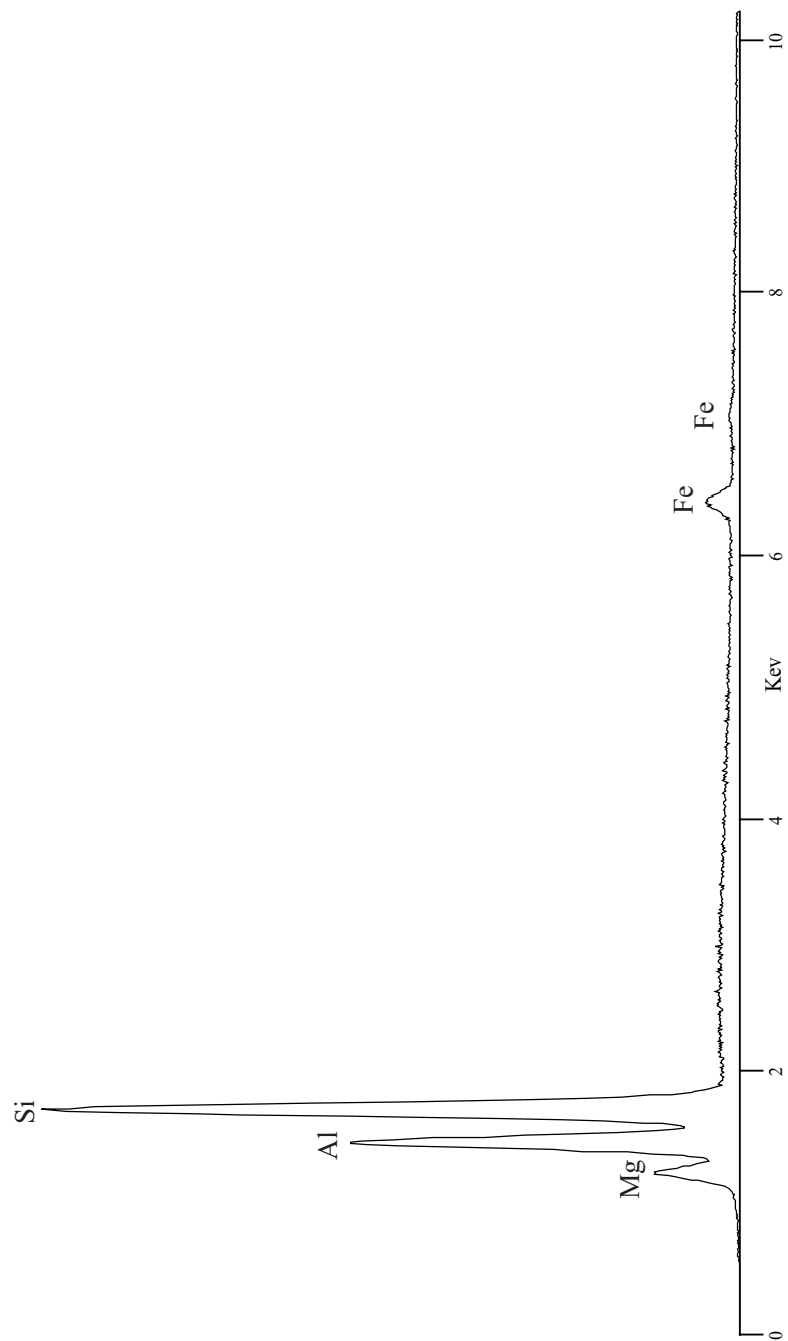
Tillyite $\text{Ca}[\text{Si}_2\text{O}_7] \cdot 2\text{CaCO}_3$



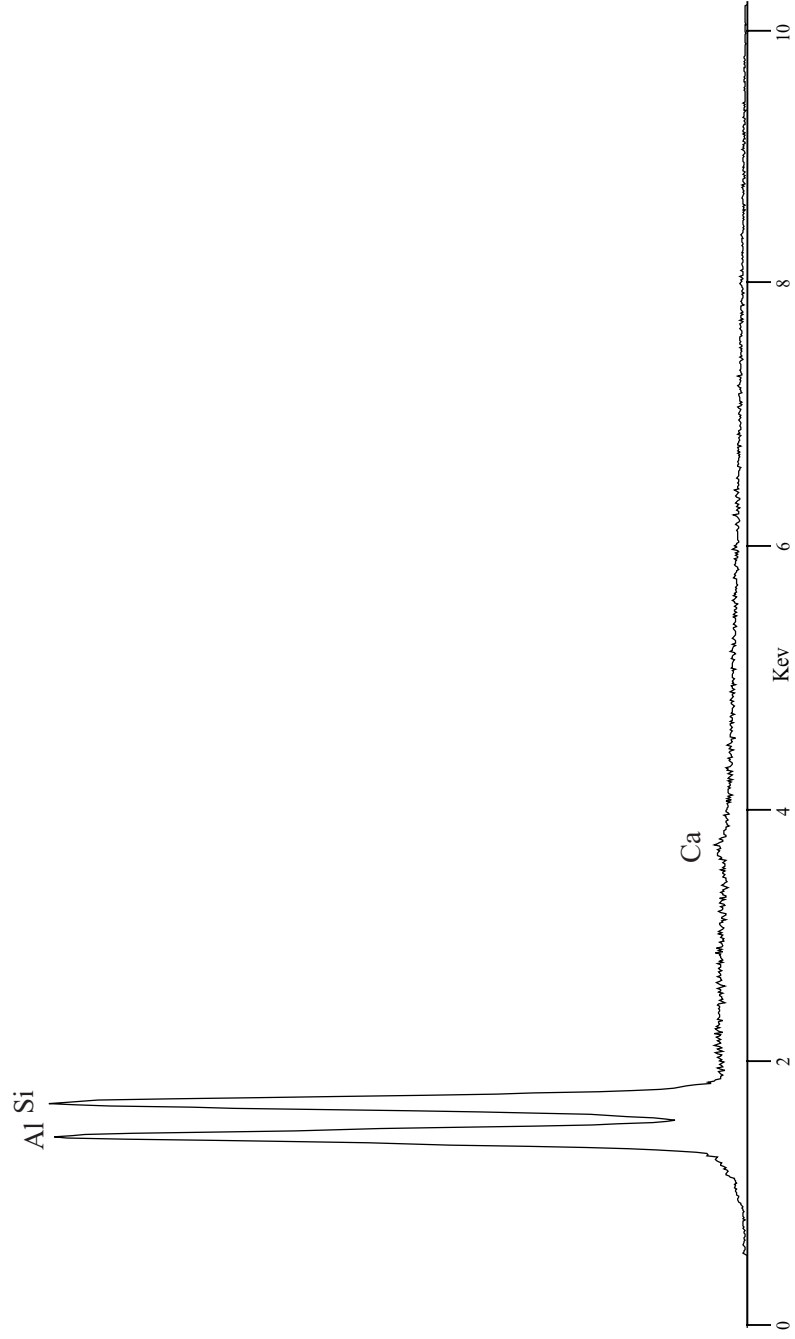
Beryl $\text{Be}_3\text{Al}_2[\text{Si}_6\text{O}_{18}]$



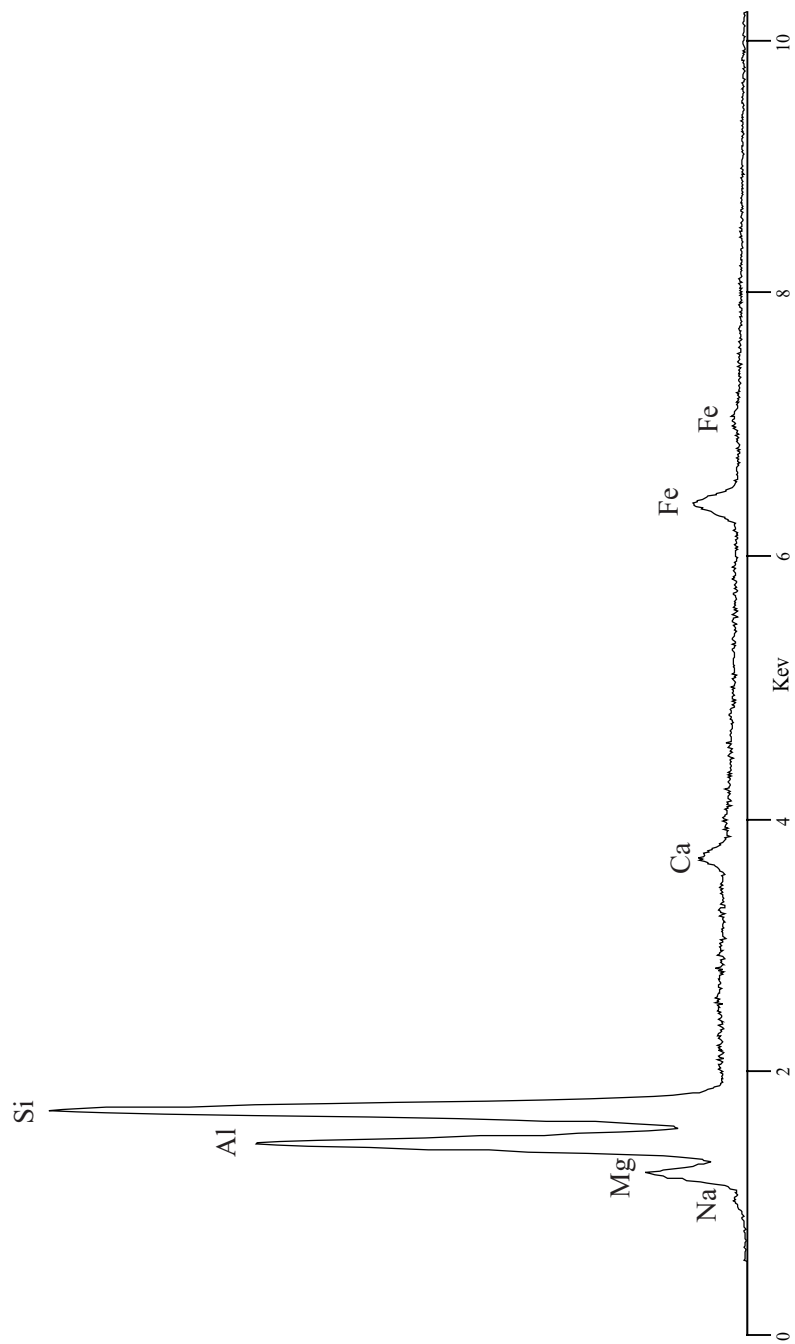
Cordierite $\text{Al}_3(\text{Mg,Fe}^{+2})_2[\text{Si}_5\text{AlO}_{18}]$



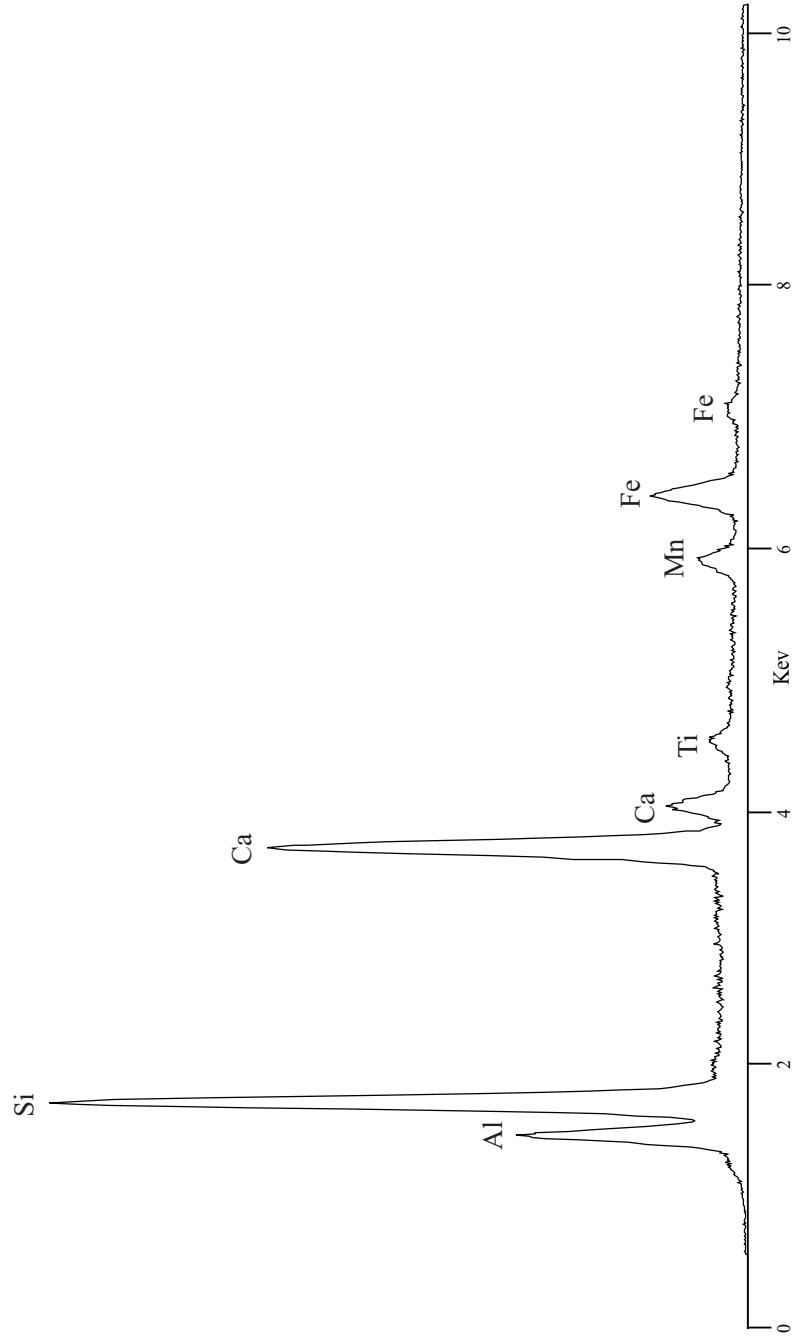
Tourmaline $\text{Na}(\text{Mg,Fe,Mn,Li,Al})_3\text{Al}_6[\text{Si}_6\text{O}_{18}][\text{BO}_3]_3(\text{OH,F})_4$



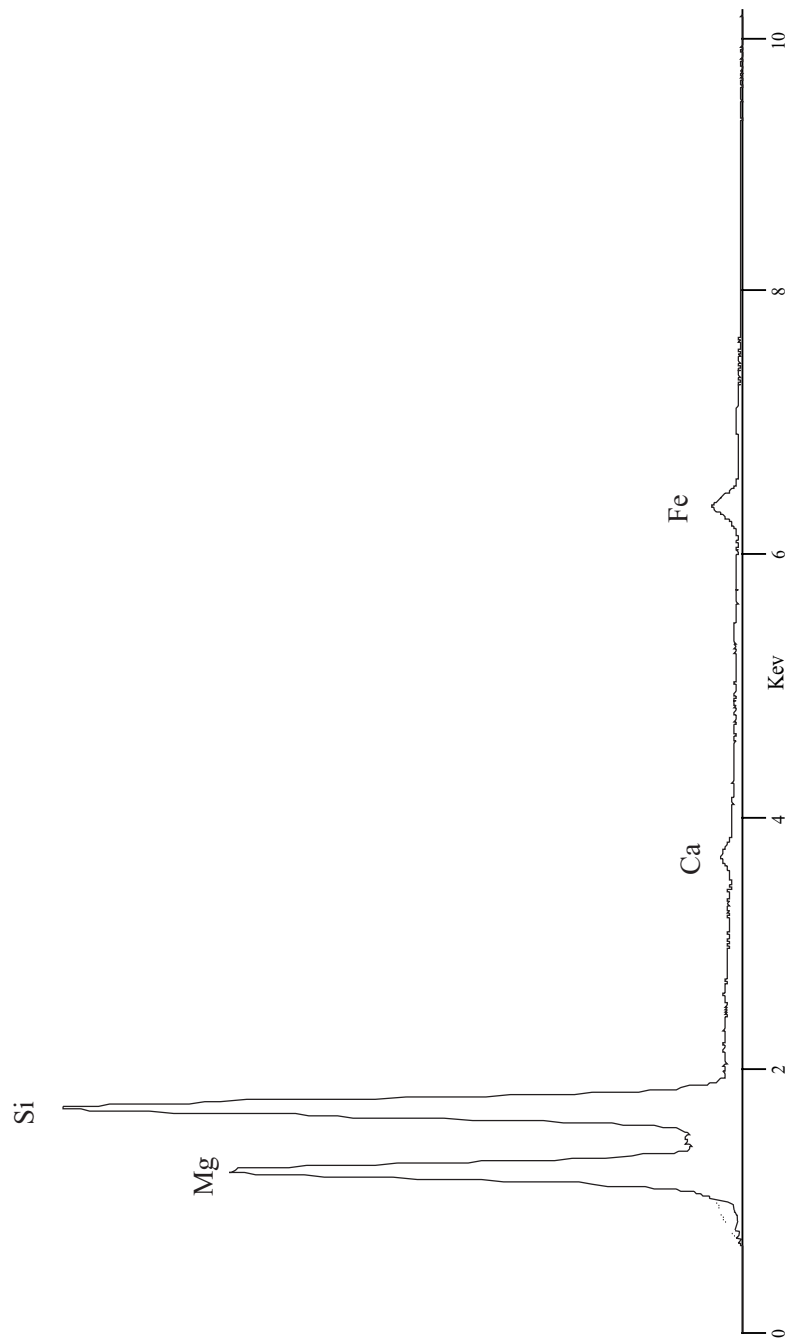
Tourmaline $\text{Na}(\text{Mg,Fe,Mn,Li,Al})_3\text{Al}_6[\text{Si}_6\text{O}_{18}](\text{BO}_3)_3(\text{OH,F})_4$



Axinite $(\text{Ca, Mn, Fe}^{+2})_3\text{Al}_2\text{BO}_3[\text{Si}_4\text{O}_{12}]\text{OH}$



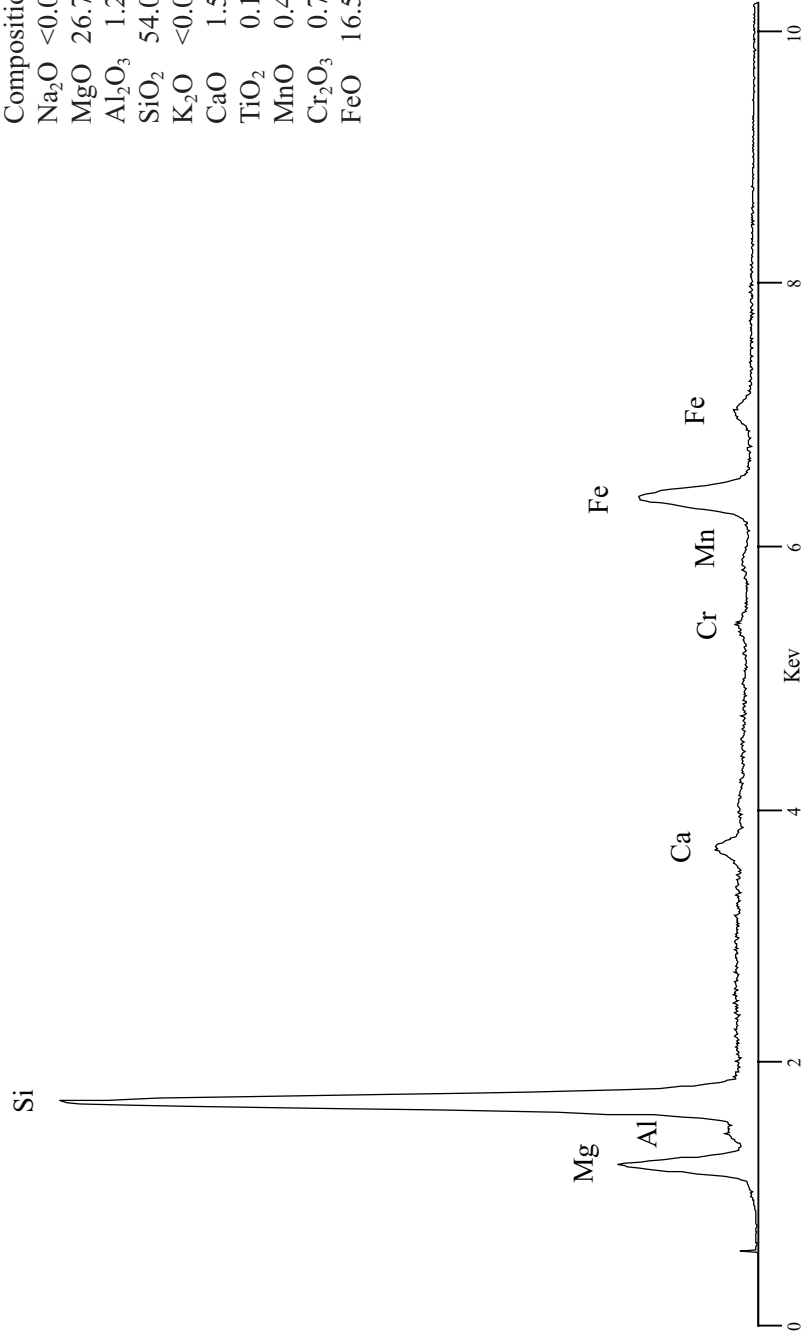
Bronzite $(\text{Mg,Fe}^{+2})[\text{SiO}_3]$
Orthopyroxene, Mg rich member in Enstatite-Orthoferrosilite solid solution series



Smithsonian Standard
USNM 746

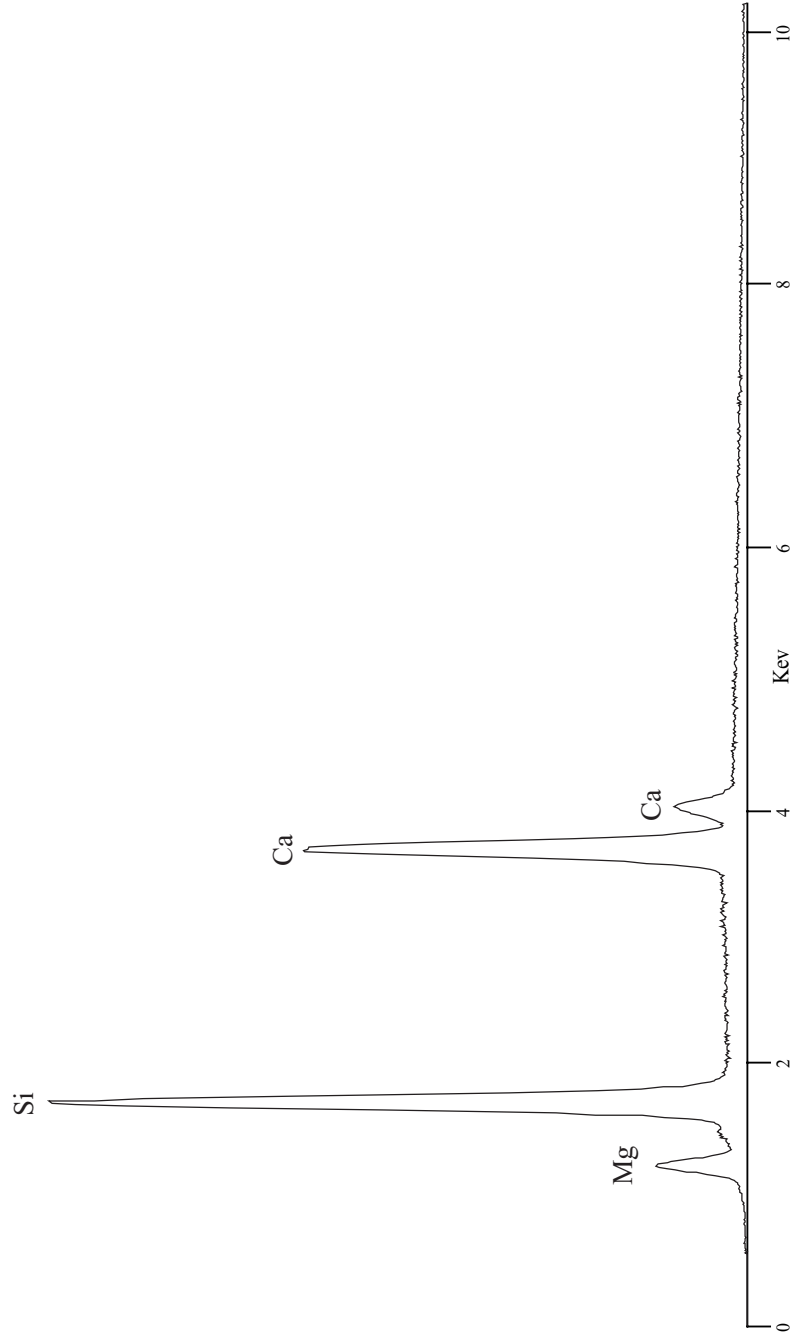
Composition
Na₂O <0.05
MgO 26.79
Al₂O₃ 1.23
SiO₂ 54.09
K₂O <0.05
CaO 1.52
TiO₂ 0.16
MnO 0.49
Cr₂O₃ 0.75
FeO 16.52

Hypersthene (Mg,Fe⁺²)[SiO₃]
Orthopyroxene in Enstatite-Orthoferrosilite solid solution series

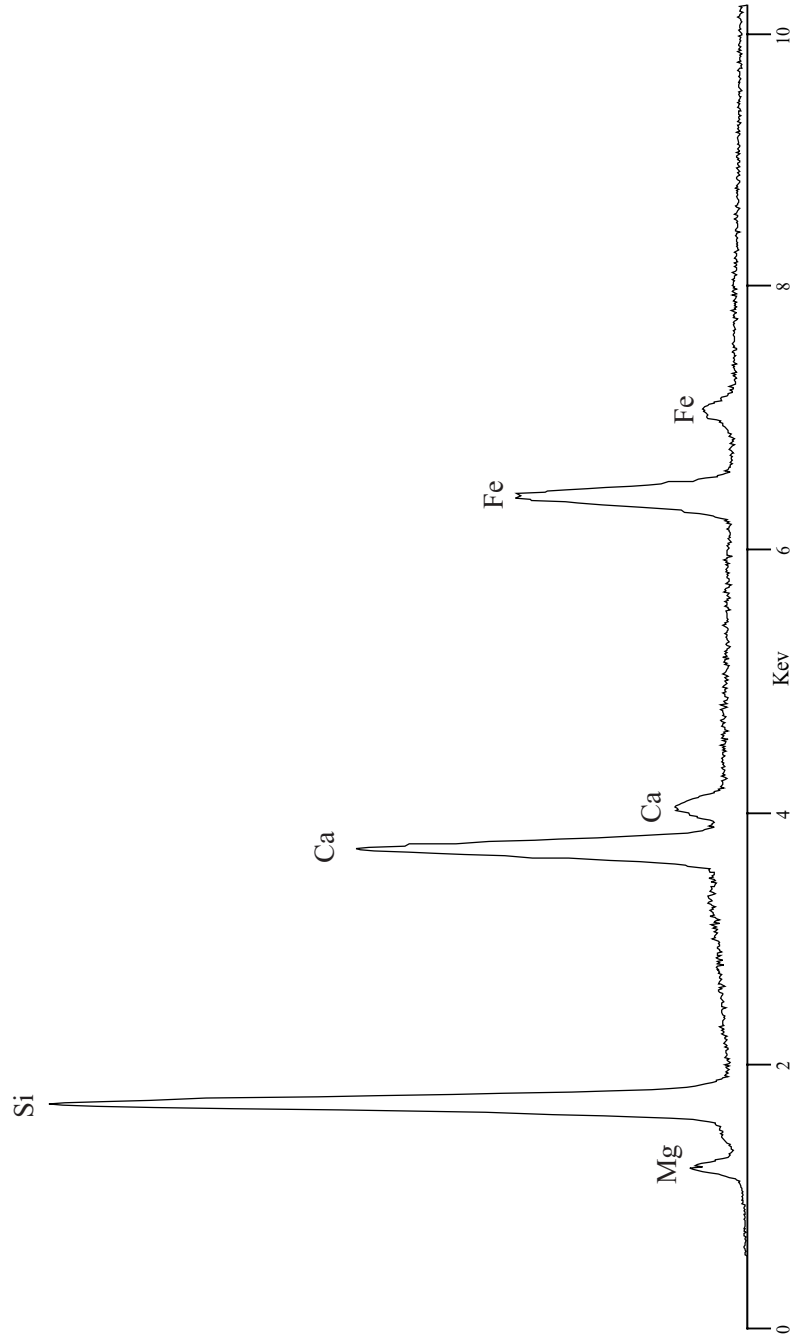


Diopside $\text{Ca}(\text{Mg,Fe})[\text{Si}_2\text{O}_6]$

Clinopyroxene in Diopside-Hedenbergite solid solution series

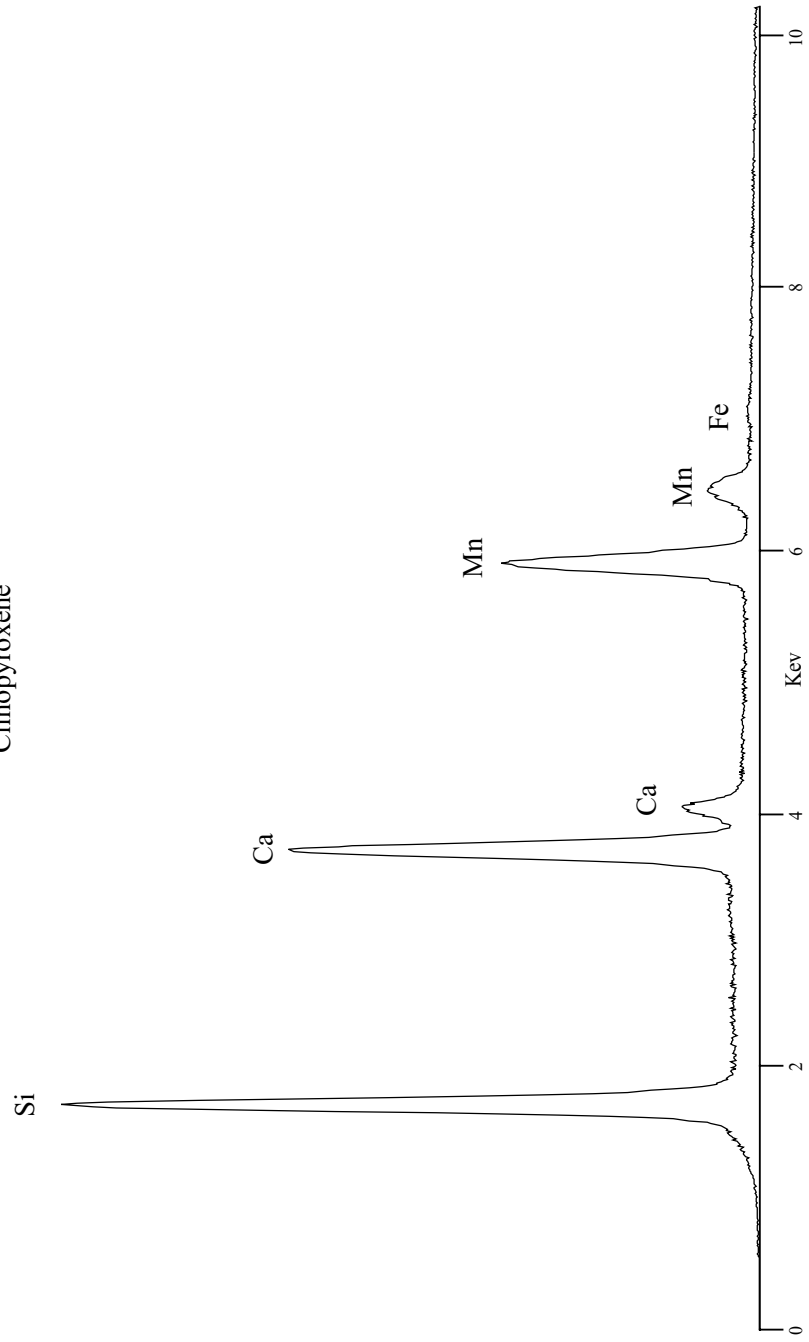


Hedenbergite $\text{Ca}(\text{Mg,Fe})[\text{Si}_2\text{O}_6]$
Clinopyroxene in Diopside-Hedenbergite solid solution series



Johansenite $\text{Ca}(\text{Mn,Fe})[\text{Si}_2\text{O}_6]$

Clinopyroxene

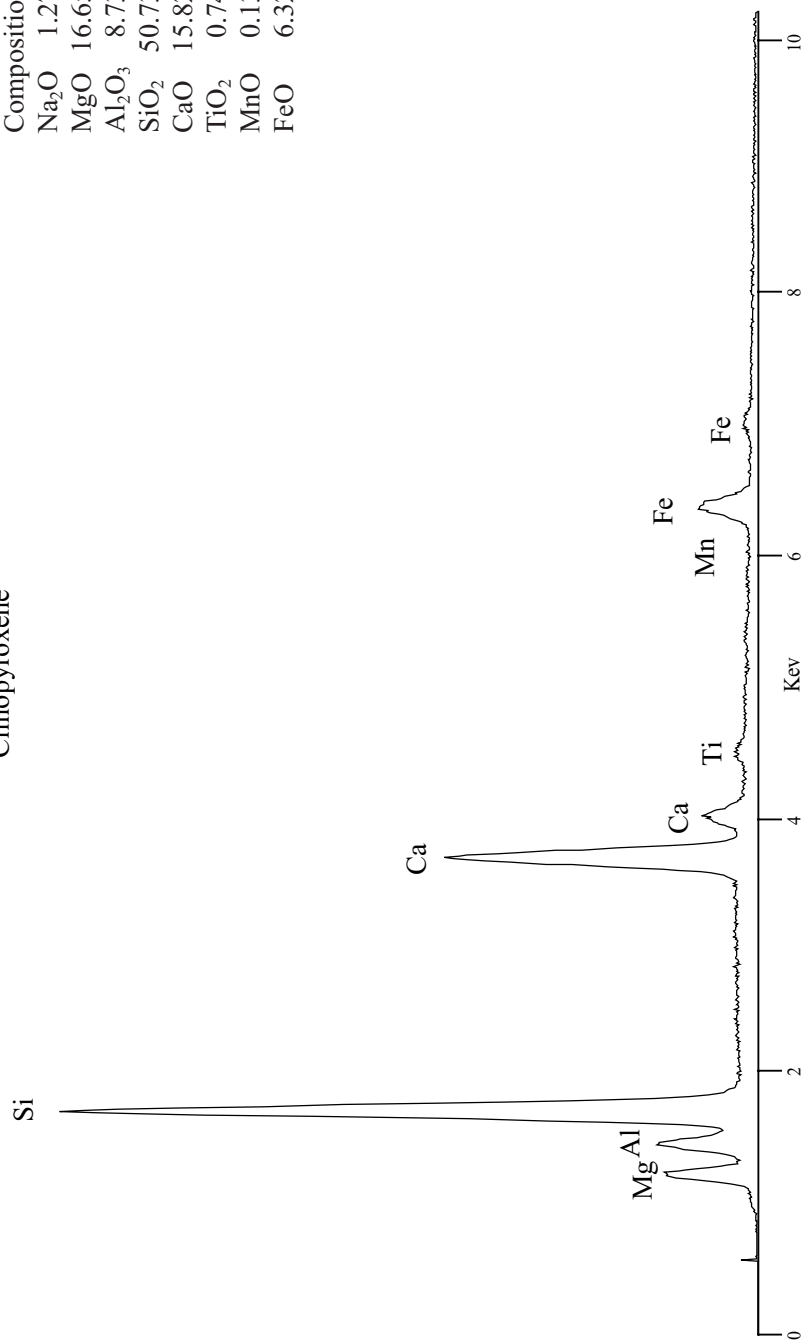


Smithsonian Standard
USNM 1222142

Augite $(Ca,Na,Mg,Fe^{+2},Mn,Fe^{+3},Al,Ti)_2[(Si,Al)_2O_6]$

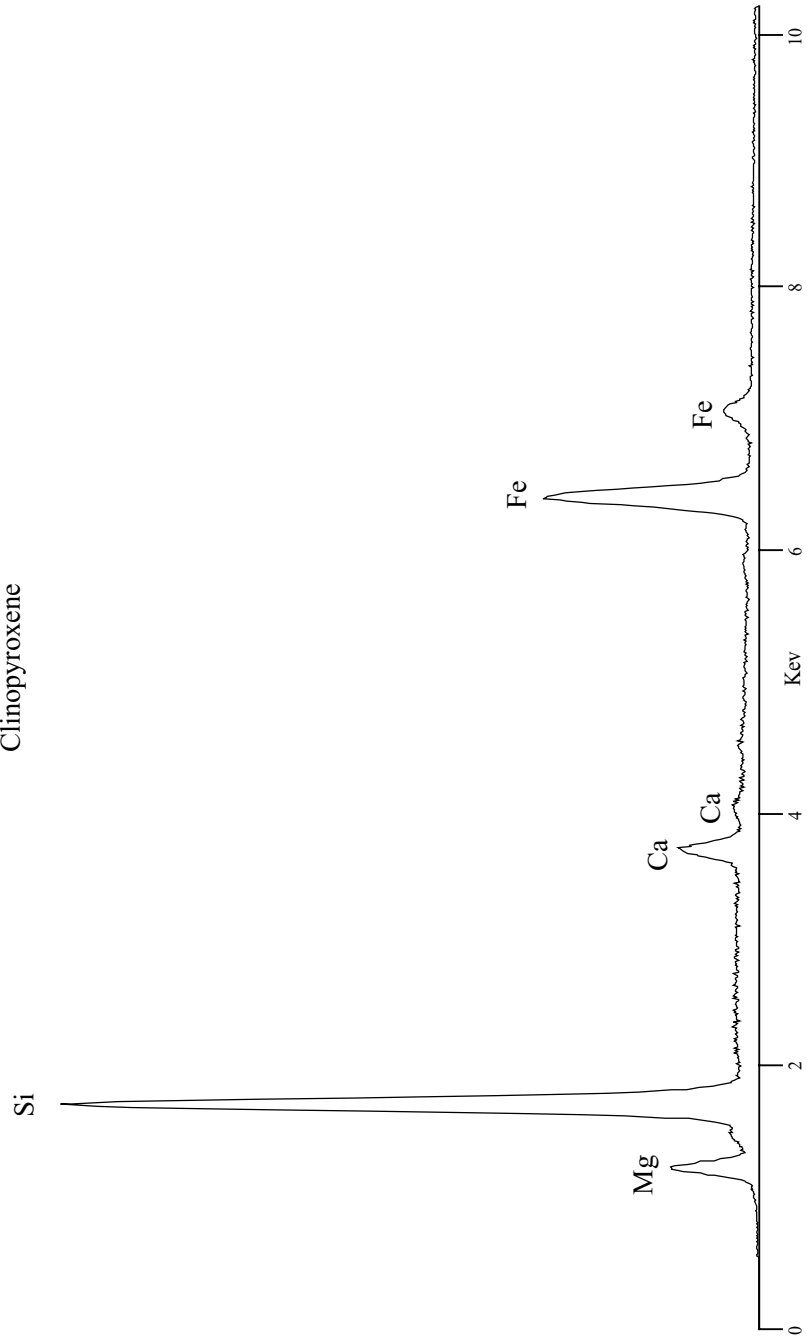
Clinopyroxene

Composition	
Na ₂ O	1.27
MgO	16.65
Al ₂ O ₃	8.73
SiO ₂	50.73
CaO	15.82
TiO ₂	0.74
MnO	0.13
FeO	6.32



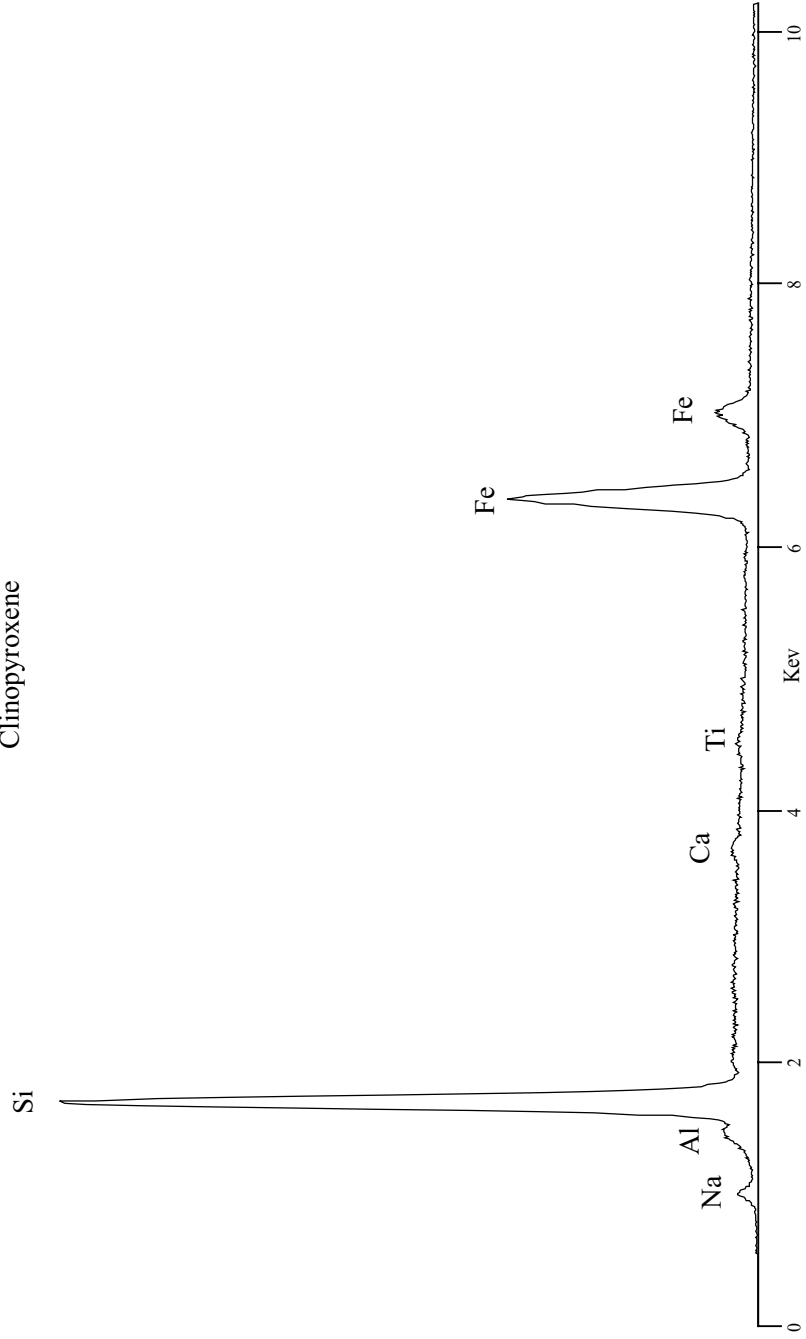
Pigeonite $(\text{Mg,Fe}^{+2},\text{Ca})(\text{Mg,Fe}^{+2})[\text{Si}_2\text{O}_6]$

Clinopyroxene



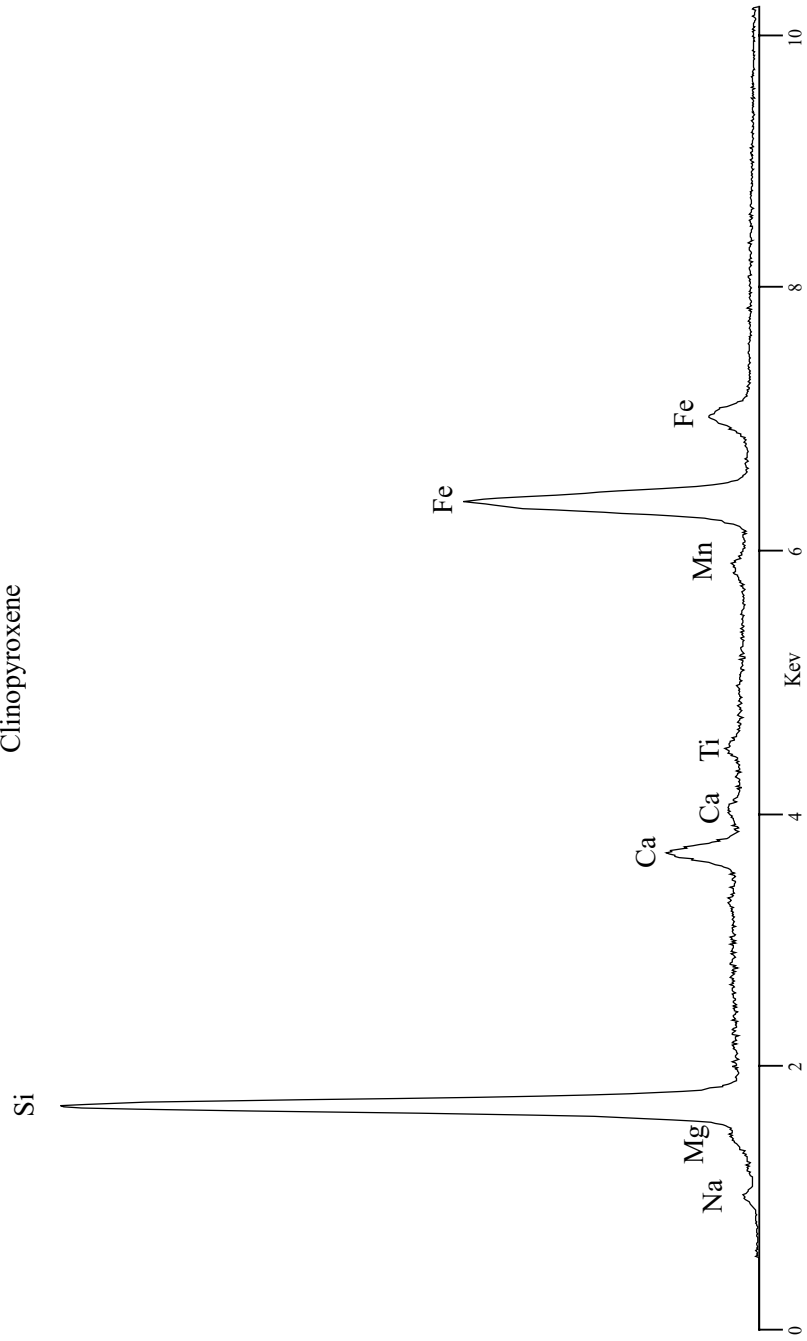
Aegerine (Acmite) $\text{NaFe}^{+3}[\text{Si}_2\text{O}_6]$

Clinopyroxene



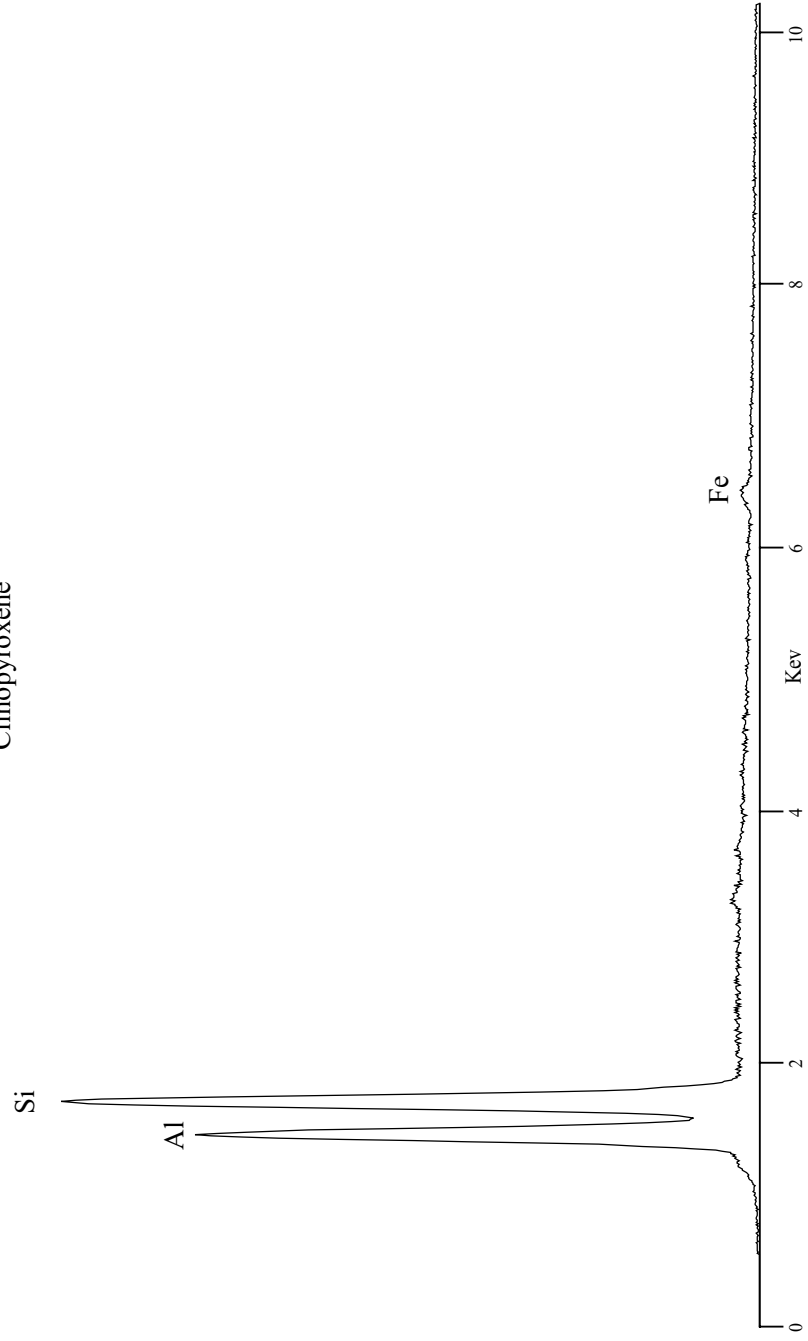
Aegerine-augite $(\text{Na,Ca})(\text{Fe}^{+3},\text{Fe}^{+3},\text{Mg})[\text{Si}_2\text{O}_6]$

Clinopyroxene



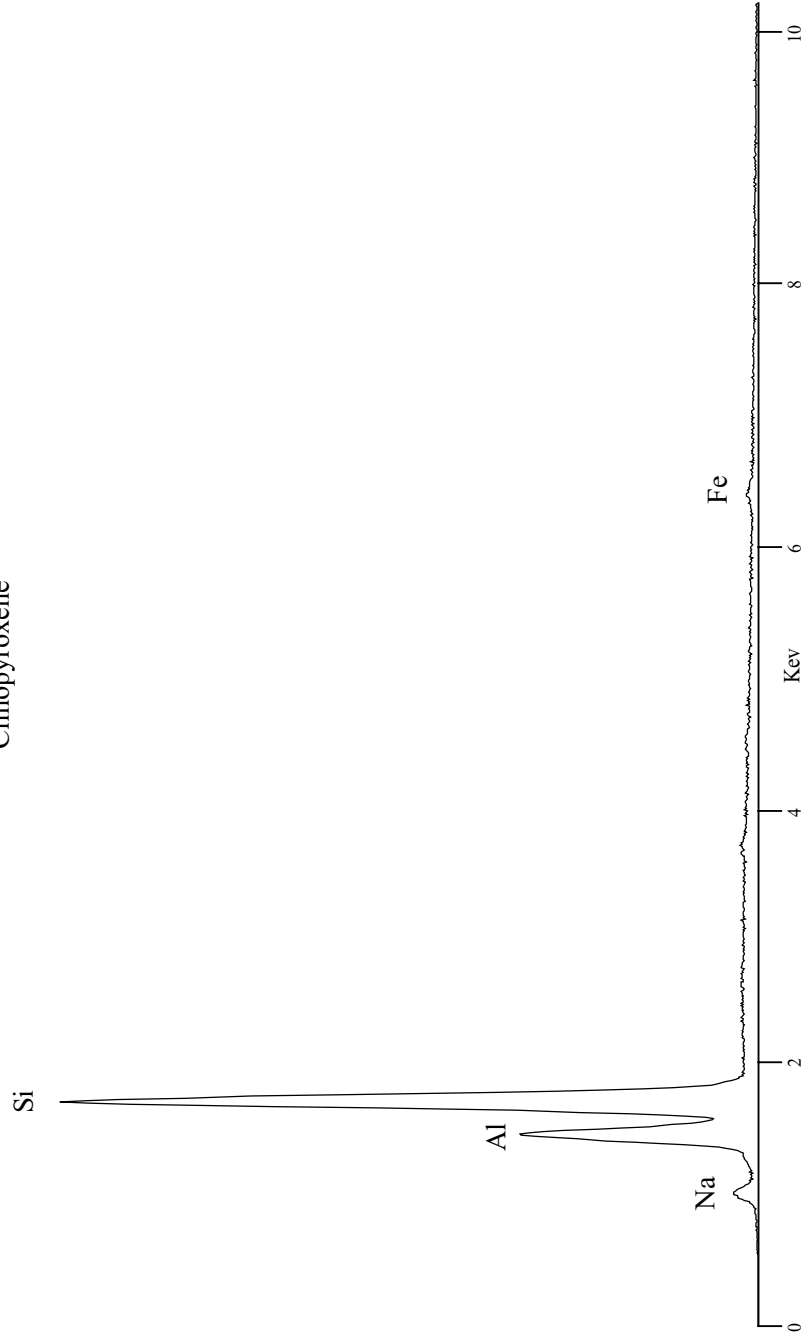
Spodumene $\text{LiAl}[\text{Si}_2\text{O}_6]$

Clinopyroxene

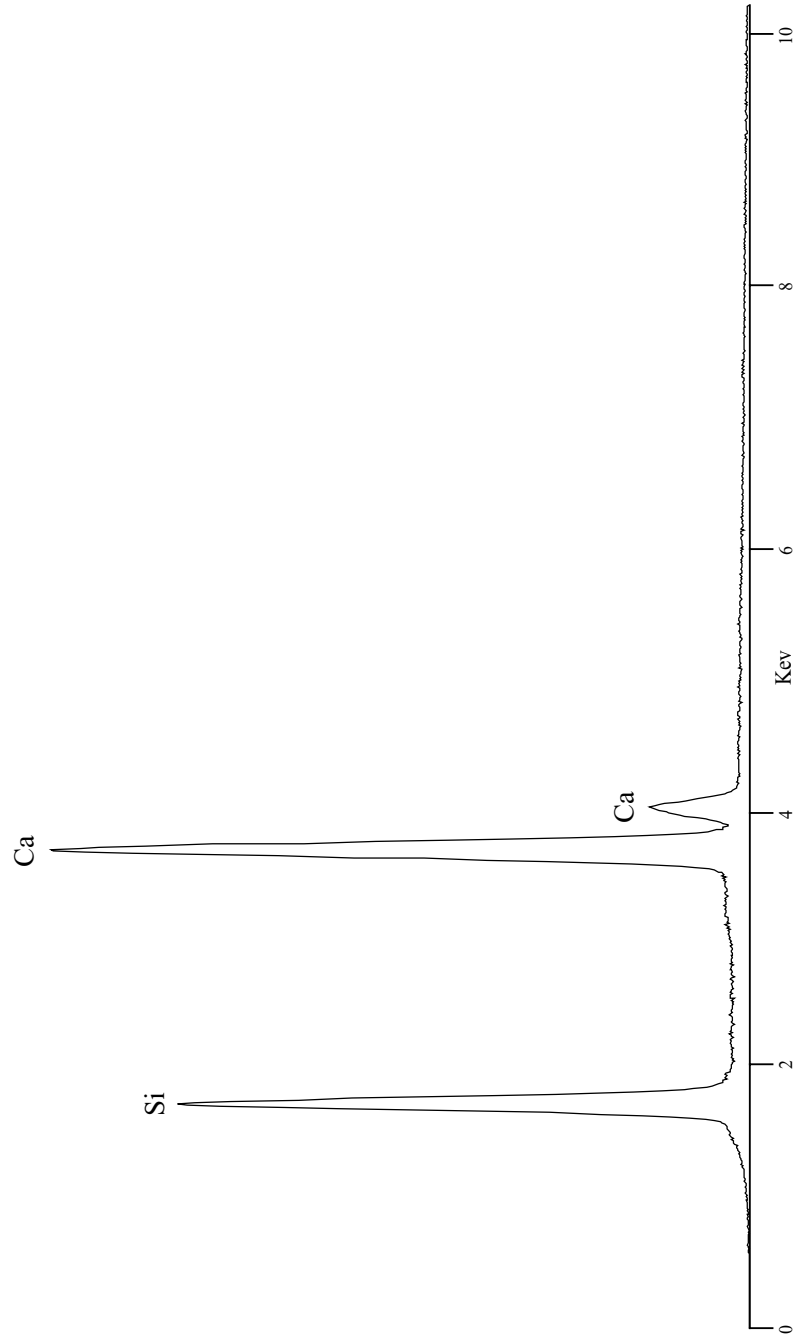


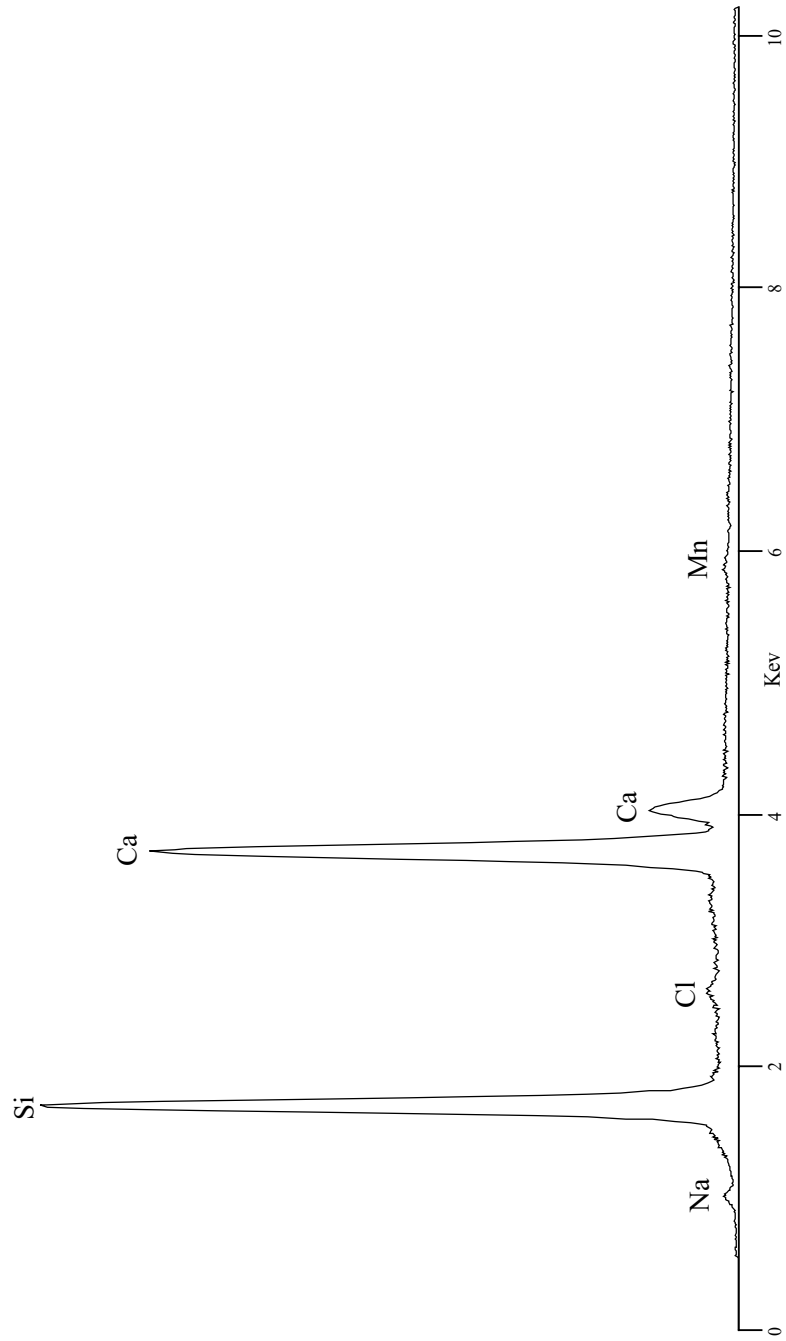
Jadeite $\text{NaAl}[\text{Si}_2\text{O}_6]$

Clinopyroxene

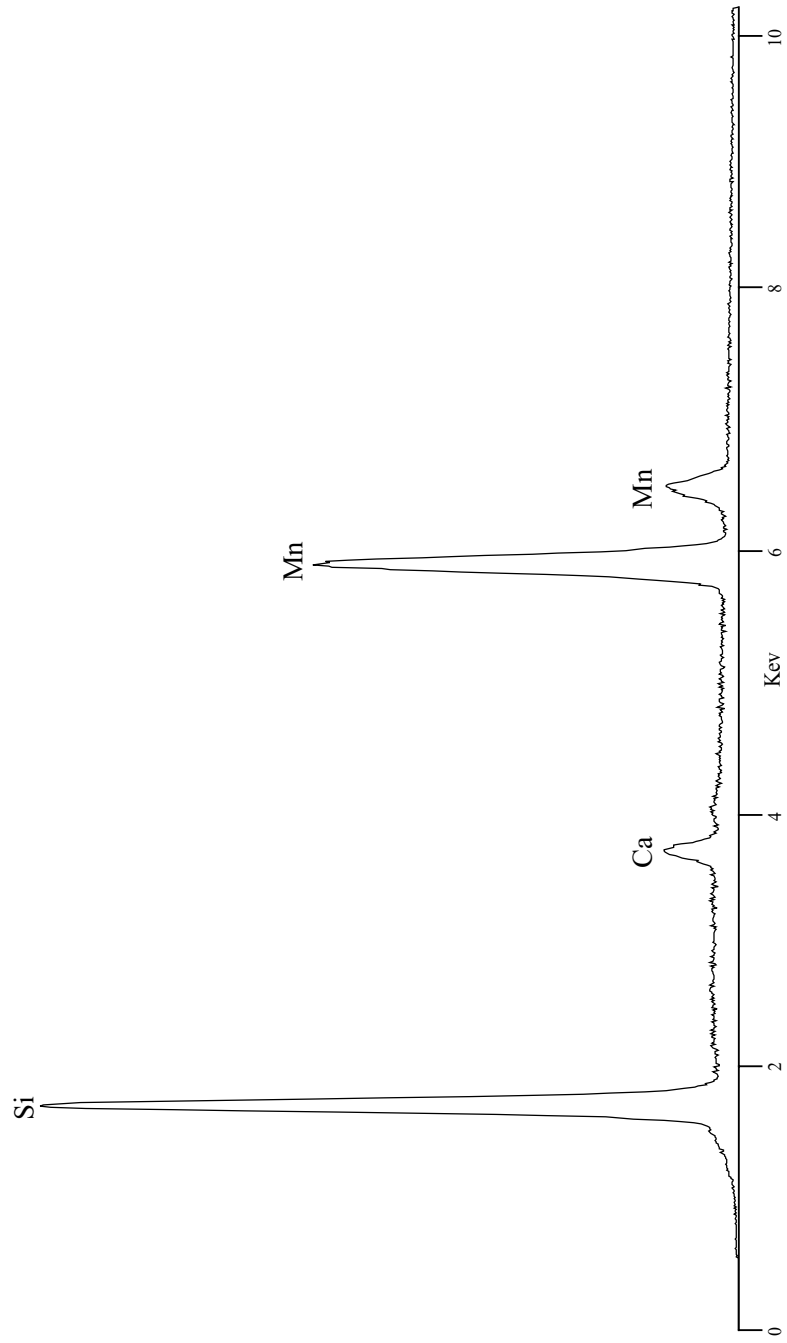


Wollastonite $\text{Ca}[\text{SiO}_3]$

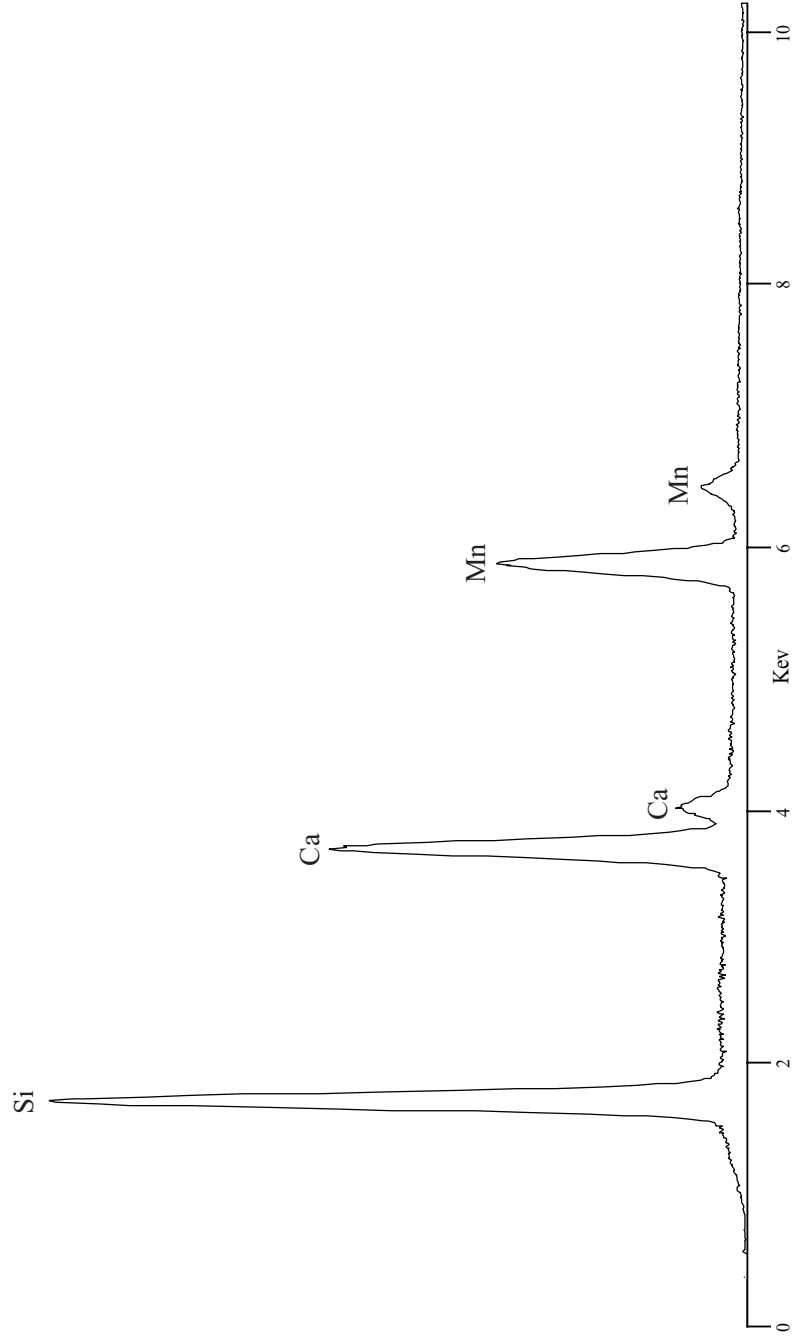


Pectolite $\text{Ca}_2\text{NaH}[\text{SiO}_3]_3$ 

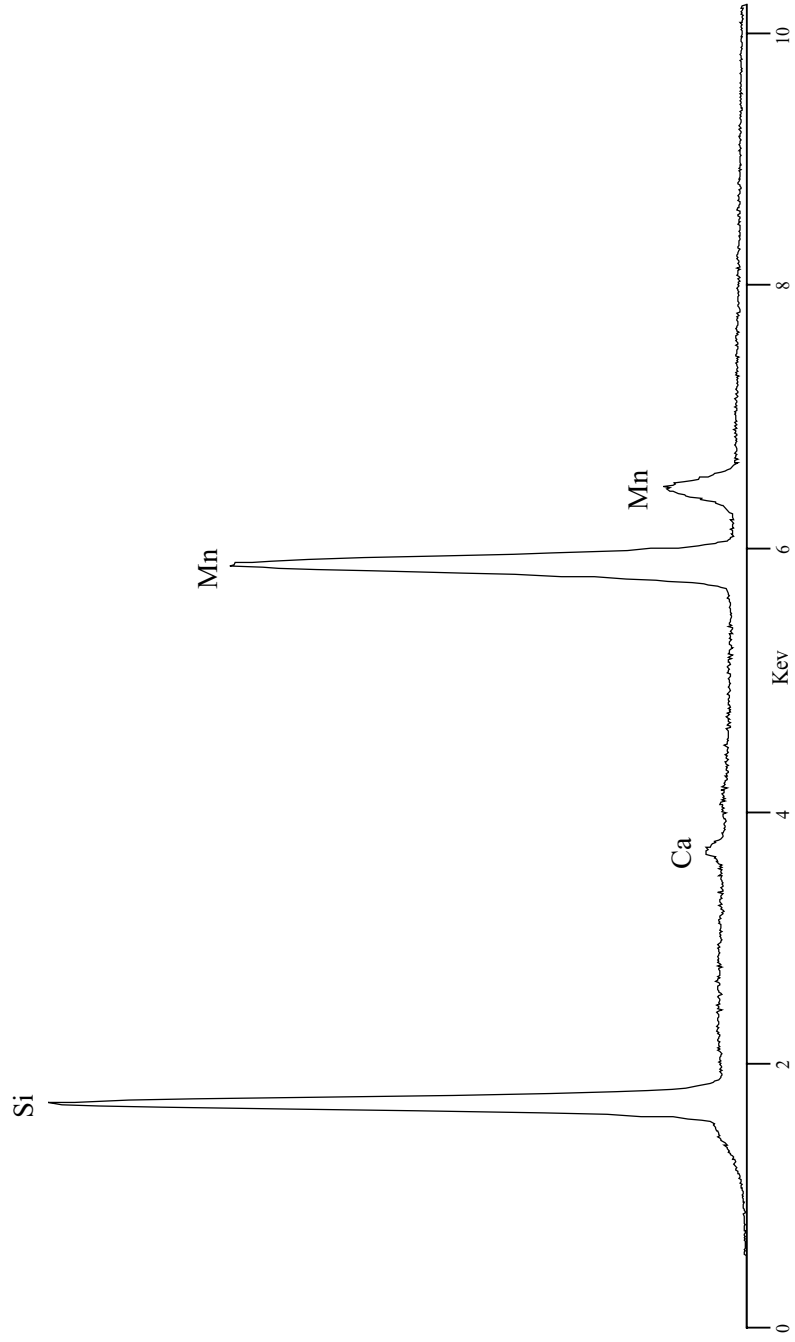
Rhodonite (Mn,Ca,Fe)[SiO₃]



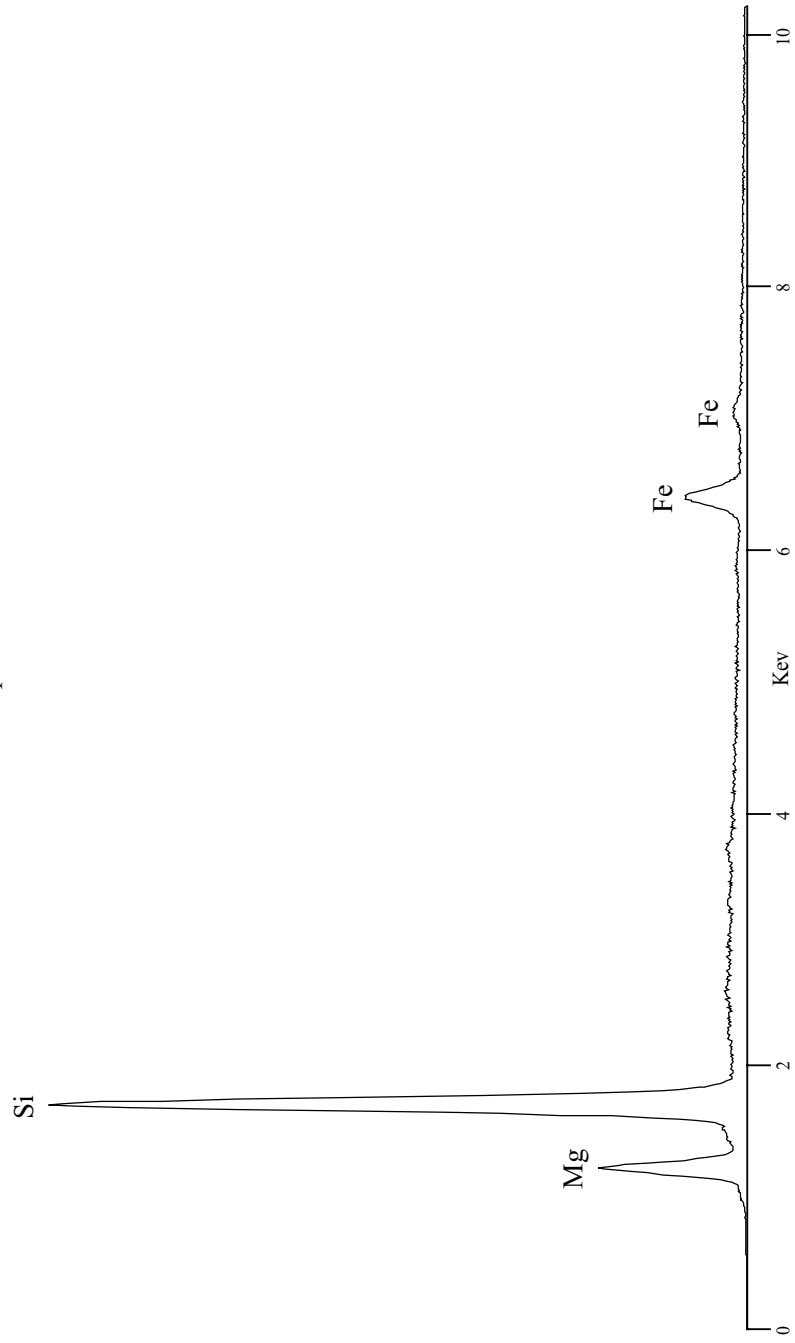
Bustamite (Mn,Ca,Fe)[SiO₃]



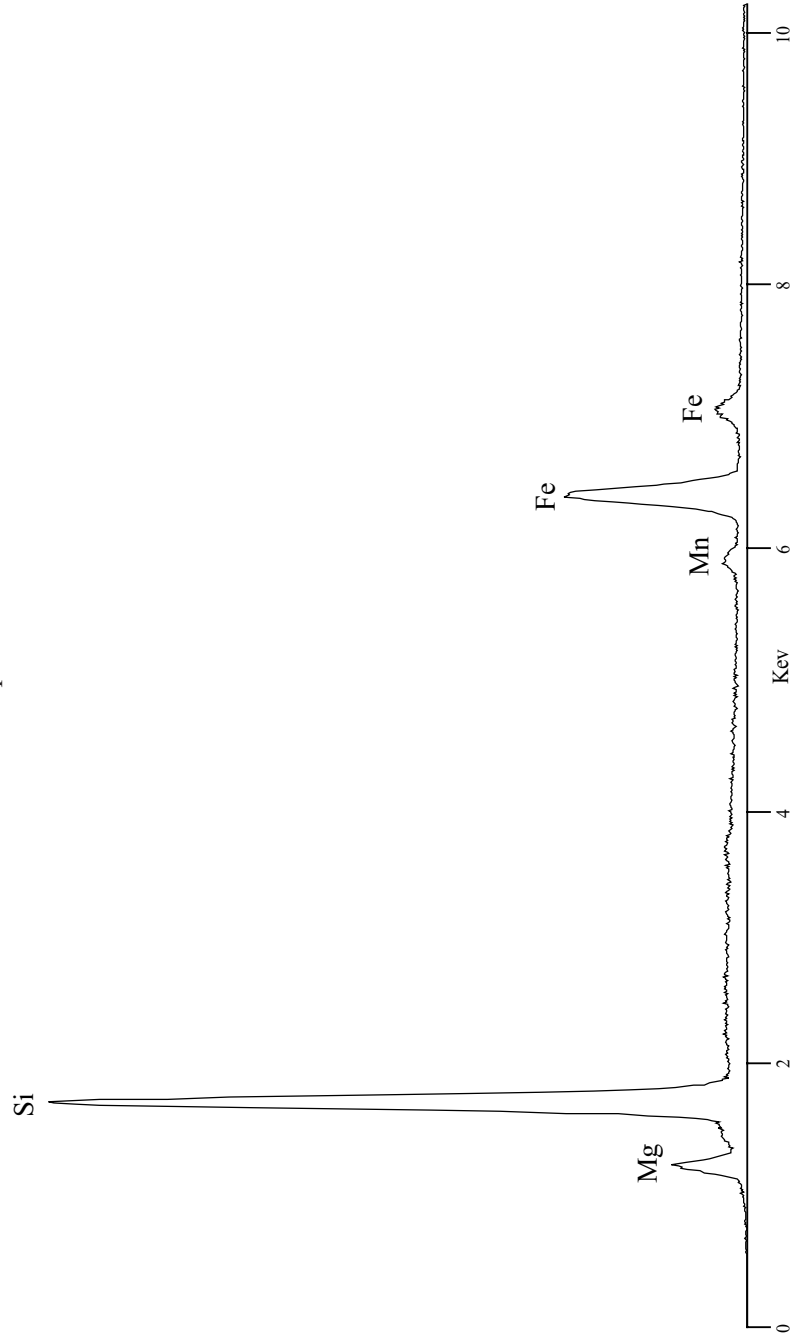
Pyroxmanginite (Mn,Fe)[SiO₃]



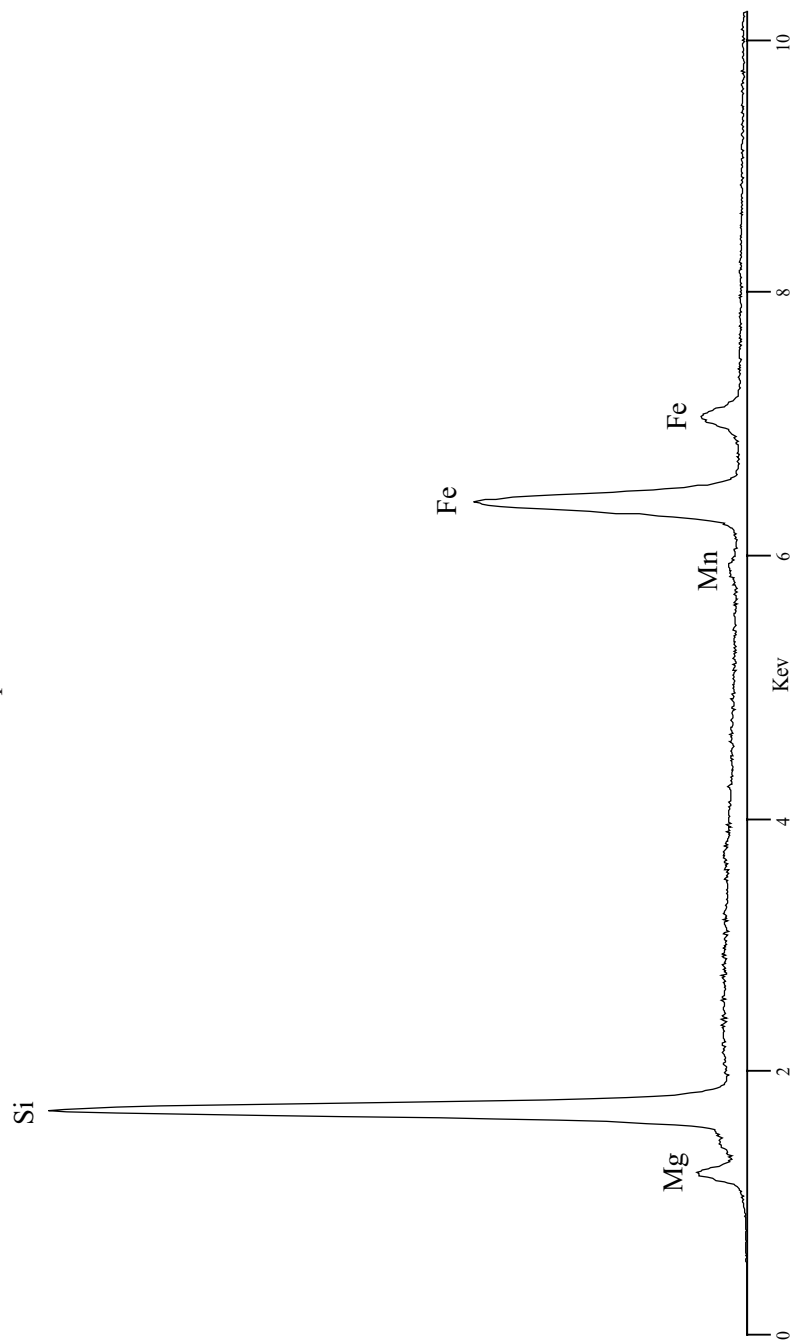
Anthophyllite $(\text{Mg,Fe}^{+2})_7[\text{Si}_8\text{O}_{22}](\text{OH,F})_2$
Amphibole



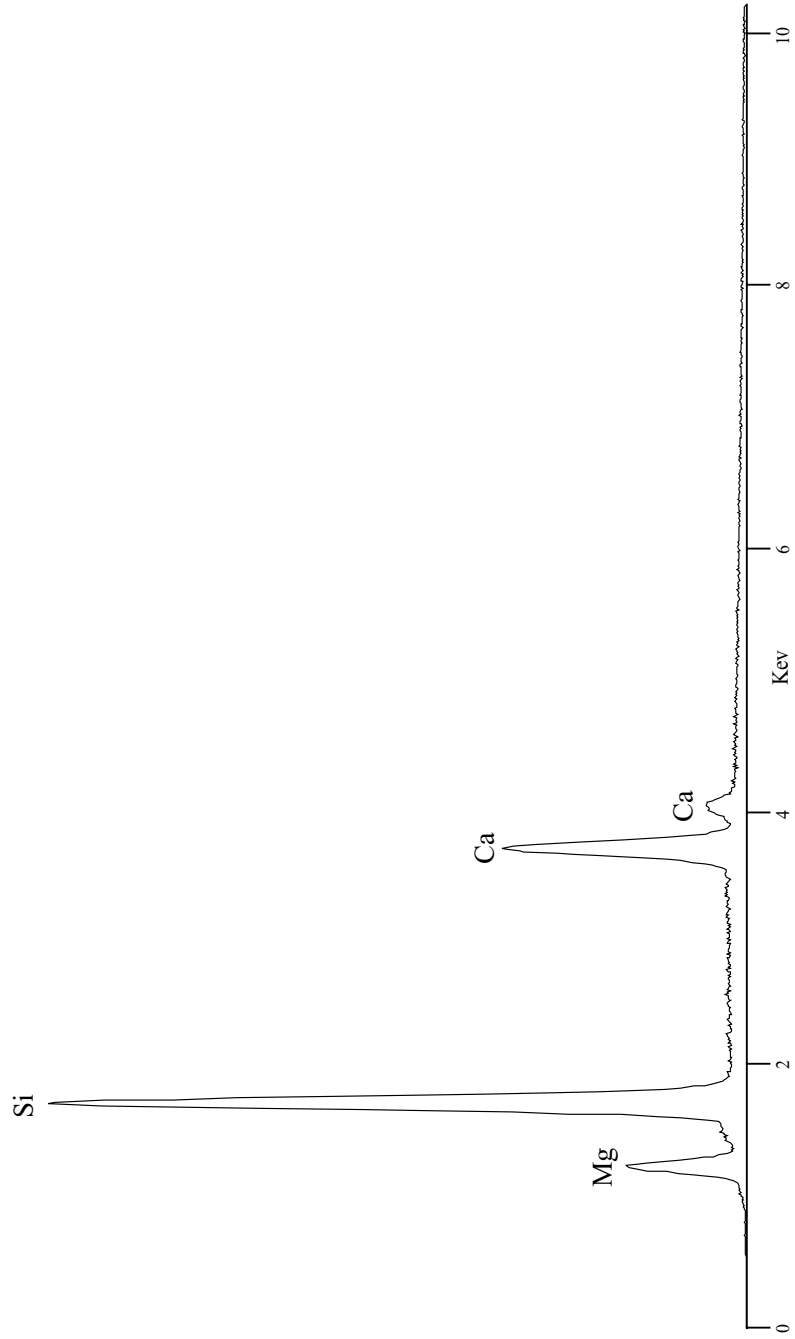
Cummingtonite $(\text{Mg}, \text{Fe}^{+2})_7[\text{Si}_8\text{O}_{22}](\text{OH})_2$
Amphibole



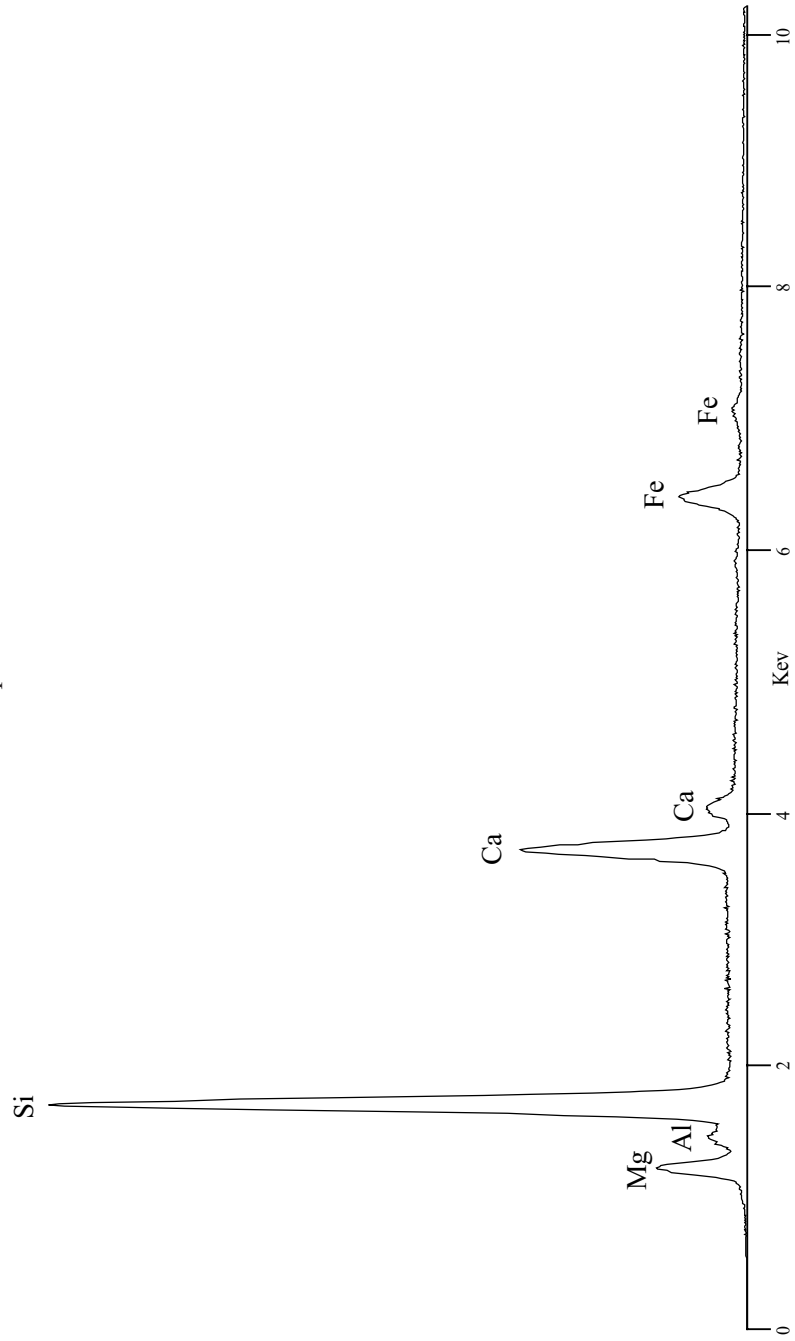
Grunerite $(\text{Fe}^{+2}, \text{Mg})_7[\text{Si}_8\text{O}_{22}](\text{OH})_2$
Amphibole



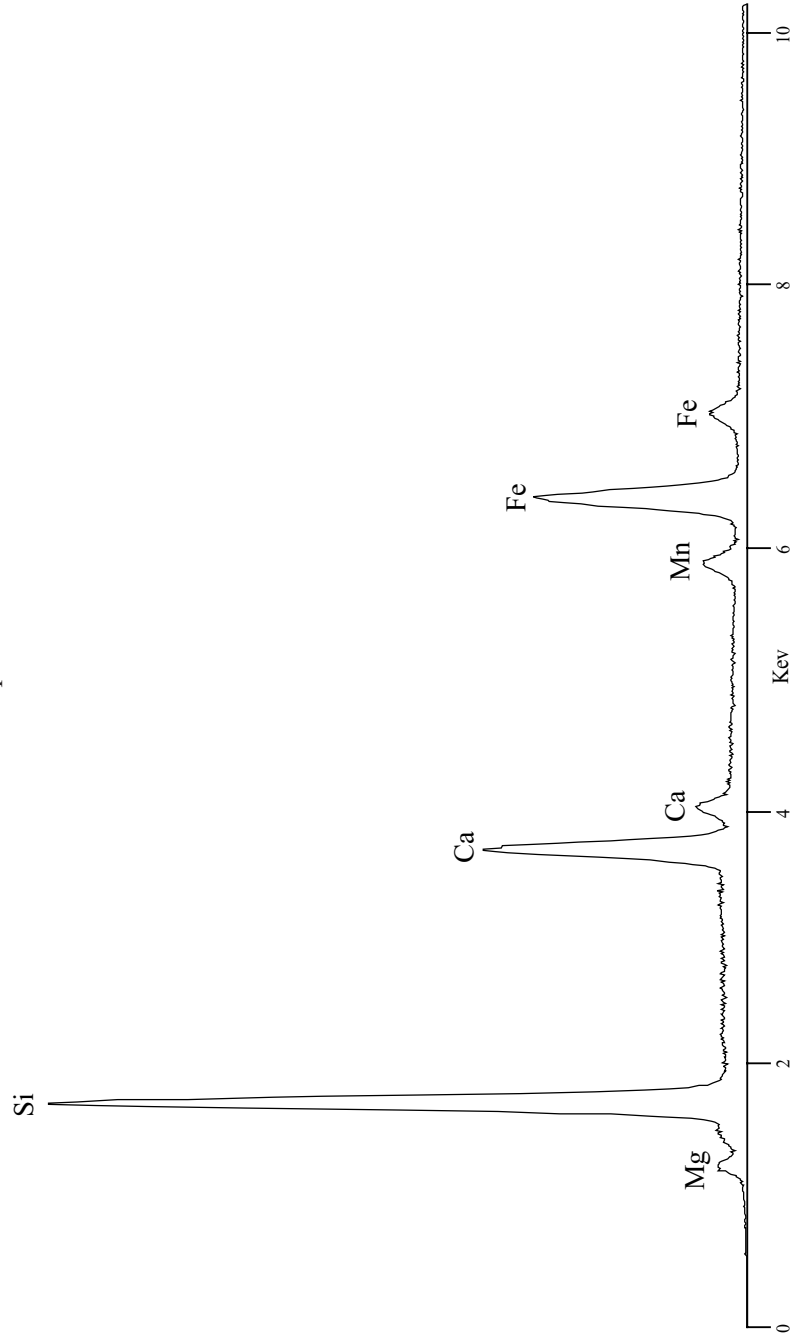
Tremolite $\text{Ca}_2\text{Mg}_5[\text{Si}_8\text{O}_{22}](\text{OH},\text{F})_2$
Amphibole



Actinolite $\text{Ca}_2(\text{Mg},\text{Fe}^{+2})_5[\text{Si}_8\text{O}_{22}](\text{OH},\text{F})_2$
Amphibole

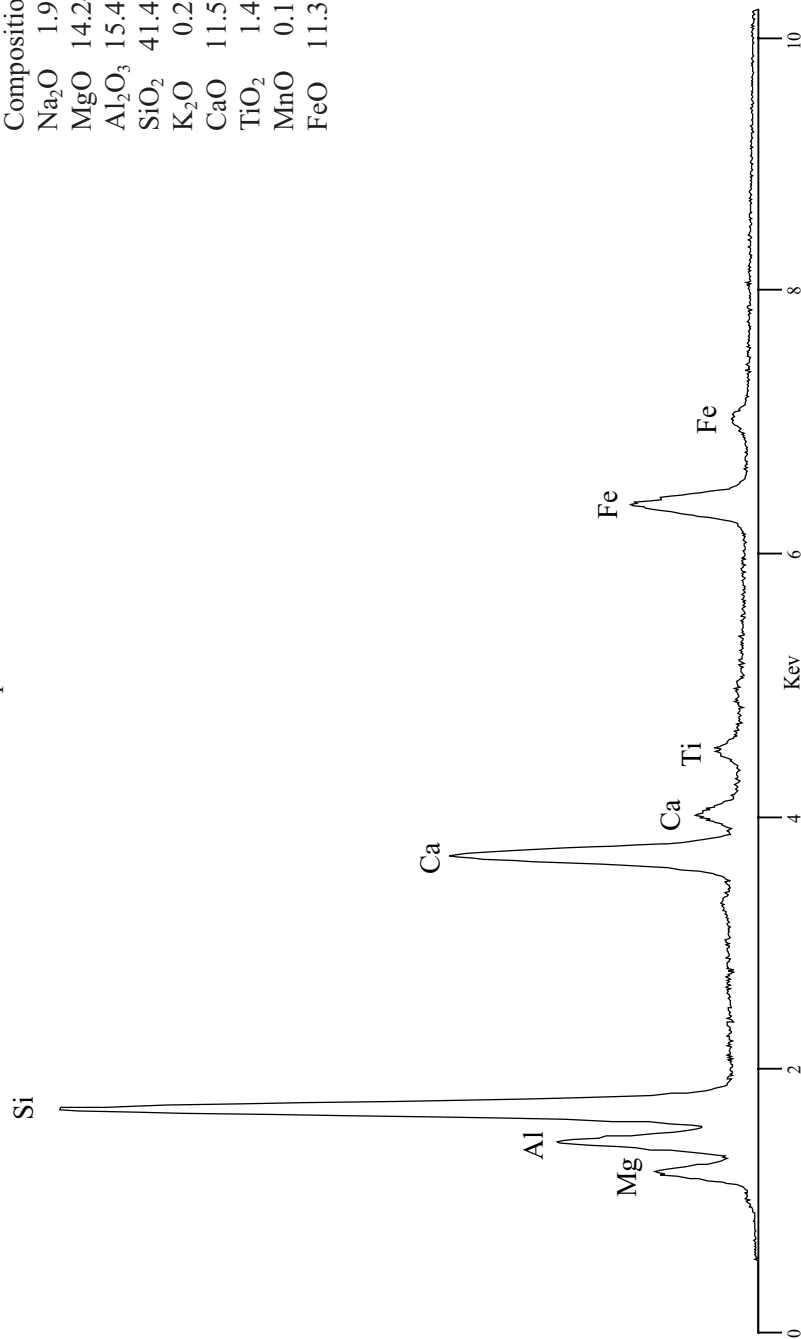


Ferroactinolite $\text{Ca}_2\text{Fe}_5^{+2}[\text{Si}_8\text{O}_{22}](\text{OH}_2)$
Amphibole



Hornblende $(\text{Na,K})_{0-1}\text{Ca}_2(\text{Mg,Fe}^{+2},\text{Fe}^{+3},\text{Al})_3[\text{Si}_{6-7}\text{Al}_{2-1}\text{O}_{22}](\text{OH,F})_2$
 Amphibole Smithsonian Standard USNM 111356

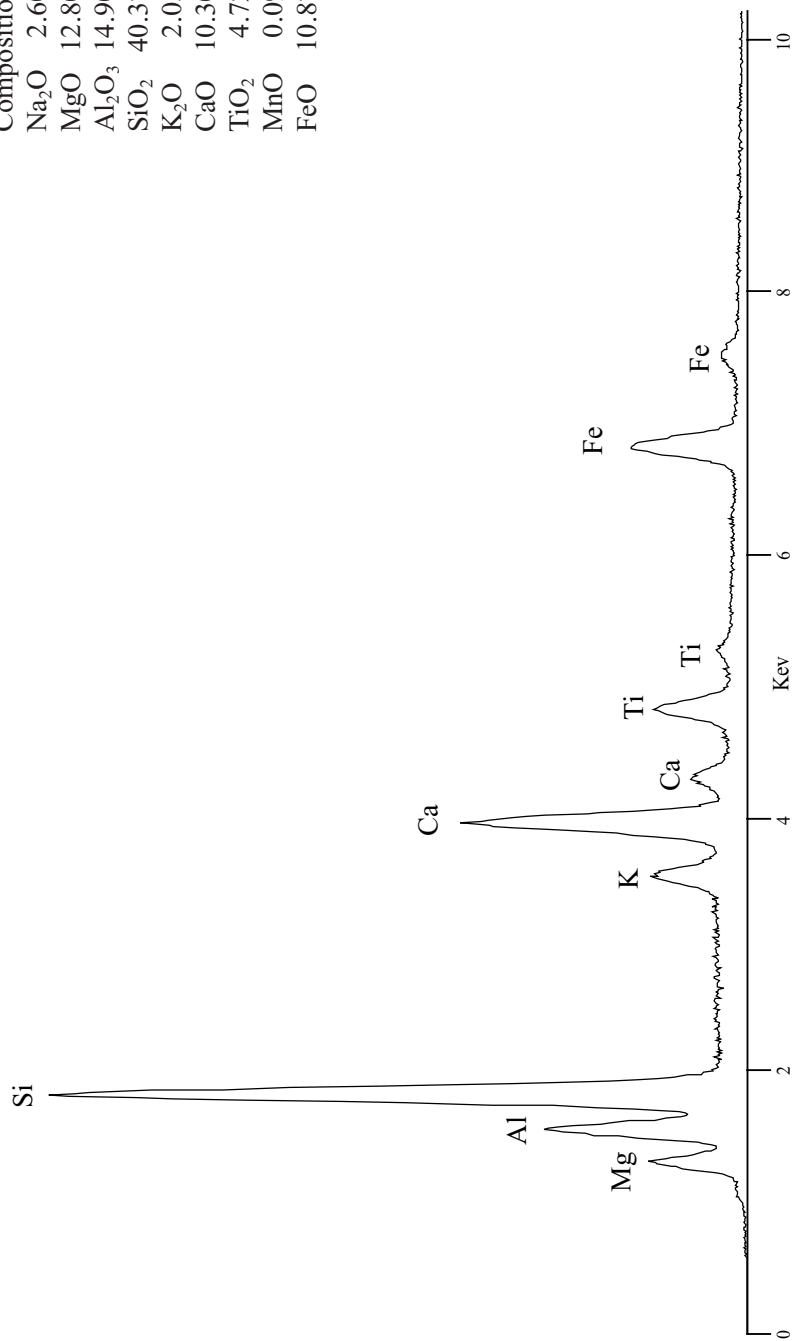
Composition	
Na ₂ O	1.91
MgO	14.24
Al ₂ O ₃	15.47
SiO ₂	41.46
K ₂ O	0.21
CaO	11.55
TiO ₂	1.41
MnO	0.15
FeO	11.38



Homblende $(\text{Na,K})_{0-1}\text{Ca}_2(\text{Mg,Fe}^{+2},\text{Fe}^{+3},\text{Al})_5[\text{Si}_{6-7}\text{Al}_{2-1}\text{O}_{22}](\text{OH,F})_2$
 Amphibole

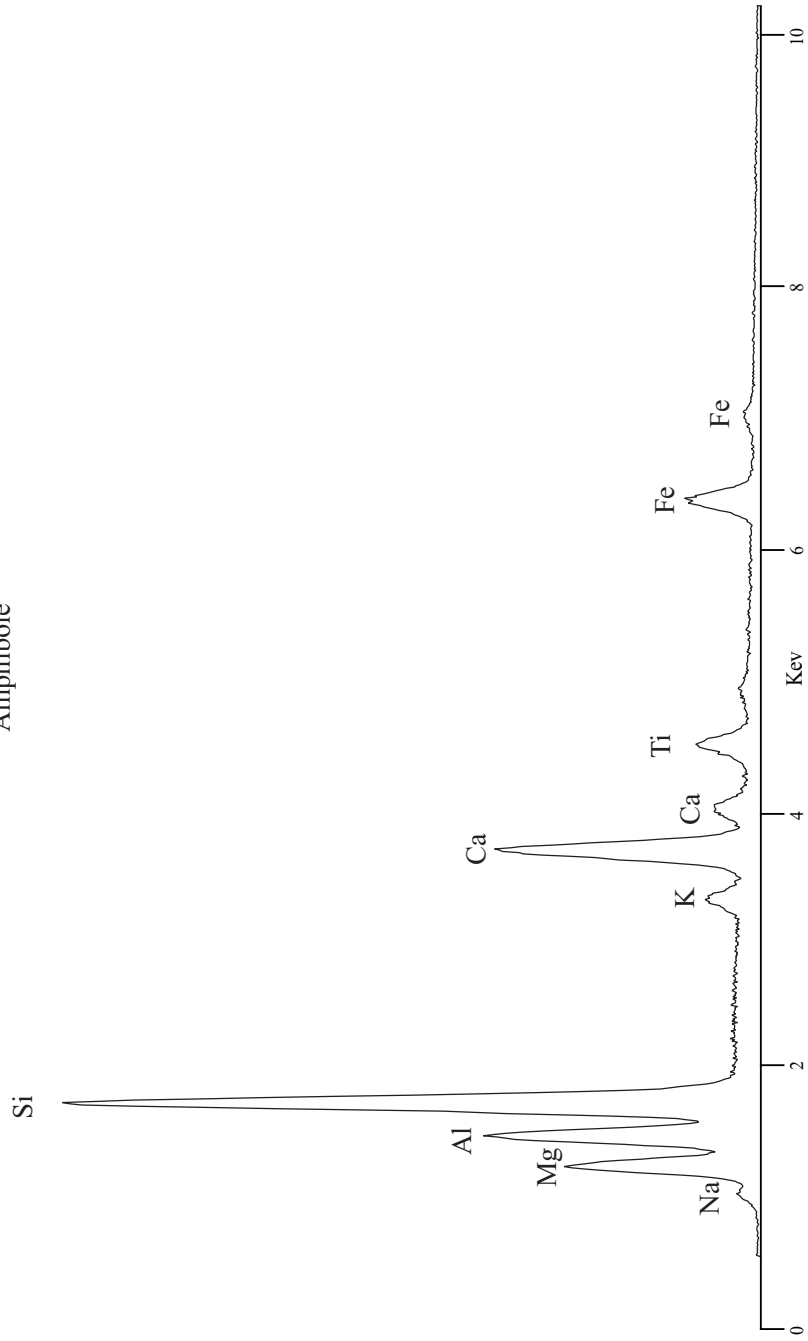
Smithsonian Standard
 USNM 143965

Composition
 Na₂O 2.60
 MgO 12.80
 Al₂O₃ 14.90
 SiO₂ 40.37
 K₂O 2.05
 CaO 10.30
 TiO₂ 4.72
 MnO 0.09
 FeO 10.87

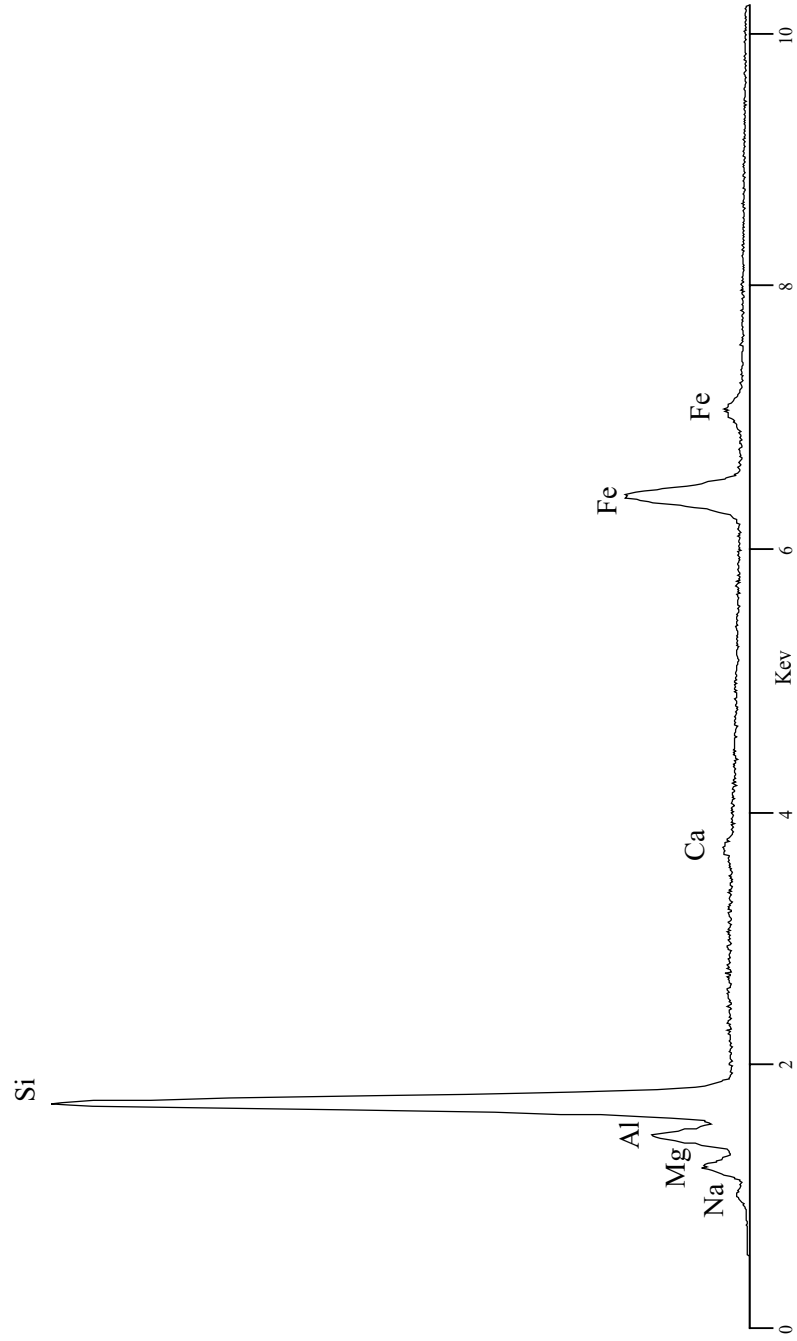


Kaersutite $\text{Ca}_2(\text{Na,K})(\text{Mg,Fe}^{+2},\text{Fe}^{+3})_4\text{Ti}[\text{Si}_6\text{Al}_2\text{O}_{22}](\text{O,OH,F})_2$

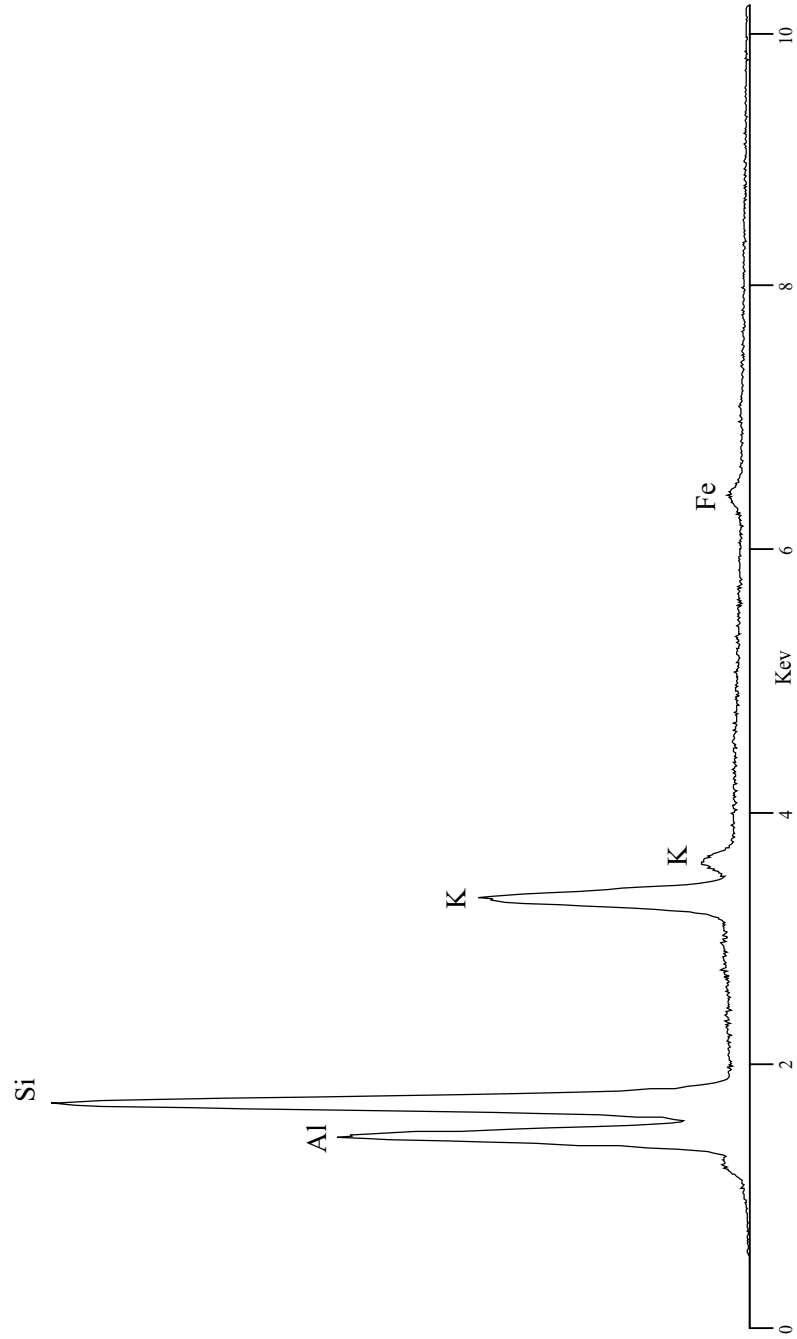
Amphibole



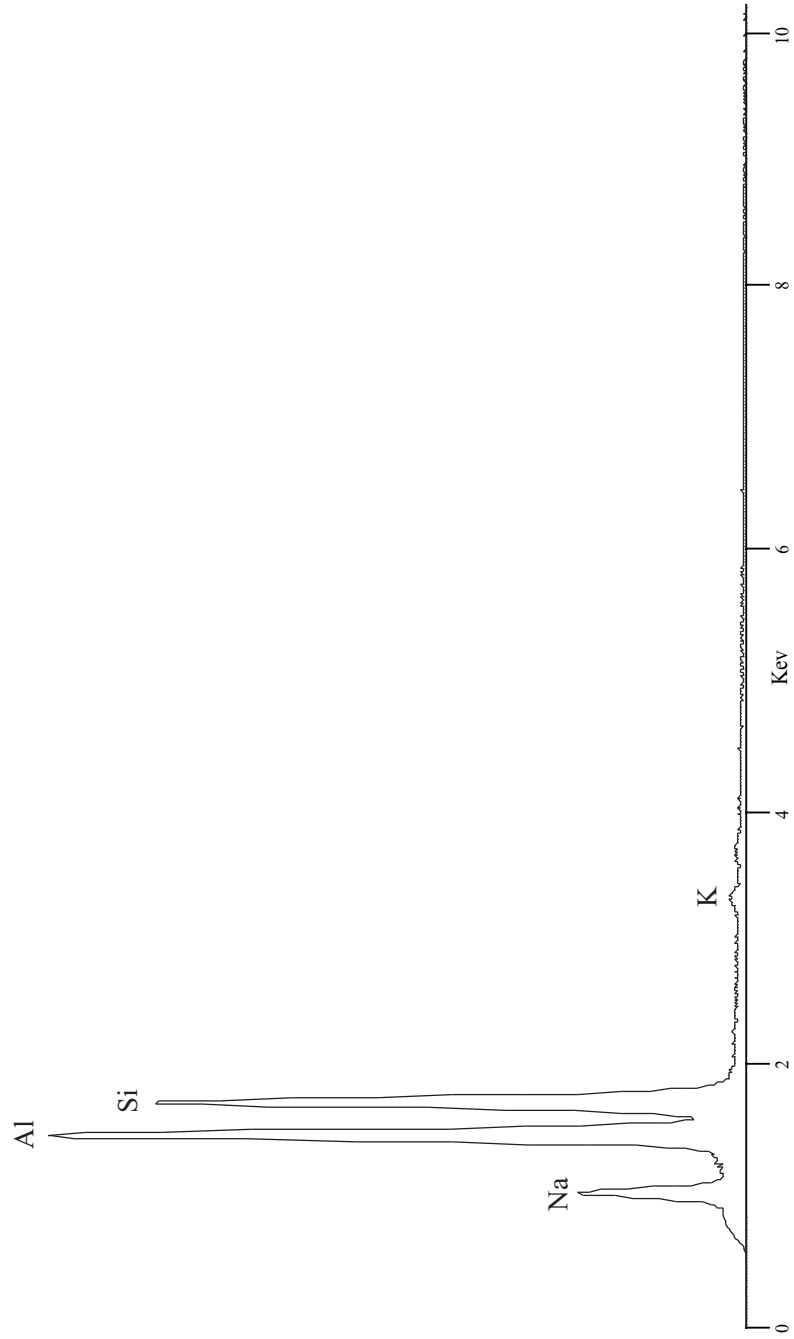
Glaucophane $\text{Na}_2\text{Mg}_3\text{Al}_2[\text{Si}_8\text{O}_{22}](\text{OH})_2$
Amphibole



Muscovite $\text{K}_2\text{Al}_4[\text{Si}_6\text{Al}_2\text{O}_{20}](\text{OH,F})_4$
Mica

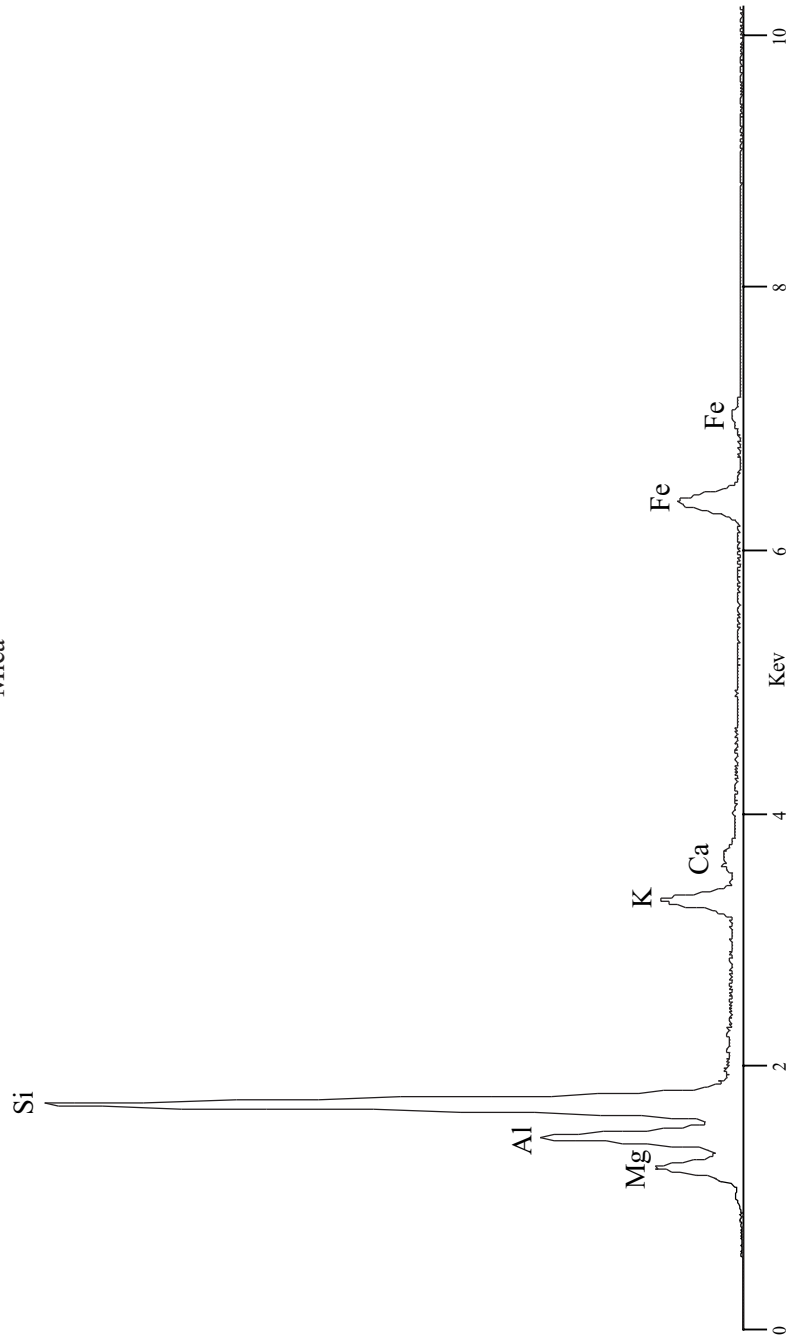


Paragonite $\text{Na}_2\text{Al}_4[\text{Si}_6\text{Al}_2\text{O}_{20}](\text{OH})_4$
Mica

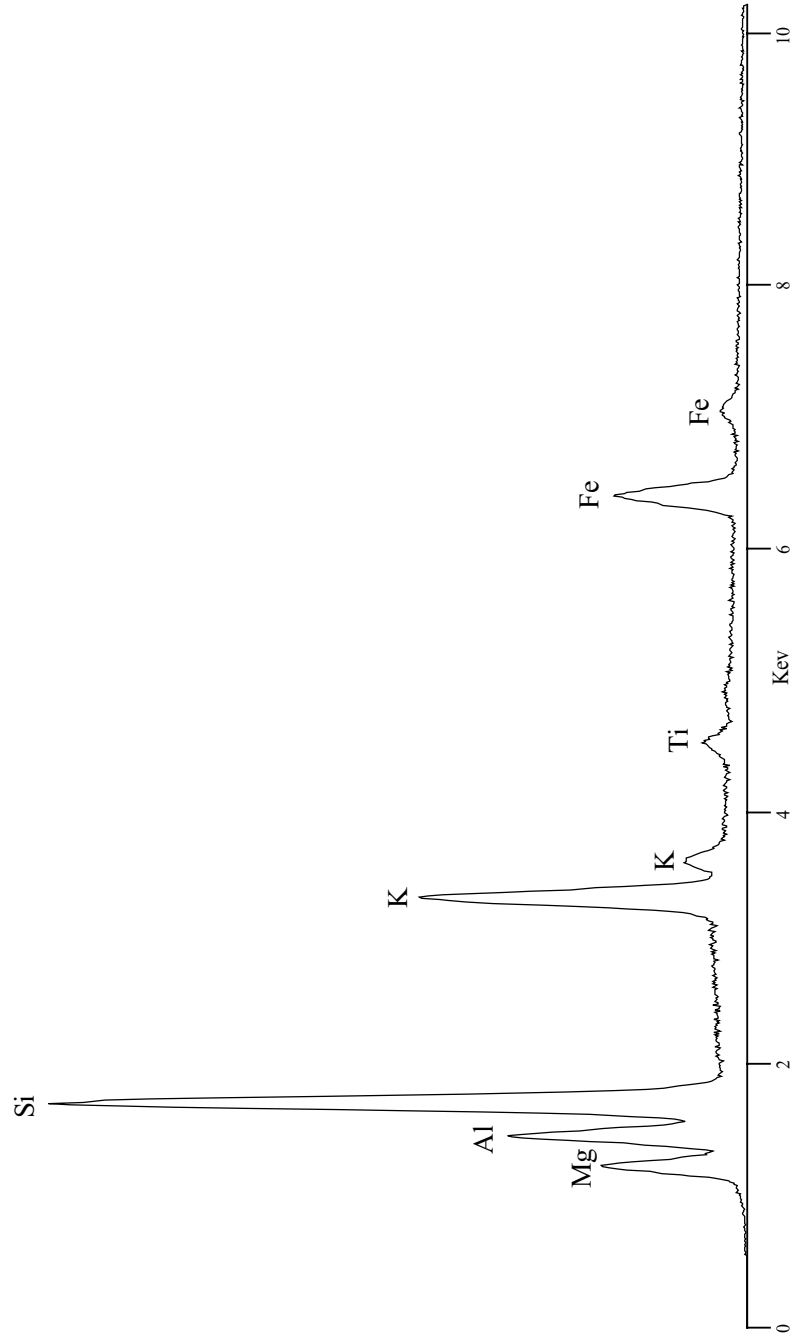


Glauconite $(K,Na,Ca)_{1.2-2.0}(Fe^{+3},Al,Fe^{+2},Mg)_{4.0}[Si_{7-7.6}Al_{1-0.4}O_{20}](OH)_4 \cdot nH_2O$

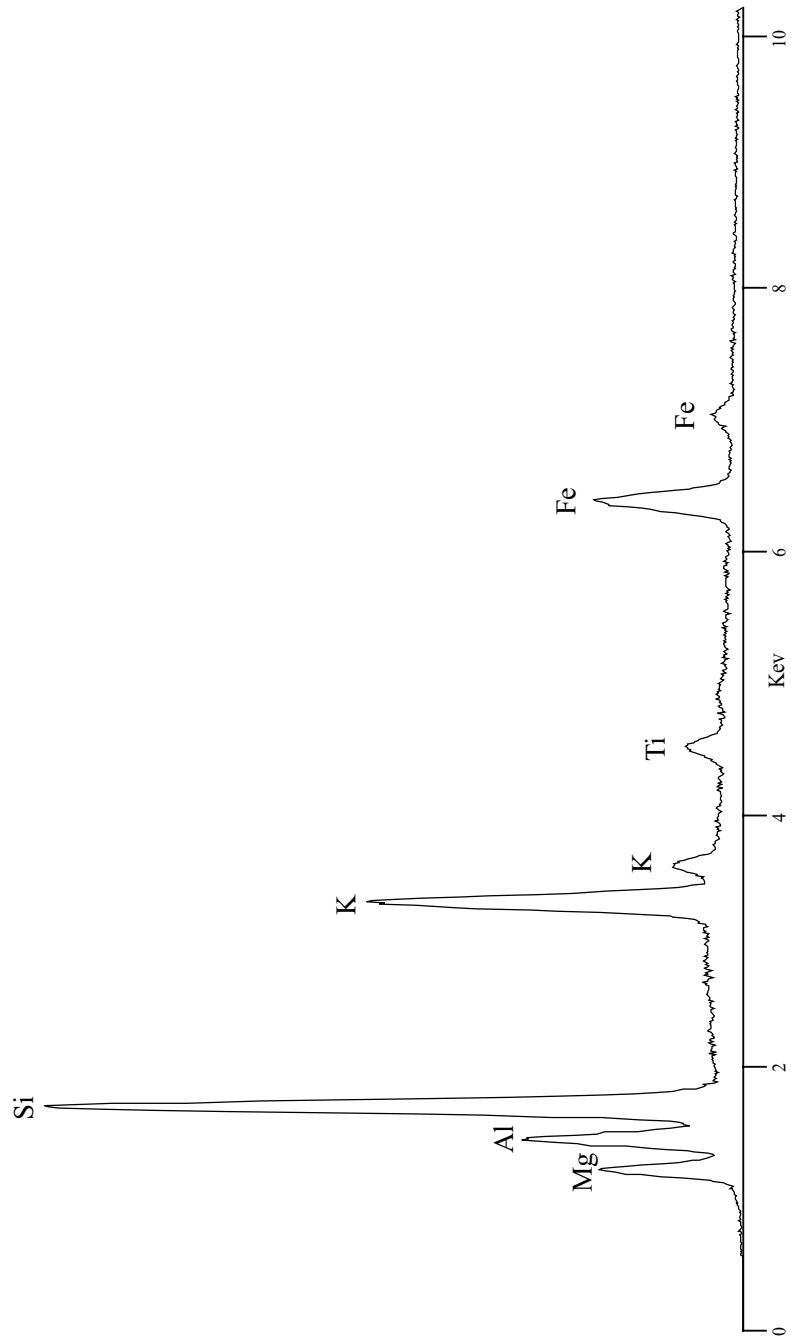
Mica



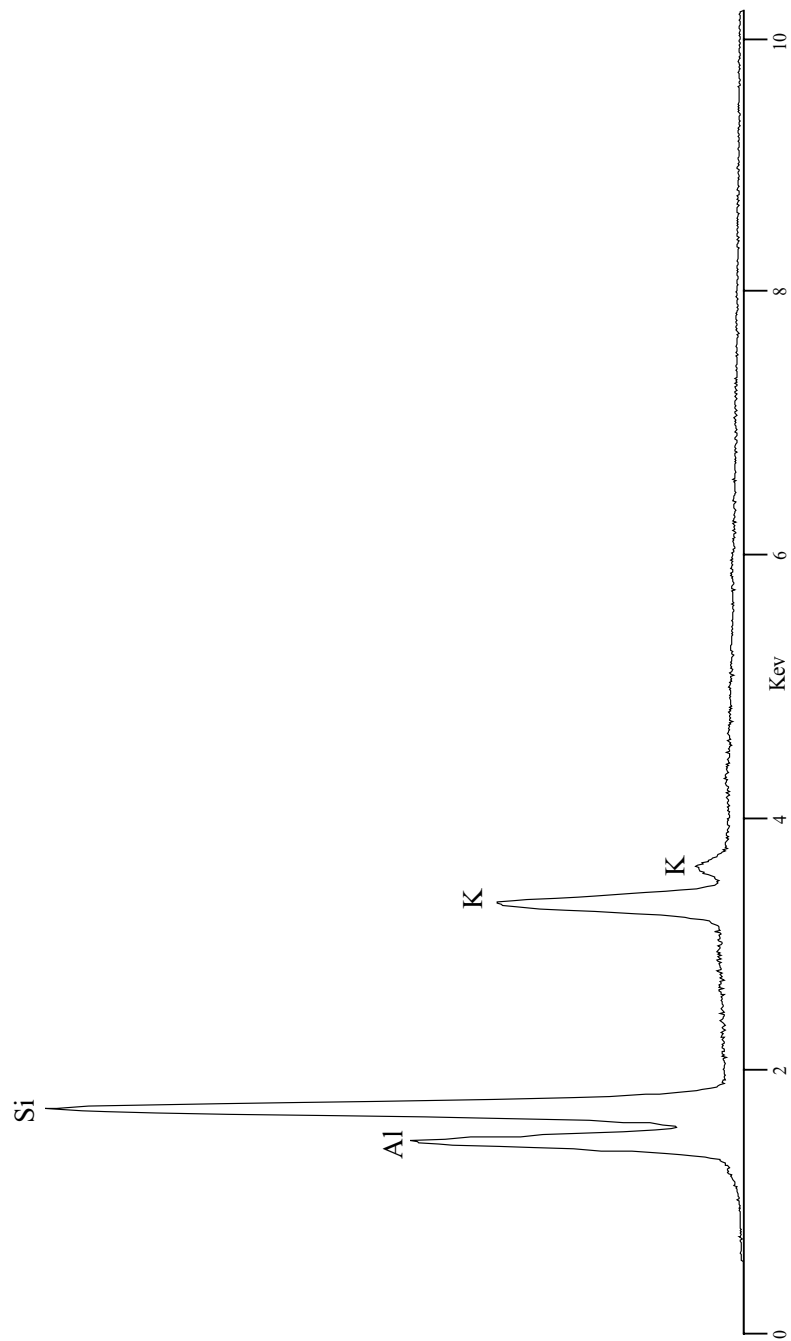
Phlogopite $K_2(Mg,Fe^{+2})_6[Si_6Al_2O_{20}](OH,F)_4$
Mica



Biotite $K_2(Mg,Fe^{+2})_{6-4}(Fe^{+3},Al,Ti)_{0-2}[Si_{6-5}Al_{2-3}O_{20}](OH,F)_4$
Mica

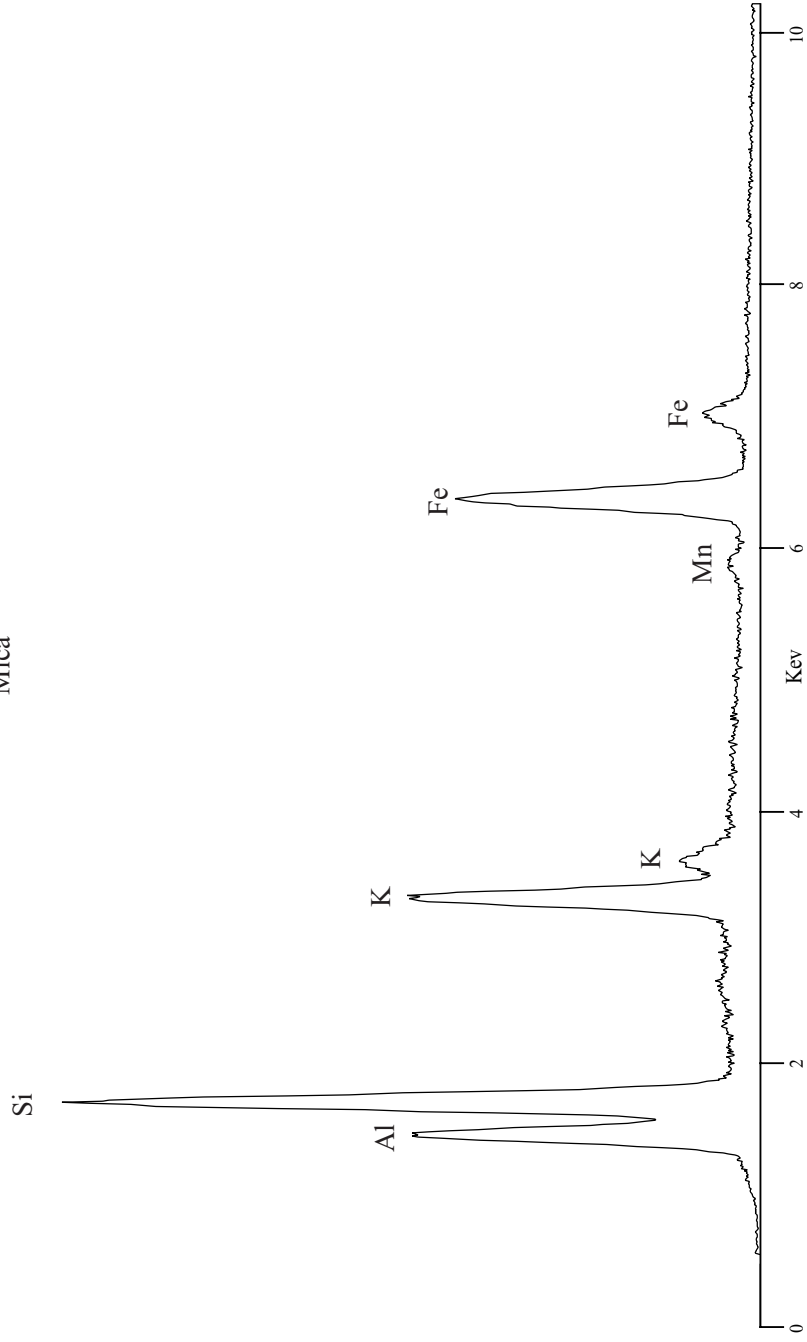


Lepidolite $K_2(Li,Al)_{5-6}[Si_{6-7}Al_{2-1}O_{20}](OH,F)_4$
Mica

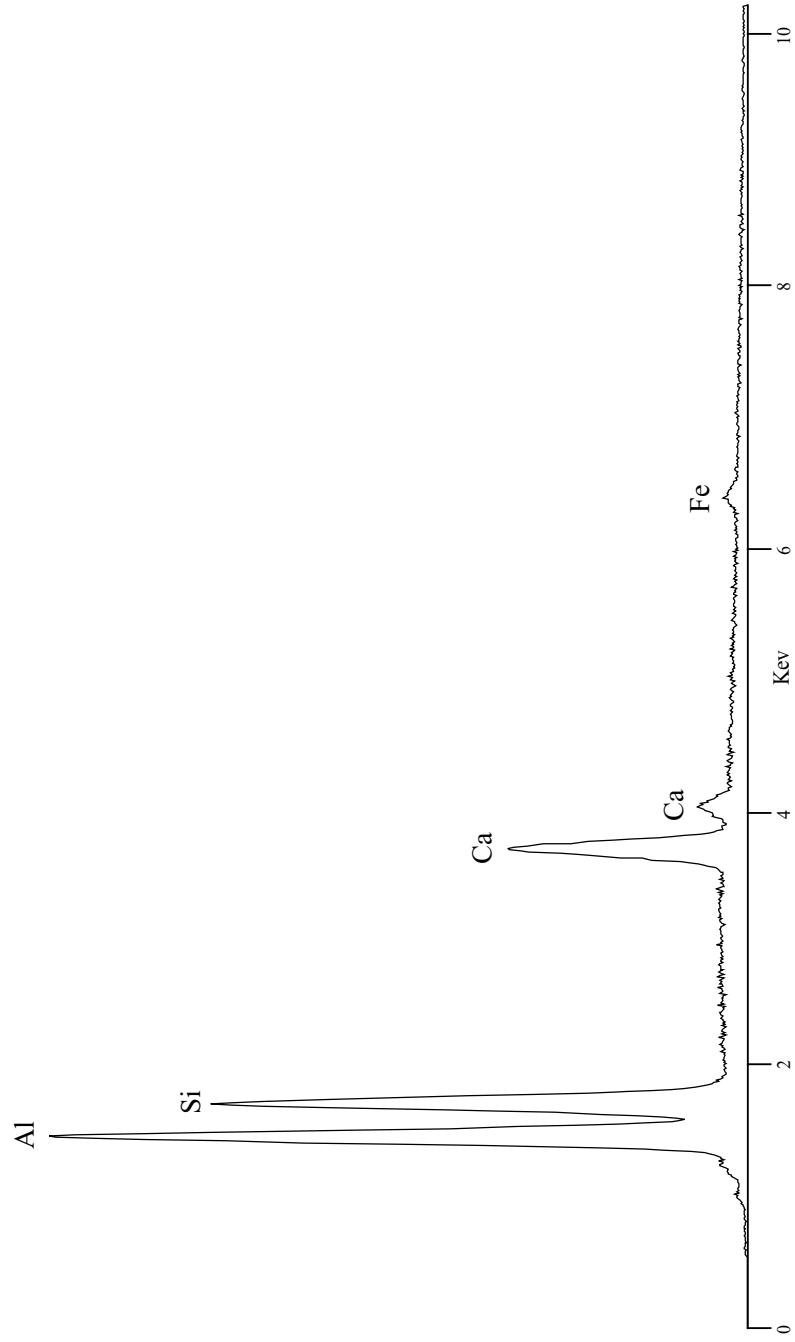


Zinnwaldite $\text{K}_2(\text{Fe}^{+2}_{2-1}, \text{Li}_{2-3}\text{Al}_2)[\text{Si}_{6-7}\text{Al}_{2-1}\text{O}_{20}](\text{F}, \text{OH})_4$

Mica

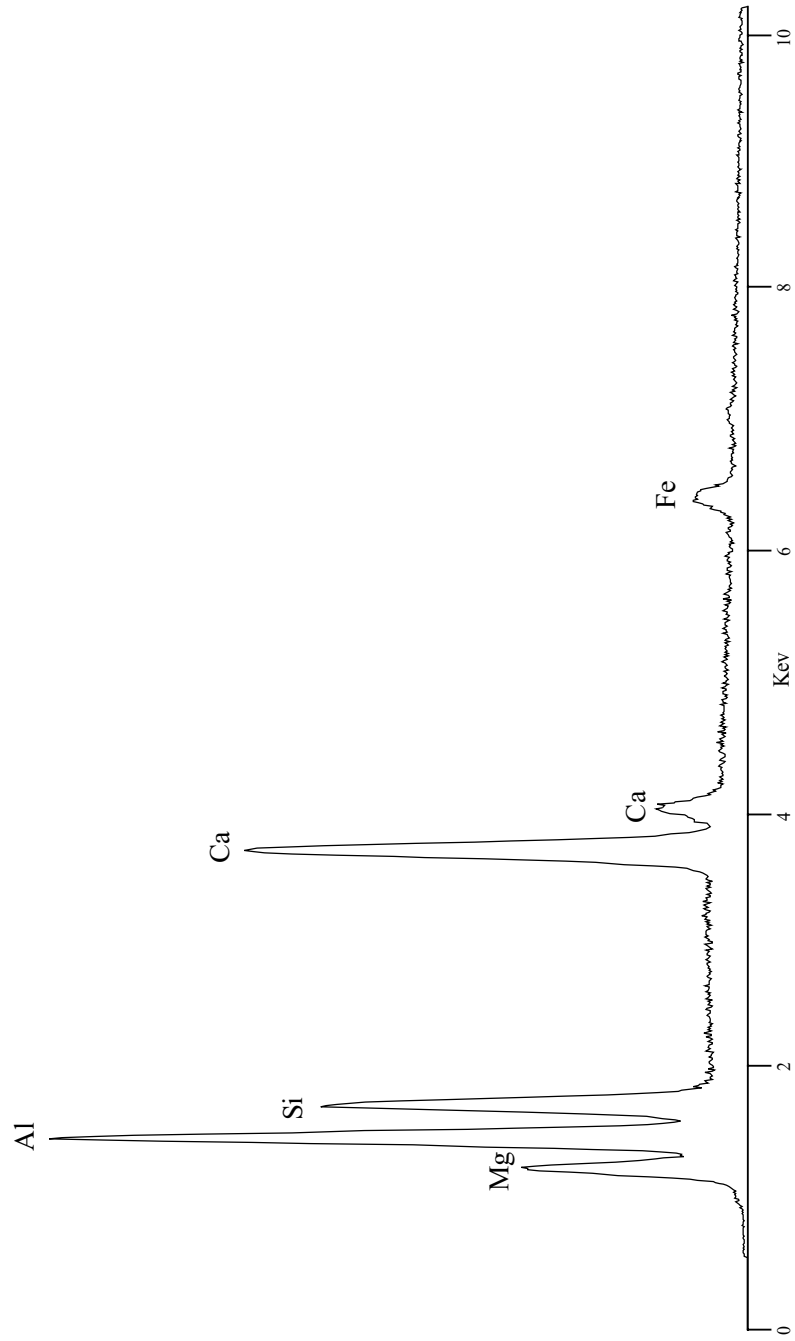


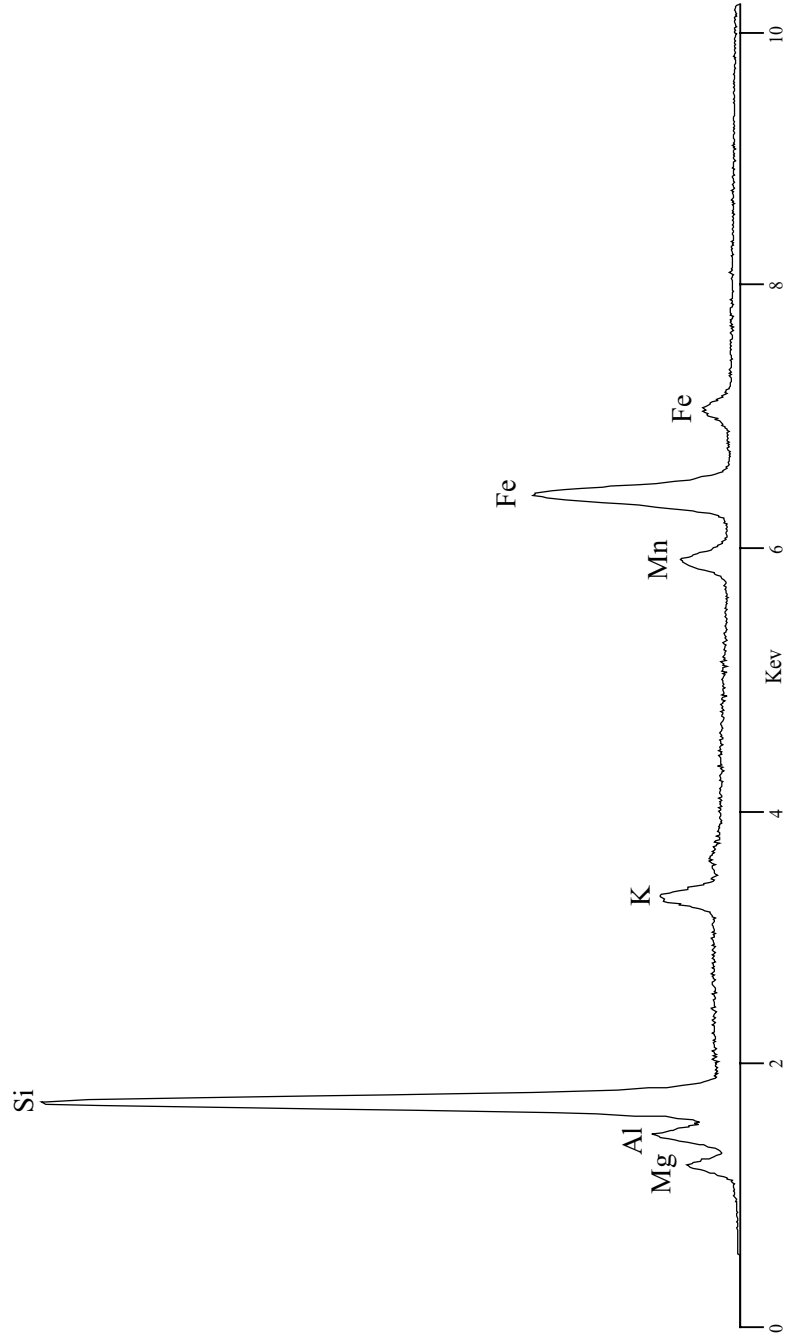
Margarite $\text{Ca}_2\text{Al}_4[\text{Si}_4\text{Al}_4\text{O}_{20}](\text{OH})_4$
Brittle Mica



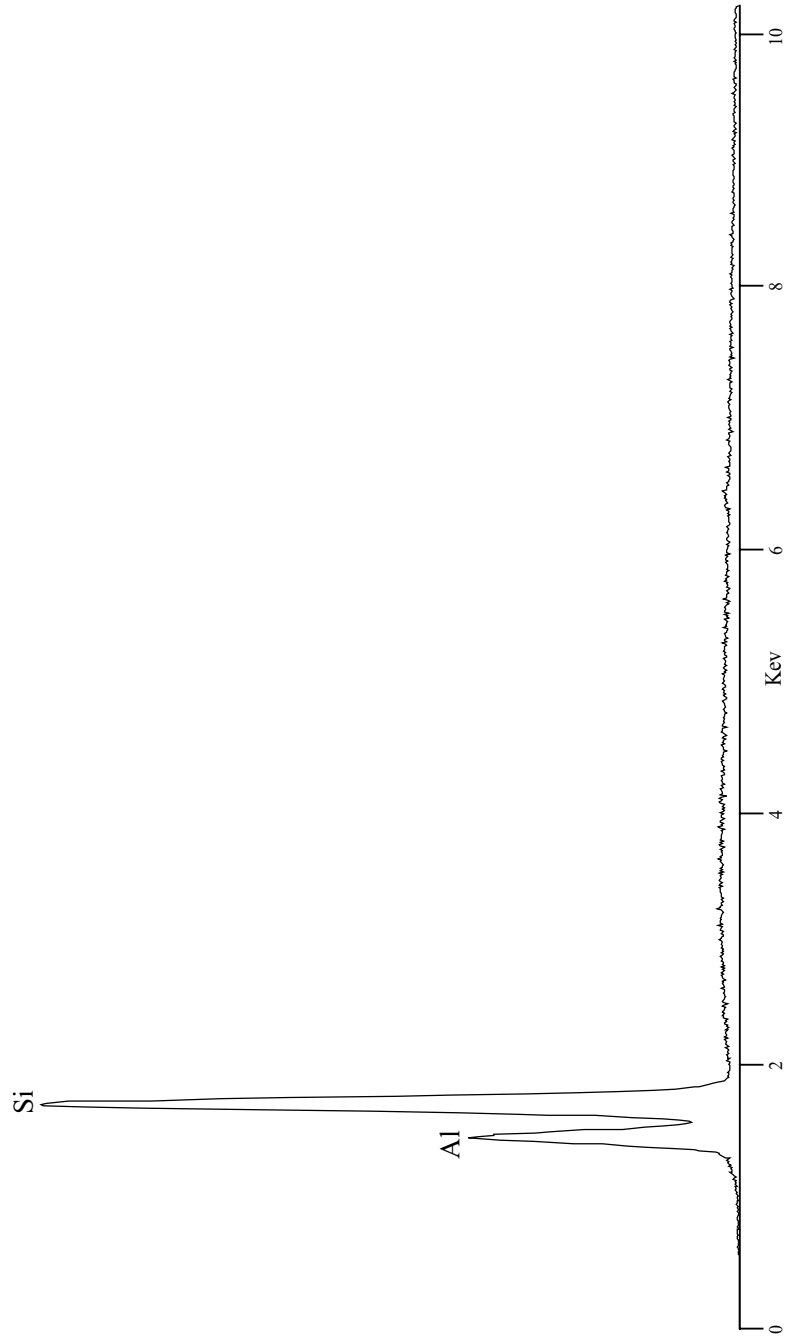
Xanthophyllite $\text{Ca}_2(\text{Mg,Fe})_4\text{Al}_{1.4}[\text{Si}_{2.5}\text{Al}_{5.5}\text{O}_{20}](\text{OH})_4$

Brittle Mica

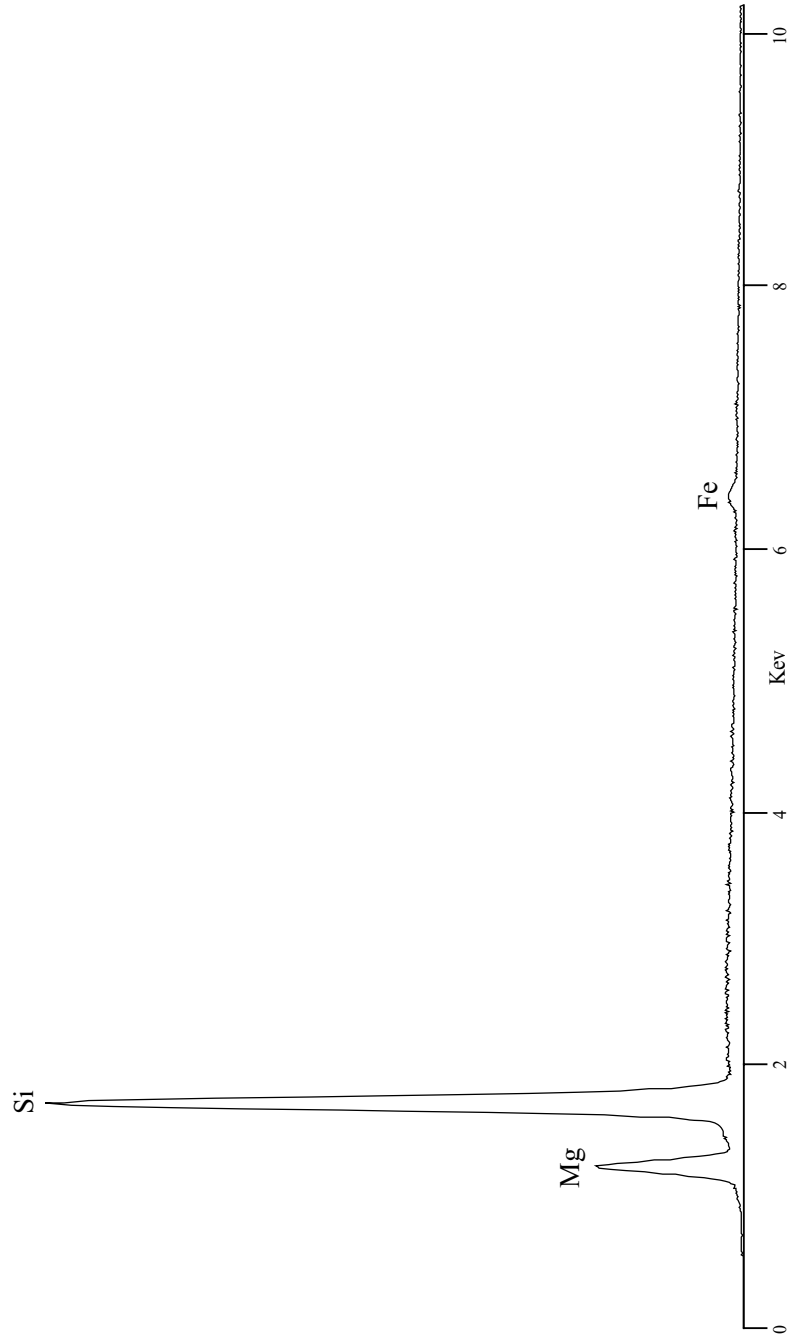


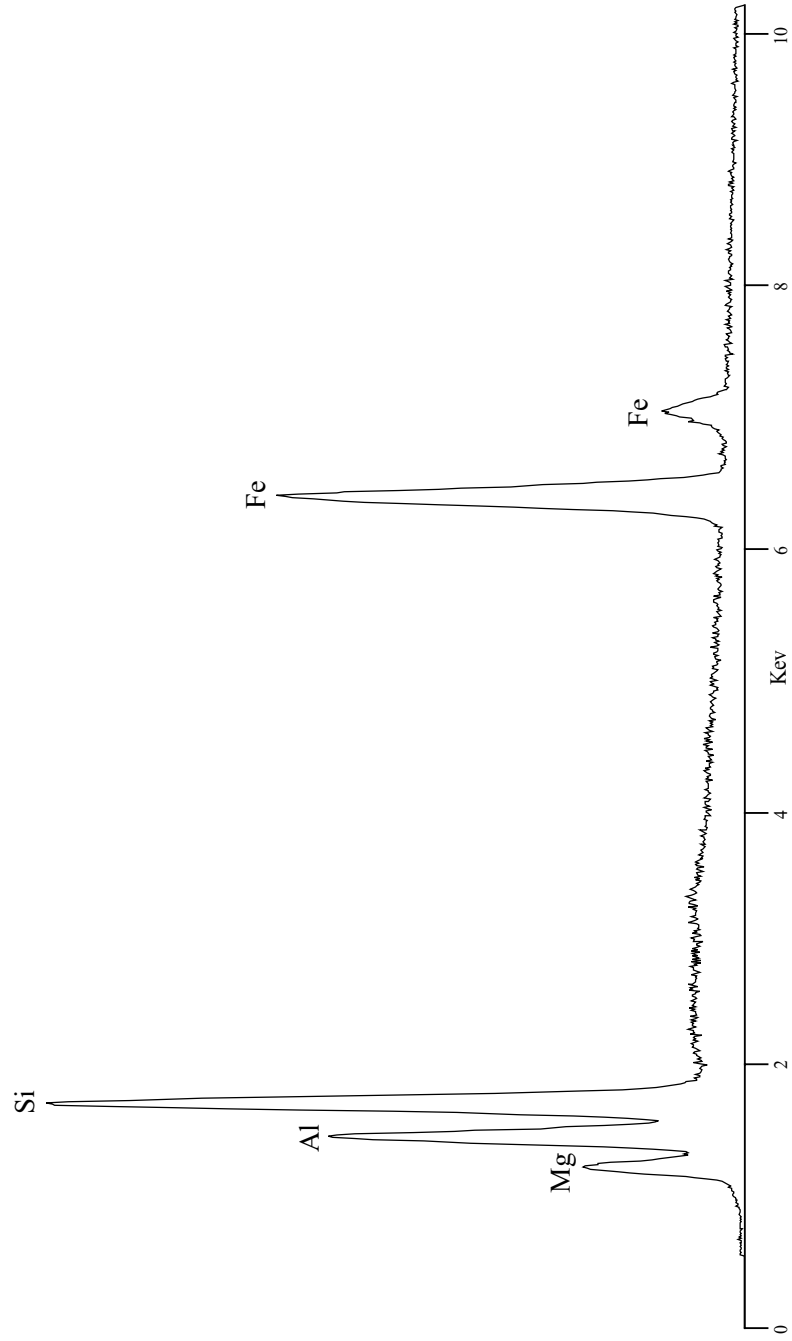


Pyrophyllite $\text{Al}_4[\text{Si}_8\text{O}_{20}](\text{OH})_4$

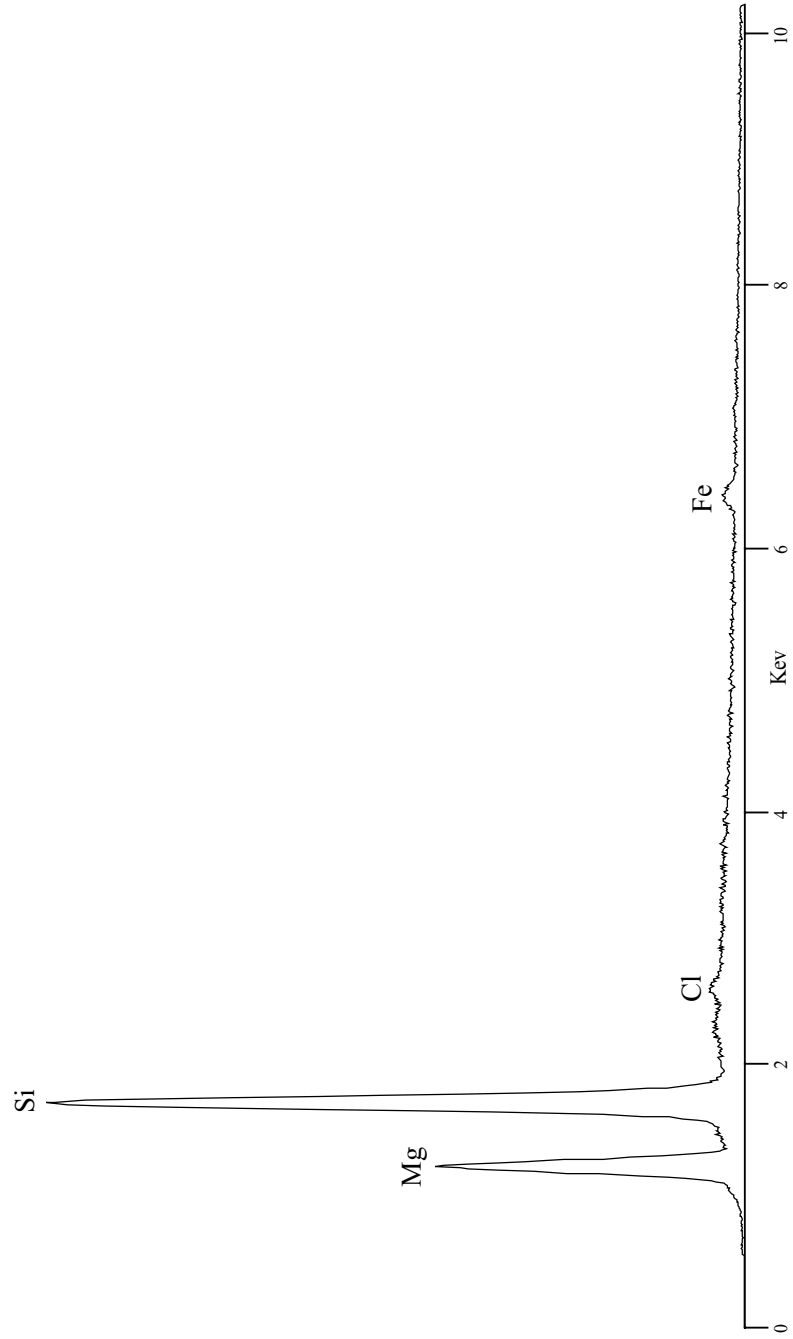


Talc $\text{Mg}_6[\text{Si}_8\text{O}_{20}](\text{OH})_4$

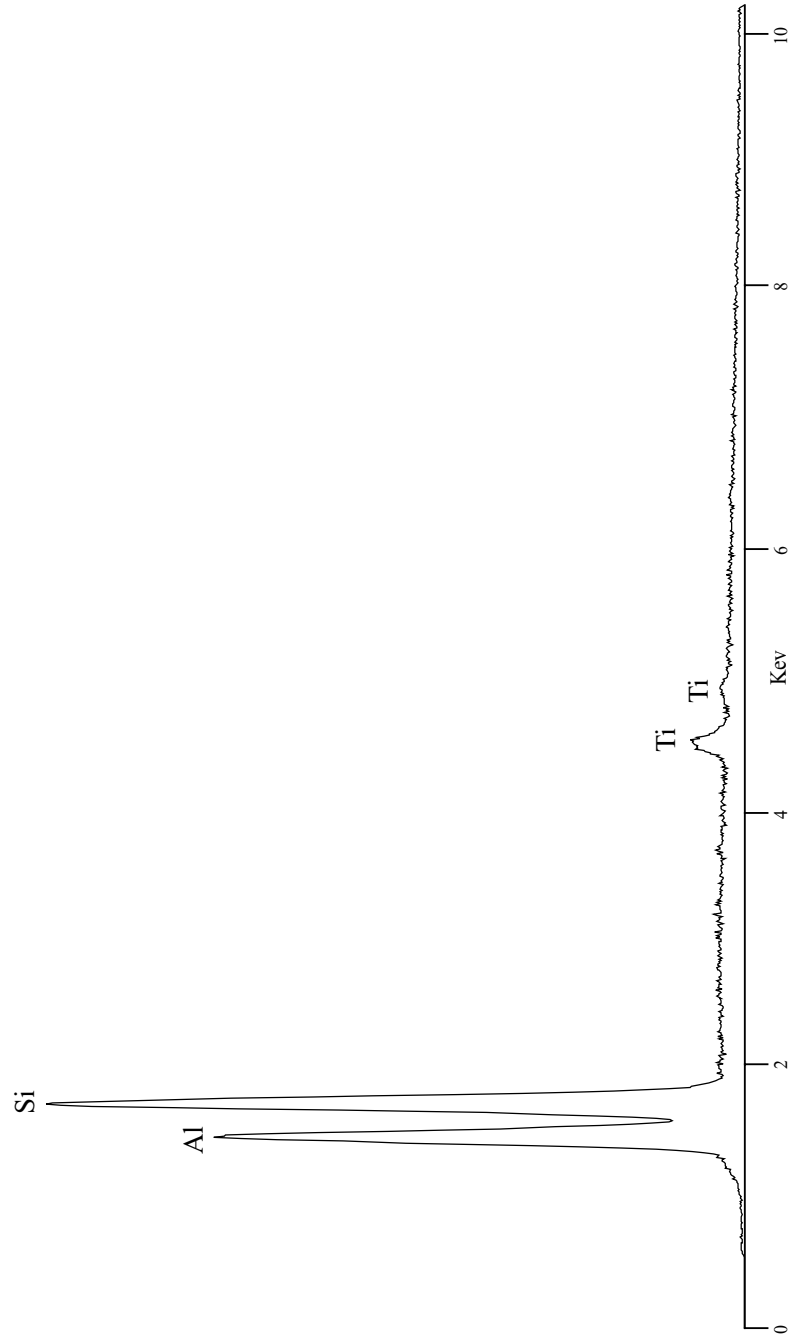


Chlorite $(\text{Mg,Al,Fe})_{12}[(\text{Si,Al})_8\text{O}_{20}](\text{OH})_{16}$ 

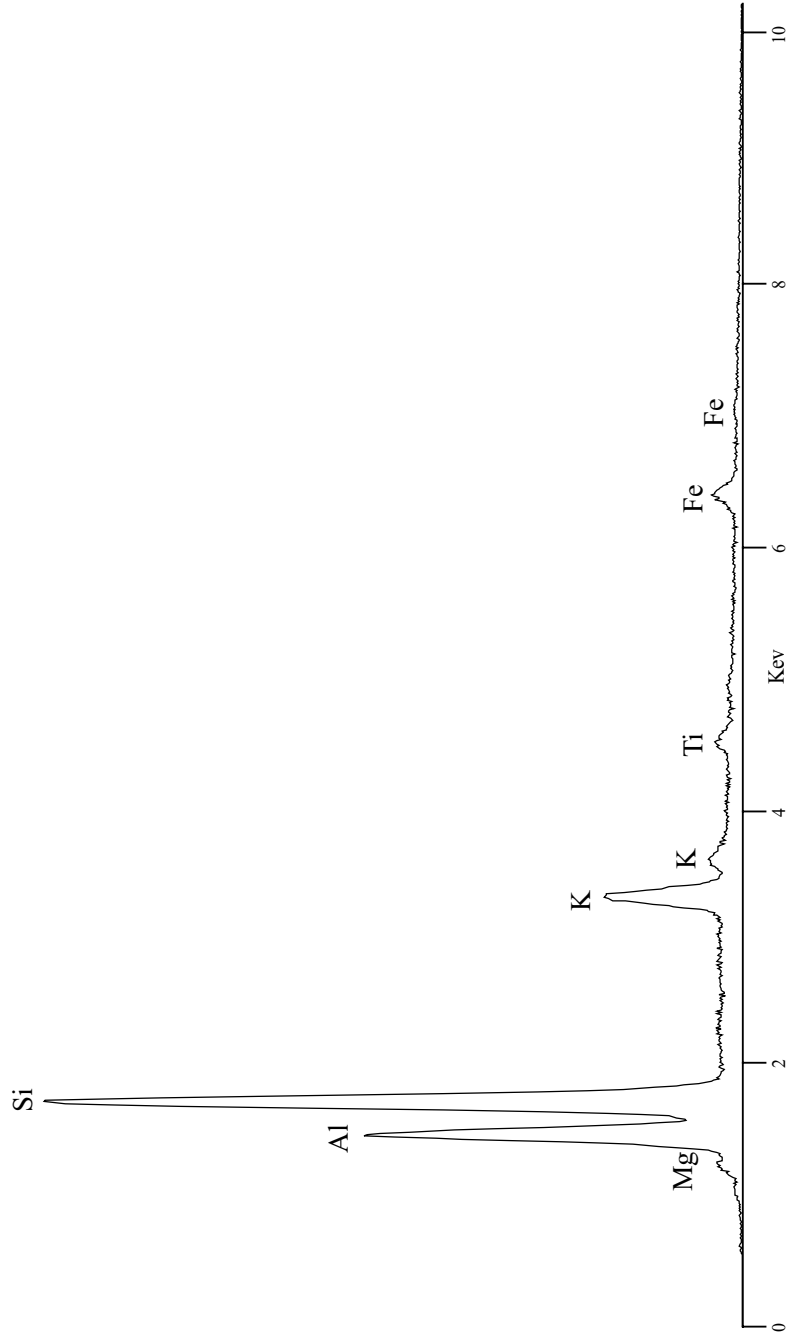
Serpentine $\text{Mg}_3[\text{Si}_2\text{O}_5](\text{OH})_4$



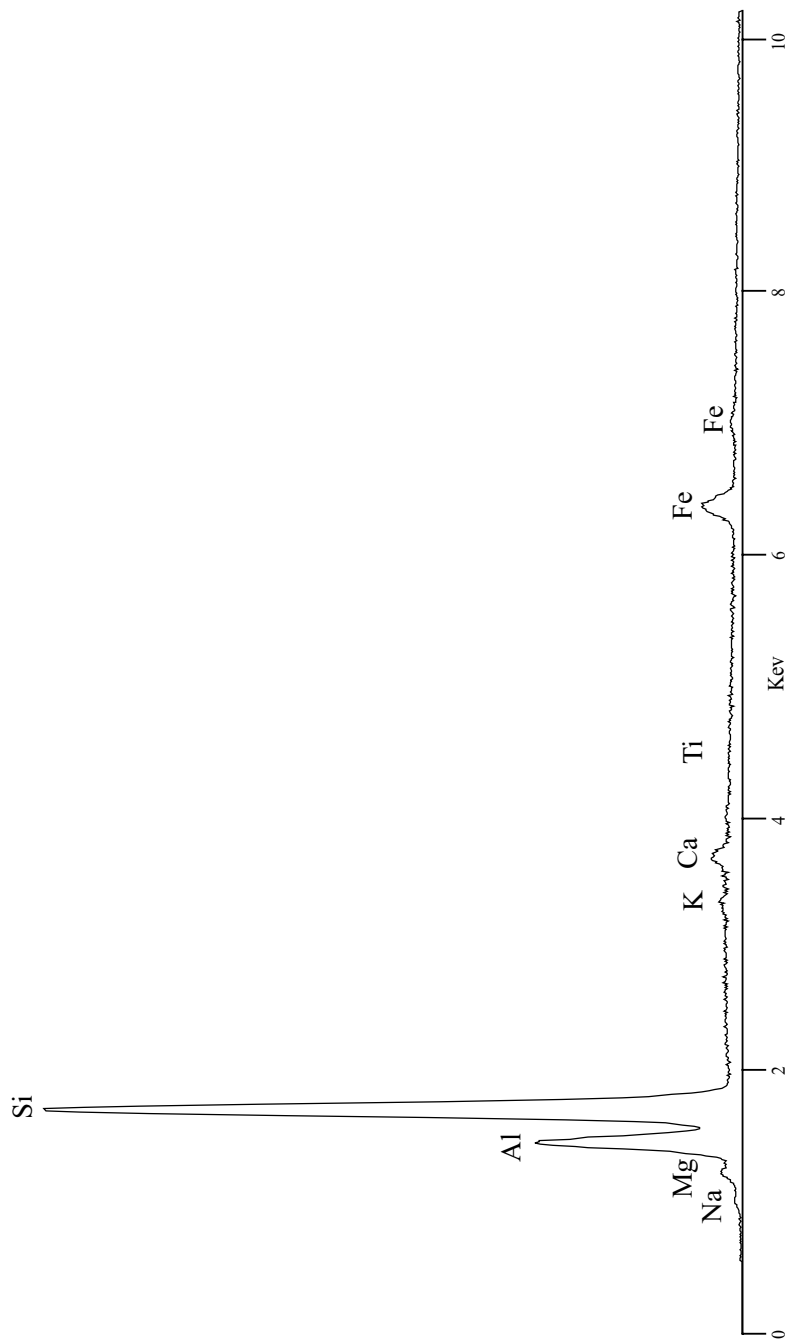
Kaolinite $\text{Al}_4[\text{Si}_4\text{O}_{10}](\text{OH})_8$
Clay

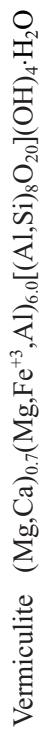


Illite $K_{1-1.5}Al_4[Si_{7-6.5}Al_{1-1.5}O_{20}](OH)_4$
Clay

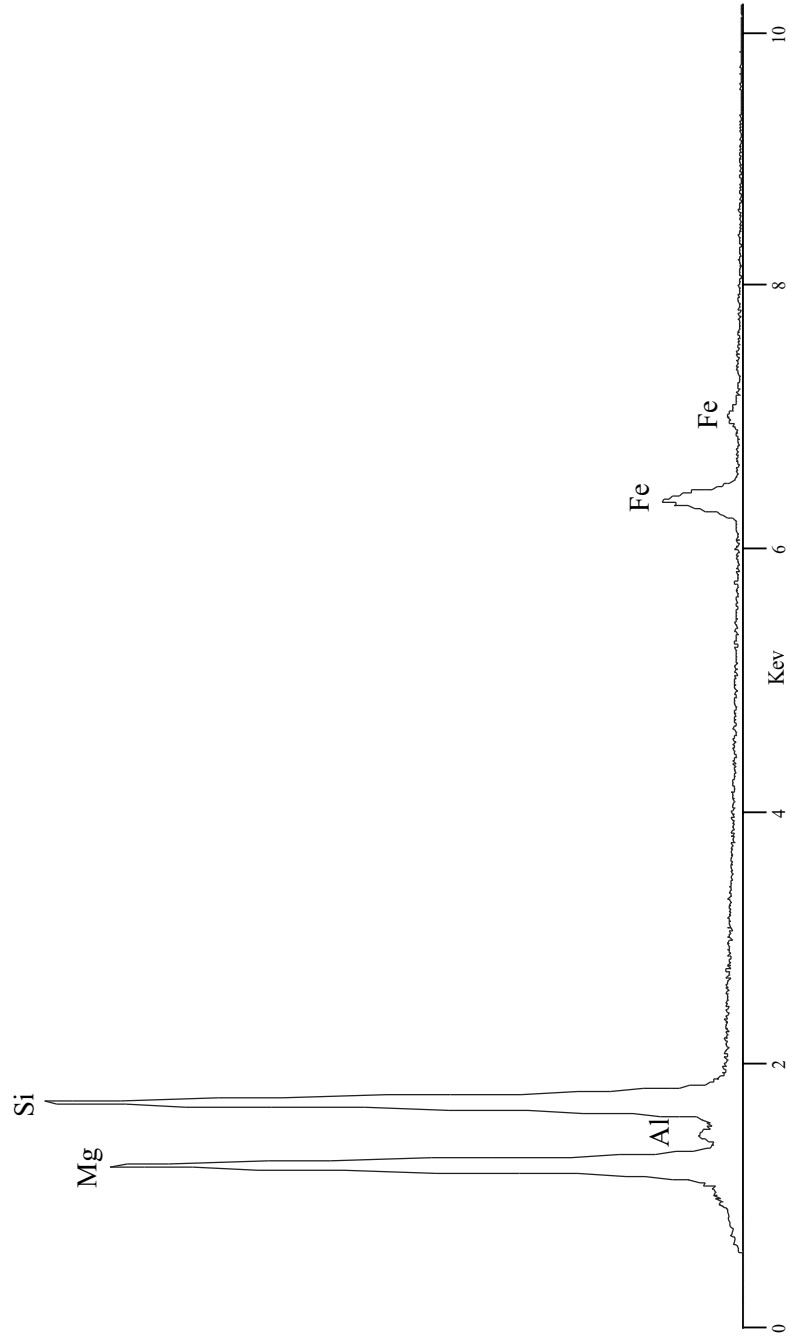


Montmorillonite (Smectite) $(\frac{1}{2}\text{Ca},\text{Na})_{0.7}(\text{Al},\text{Mg},\text{Fe})_4[(\text{Si},\text{Al})_8\text{O}_{20}](\text{OH})_4 \cdot n\text{H}_2\text{O}$
Clay



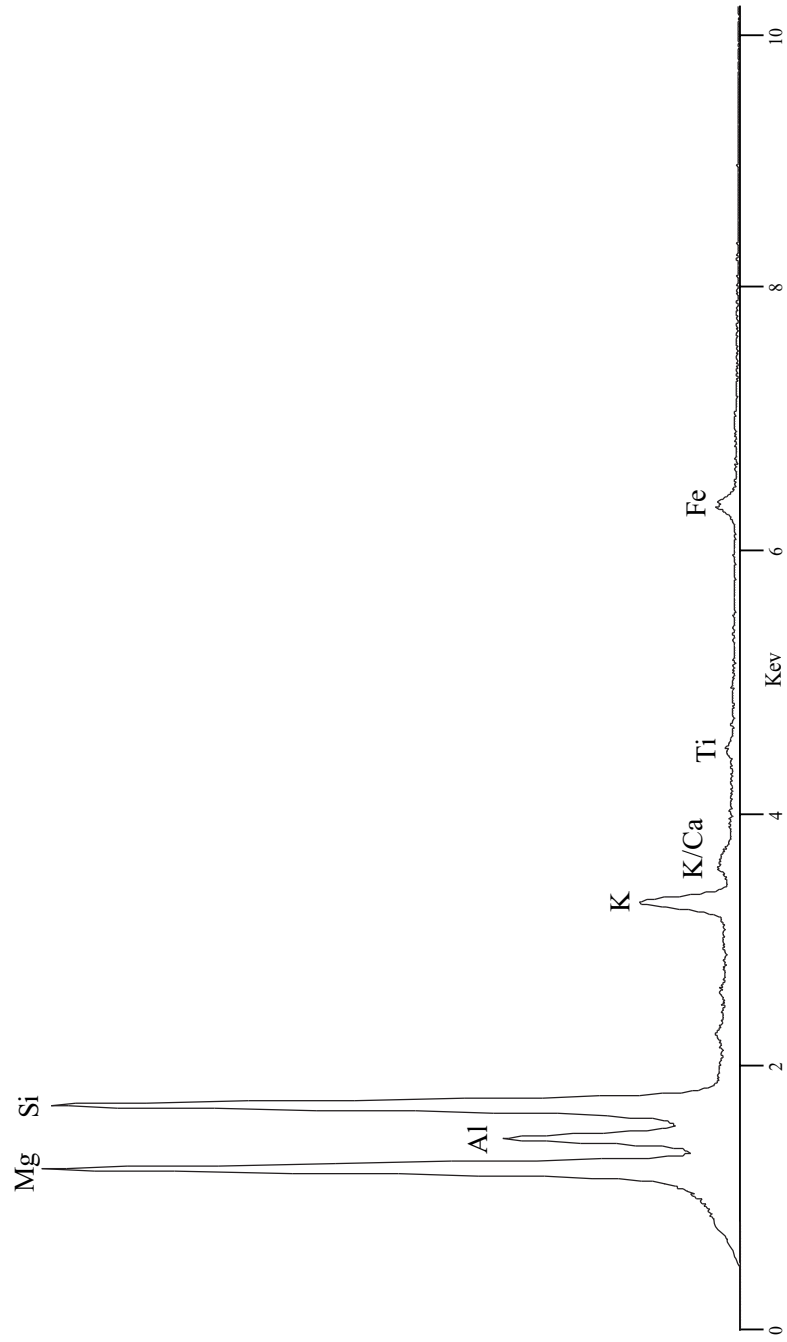


Clay

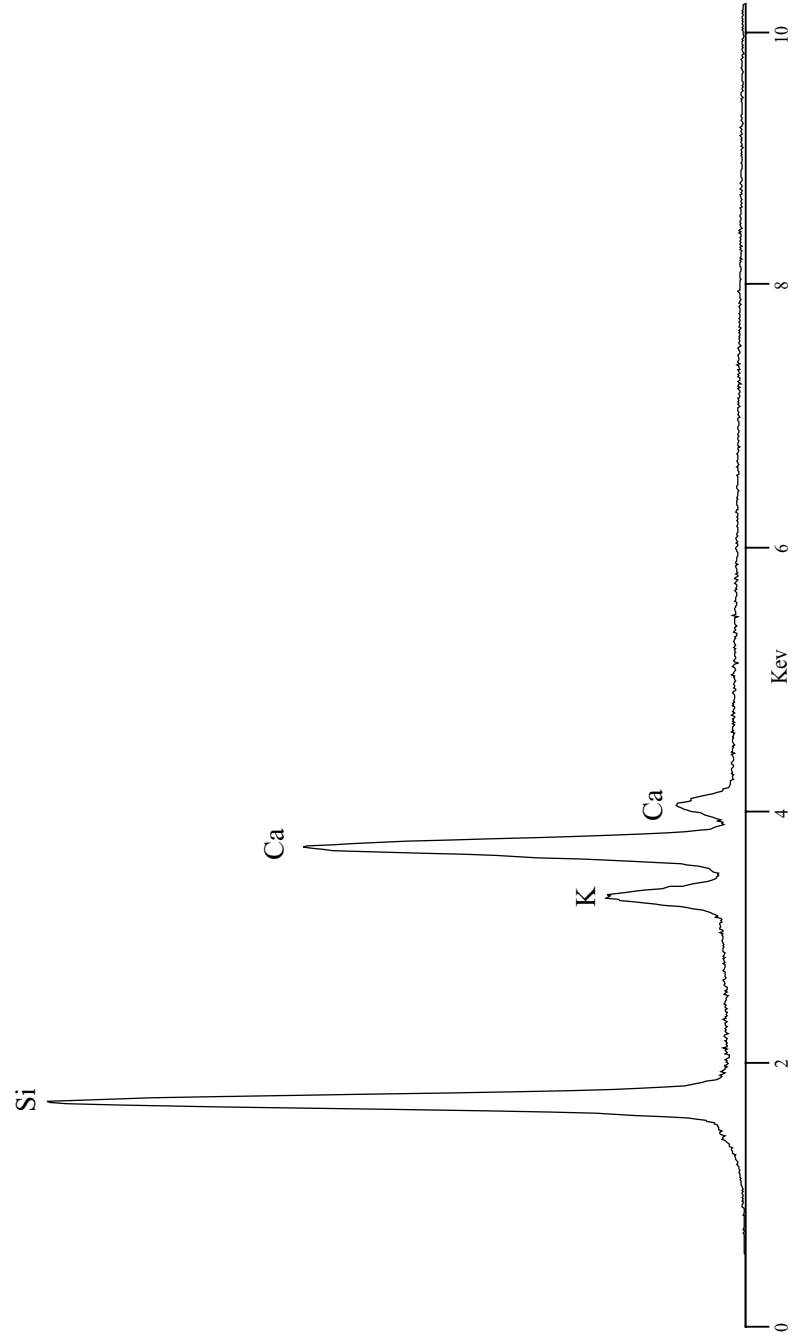


Vermiculite $(\text{Mg,Ca})_{0.7}(\text{Mg,Fe}^{+3},\text{Al})_{6.0}[\text{Al,Si}_8\text{O}_{20}](\text{OH})_4 \cdot \text{H}_2\text{O}$

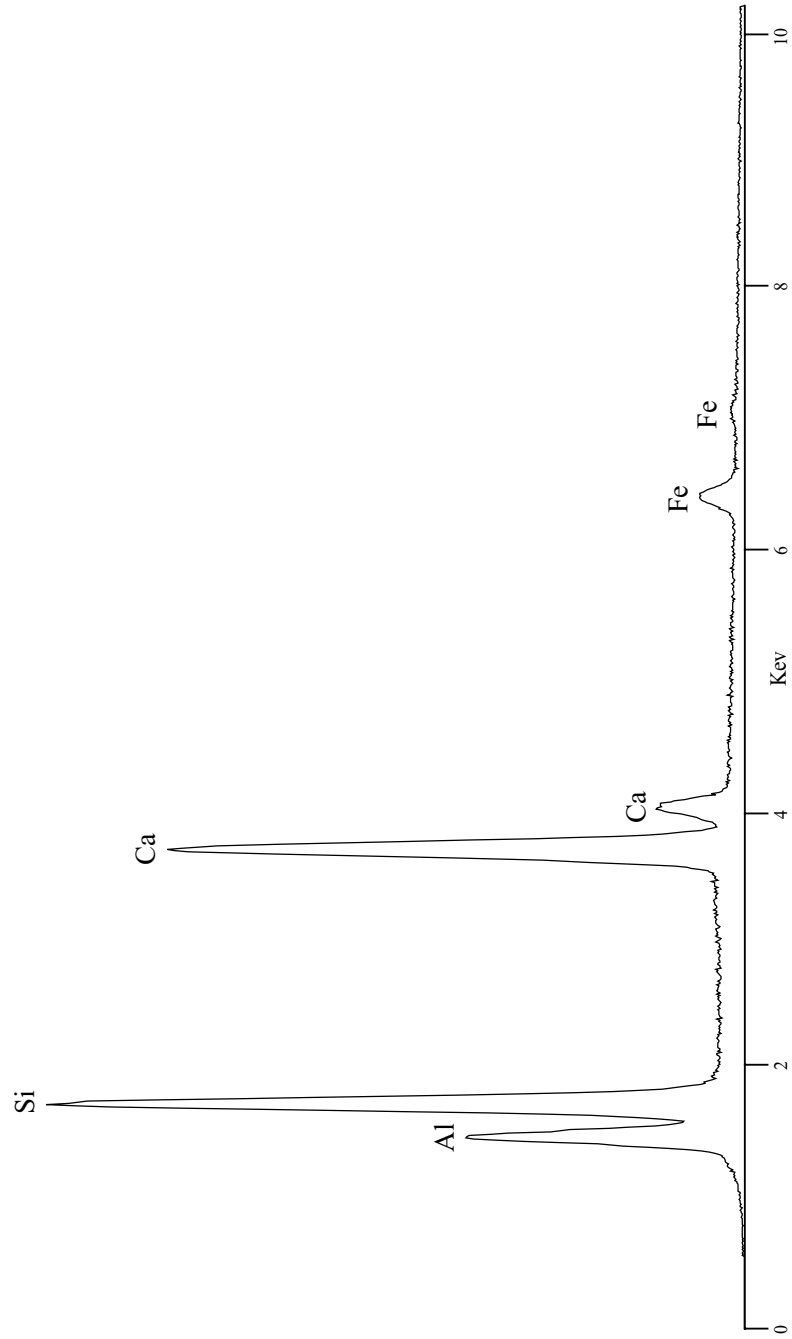
Clay



Apophyllite $\text{KFCa}_4[\text{Si}_8\text{O}_{20}] \cdot 8\text{H}_2\text{O}$

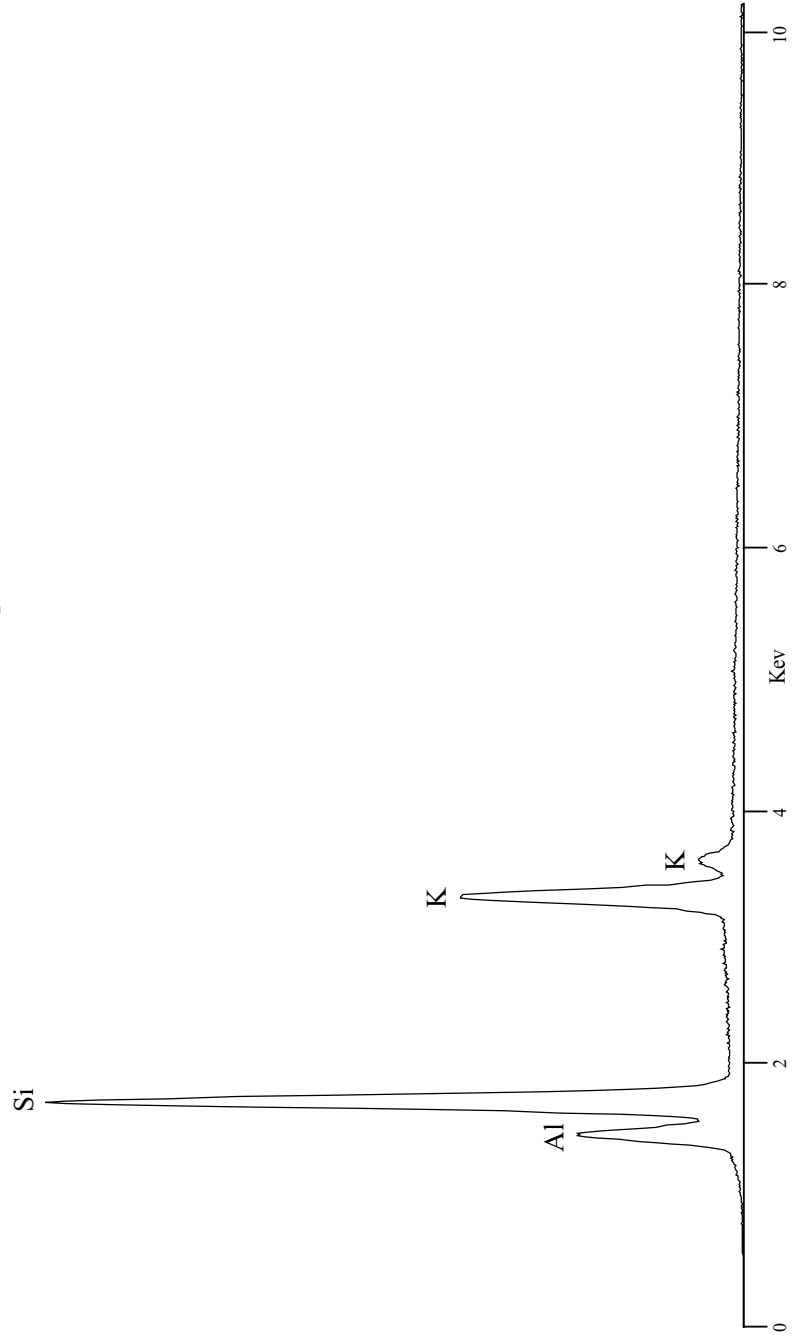


Prehnite $\text{Ca}_2\text{Al}[\text{AlSi}_3\text{O}_{10}](\text{OH})_2$



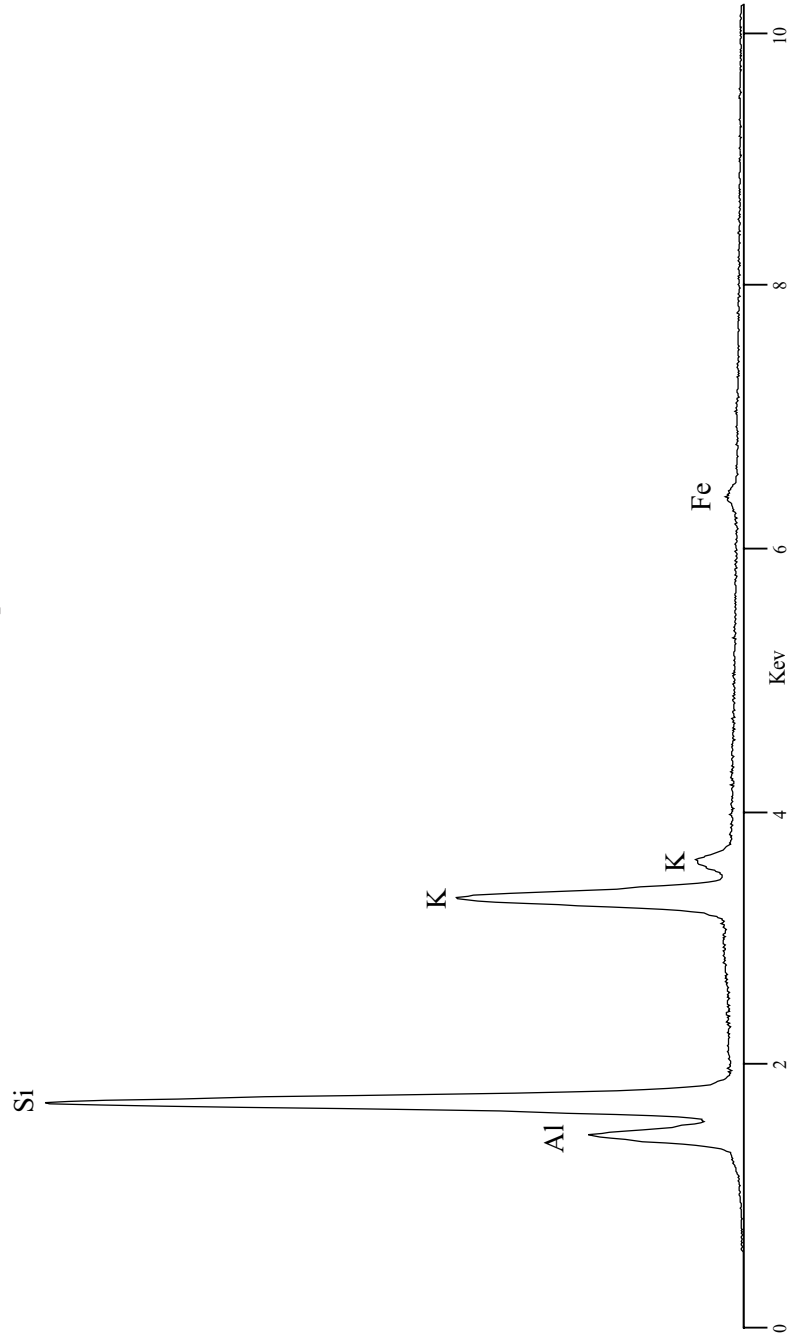
Microcline (K_2Na)[$AlSi_3O_8$]

Alkali Feldspar



Orthoclase (K,Na)[AlSi₃O₈]

Alkali Feldspar

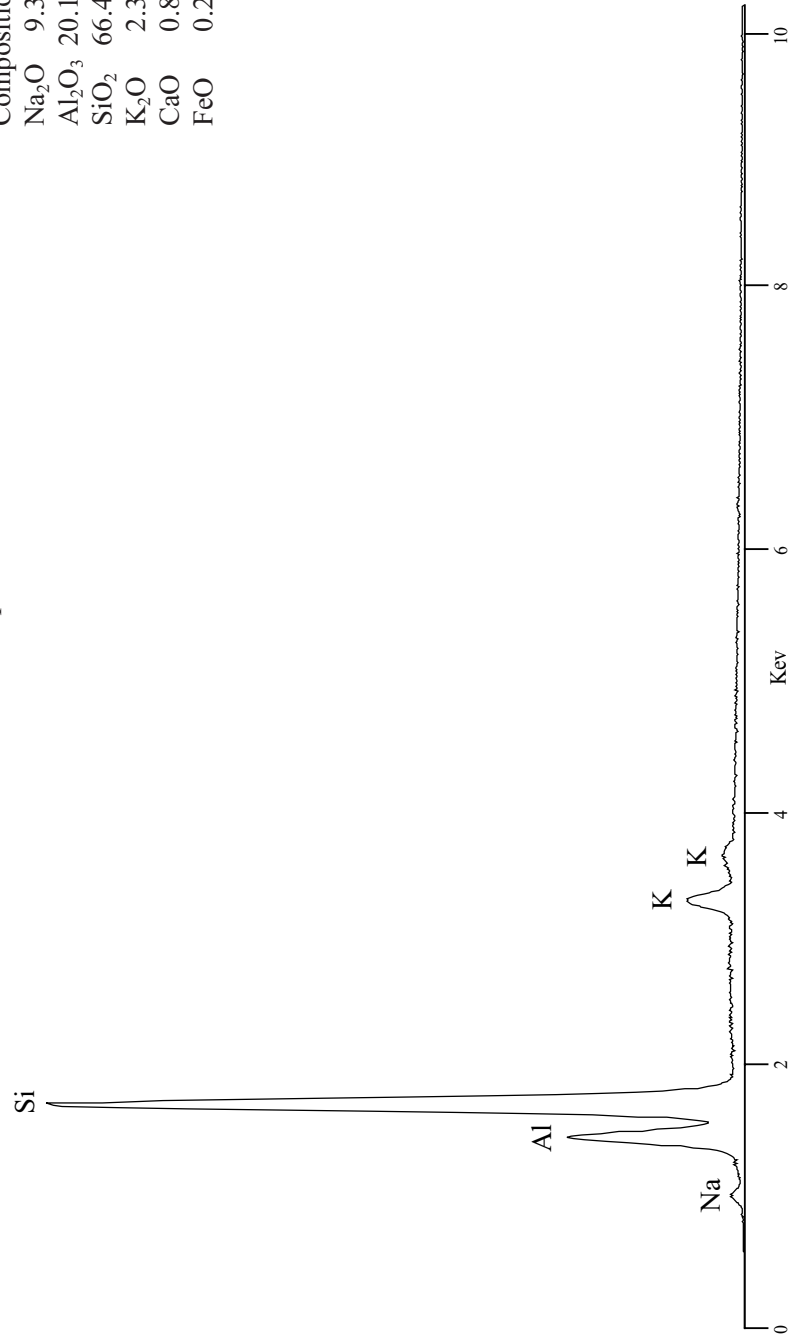


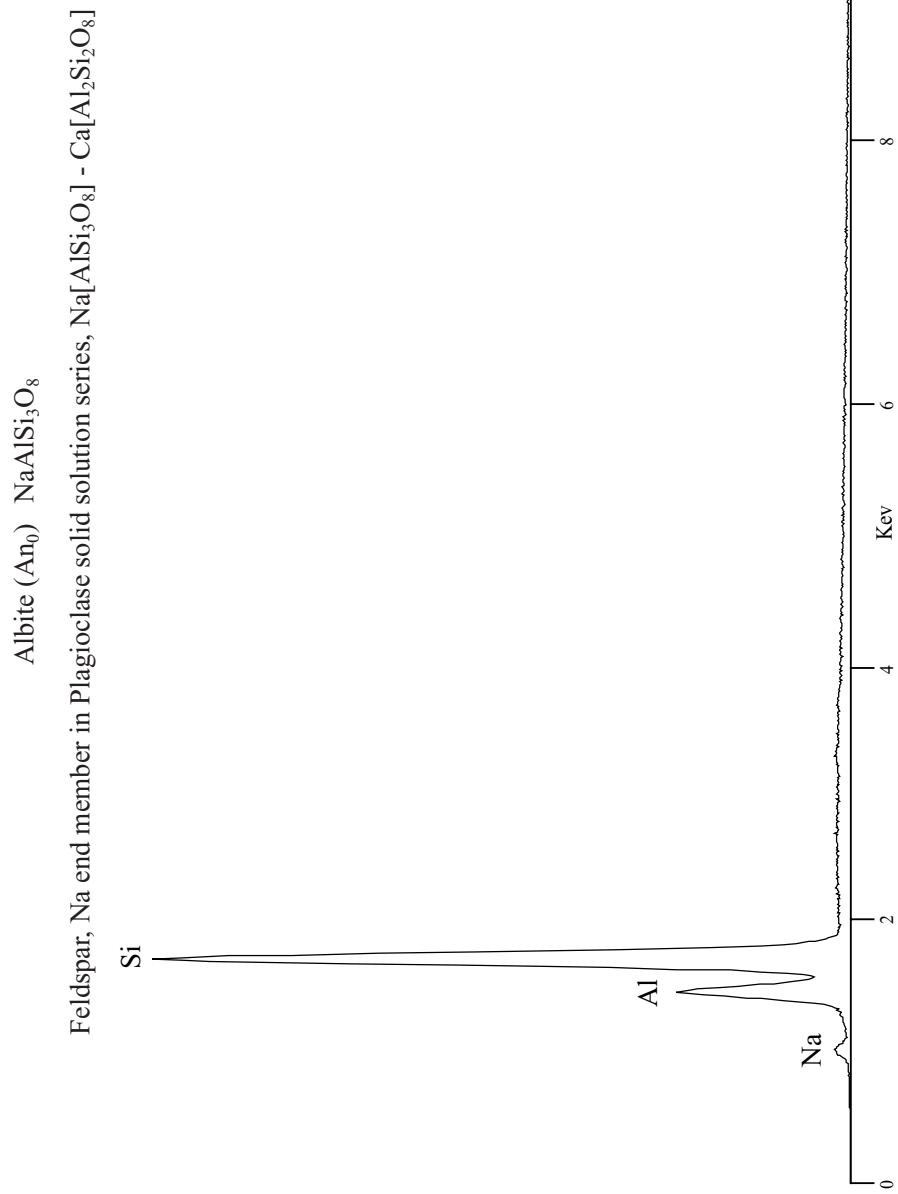
Anorthoclase (K,Na)[AlSi₃O₈]

Alkali Feldspar

Smithsonian Standard
USNM 113860

Composition	
Na ₂ O	9.31
Al ₂ O ₃	20.12
SiO ₂	66.44
K ₂ O	2.35
CaO	0.87
FeO	0.20

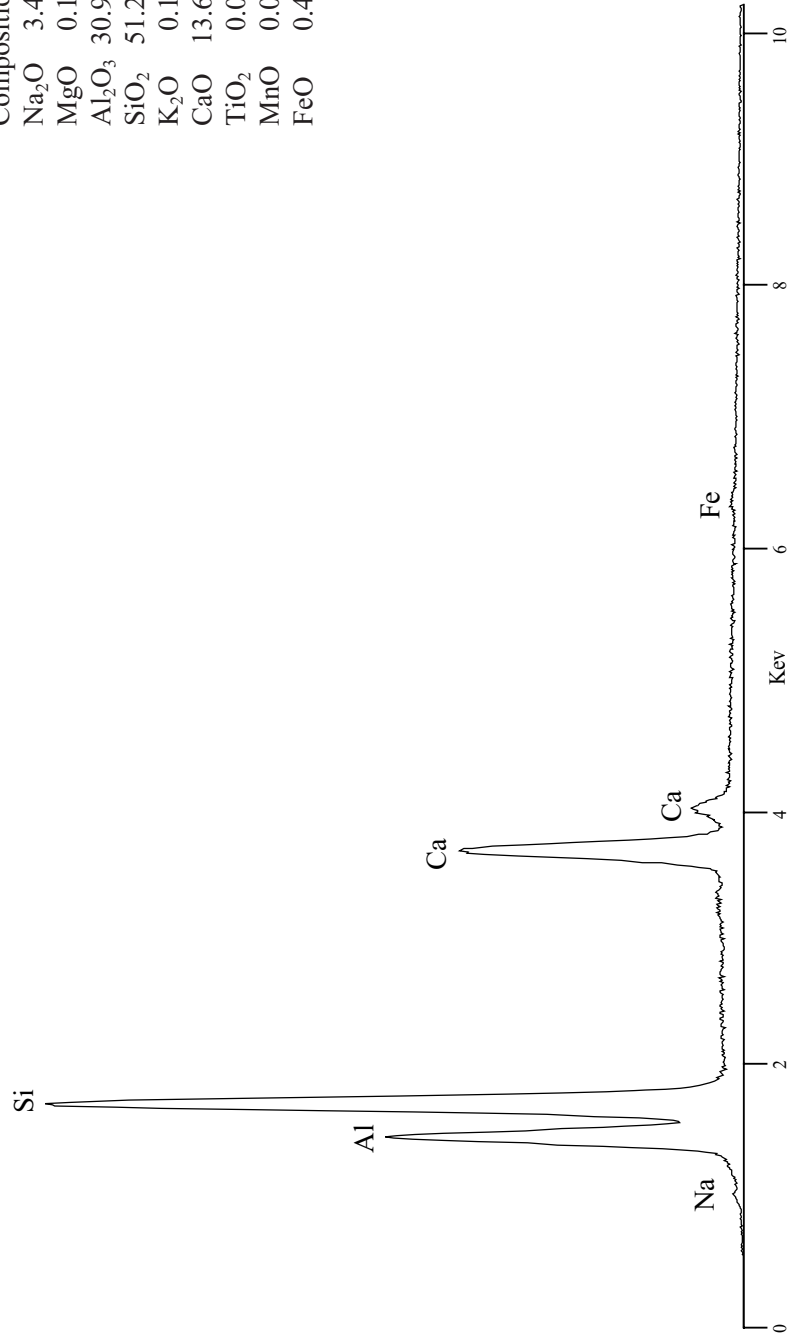




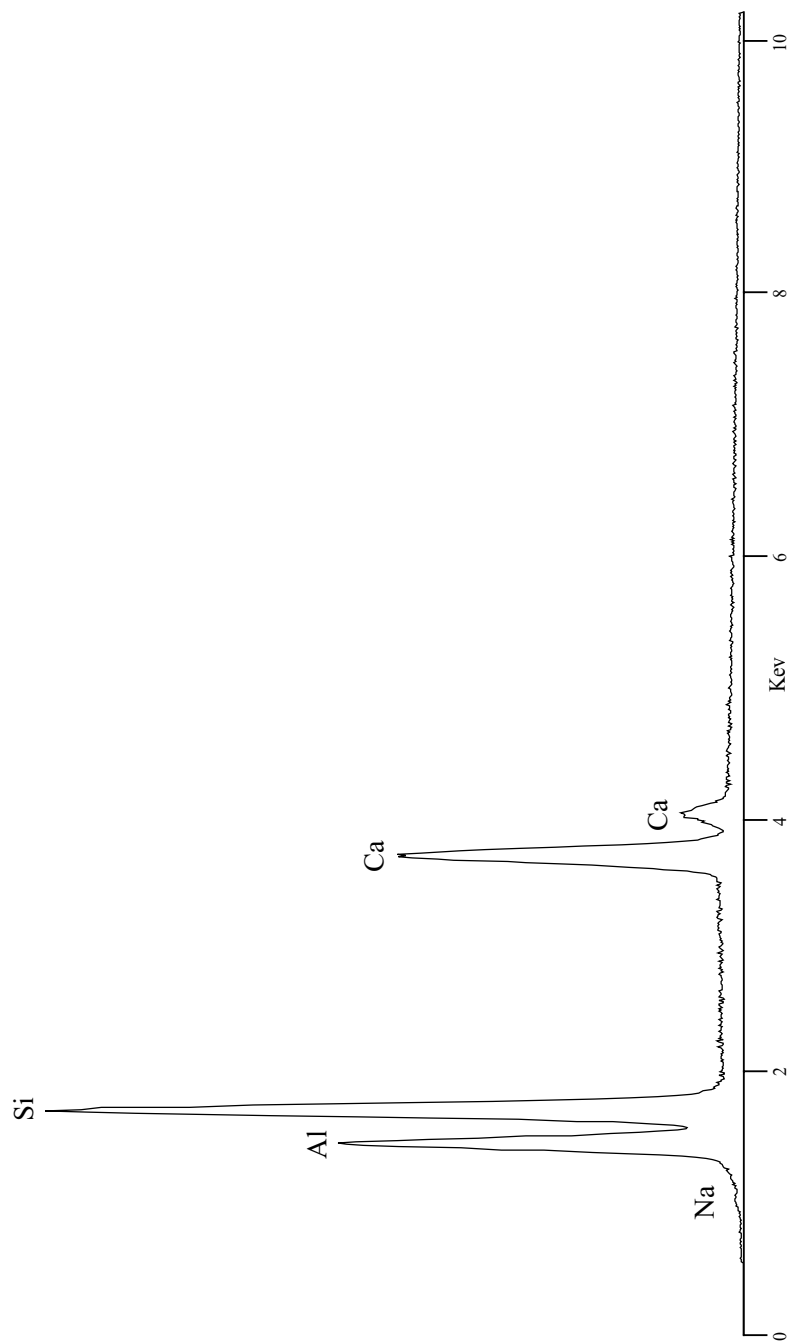
Labradorite (An₅₀₋₇₀)
Smithsonian Standard
USNM 115900

Feldspar in Plagioclase solid solution series, Na[AlSi₃O₈] - Ca[Al₂Si₂O₈]

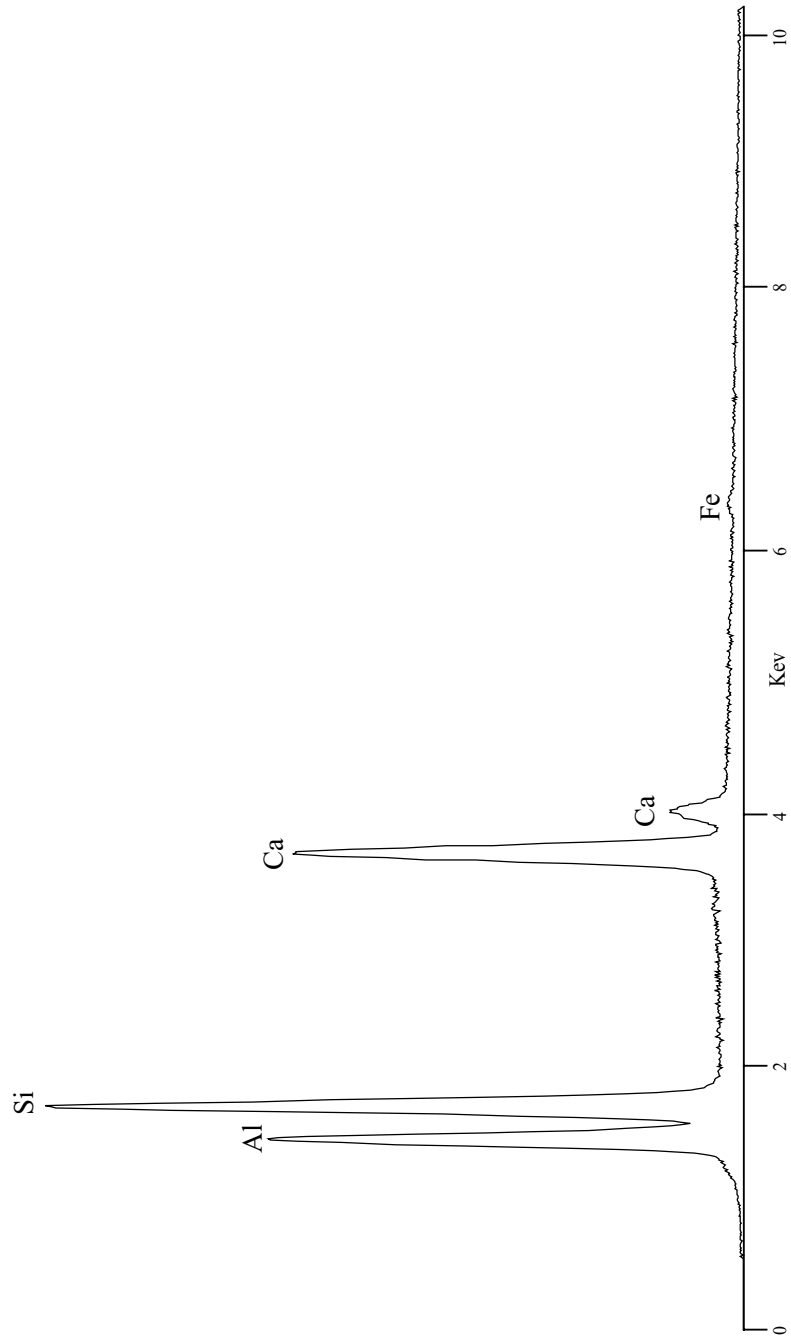
Composition	
Na ₂ O	3.45
MgO	0.14
Al ₂ O ₃	30.91
SiO ₂	51.25
K ₂ O	0.18
CaO	13.64
TiO ₂	0.05
MnO	0.01
FeO	0.45



Bytownite (An₈₀)
Feldspar, Ca rich member in Plagioclase solid solution series, Na[AlSi₃O₈] - Ca[Al₂Si₂O₈]

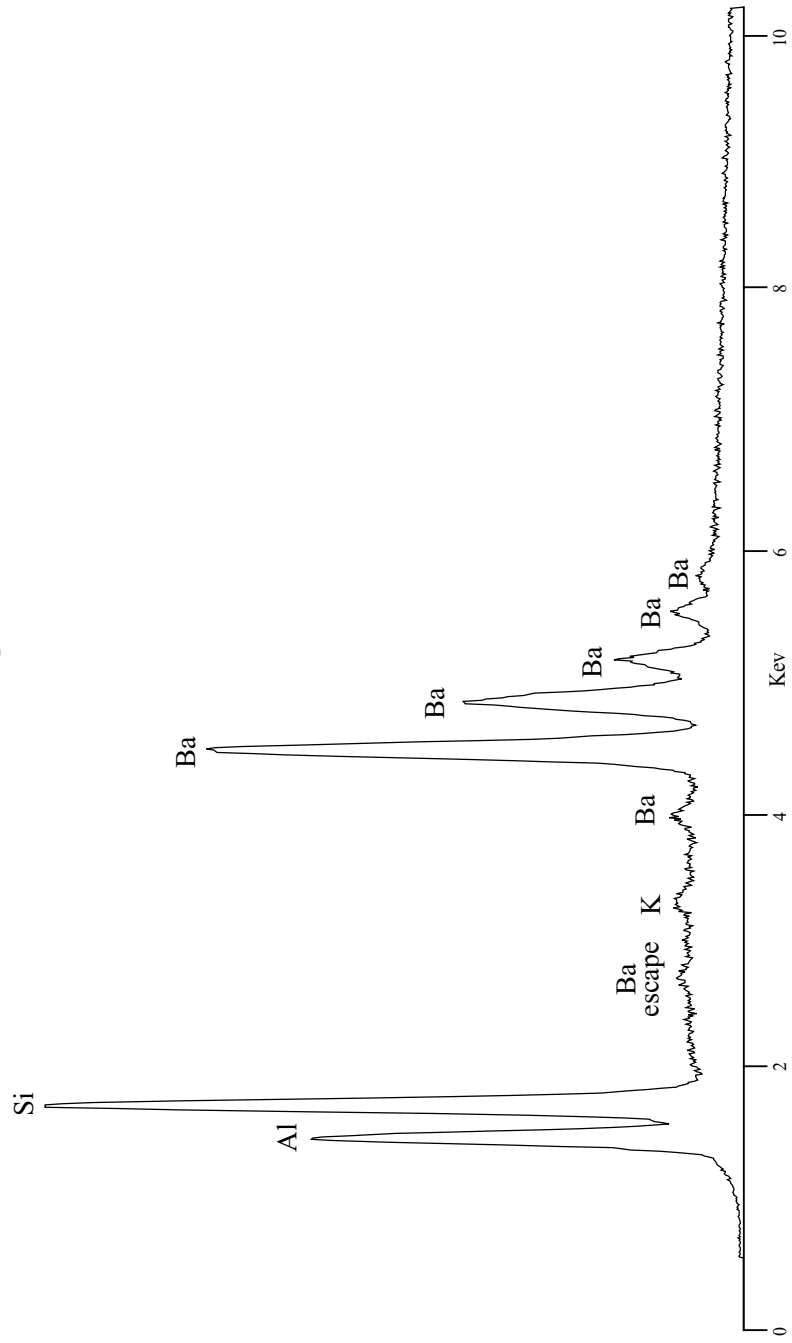


Anorthite (An₁₀₀) Ca[Al₂Si₂O₈]
Feldspar, Ca end member in Plagioclase solid solution series, Na[AlSi₃O₈] - Ca[Al₂Si₂O₈]



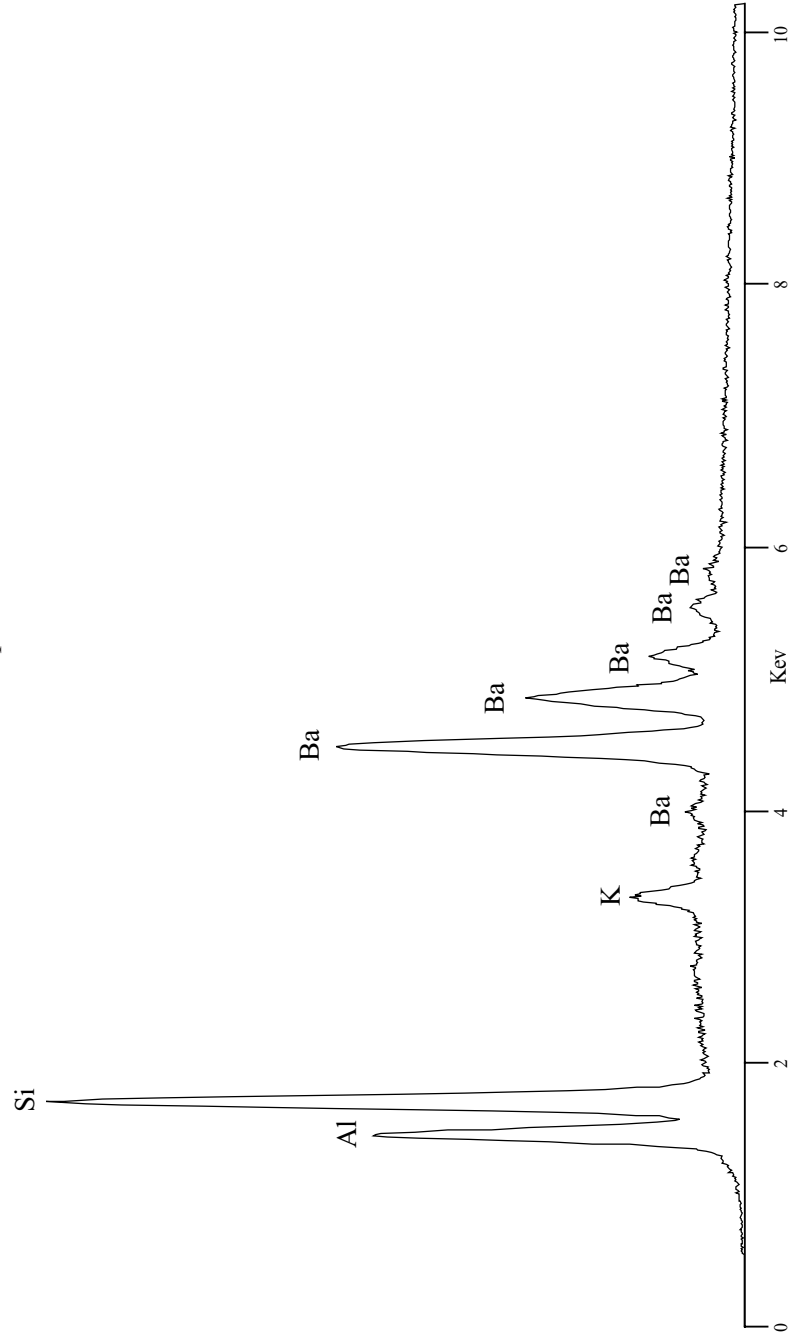
Celsian $Ba[Al_2Si_2O_8]$

Feldspar



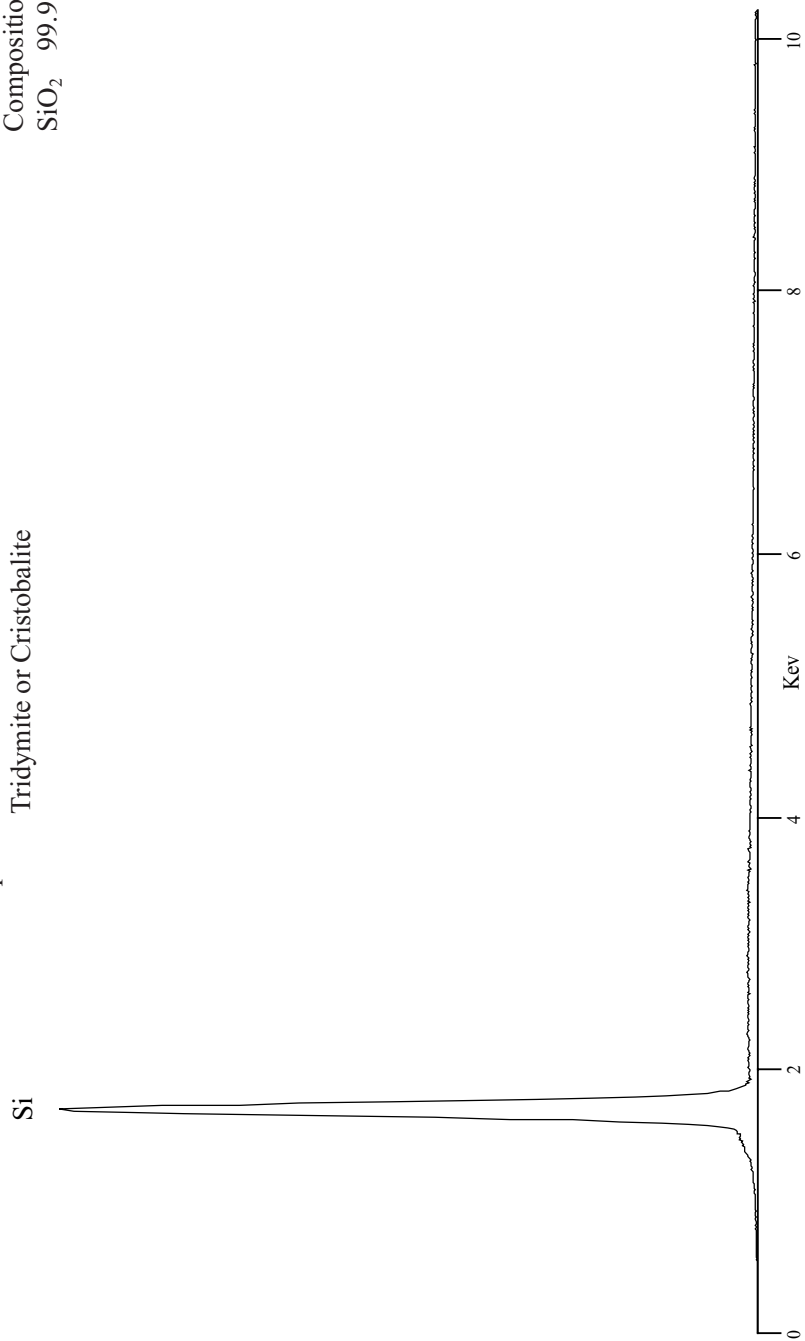
Hyalophane (K,Na,Ba) $[(Al,Si)_4O_8]$

Feldspar

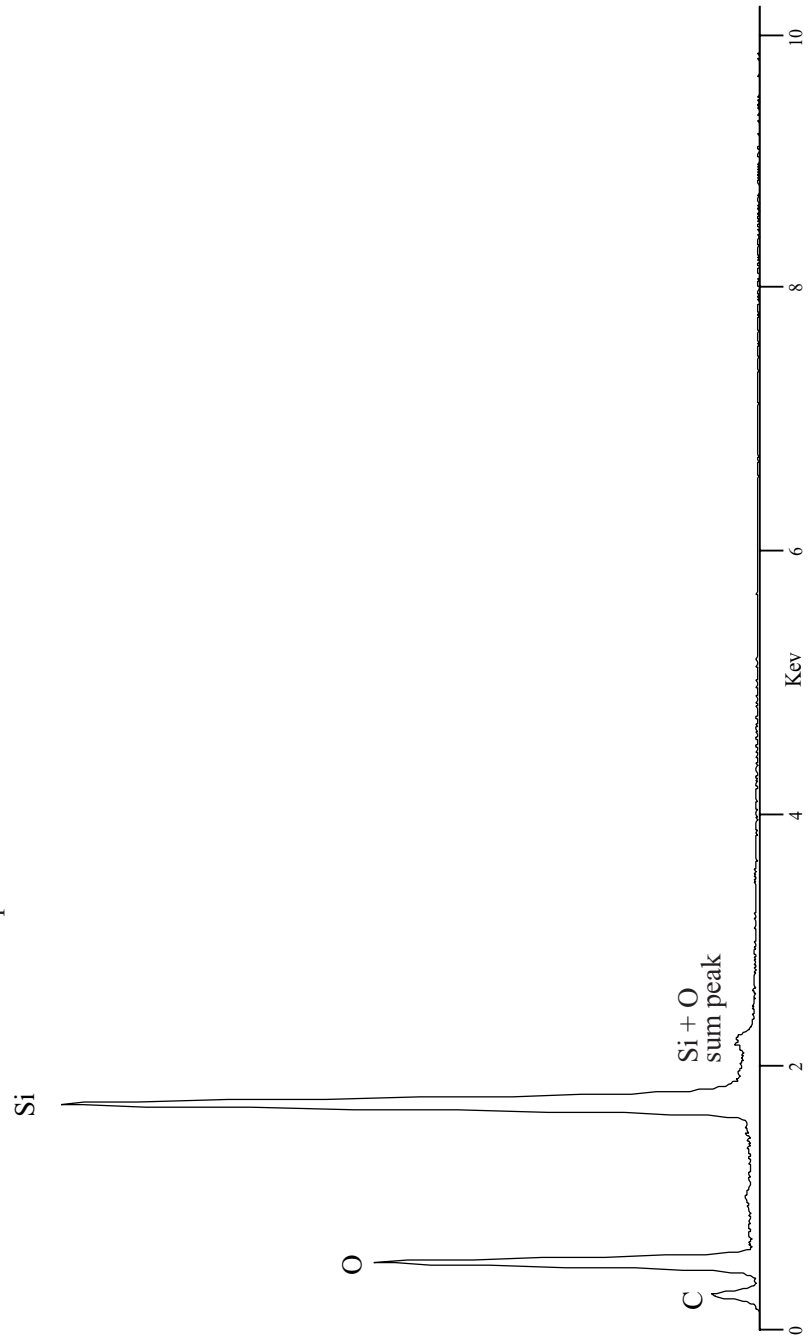


Smithsonian Standard
USNM R17701
Composition
SiO₂ 99.99

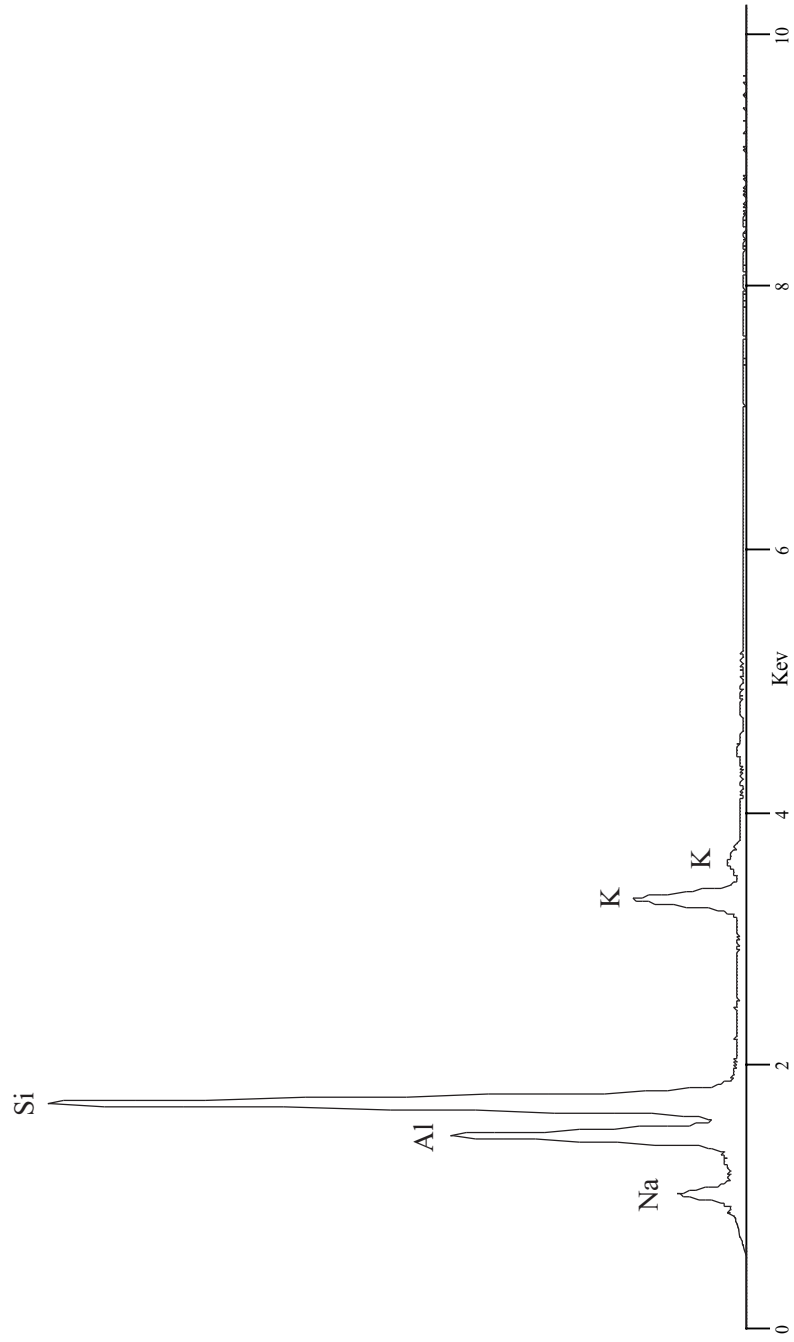
Quartz SiO₂
Spectra similar to this would be seen for
Tridymite or Cristobalite



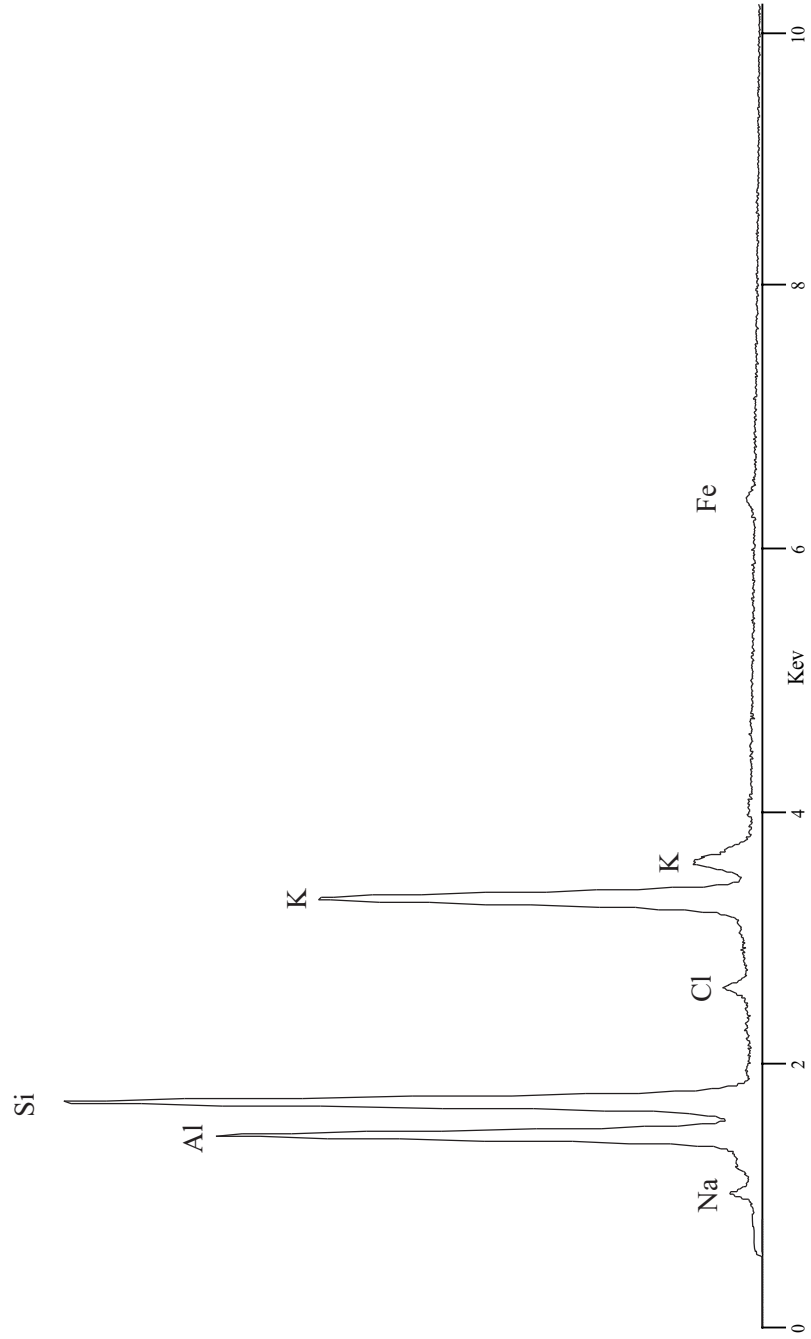
Quartz SiO_2
Spectrum collected with thin window detector

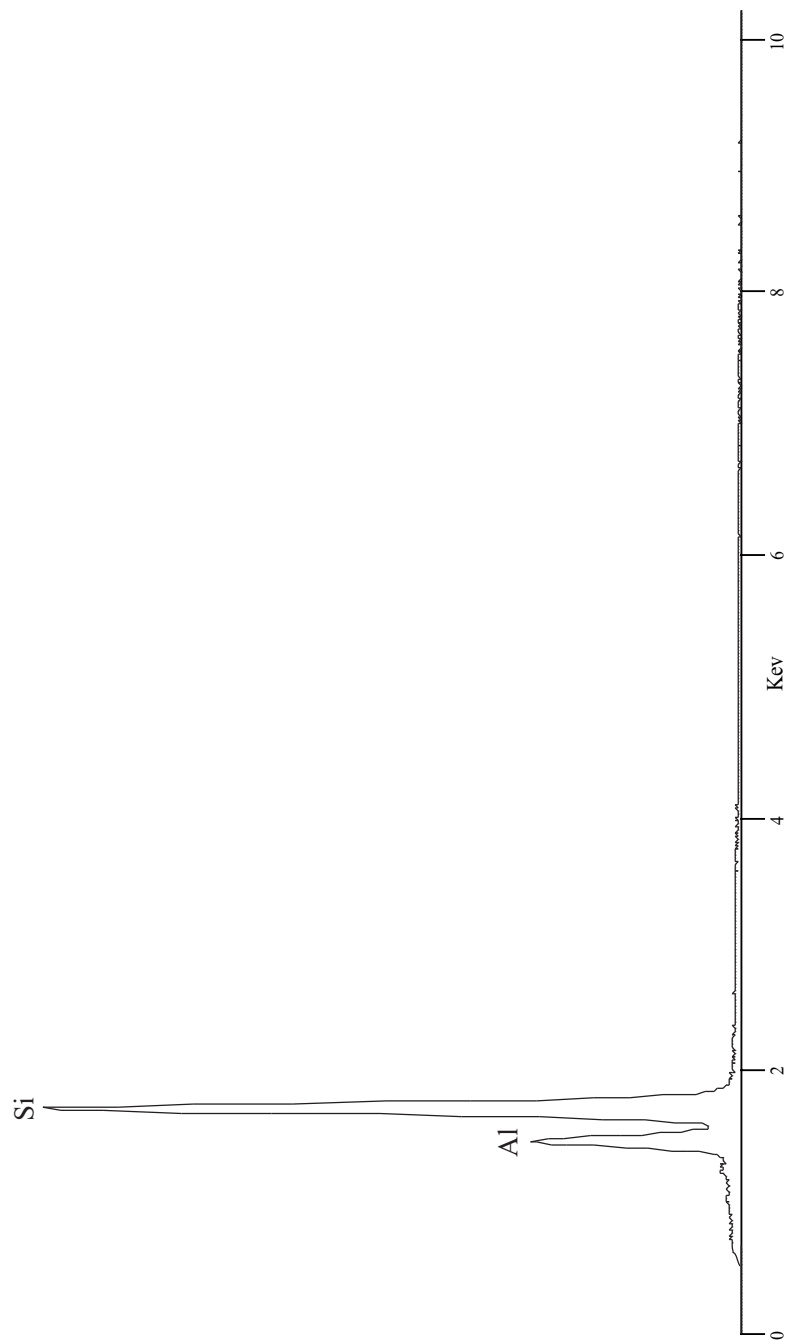


Nepheline $\text{Na}_3(\text{Na,K})[\text{Al}_4\text{Si}_4\text{O}_{16}]$

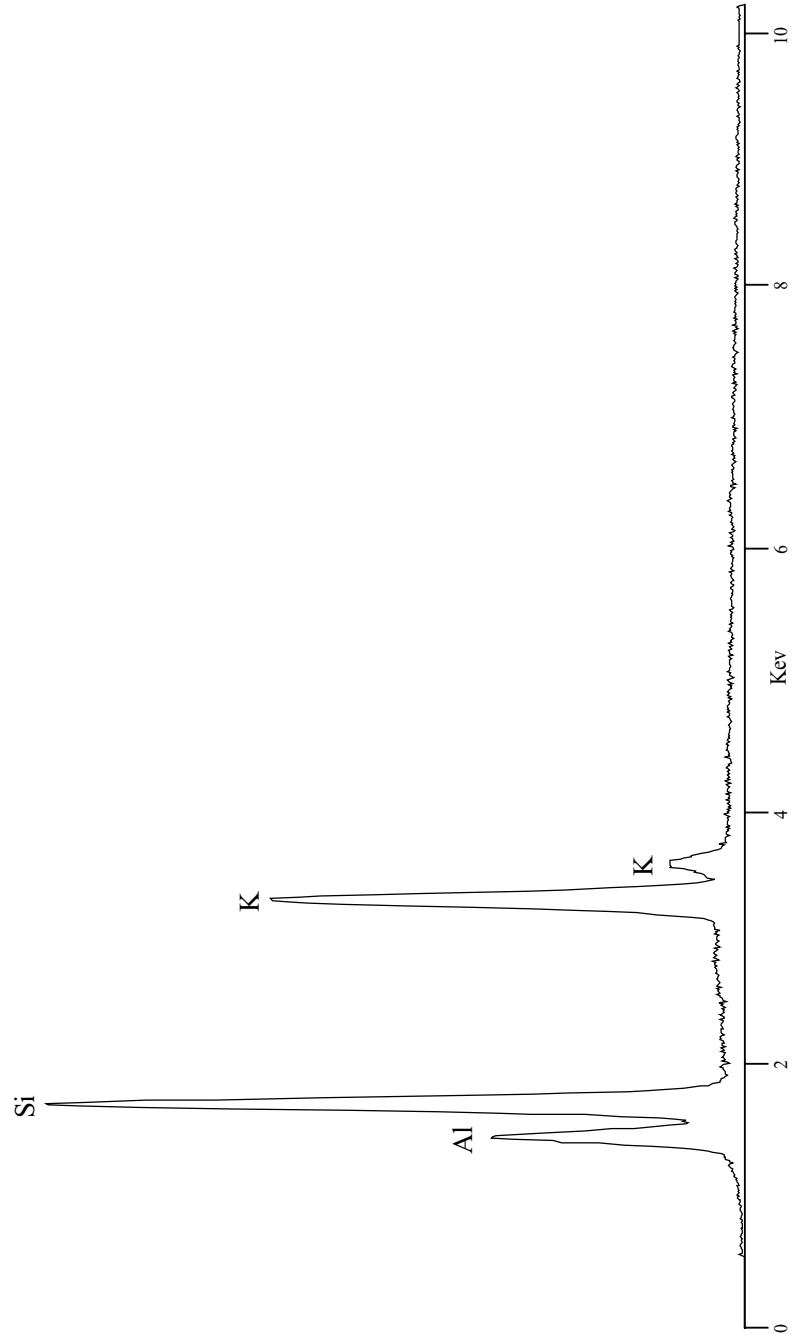


Kalsilite $K[AlSiO_4]$



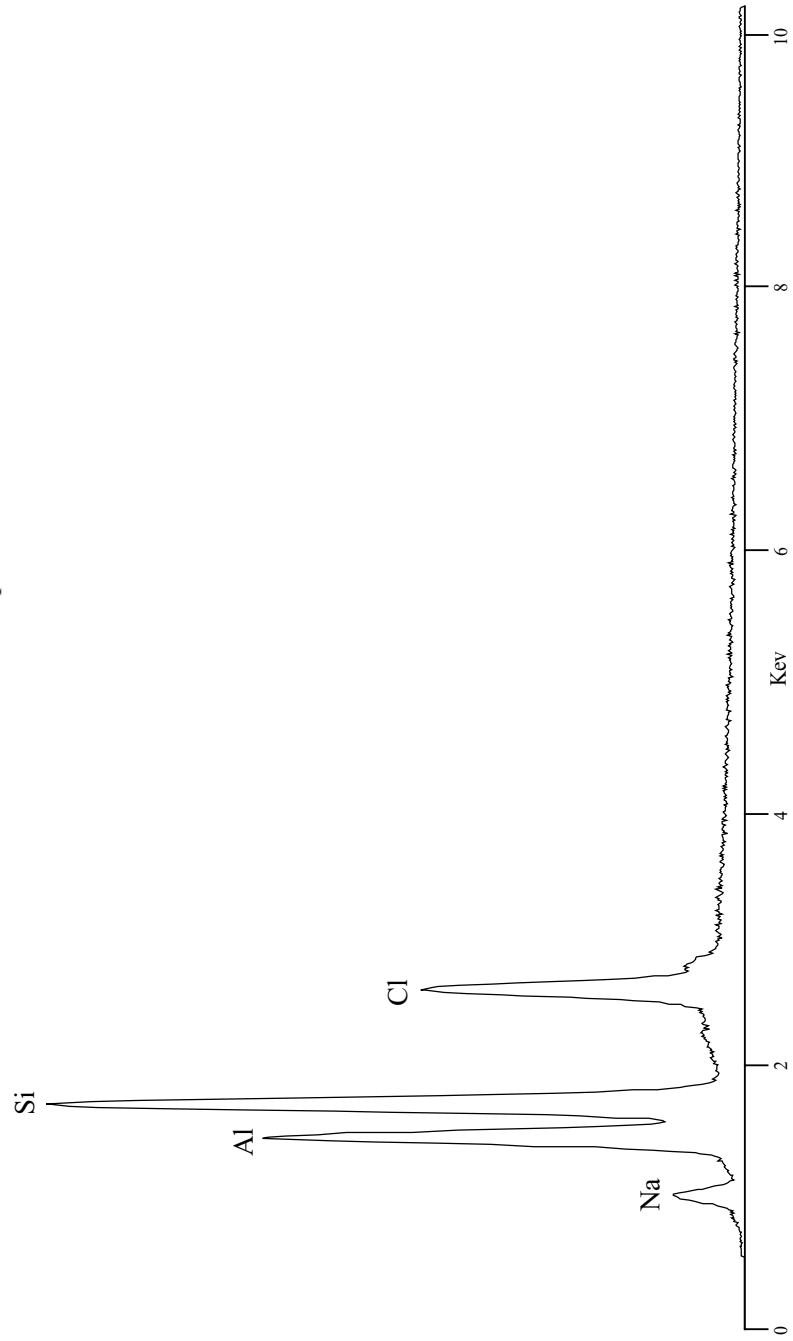
Petalite $\text{Li}[\text{AlSi}_4\text{O}_{10}]$ 

Leucite $K[AlSi_2O_6]$



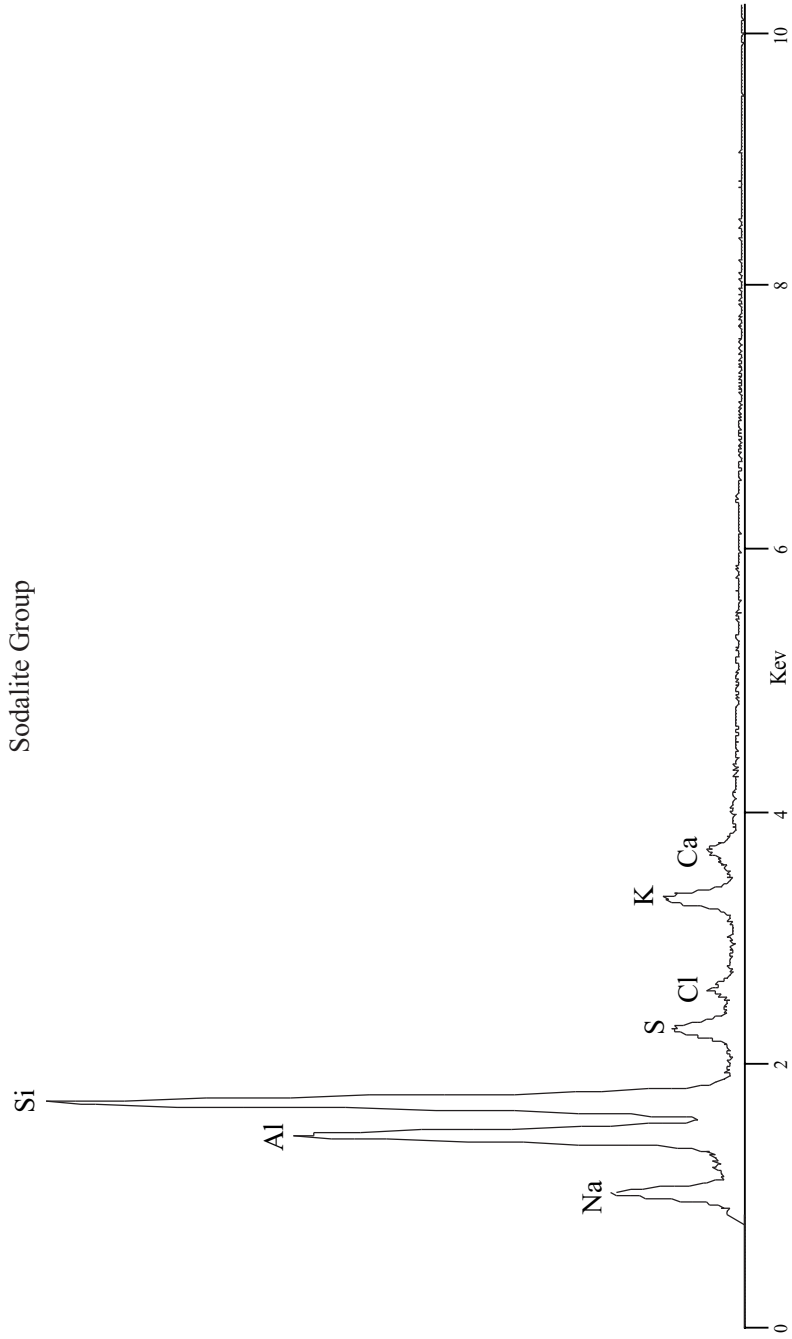
Sodalite $\text{Na}_8[\text{Al}_6\text{Si}_6\text{O}_{24}]\text{Cl}_2$

Sodalite Group

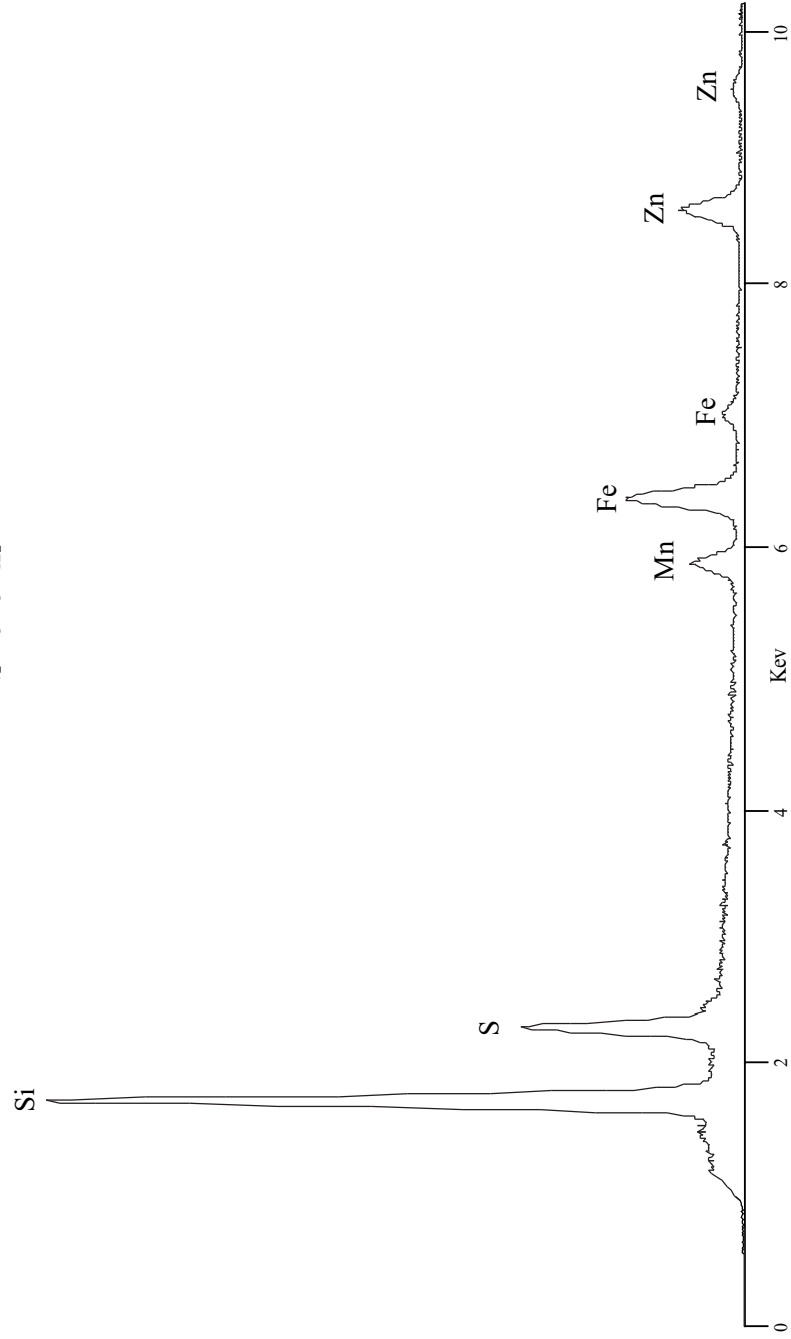


Nosean $\text{Na}_8[\text{Al}_6\text{Si}_6\text{O}_{24}]\text{SO}_4$
Häuyne $(\text{Na,Ca})_{4-8}[\text{Al}_6\text{Si}_6\text{O}_{24}](\text{SO}_4,\text{S})_{1-2}$

Sodalite Group



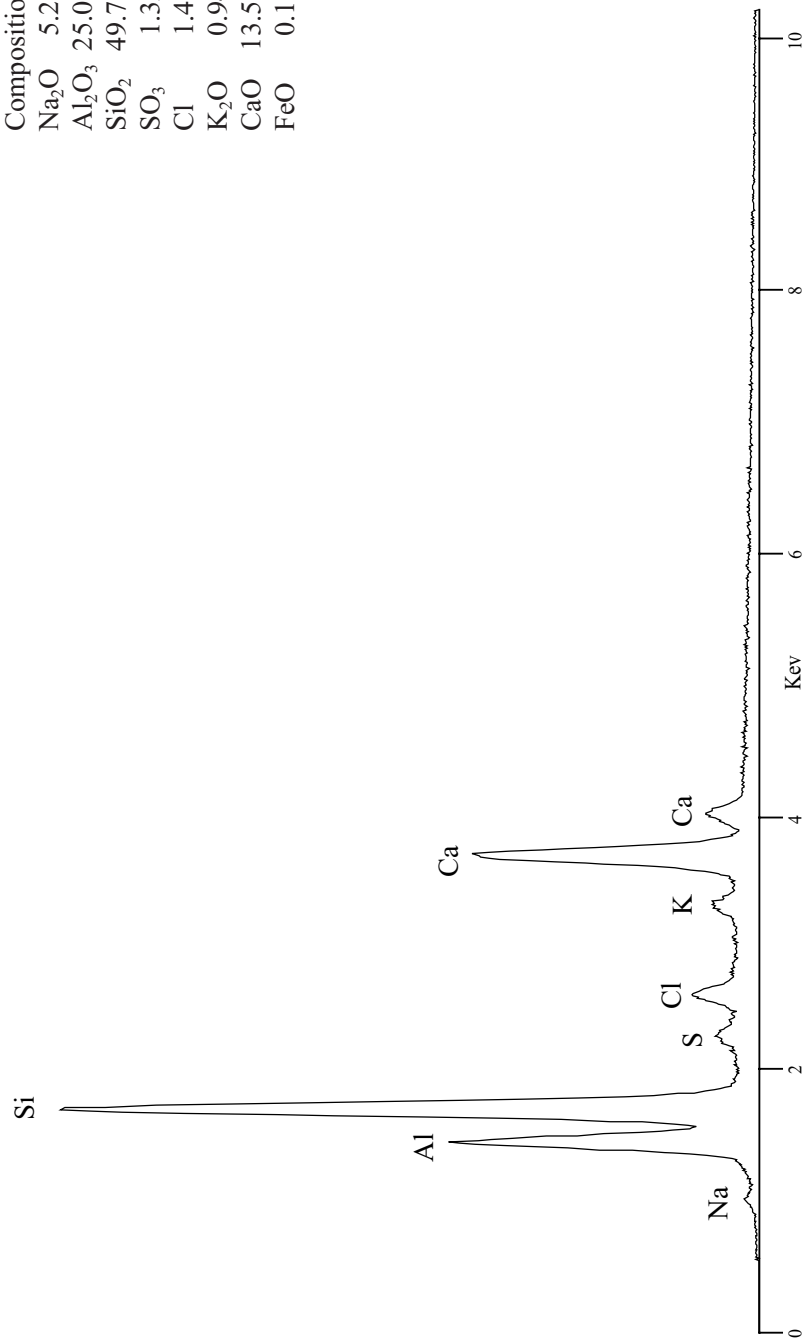
Helvite $\text{Mn}_4[\text{Be}_3\text{Si}_3\text{O}_{12}]_2\text{S} \sim 10\%$
Danalite $\text{Fe}_4[\text{Be}_3\text{Si}_3\text{O}_{12}]_2\text{S} \sim 35\%$
Genthelvite $\text{Zn}_4[\text{Be}_3\text{Si}_3\text{O}_{12}]_2\text{S} \sim 55\%$



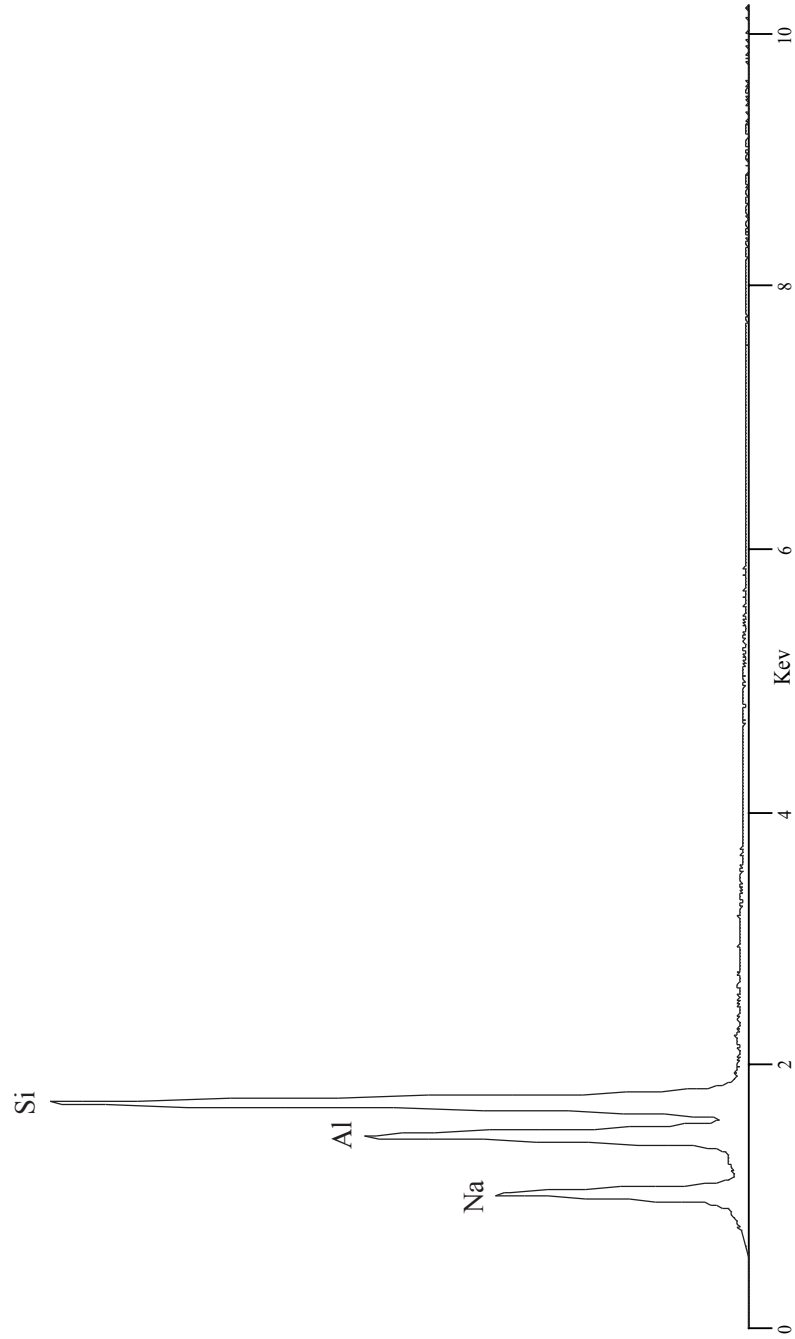
Smithsonian Standard
USNM R6600-1

Composition	
Na ₂ O	5.20
Al ₂ O ₃	25.05
SiO ₂	49.78
SO ₃	1.32
Cl	1.43
K ₂ O	0.94
CaO	13.58
FeO	0.17

Scapolite (Na,Ca,K)₄[Al₃(Al,Si)₃Si₆O₂₄](Cl,CO₃,SO₄,OH)

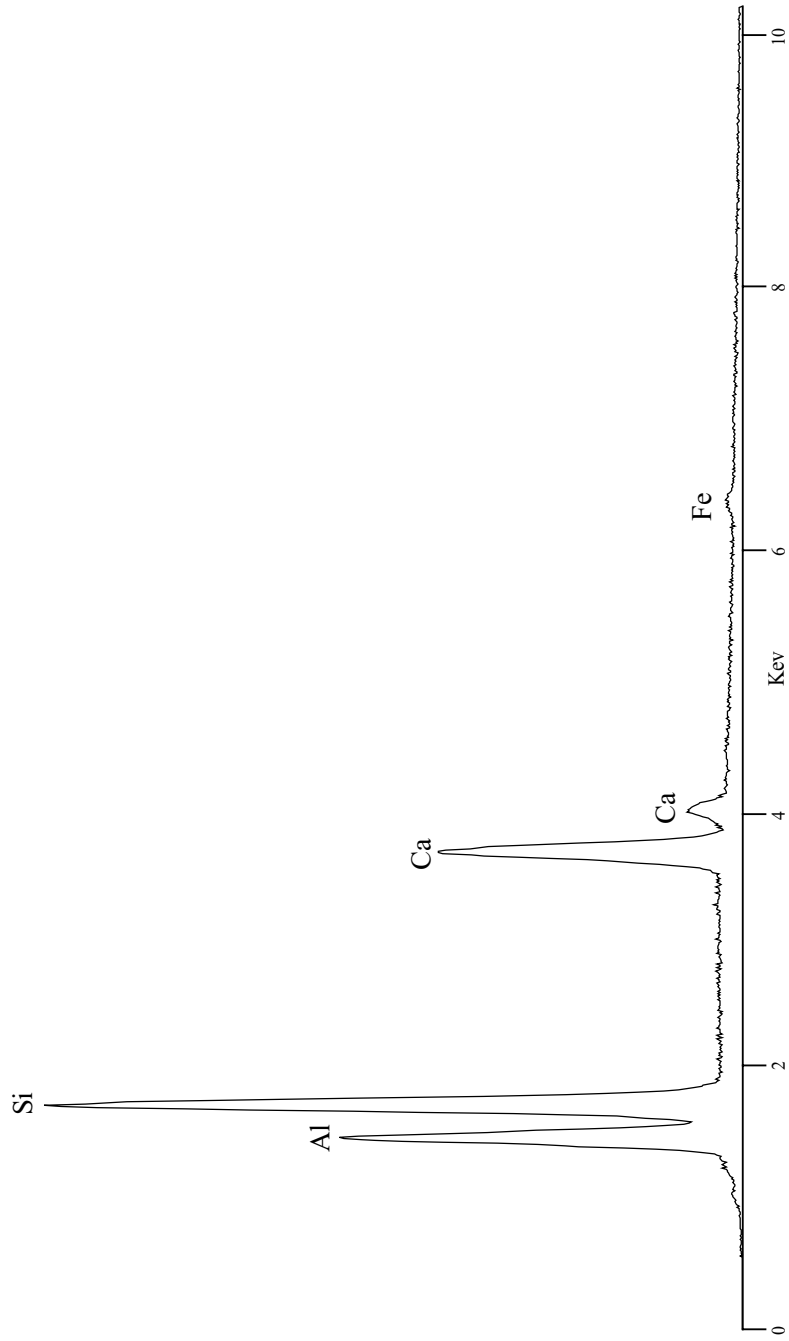


Analcite $\text{Na}[\text{AlSi}_2\text{O}_6] \cdot \text{H}_2\text{O}$



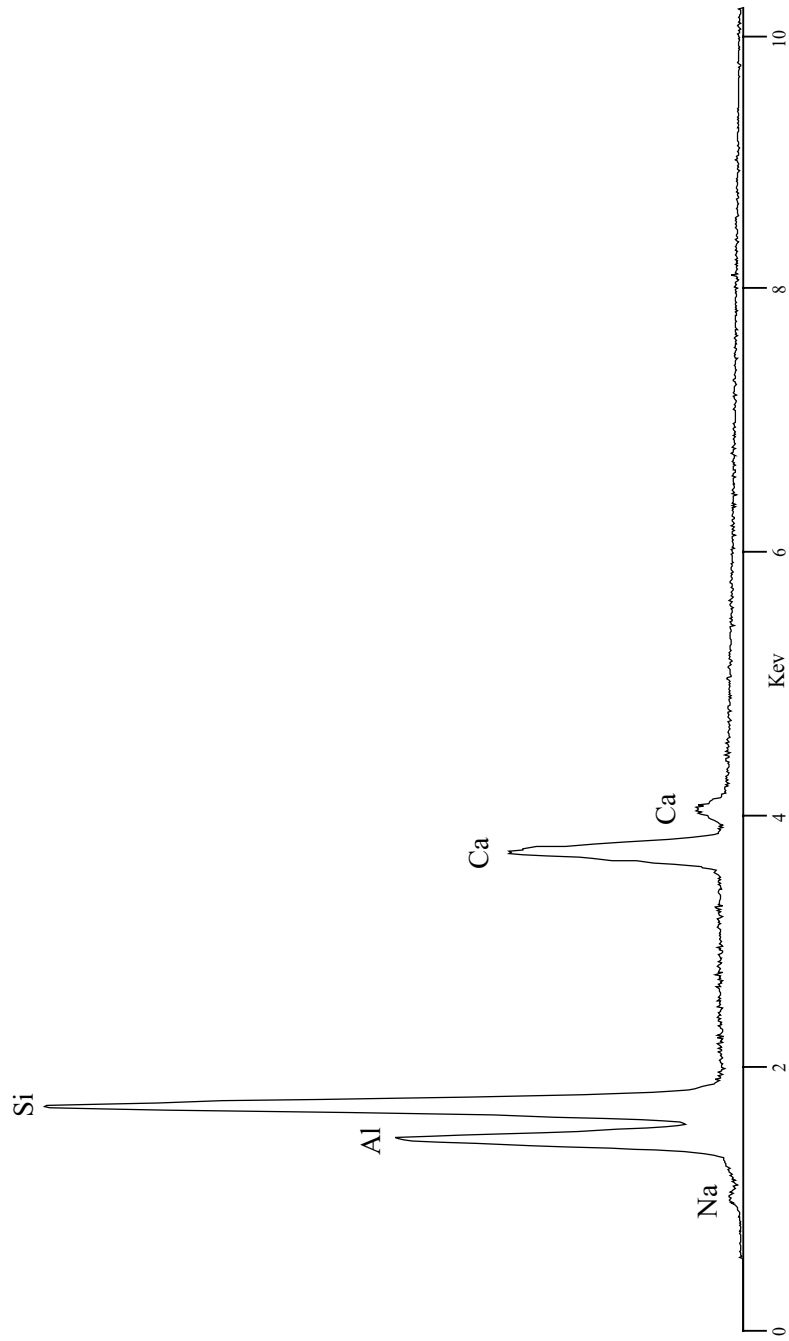
Scolecite $\text{Ca}[\text{Al}_2\text{Si}_3\text{O}_{10}] \cdot 3\text{H}_2\text{O}$

Zeolite

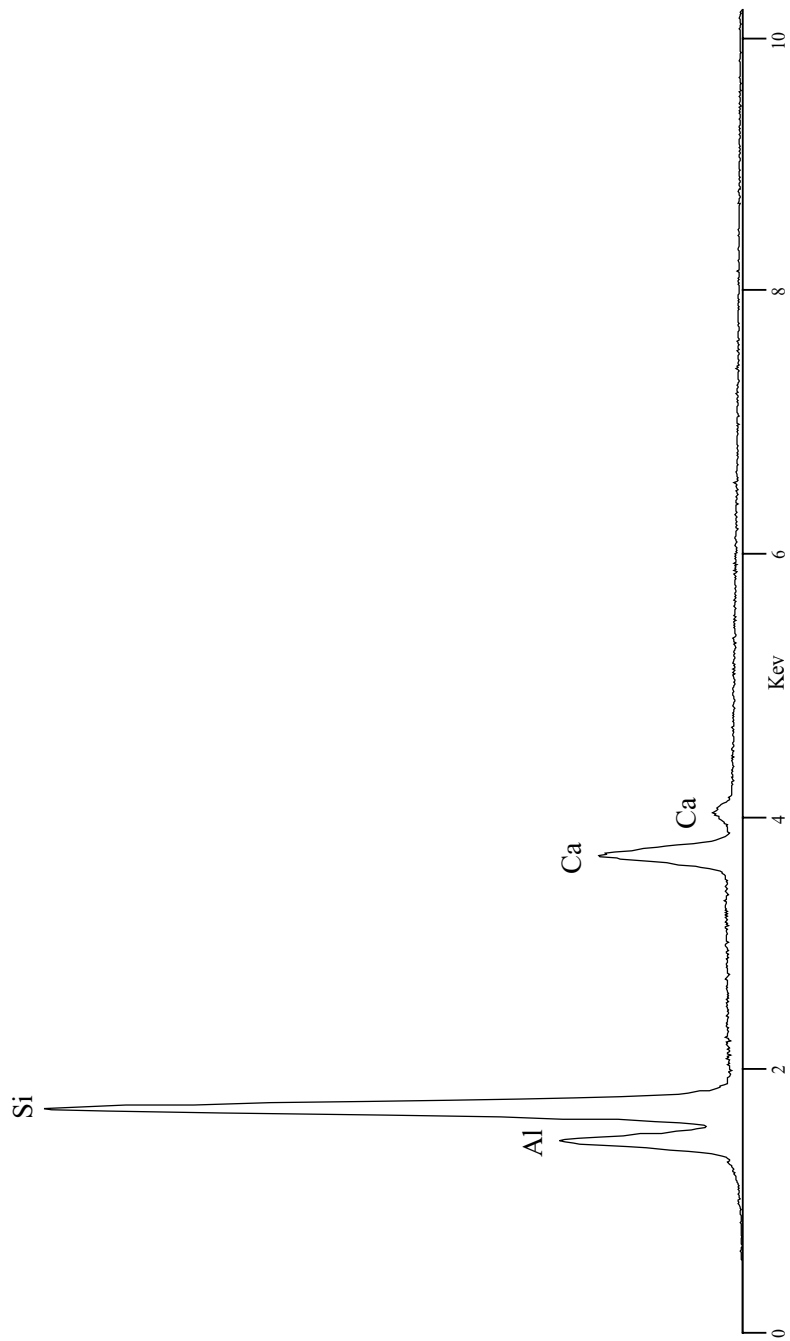


Thomsonite $\text{NaCa}_2[(\text{Al},\text{Si})_{10}\text{O}_{10}]_2 \cdot 6\text{H}_2\text{O}$

Zeolite

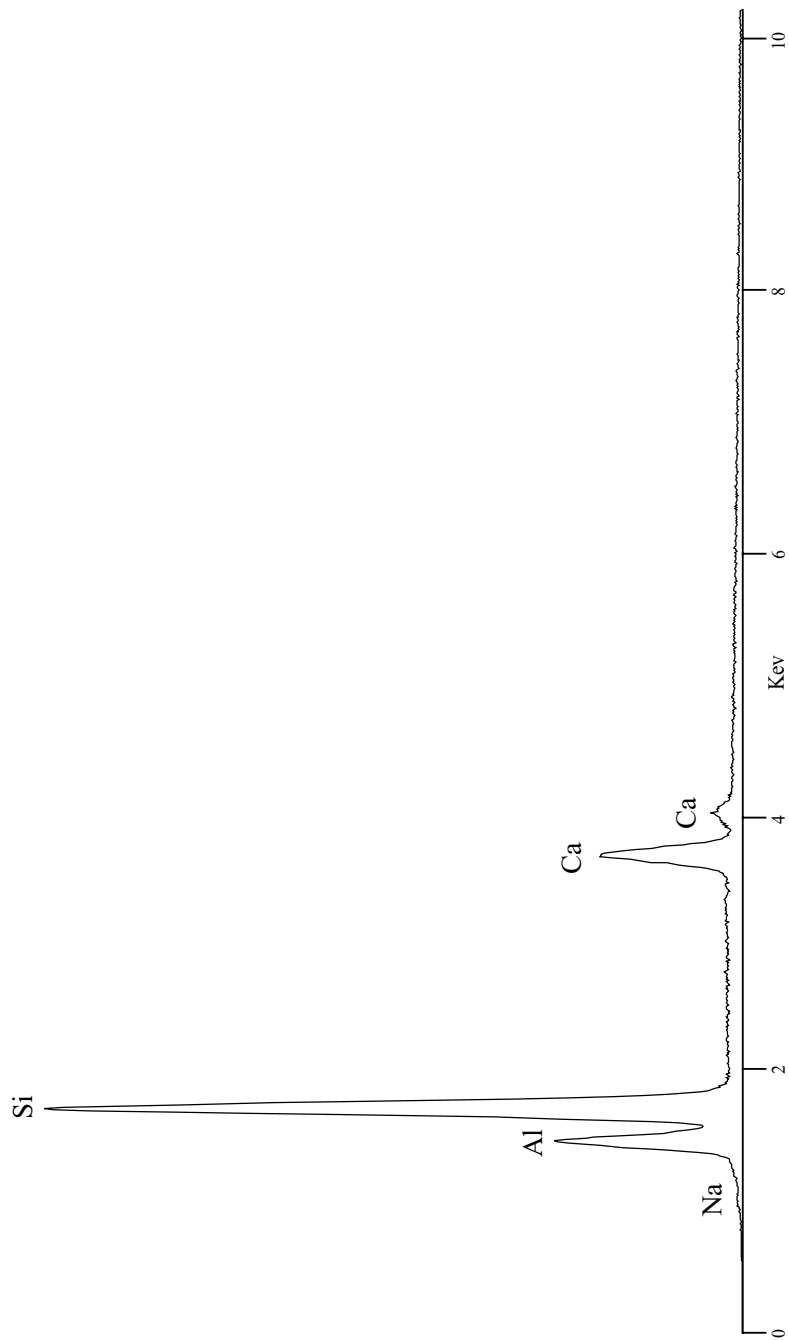


Chabazite $\text{Ca}[\text{Al}_2\text{Si}_4\text{O}_{12}] \cdot 6\text{H}_2\text{O}$
Zeolite



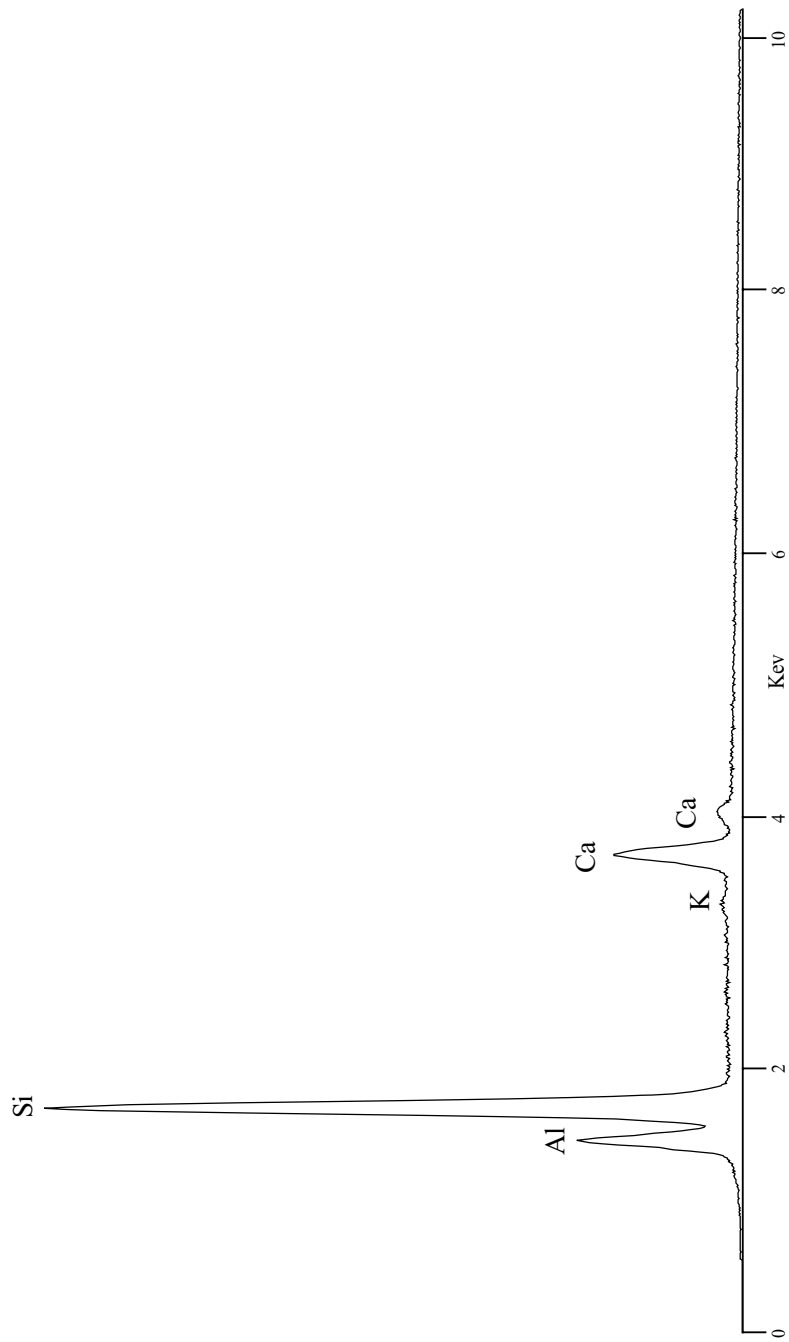
Heulandite $(\text{Ca},\text{Na}_2)[\text{Al}_2\text{Si}_7\text{O}_{18}] \cdot 6\text{H}_2\text{O}$

Zeolite



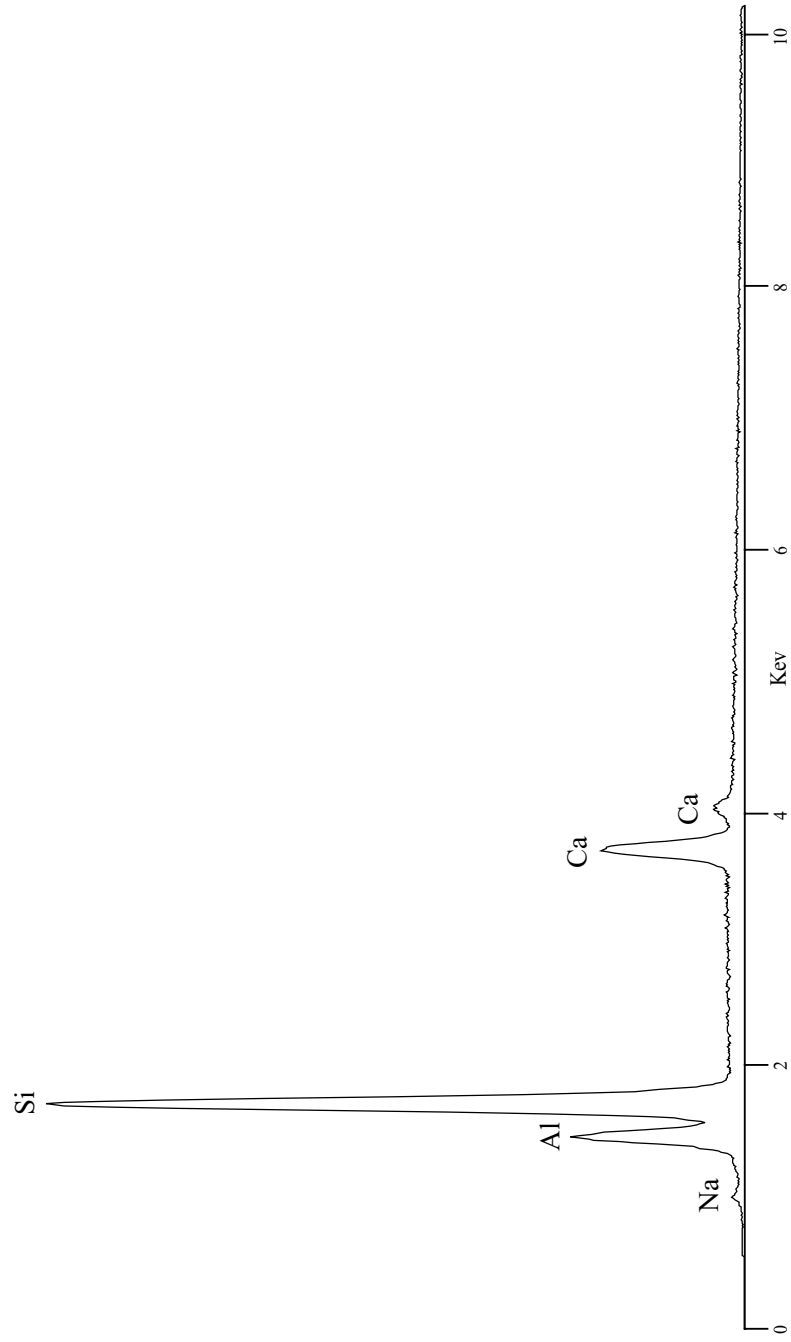
Stilbite $(Ca,Na_2,K_2)[Al_2Si_7O_{18}] \cdot 7H_2O$

Zeolite

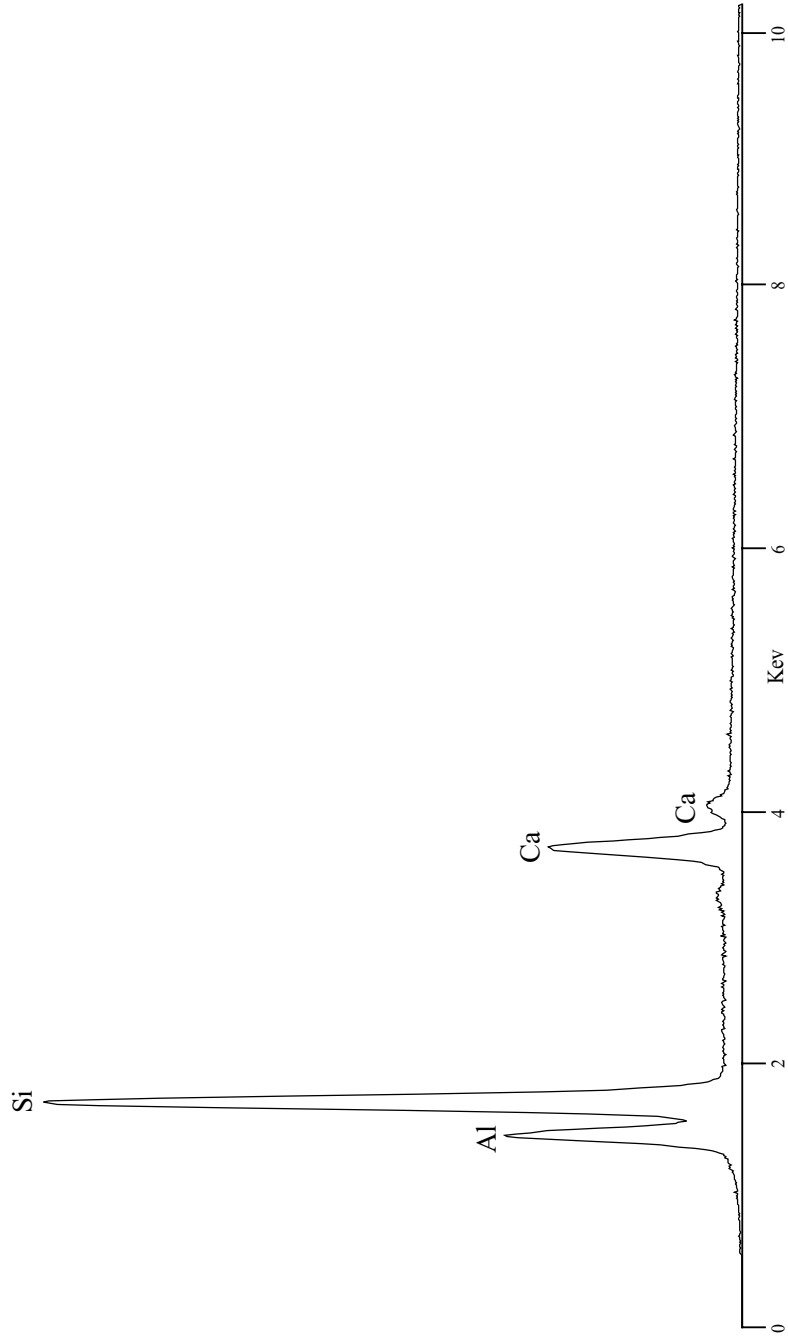


Stilbite $(\text{Ca}, \text{Na}_2, \text{K}_2)[\text{Al}_2\text{Si}_7\text{O}_{18}] \cdot 7\text{H}_2\text{O}$

Zeolite

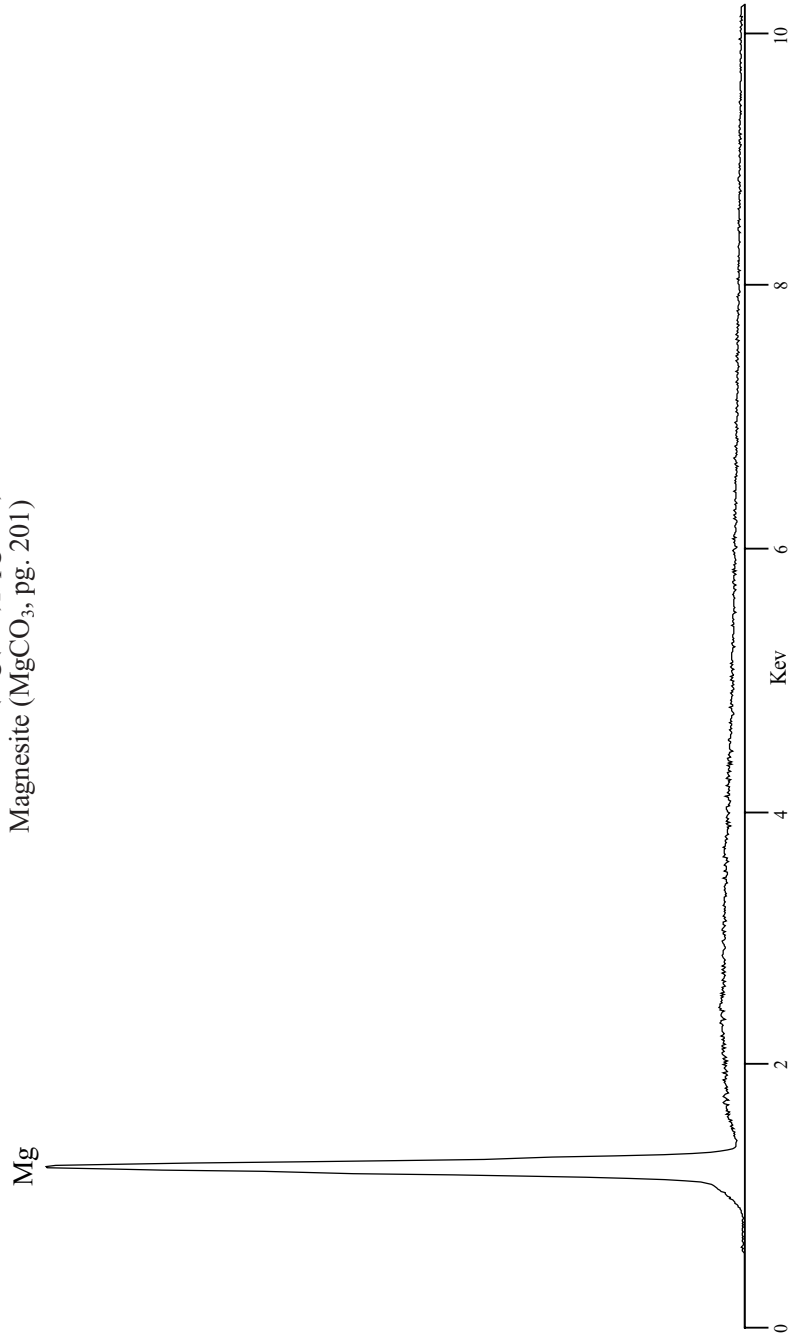


Laumontite $\text{Ca}[\text{Al}_2\text{Si}_4\text{O}_{12}] \cdot 4\text{H}_2\text{O}$
Zeolite



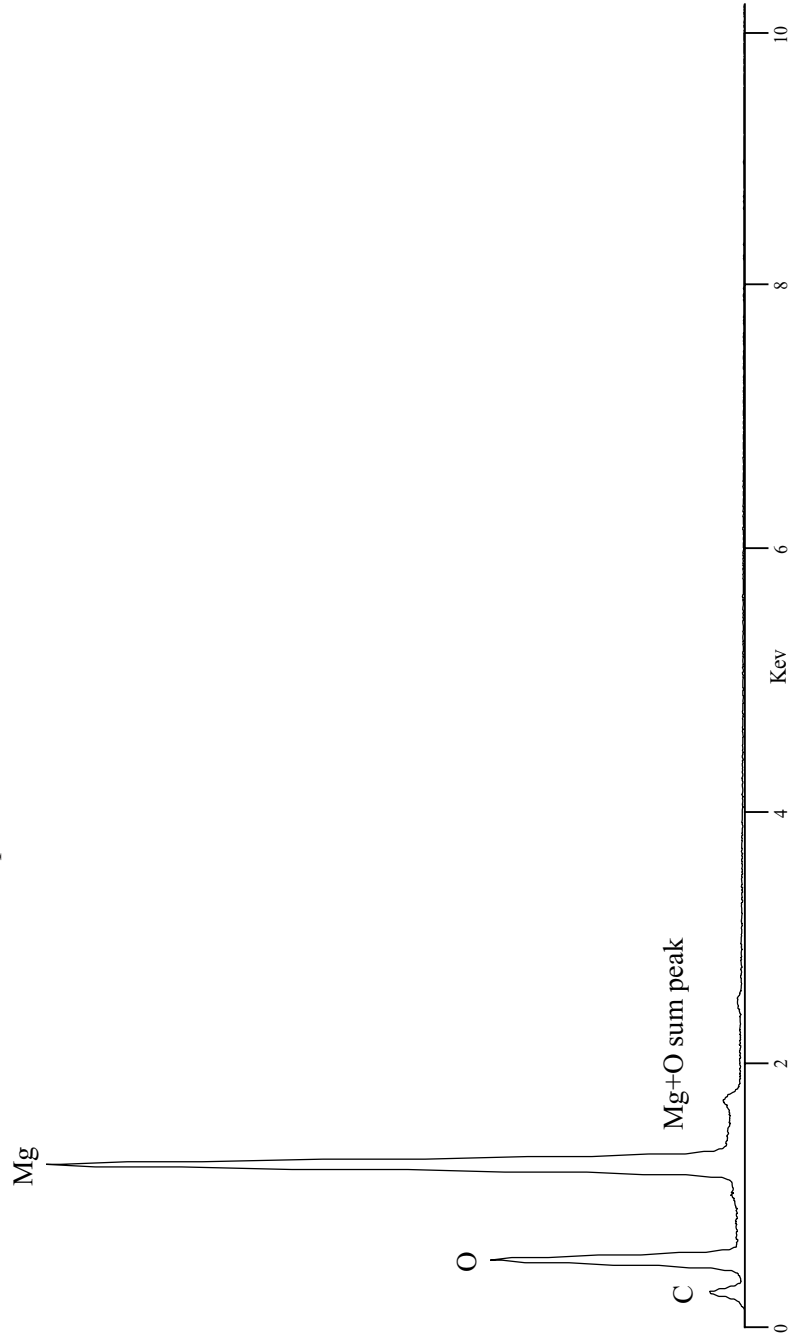
Periclase MgO

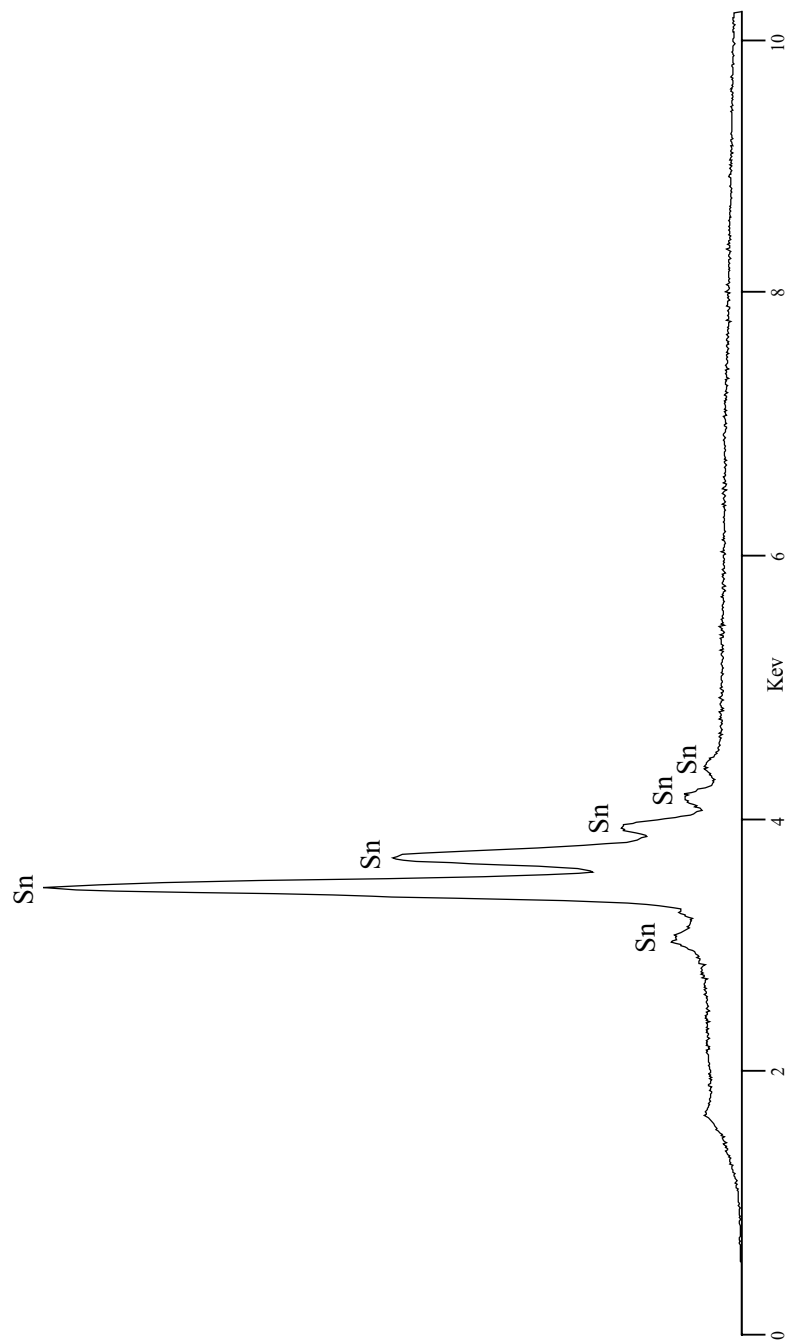
see also Brucite $(\text{Mg}(\text{OH})_2)$, pg.179) and
Magnesite (MgCO_3) , pg. 201)



Periclase MgO

Spectrum collected with thin window detector

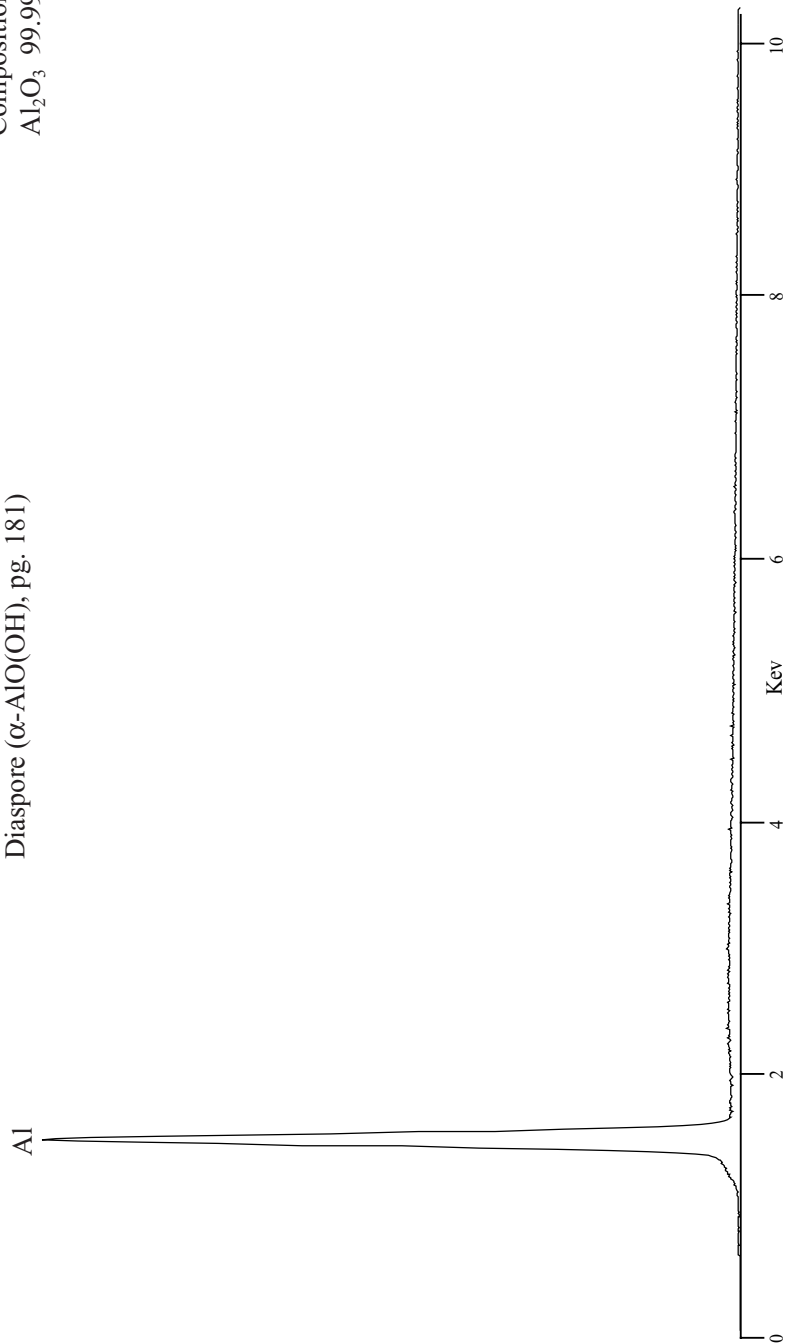


Cassiterite SnO_2 

Smithsonian Standard
USNM 657S
Composition
Al₂O₃ 99.99

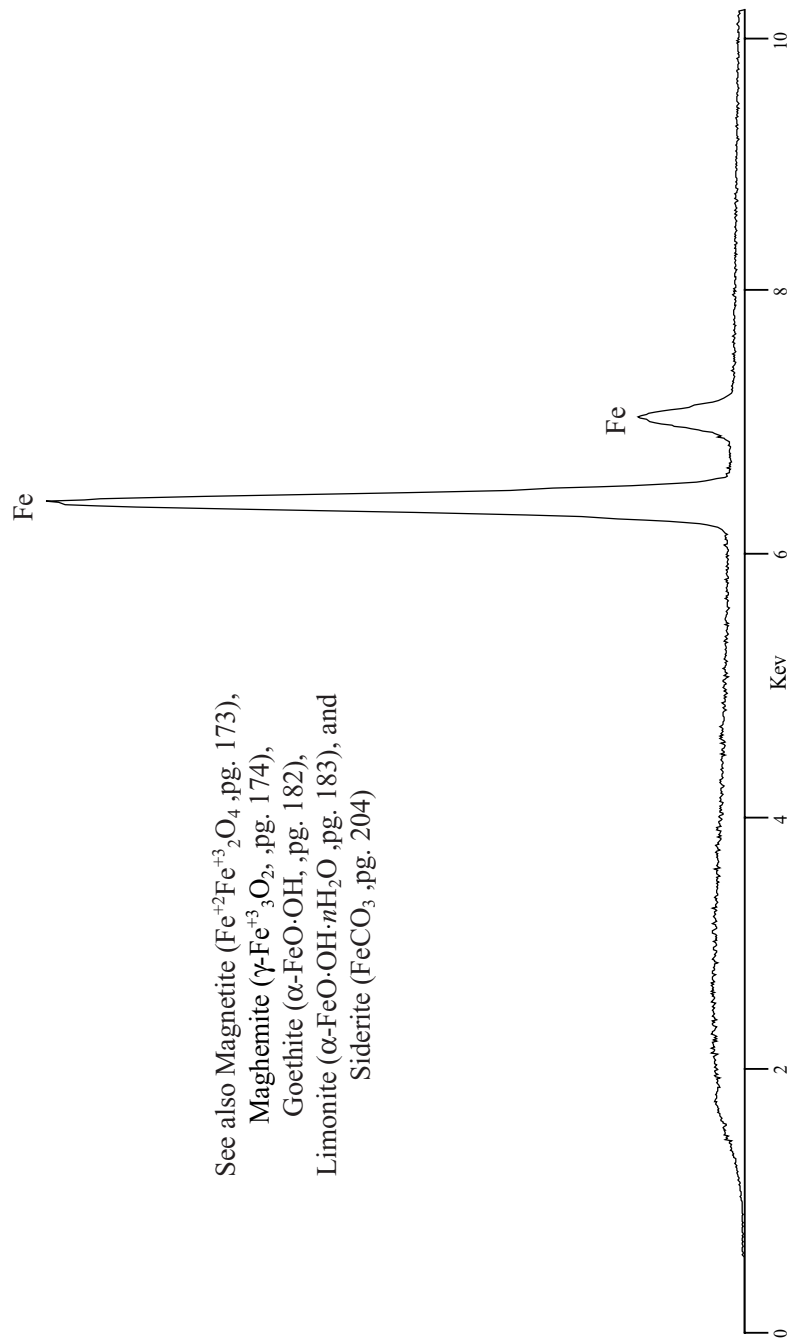
Corundum α -Al₂O₃

See also Gibbsite (Al(OH)₃, pg. 180) and
Diaspore (α -AlO(OH), pg. 181)



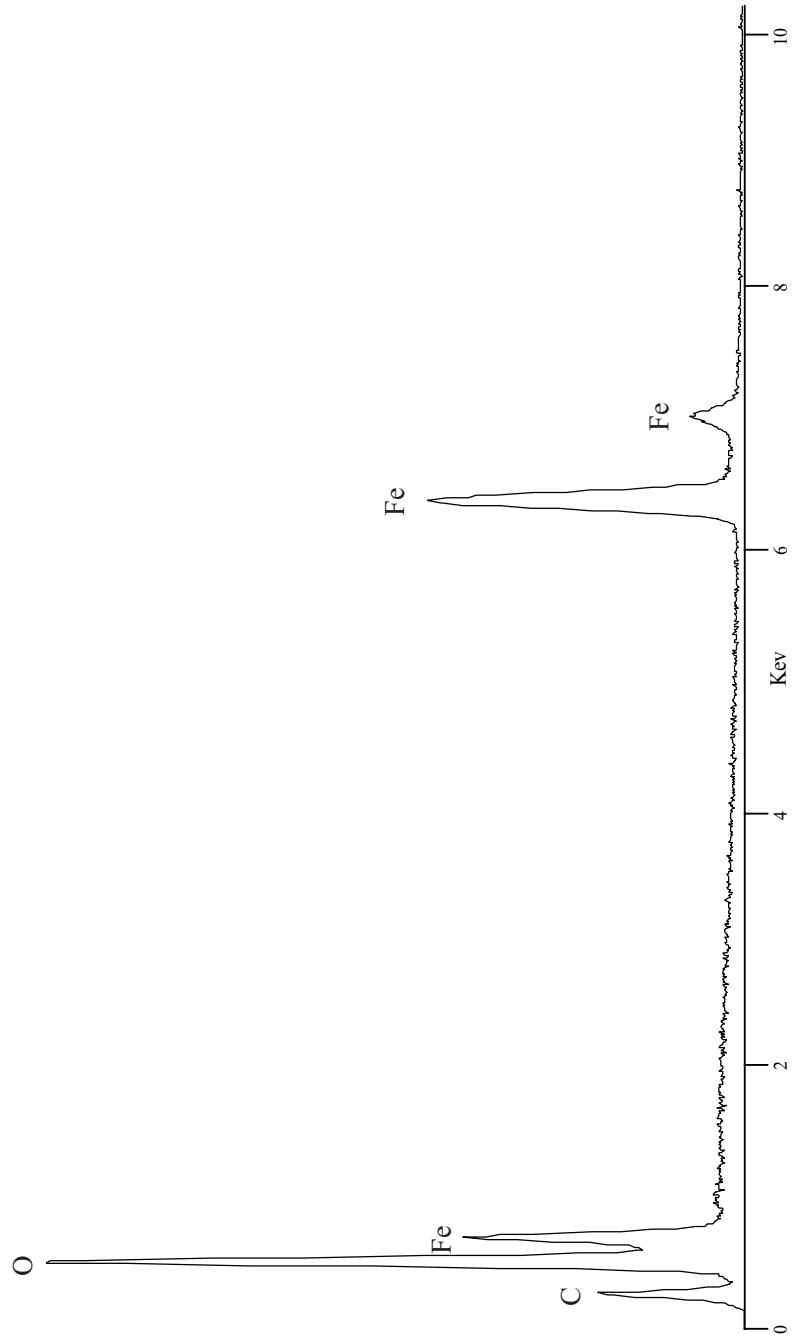
Hæmatite $\alpha\text{-Fe}_2\text{O}_3$

See also Magnetite ($\text{Fe}^{+2}\text{Fe}^{+3}_2\text{O}_4$, pg. 173),
Maghemite ($\gamma\text{-Fe}^{+3}_3\text{O}_2$, pg. 174),
Goethite ($\alpha\text{-FeO}\cdot\text{OH}$, pg. 182),
Limonite ($\alpha\text{-FeO}\cdot\text{OH}\cdot n\text{H}_2\text{O}$, pg. 183), and
Siderite (FeCO_3 , pg. 204)



Hematite α -Fe₂O₃

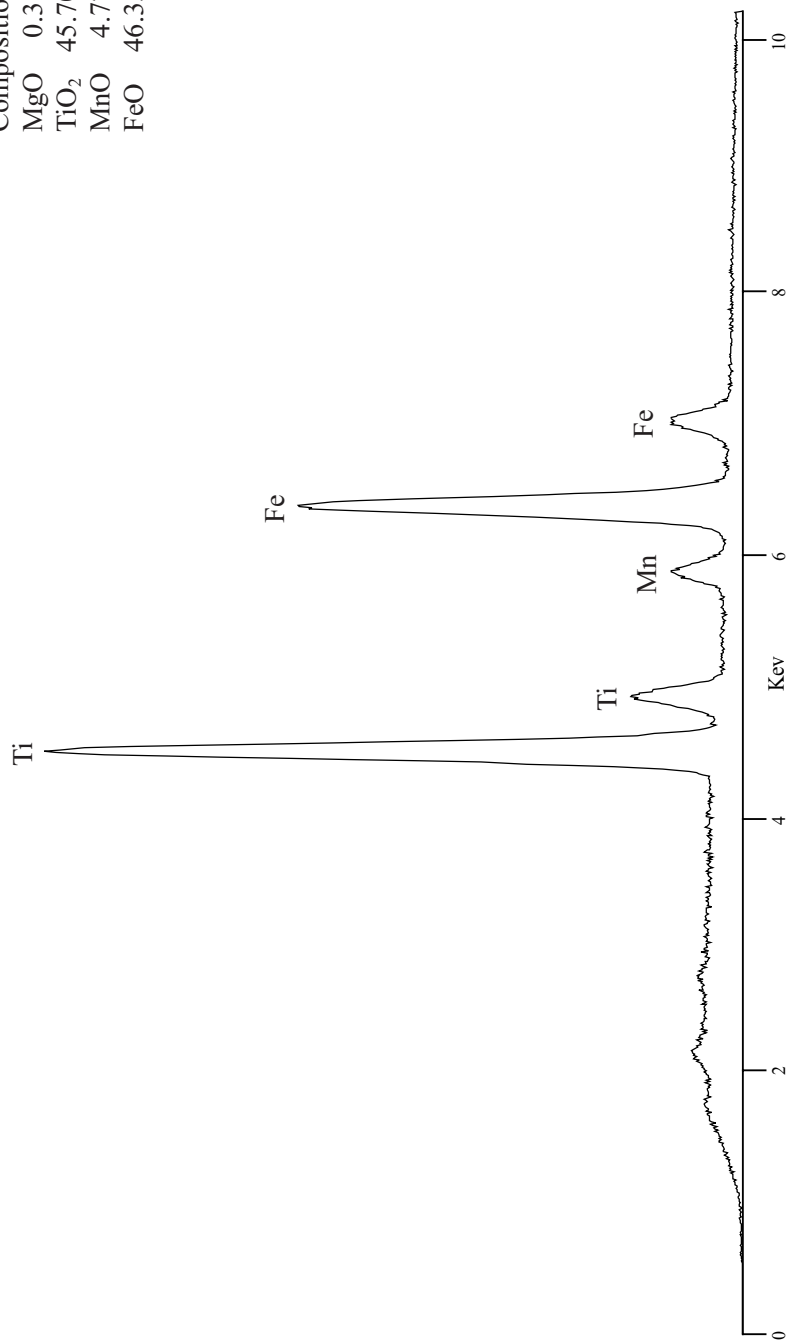
Spectrum collected with thin window detector



Smithsonian Standard
USNM 96189

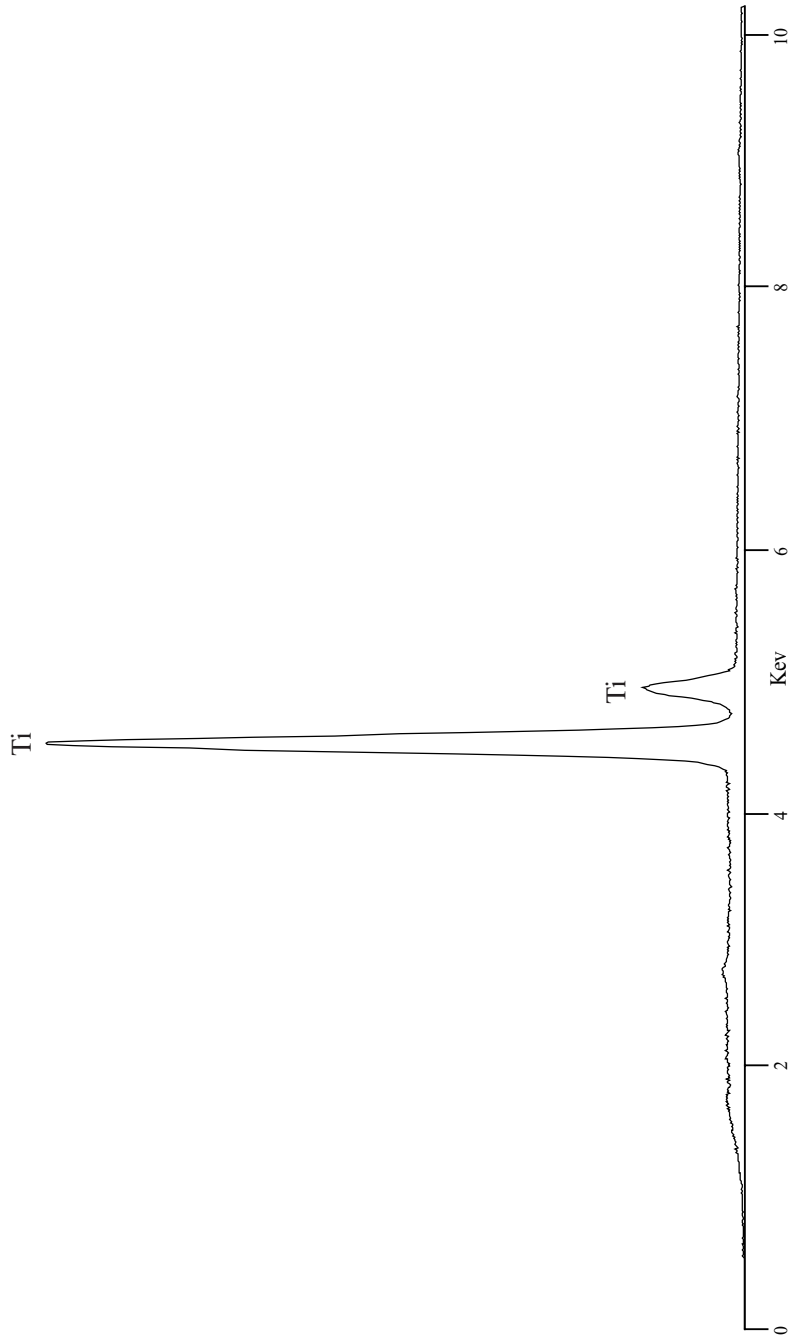
Composition
MgO 0.31
TiO₂ 45.70
MnO 4.77
FeO 46.35

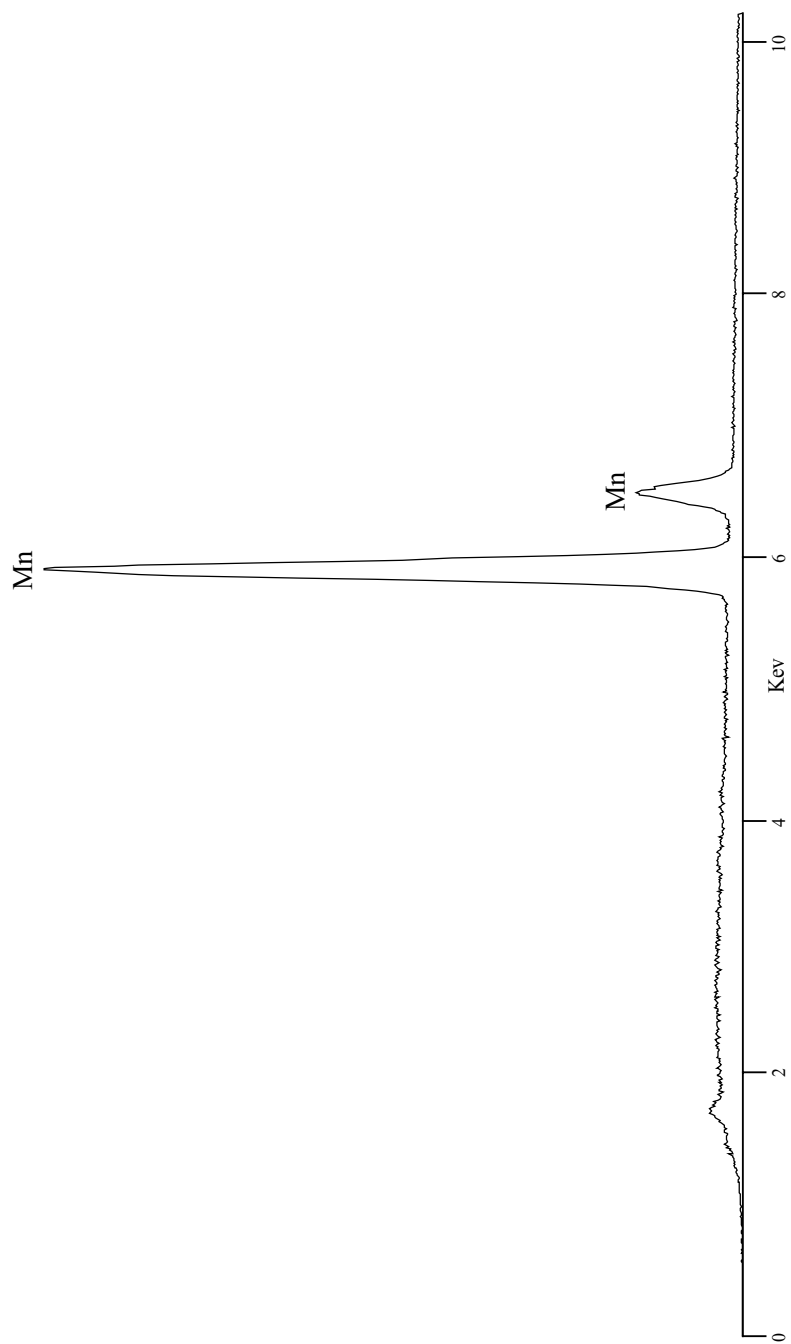
Ilmenite FeTiO₃



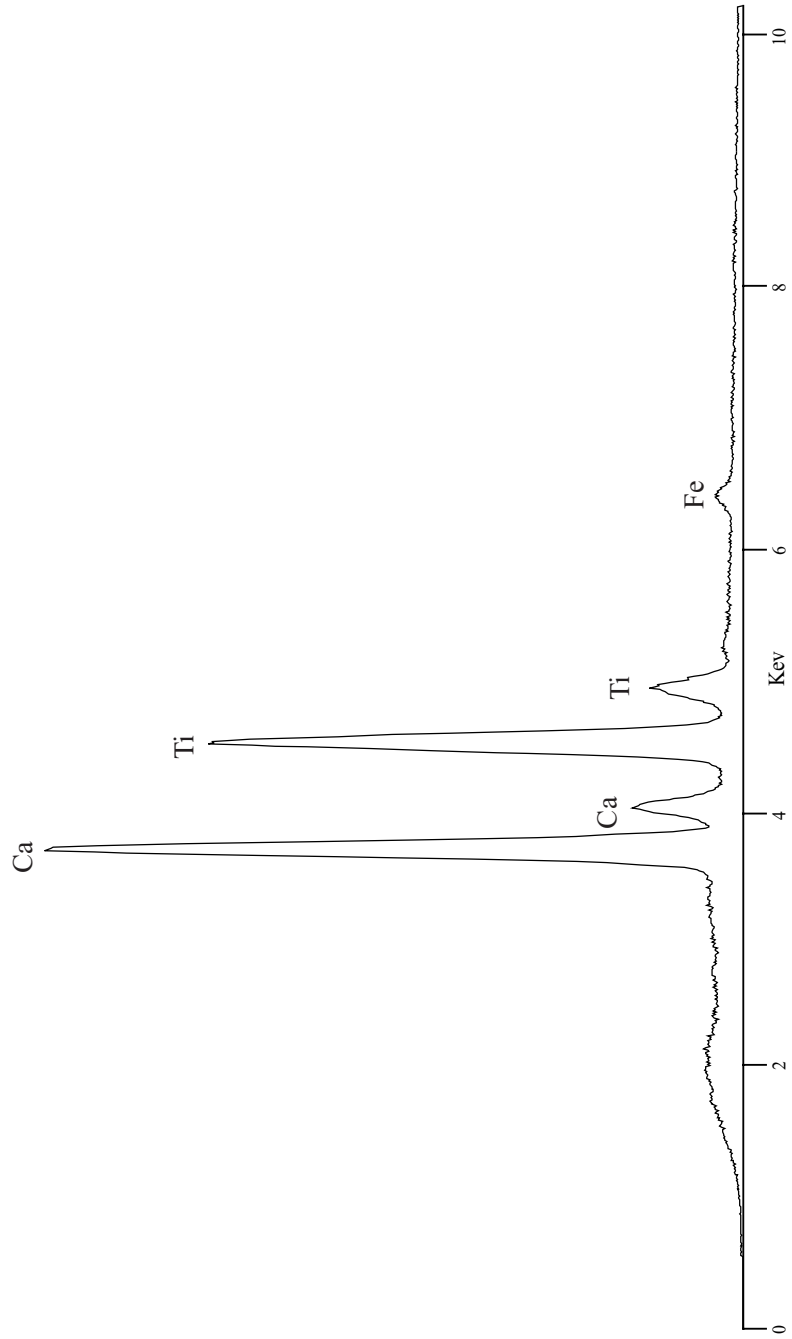
Rutile TiO_2

Similar spectra would be obtained from Anatase or Brookite

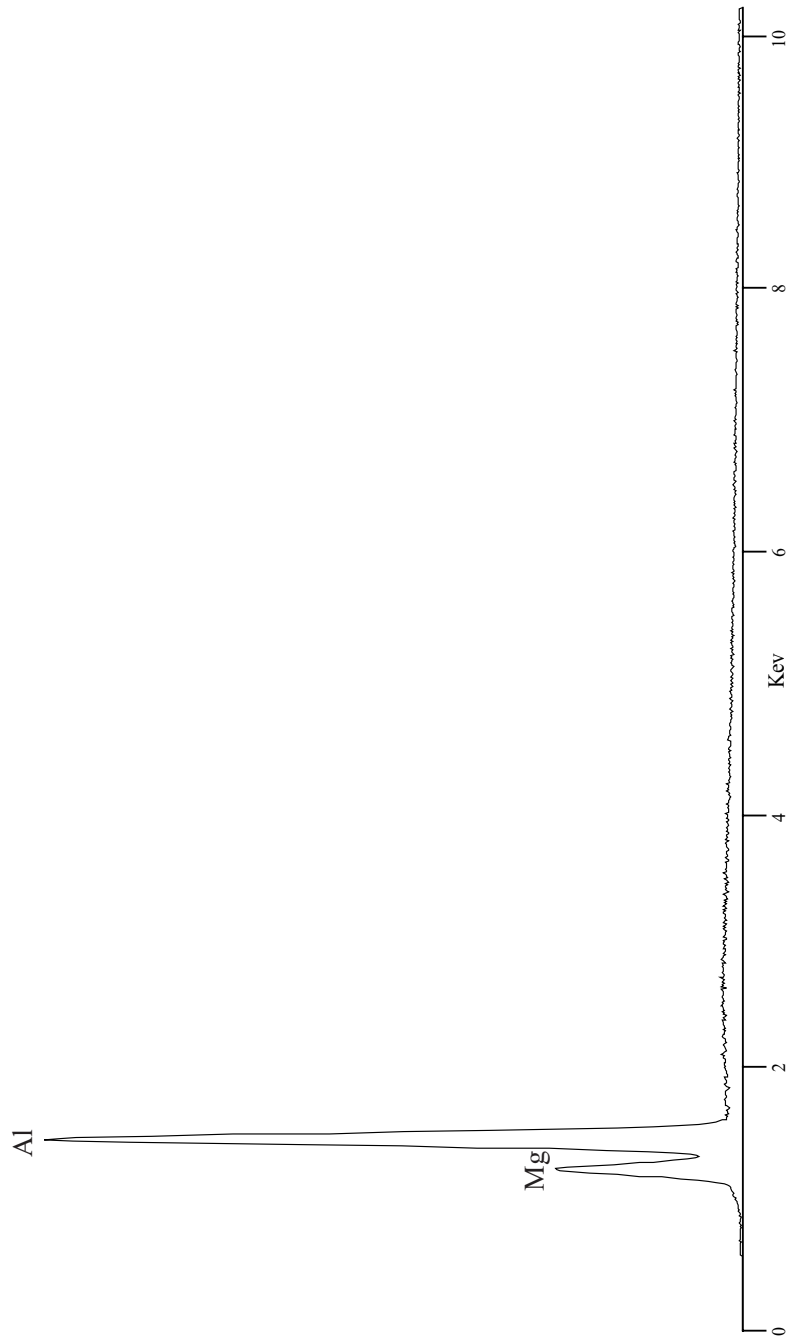


Pyrolusite MnO_2 

Perovskite $(\text{Ca}, \text{Na}, \text{Fe}^{+2}, \text{Ce})(\text{Ti}, \text{Nb})\text{O}_3$



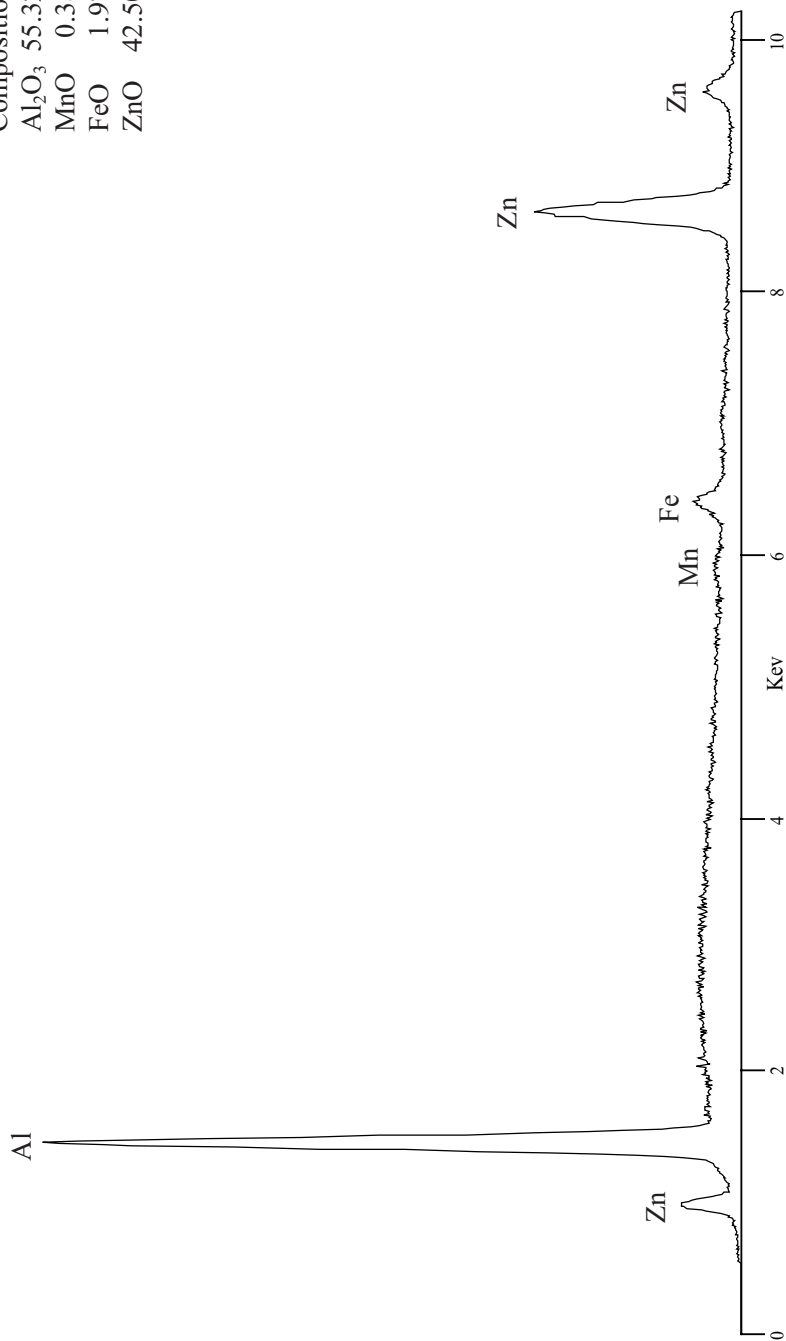
Spinel $MgAl_2O_4$
Spinel



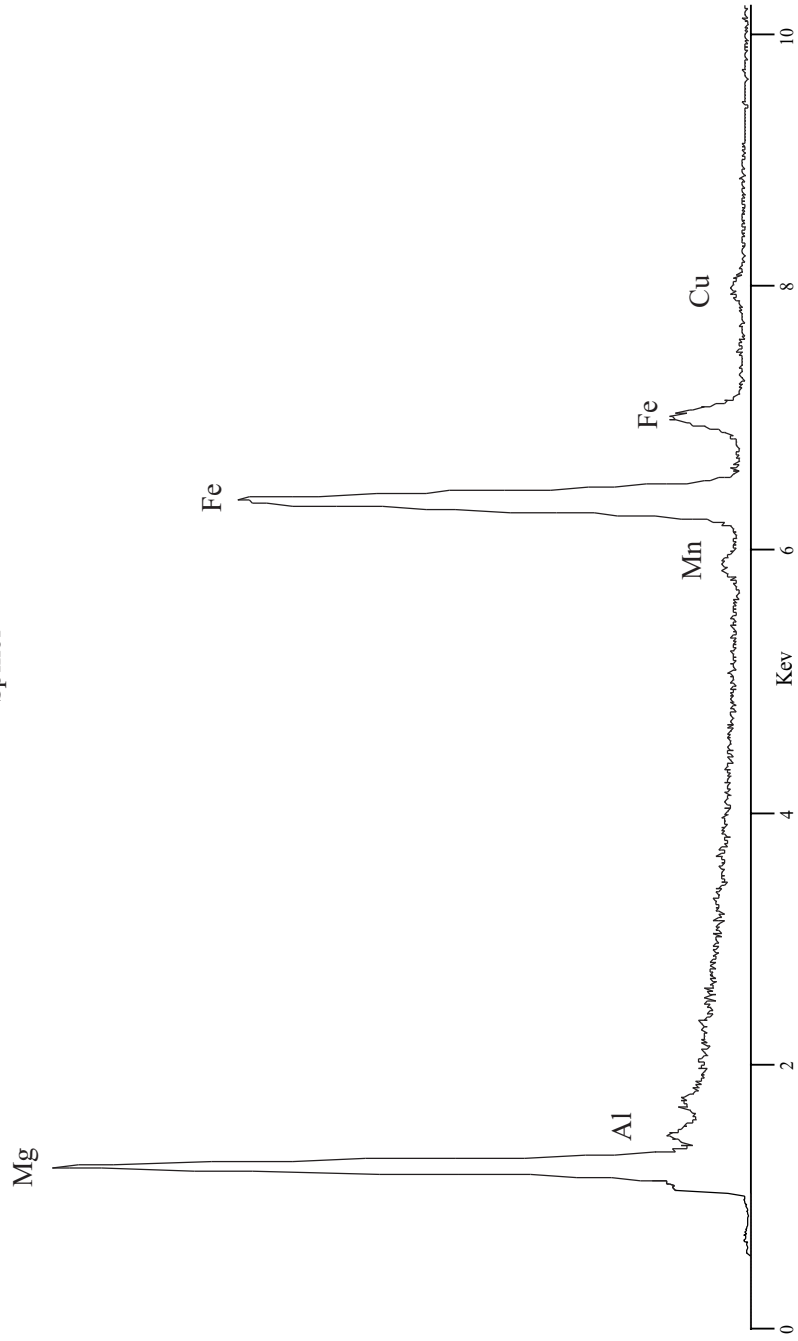
Gahnite $ZnAl_2O_4$
Spinel

Smithsonian Standard
USNM 145883

Composition
 Al_2O_3 55.32
MnO 0.38
FeO 1.97
ZnO 42.50



Magnesioferrite $MgFe^{+3}O_4$
Spinel

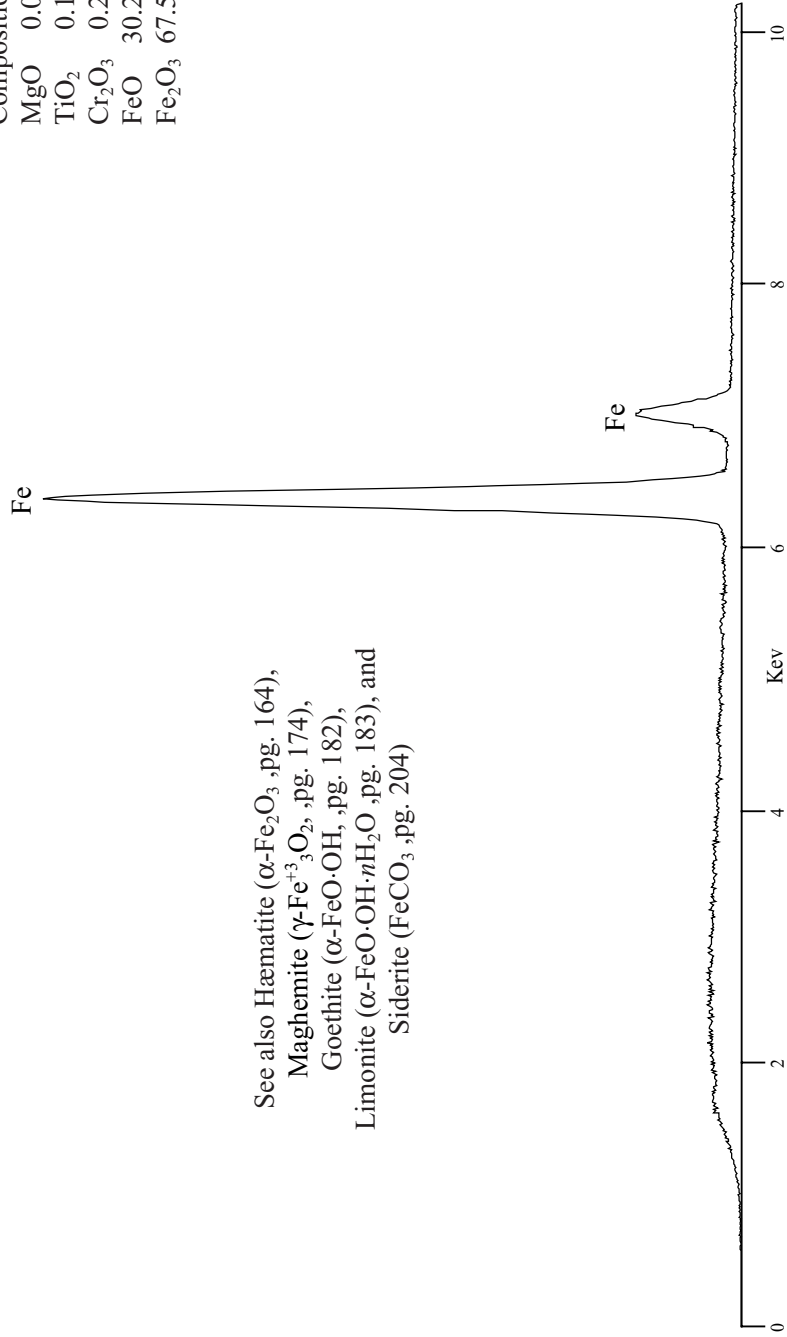


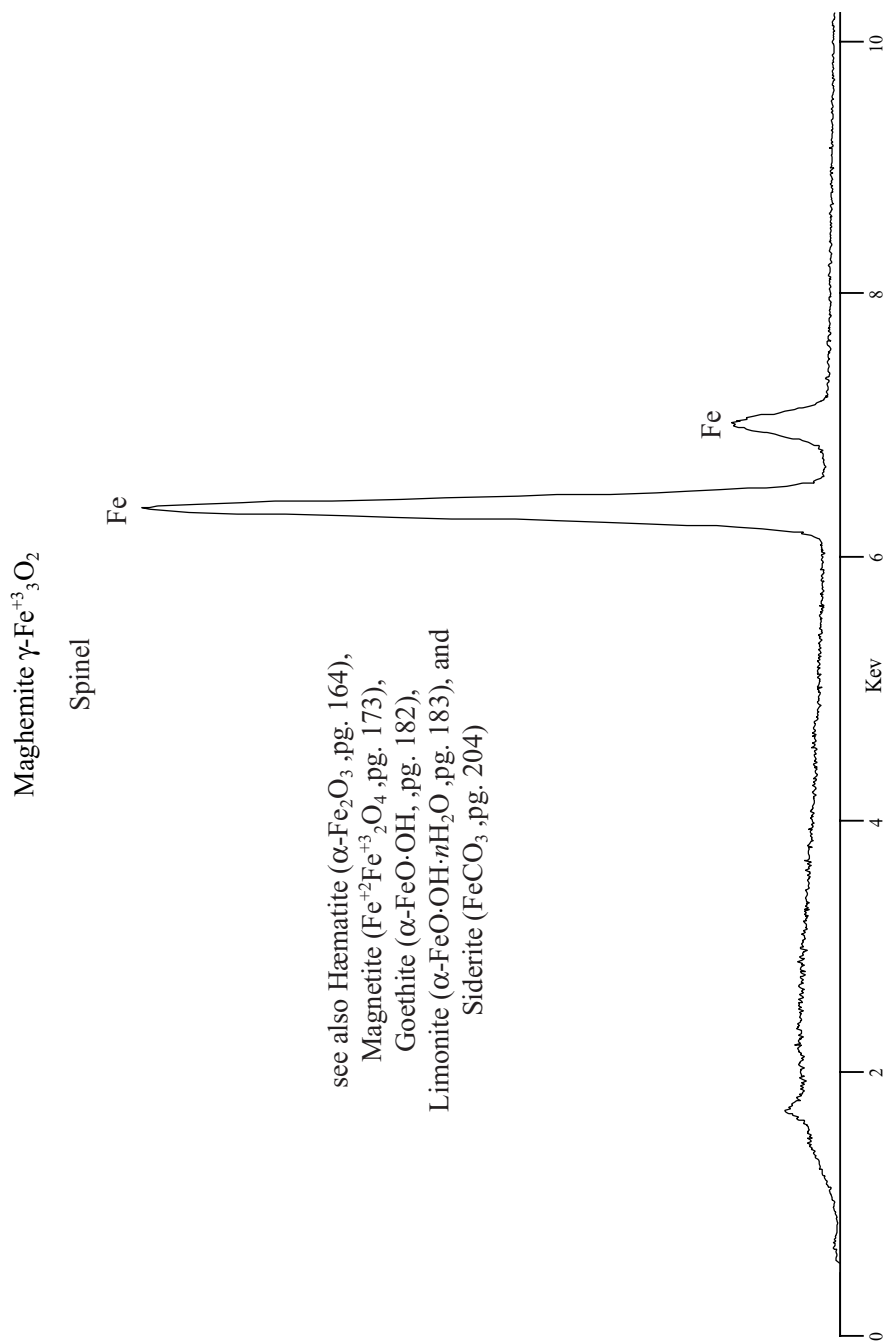
Smithsonian Standard
USNM 114887

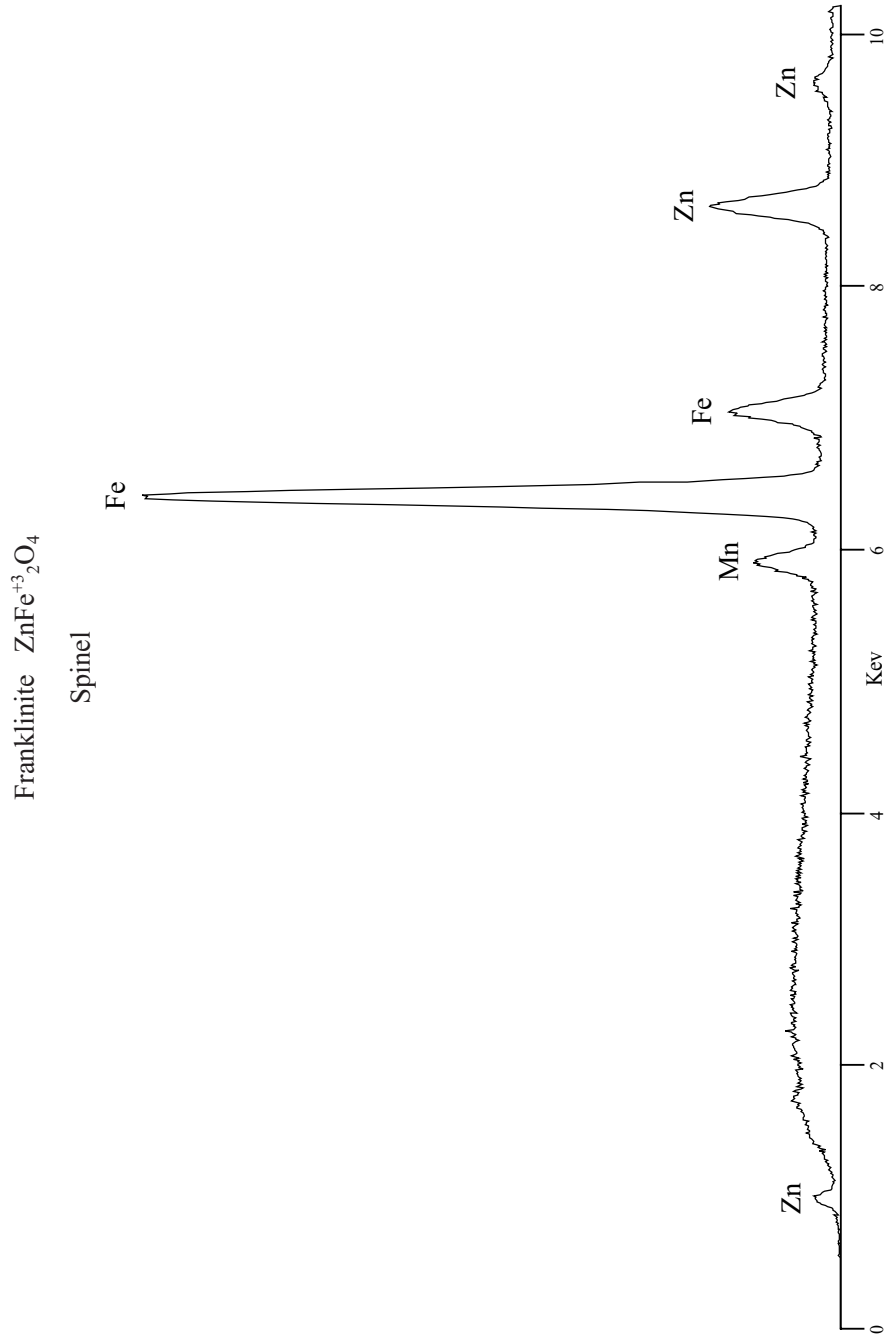
Composition	
MgO	0.05
TiO ₂	0.16
Cr ₂ O ₃	0.25
FeO	30.20
Fe ₂ O ₃	67.50

Magnetite Fe²⁺Fe³⁺O₄
Spinel

See also Häematite (α -Fe₂O₃, pg. 164),
Magnetite (γ -Fe₃O₄, pg. 174),
Goethite (α -FeO·OH, pg. 182),
Limonite (α -FeO·OH·*n*H₂O, pg. 183), and
Siderite (FeCO₃, pg. 204)

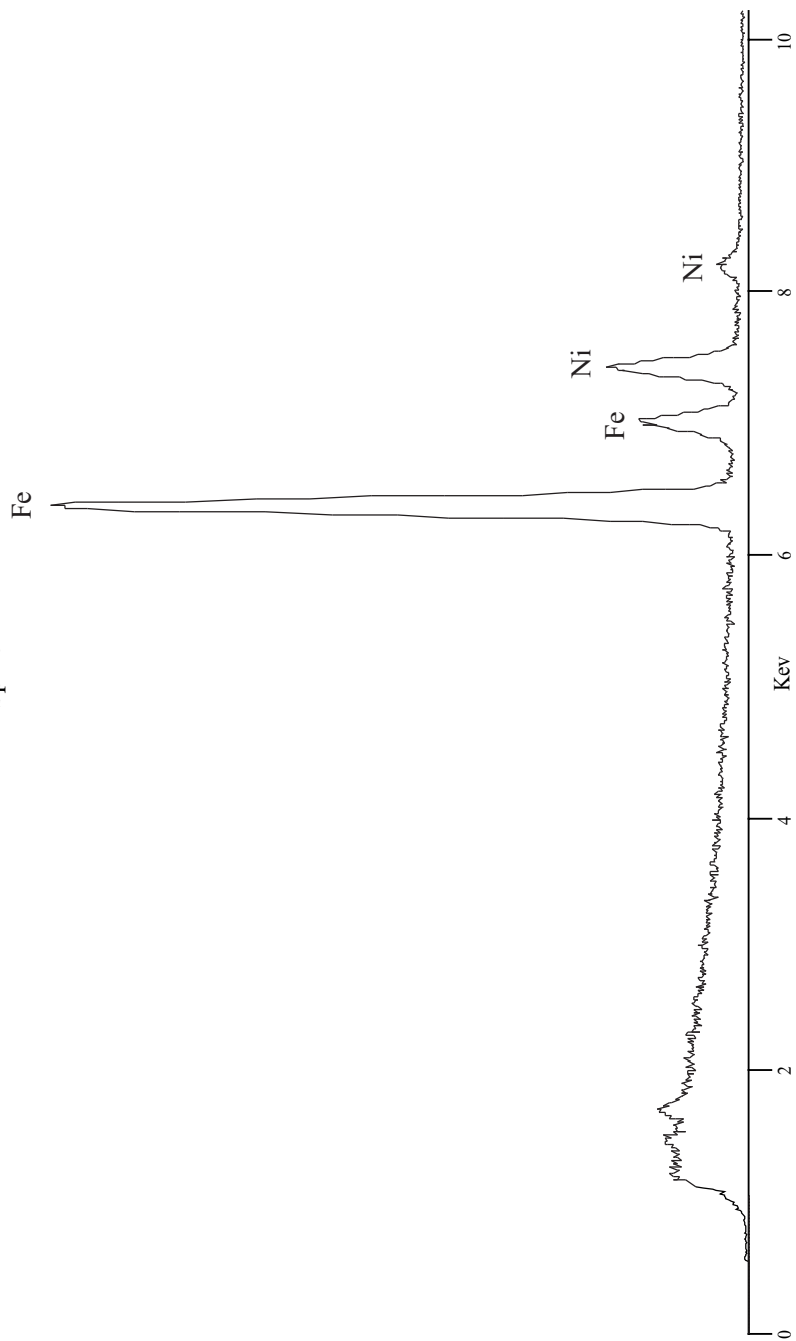






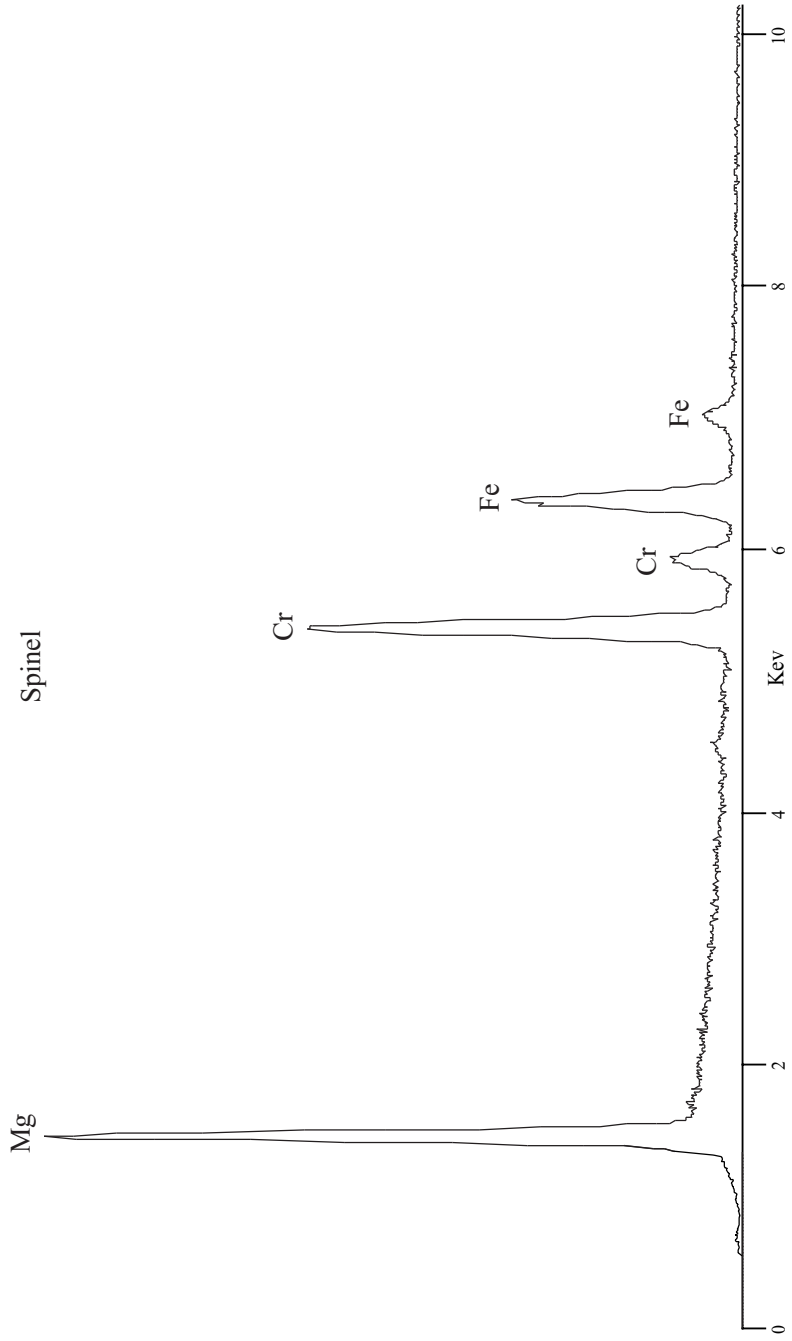
Trevorite $\text{NiFe}^{+3}\text{O}_4$

Spinel



Magnesiochromite $MgCr_2O_4$

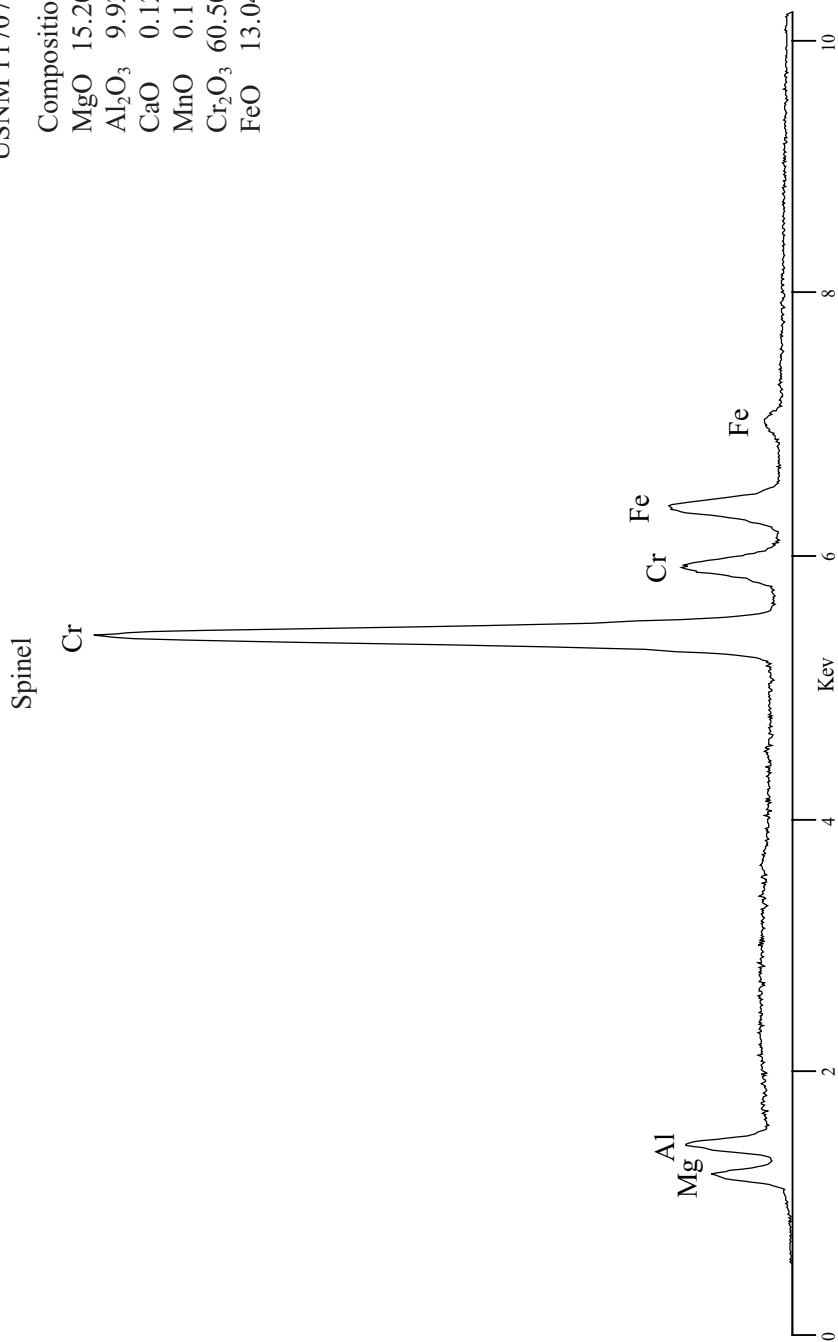
Spinel



Chromite $\text{Fe}^{2+}\text{Cr}_2\text{O}_4$
 Spinel

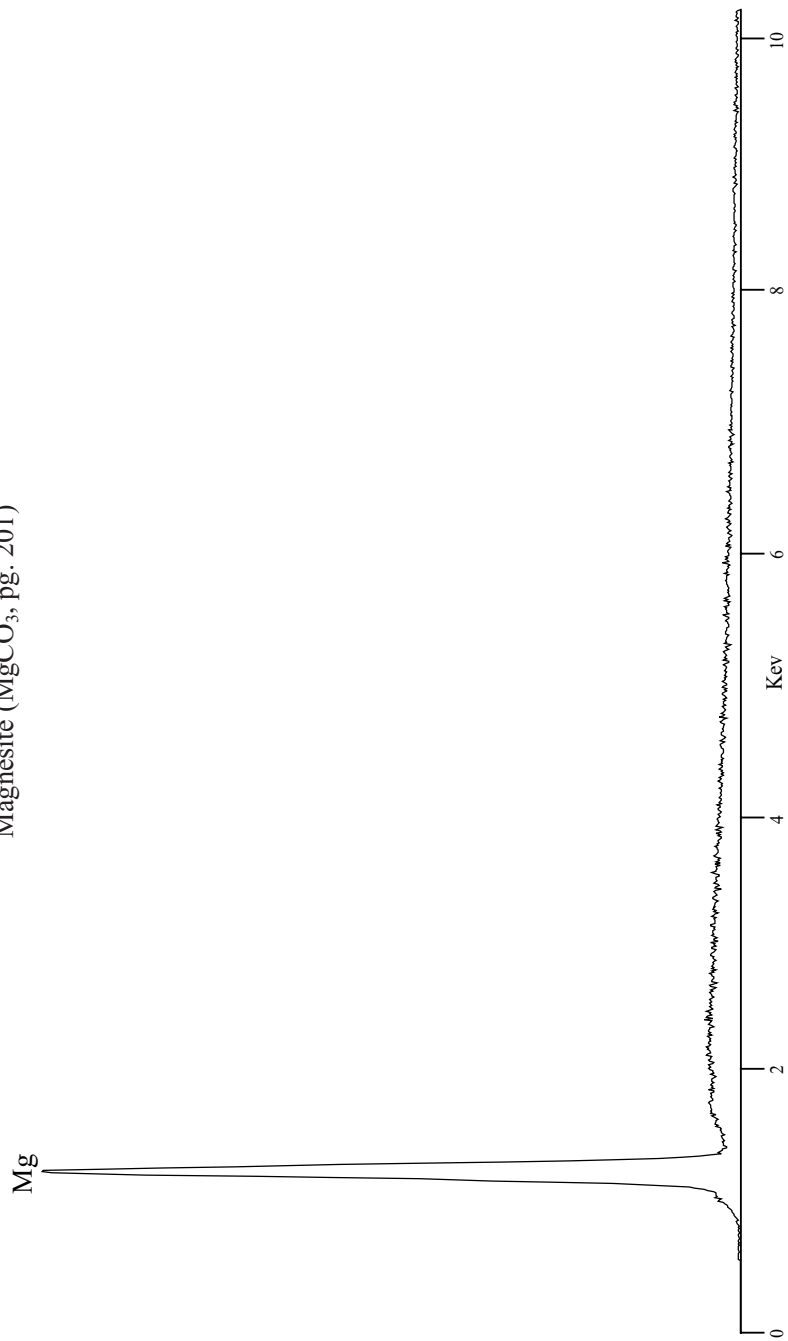
Smithsonian Standard
 USNM 117075

Composition
 MgO 15.20
 Al_2O_3 9.92
 CaO 0.12
 MnO 0.11
 Cr_2O_3 60.50
 FeO 13.04



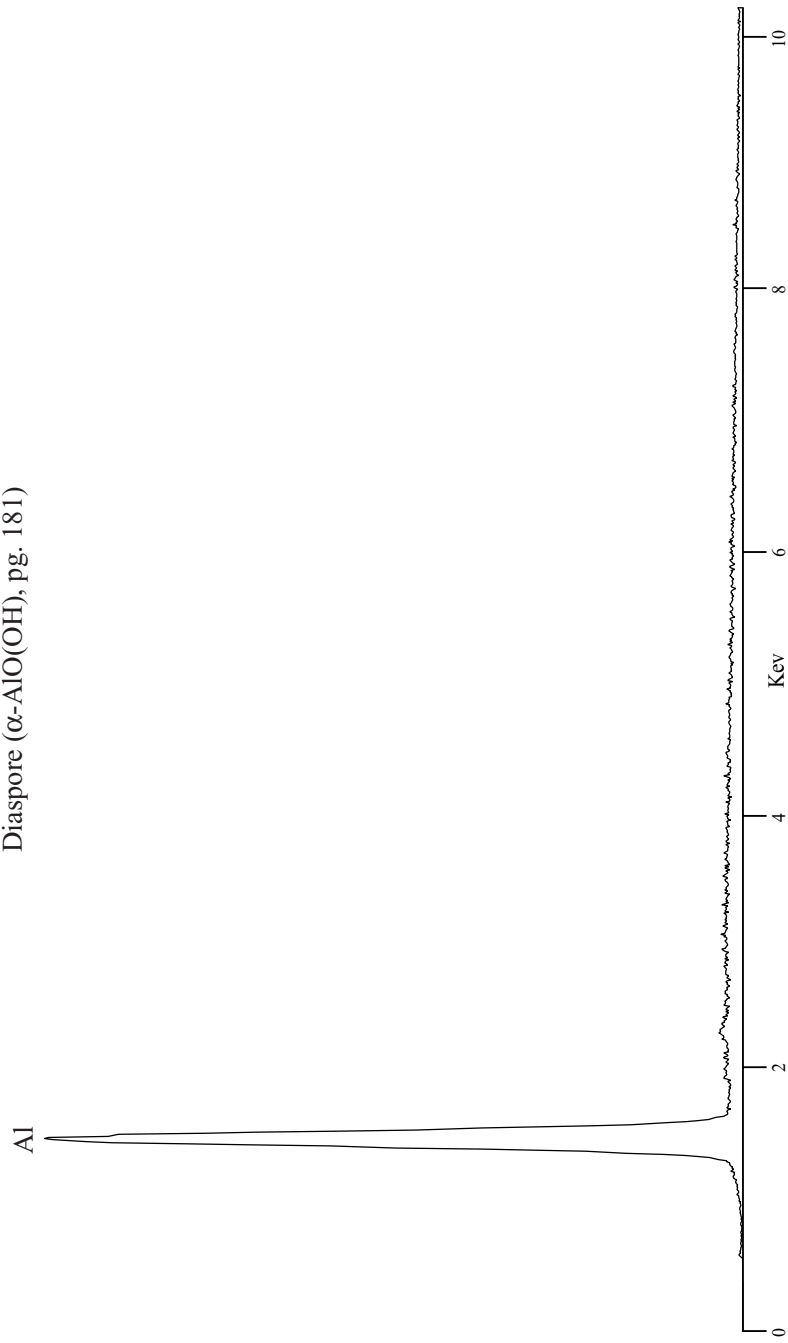
Brucite Mg(OH)_2

See also Periclase (MgO , pg. 160) and
Magnesite (MgCO_3 , pg. 201)



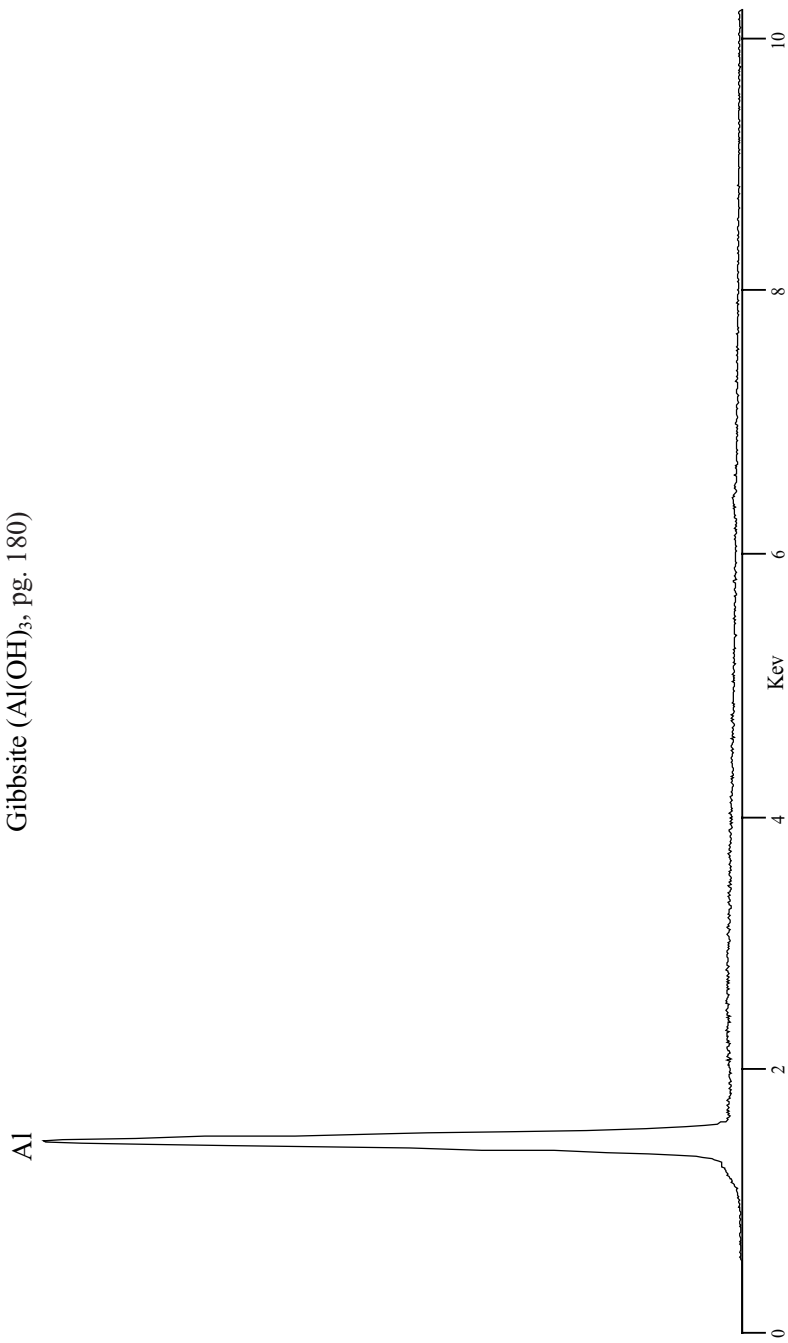
Gibbsite $\text{Al}(\text{OH})_3$

See also Corundum ($\alpha\text{-Al}_2\text{O}_3$, pg. 163) and
Diaspore ($\alpha\text{-AlO}(\text{OH})$, pg. 181)



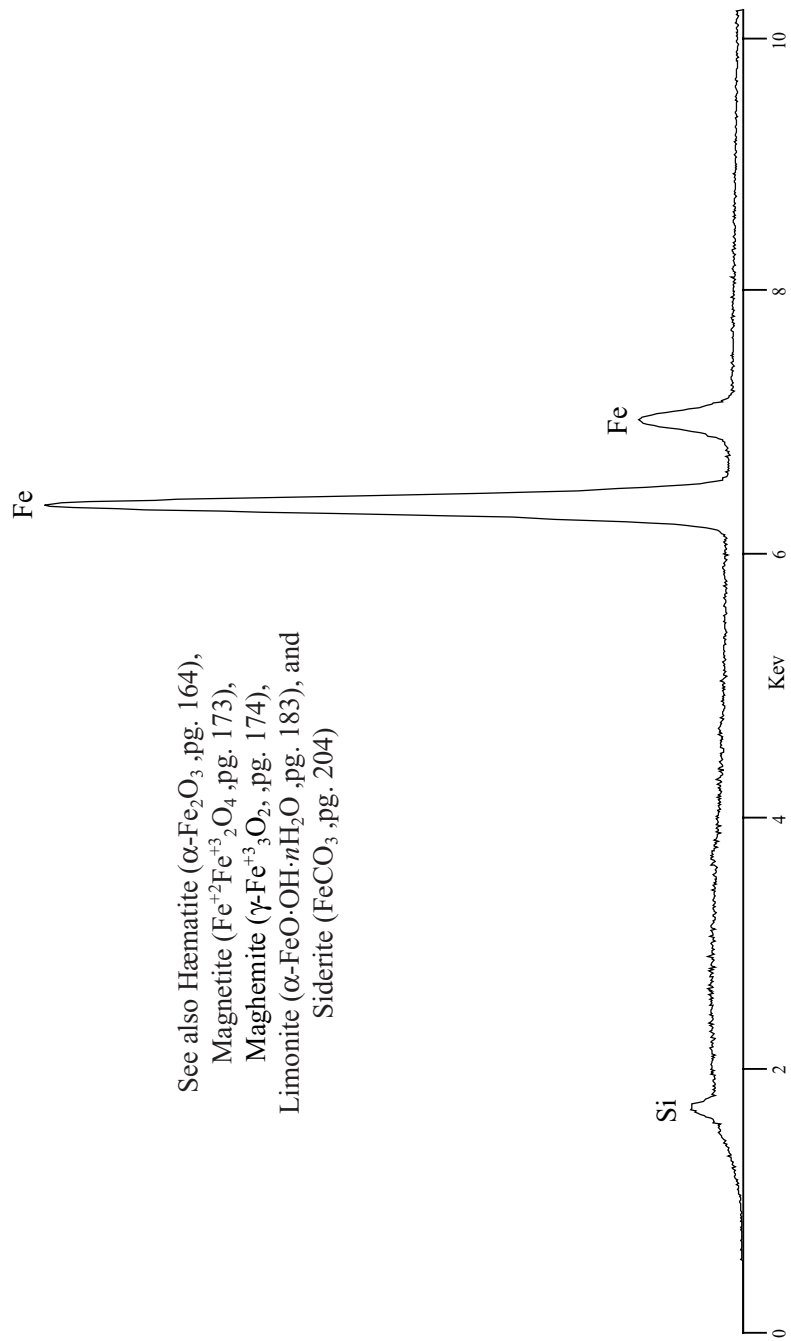
Diaspore α -AlO(OH)

See also Corundum (α -Al₂O₃, pg. 163) and
Gibbsite (Al(OH)₃, pg. 180)



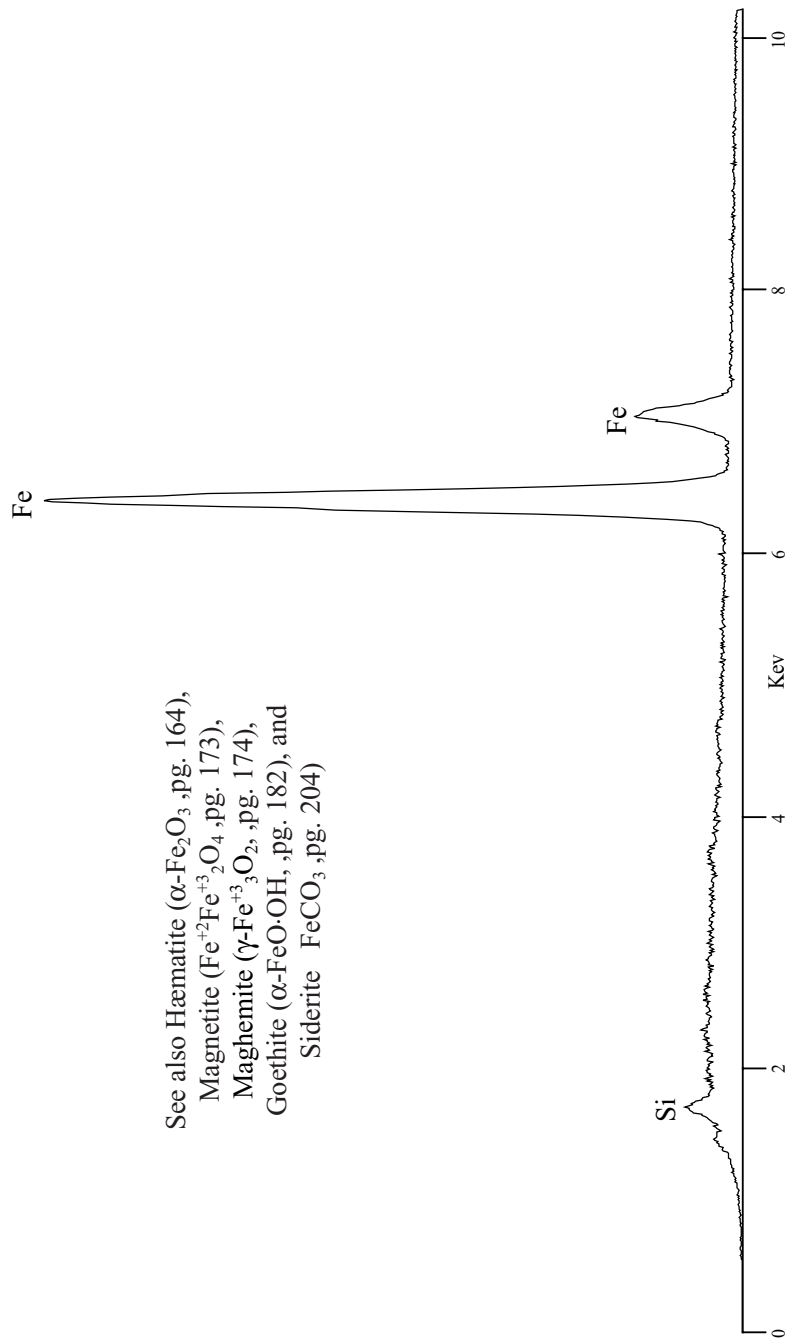
Goethite $\alpha\text{-FeO}\cdot\text{OH}$

See also Häematite ($\alpha\text{-Fe}_2\text{O}_3$, pg. 164),
Magnetite ($\text{Fe}^{+2}\text{Fe}^{+3}_2\text{O}_4$, pg. 173),
Maghemite ($\gamma\text{-Fe}^{+3}_3\text{O}_2$, pg. 174),
Limonite ($\alpha\text{-FeO}\cdot\text{OH}\cdot n\text{H}_2\text{O}$, pg. 183), and
Siderite (FeCO_3 , pg. 204)

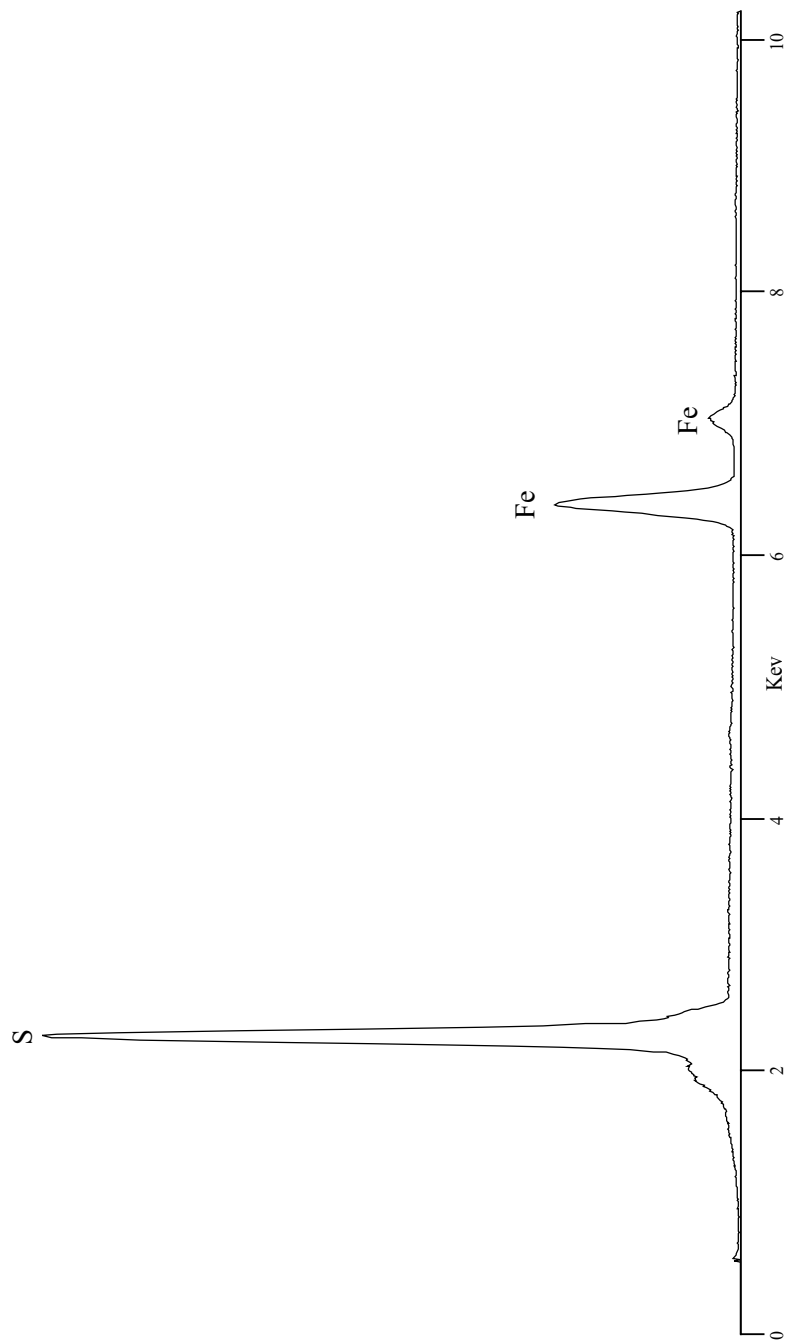


Limonite $\alpha\text{-FeO}\cdot\text{OH}\cdot n\text{H}_2\text{O}$

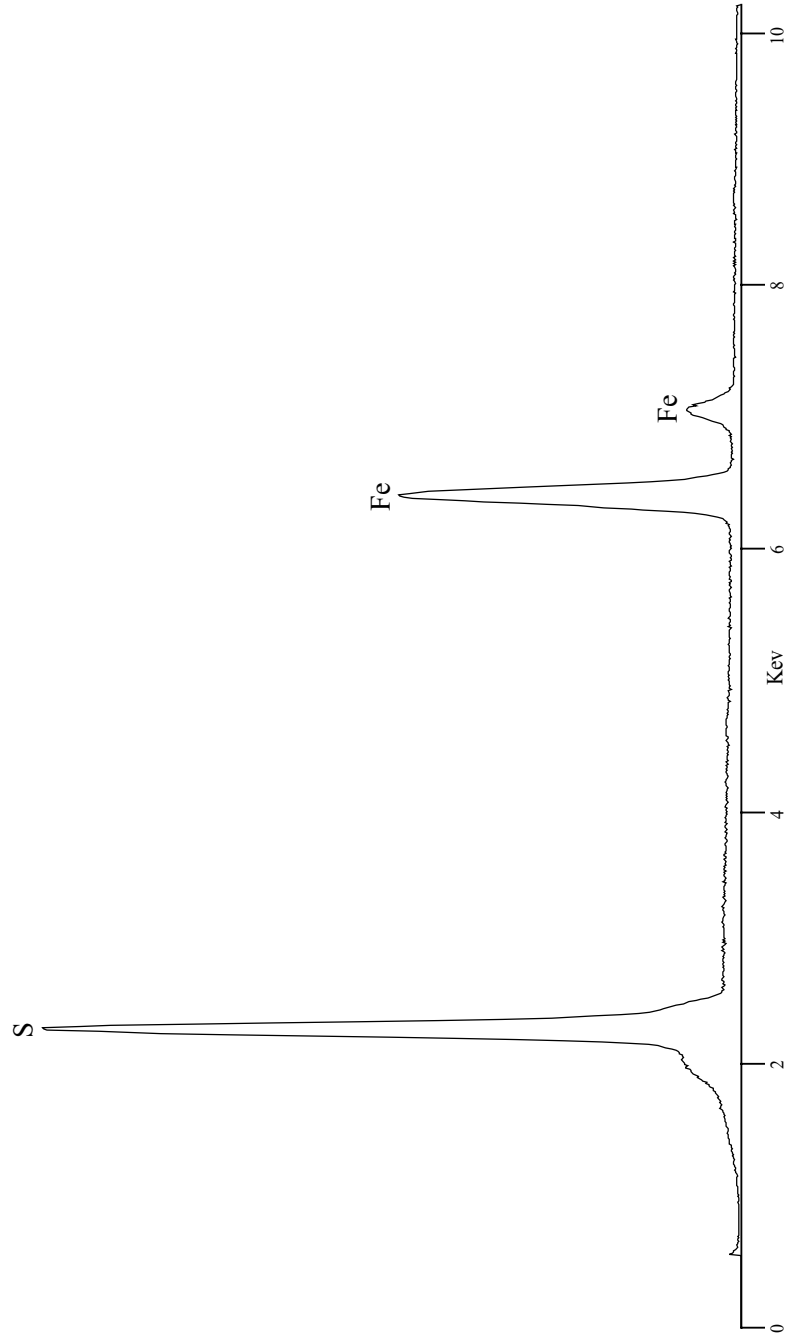
See also Hämatite ($\alpha\text{-Fe}_2\text{O}_3$, pg. 164),
Magnetite ($\text{Fe}^{+2}\text{Fe}^{+3}_2\text{O}_4$, pg. 173),
Maghemite ($\gamma\text{-Fe}^{+3}_3\text{O}_2$, pg. 174),
Goethite ($\alpha\text{-FeO}\cdot\text{OH}$, pg. 182), and
Siderite FeCO_3 , pg. 204



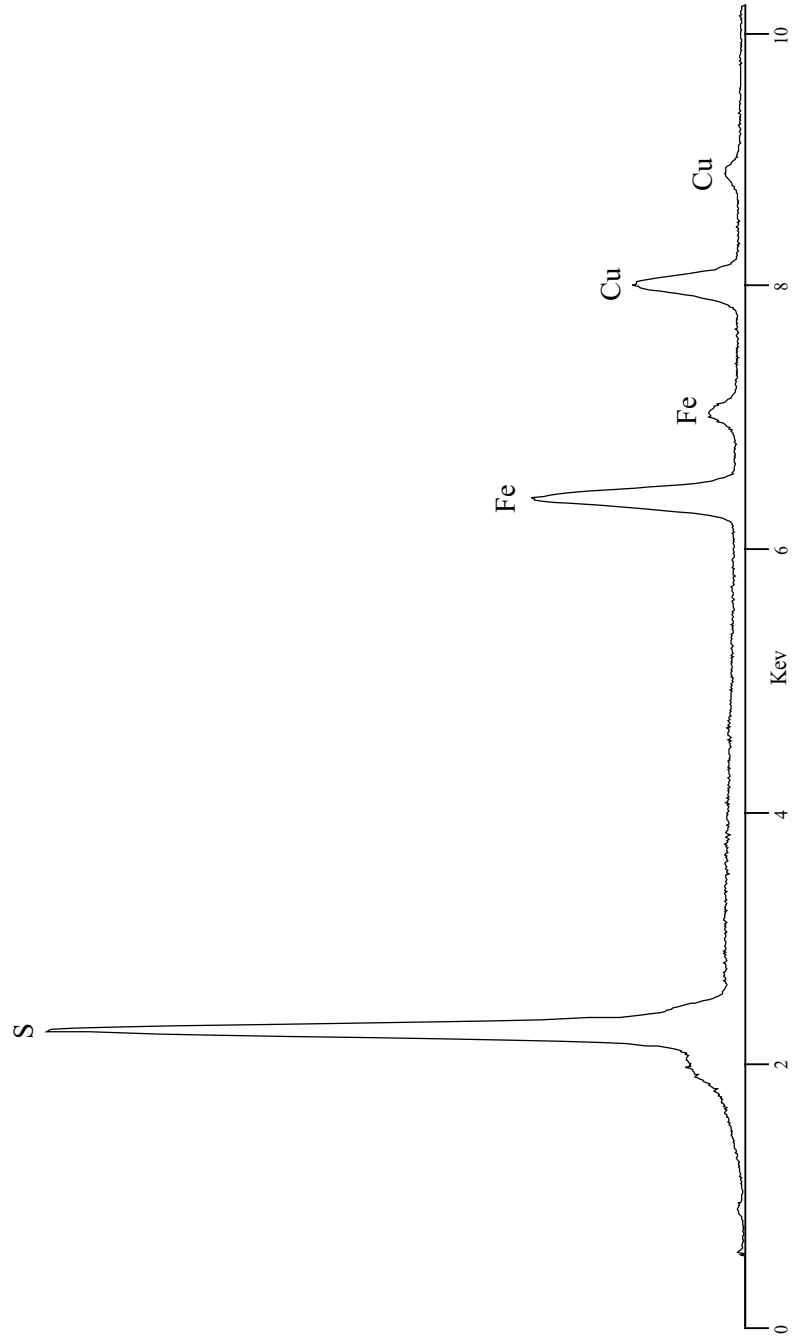
Pyrite FeS_2
Sulfide



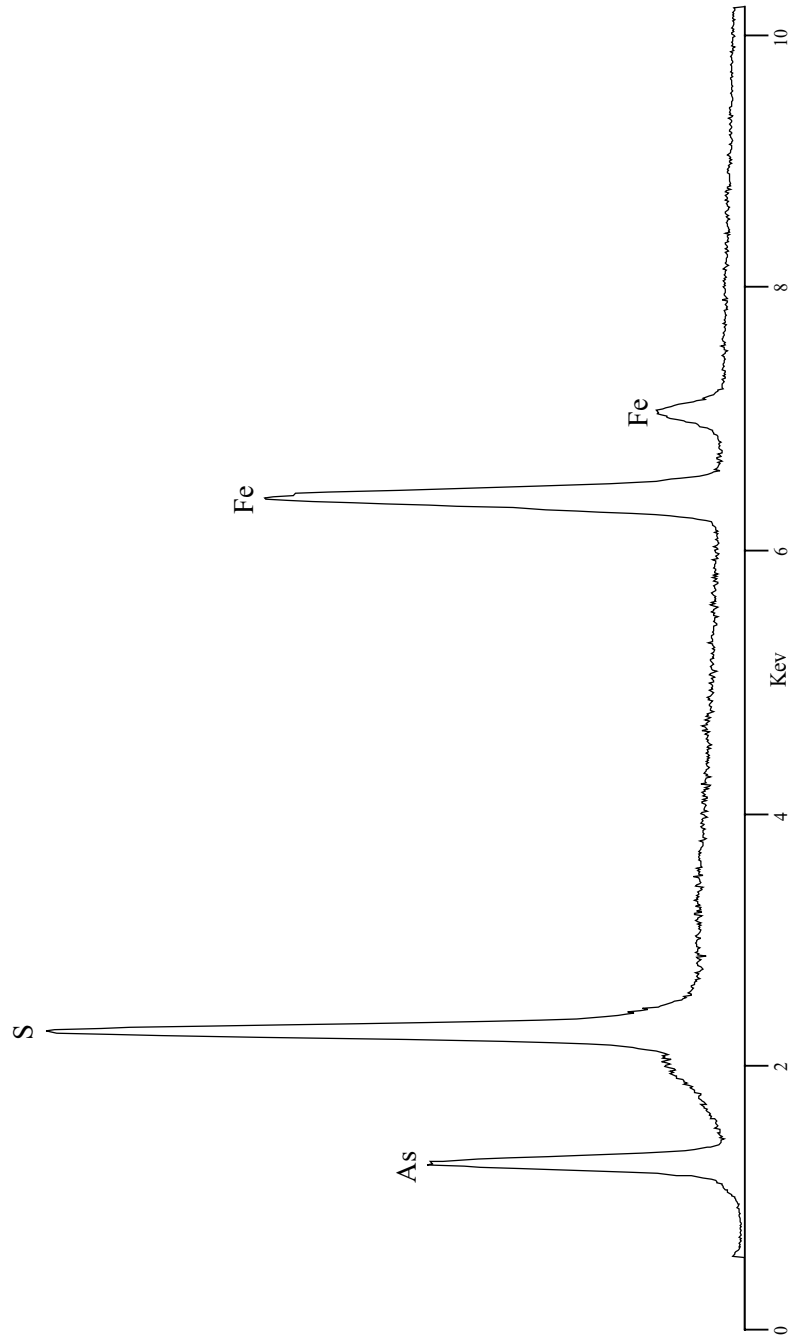
Pyrrhotite Fe_7S_8 - FeS
Sulfide



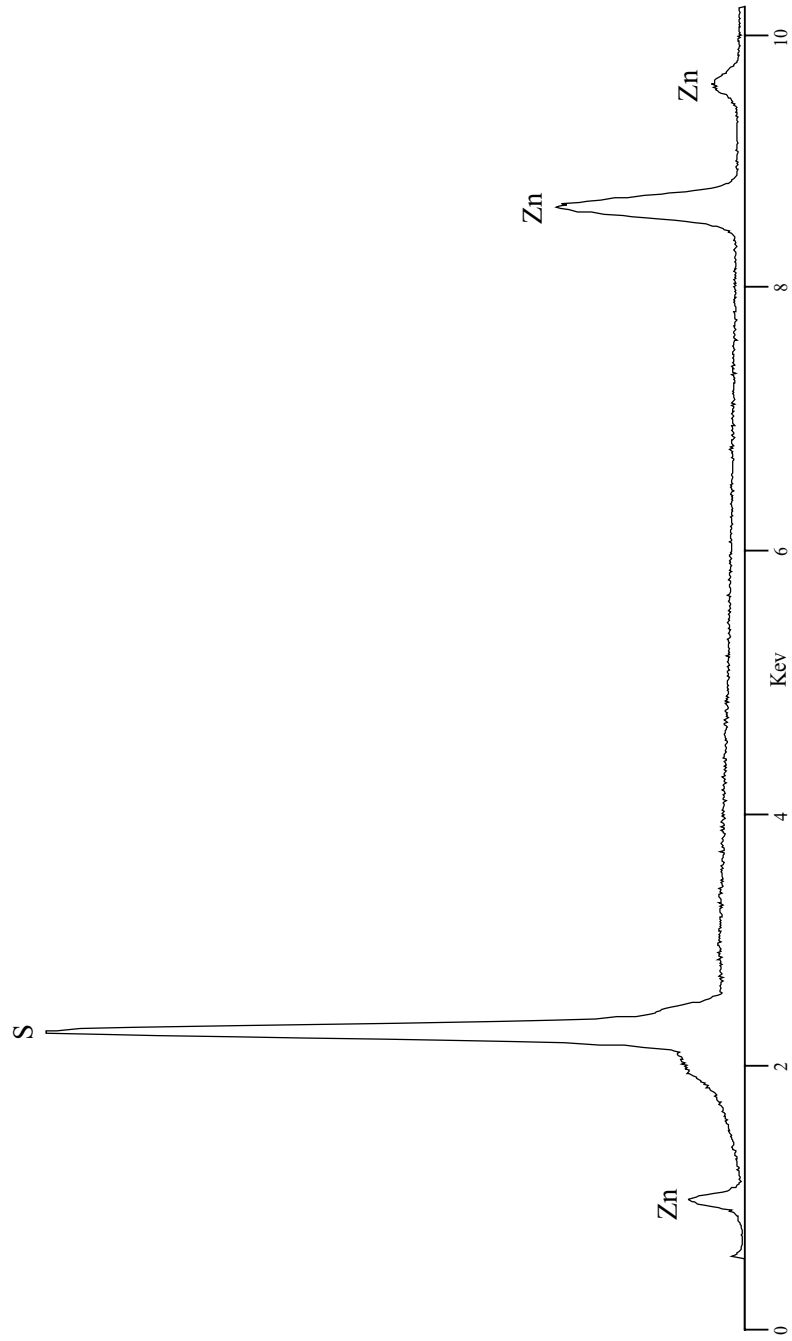
Chalcopyrite CuFeS_2
Sulfide

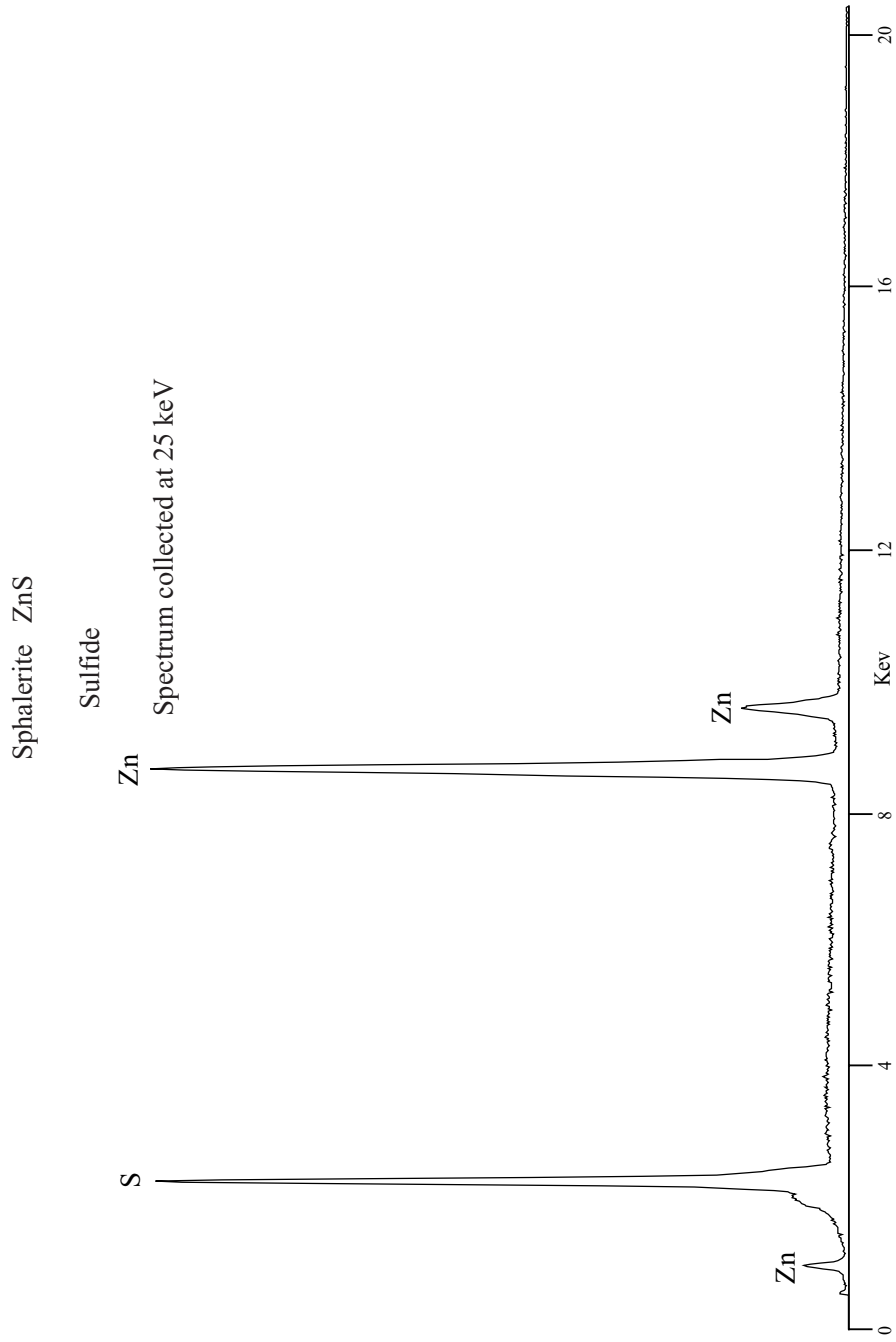


Arsenopyrite FeAsS
Sulfide



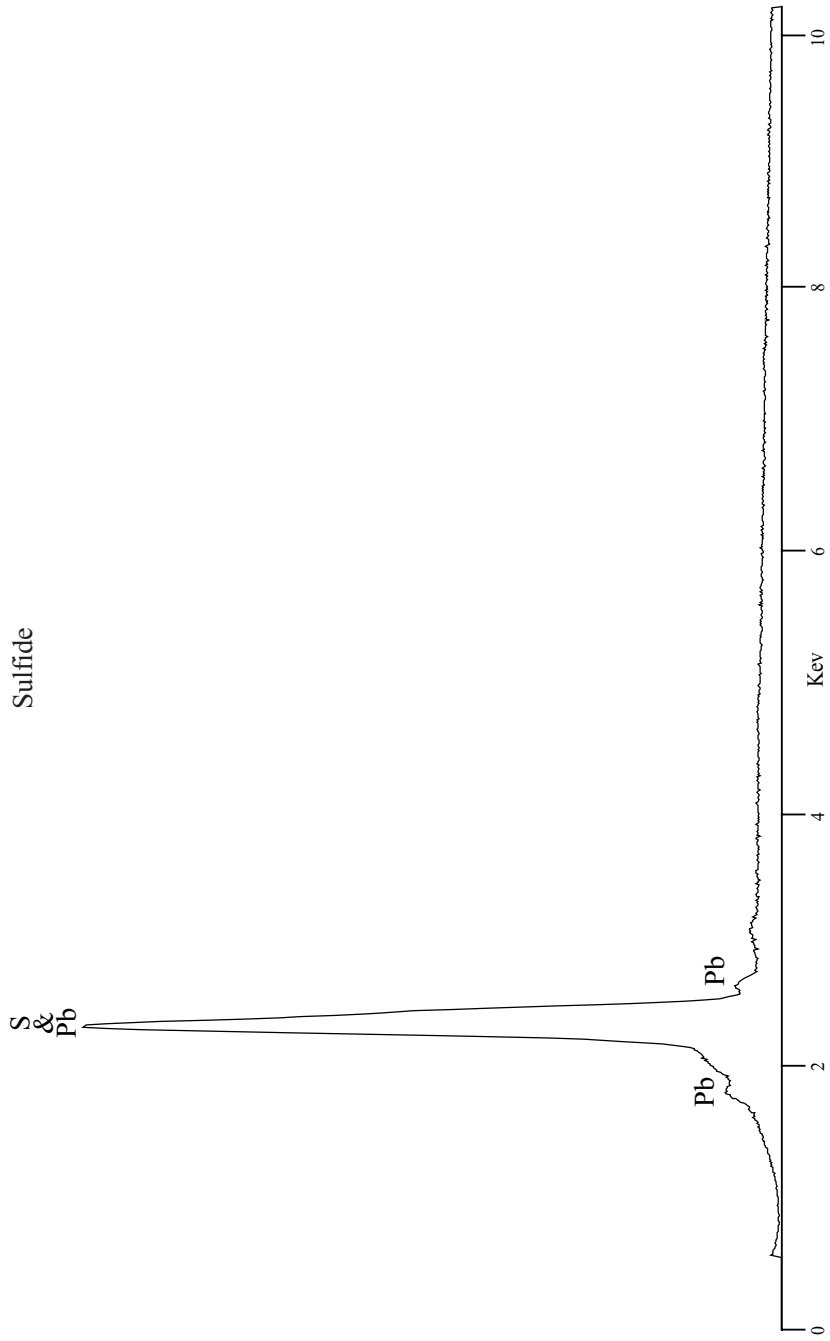
Sphalerite ZnS
Sulfide





Galena PbS

Sulfide



Galena PbS

S
&
Pb

Sulfide

Expanded Horizontal Scale

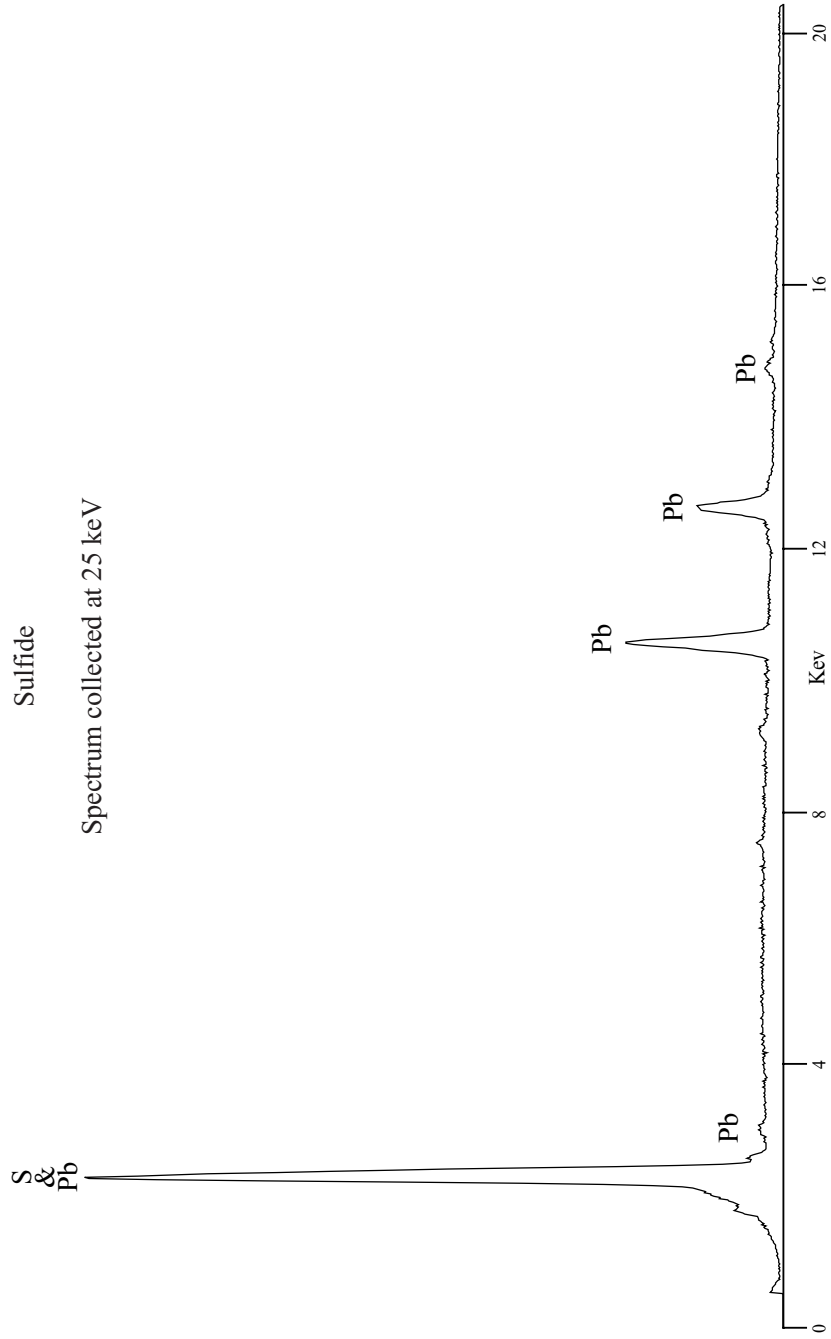
Pb

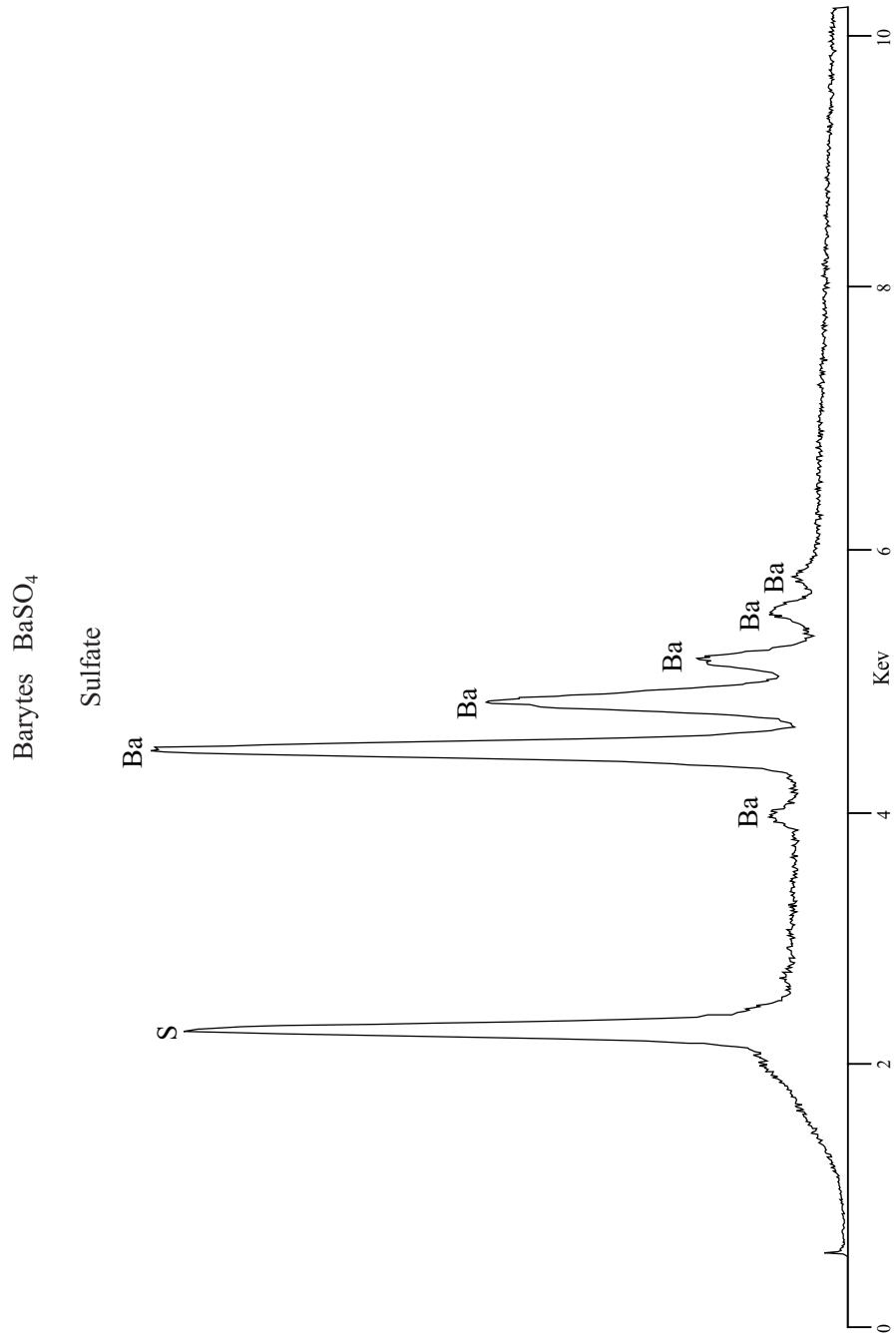
Pb



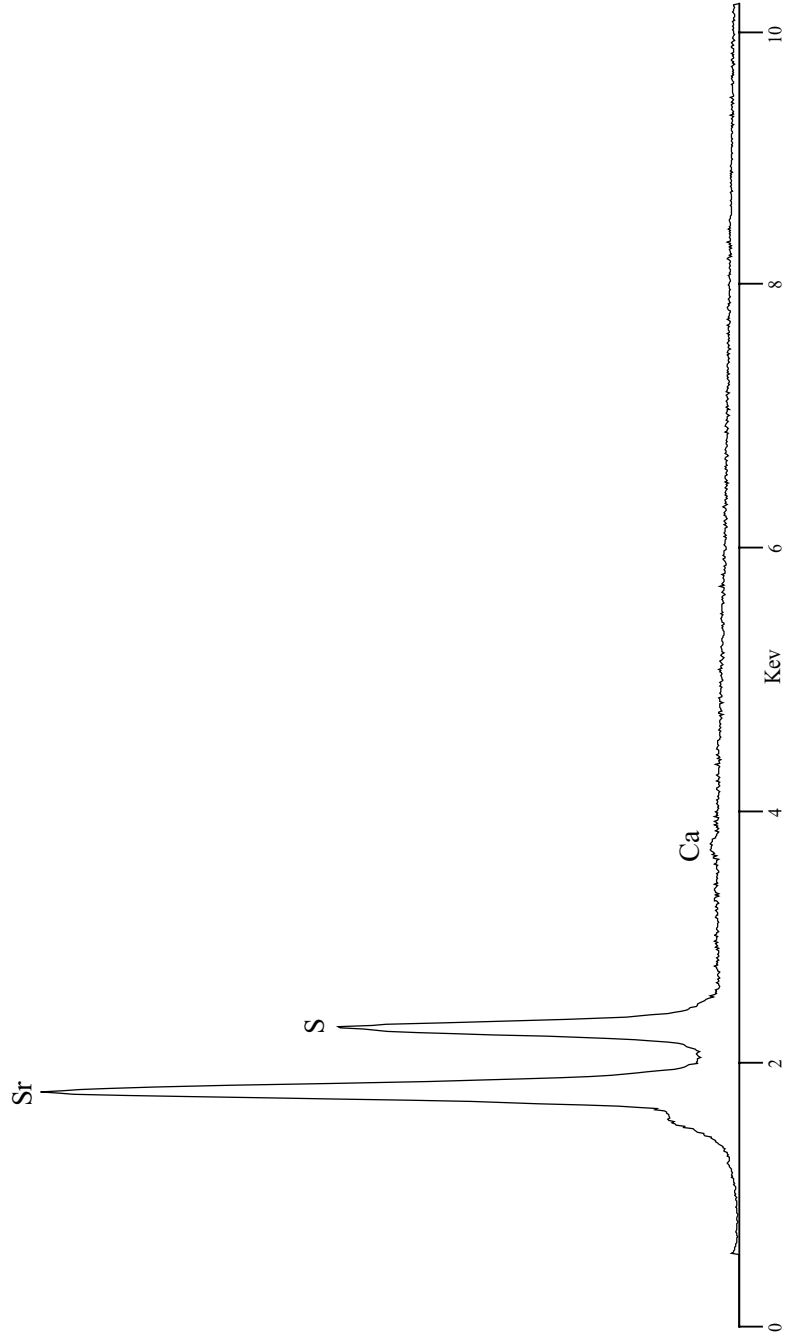
Galena PbS
Sulfide

Spectrum collected at 25 keV





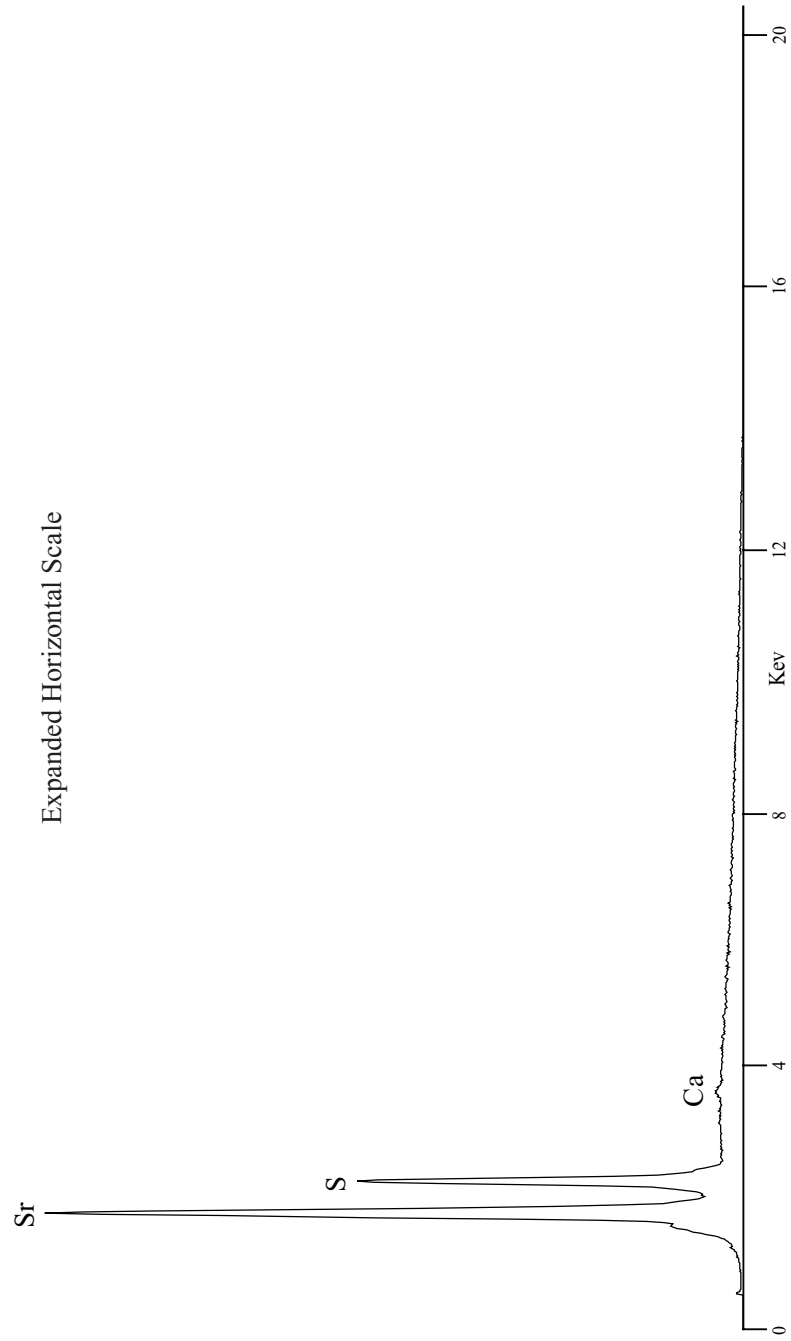
Celestine SrSO_4
Sulfate



Celestine SrSO_4

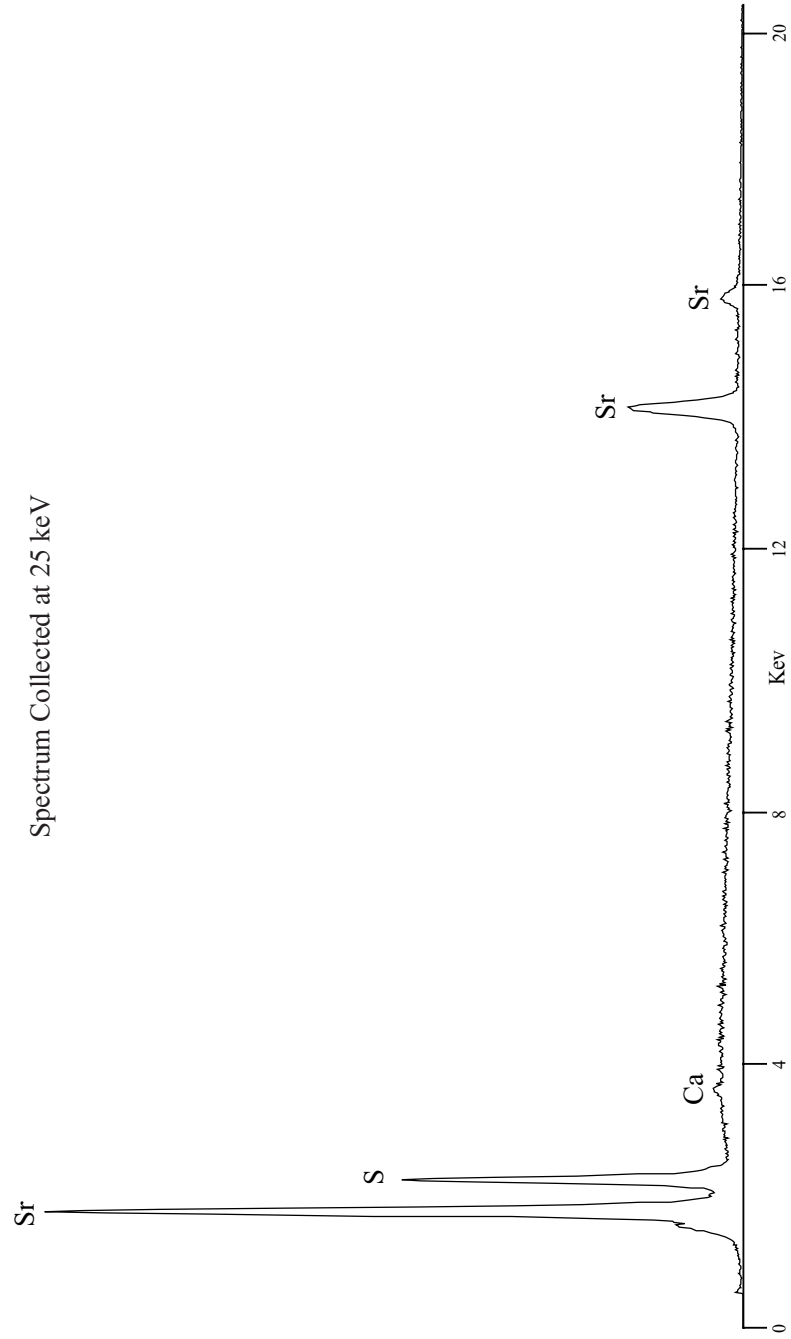
Sulfate

Expanded Horizontal Scale



Celestine SrSO_4
Sulfate

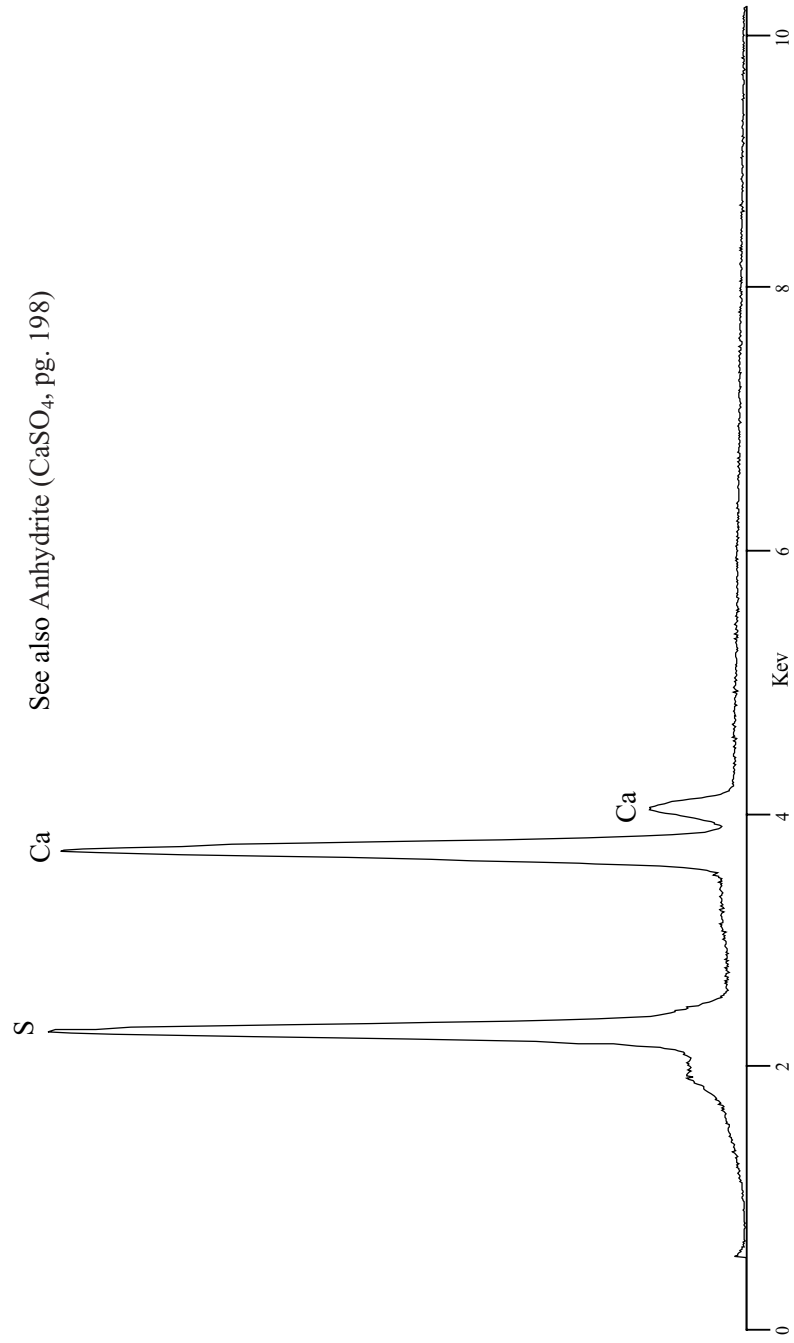
Spectrum Collected at 25 keV



Gypsum $\text{CaSO}_4 \cdot 2\text{H}_2\text{O}$

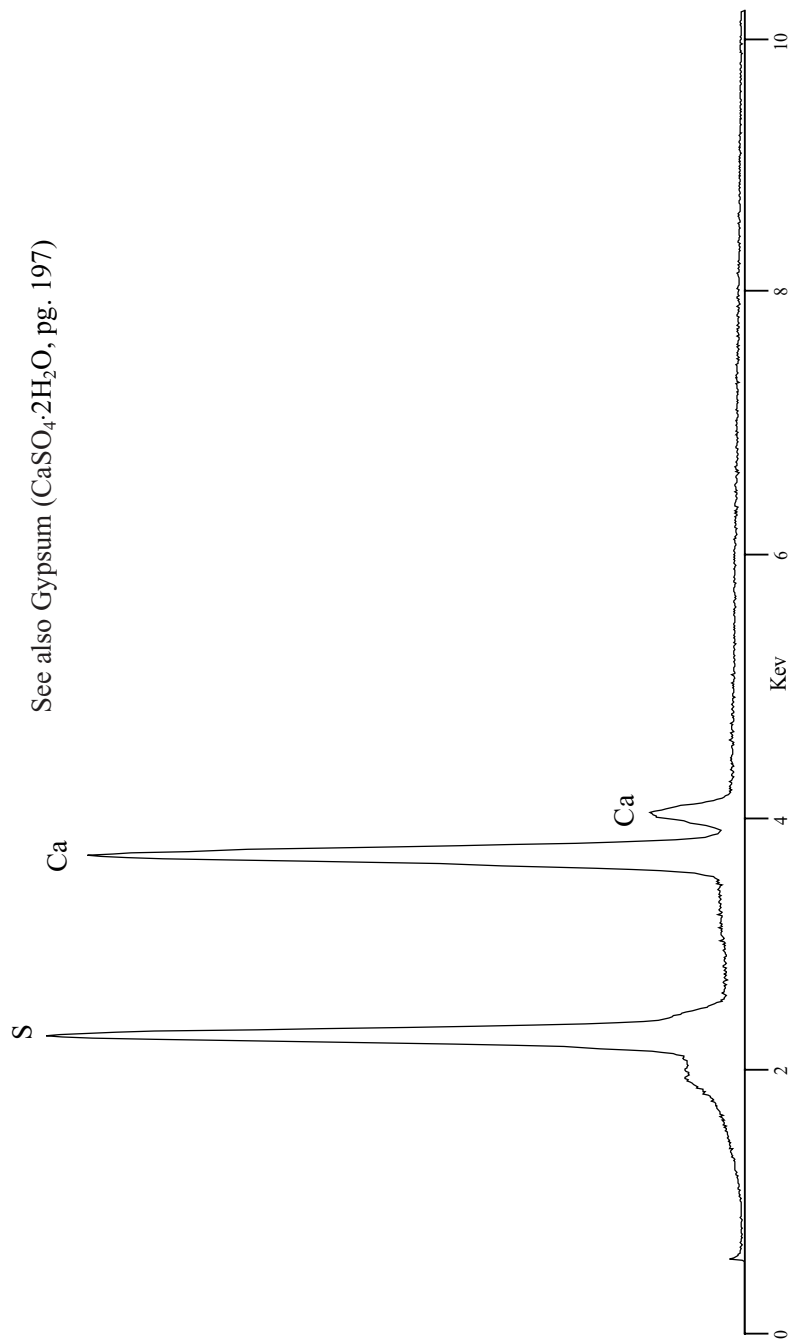
Sulfate

See also Anhydrite (CaSO_4 , pg. 198)



Anhydrite CaSO_4
Sulfate

See also Gypsum ($\text{CaSO}_4 \cdot 2\text{H}_2\text{O}$, pg. 197)

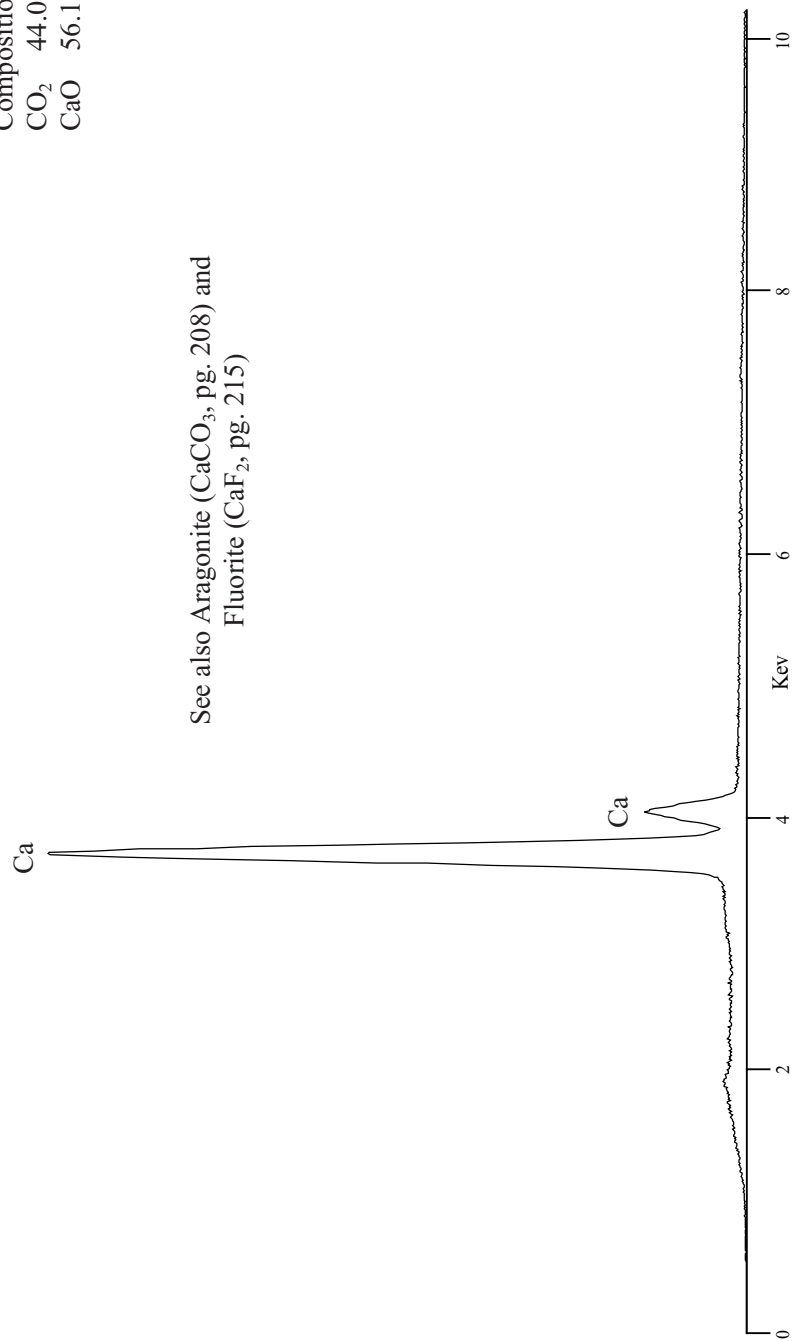


Calcite CaCO_3
Carbonate

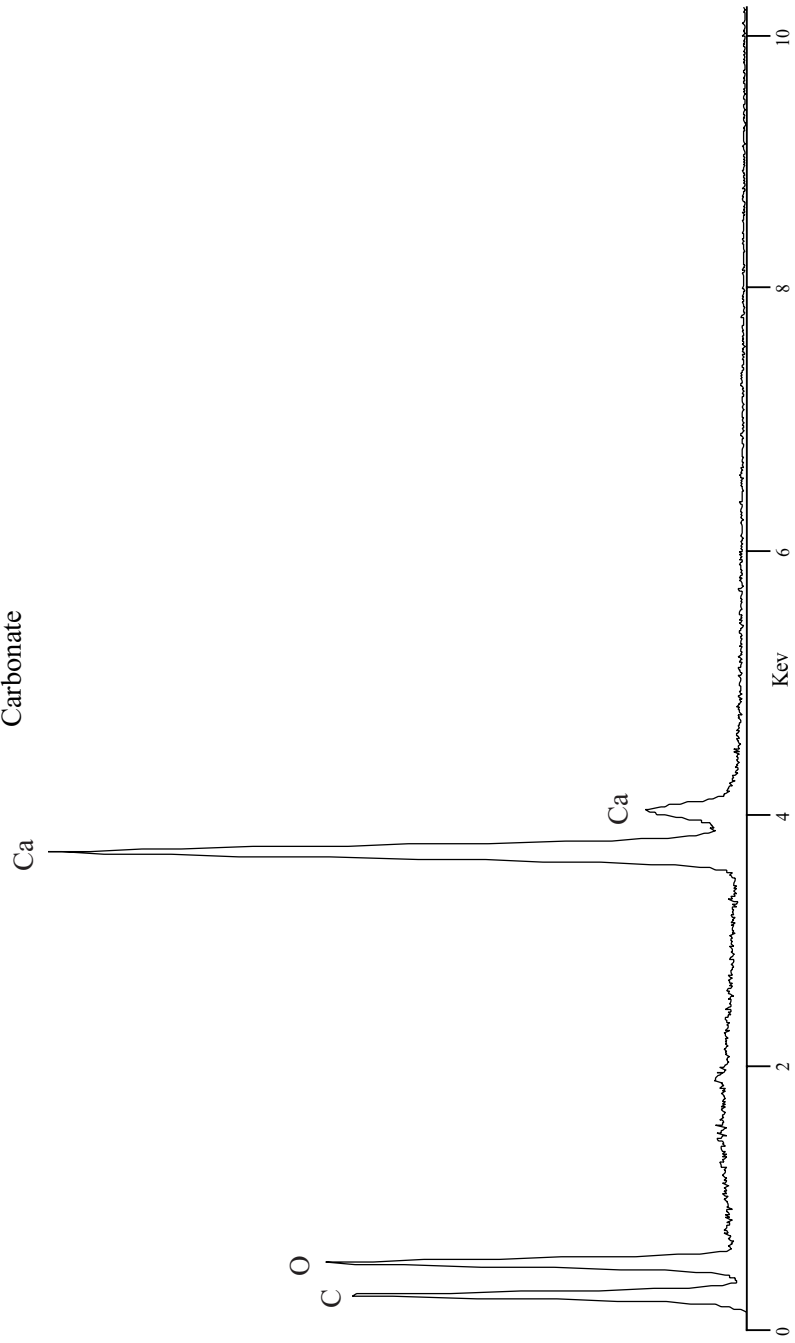
Smithsonian Standard
USNM 136321

Composition
 CO_2 44.01
 CaO 56.10

See also Aragonite (CaCO_3 , pg. 208) and
Fluorite (CaF_2 , pg. 215)



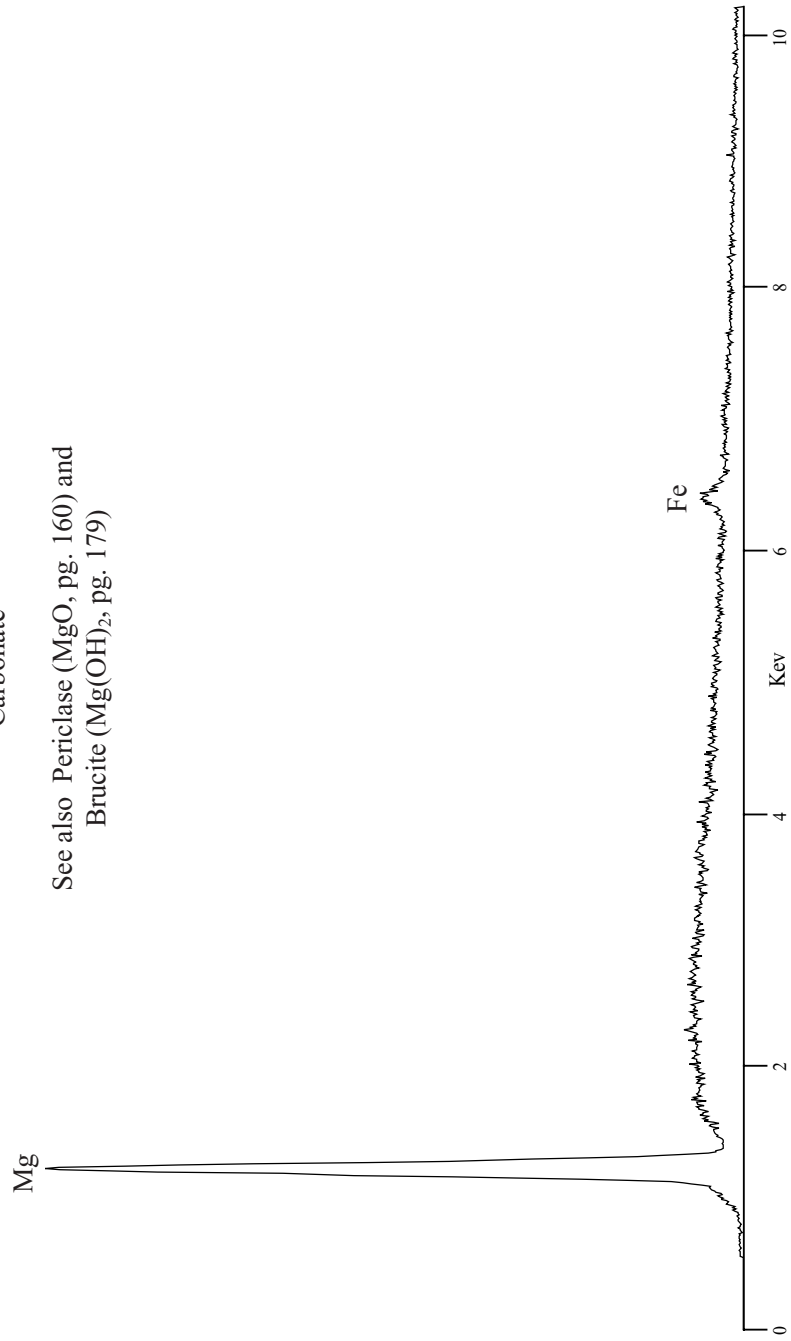
Calcite CaCO_3
Spectrum collected with thin window detector
Carbonate



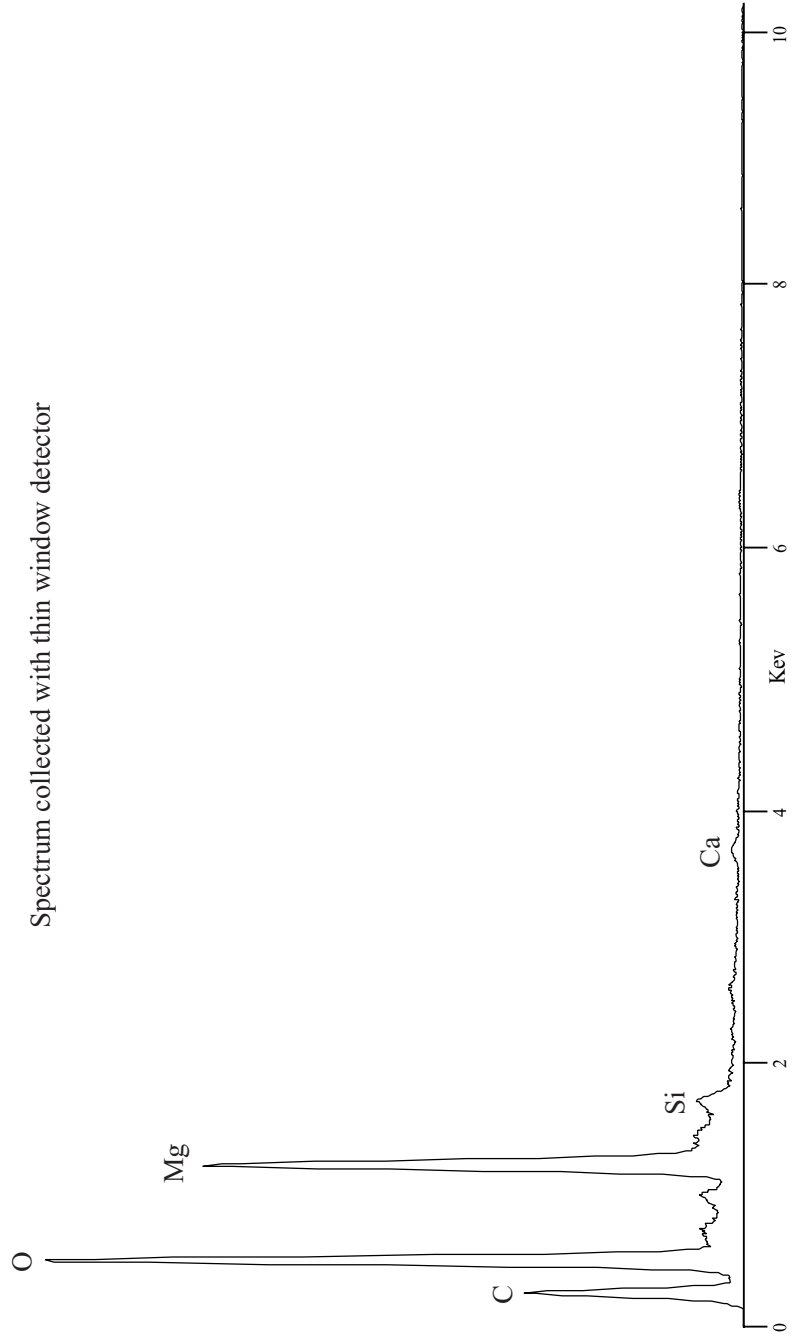
Magnesite $MgCO_3$

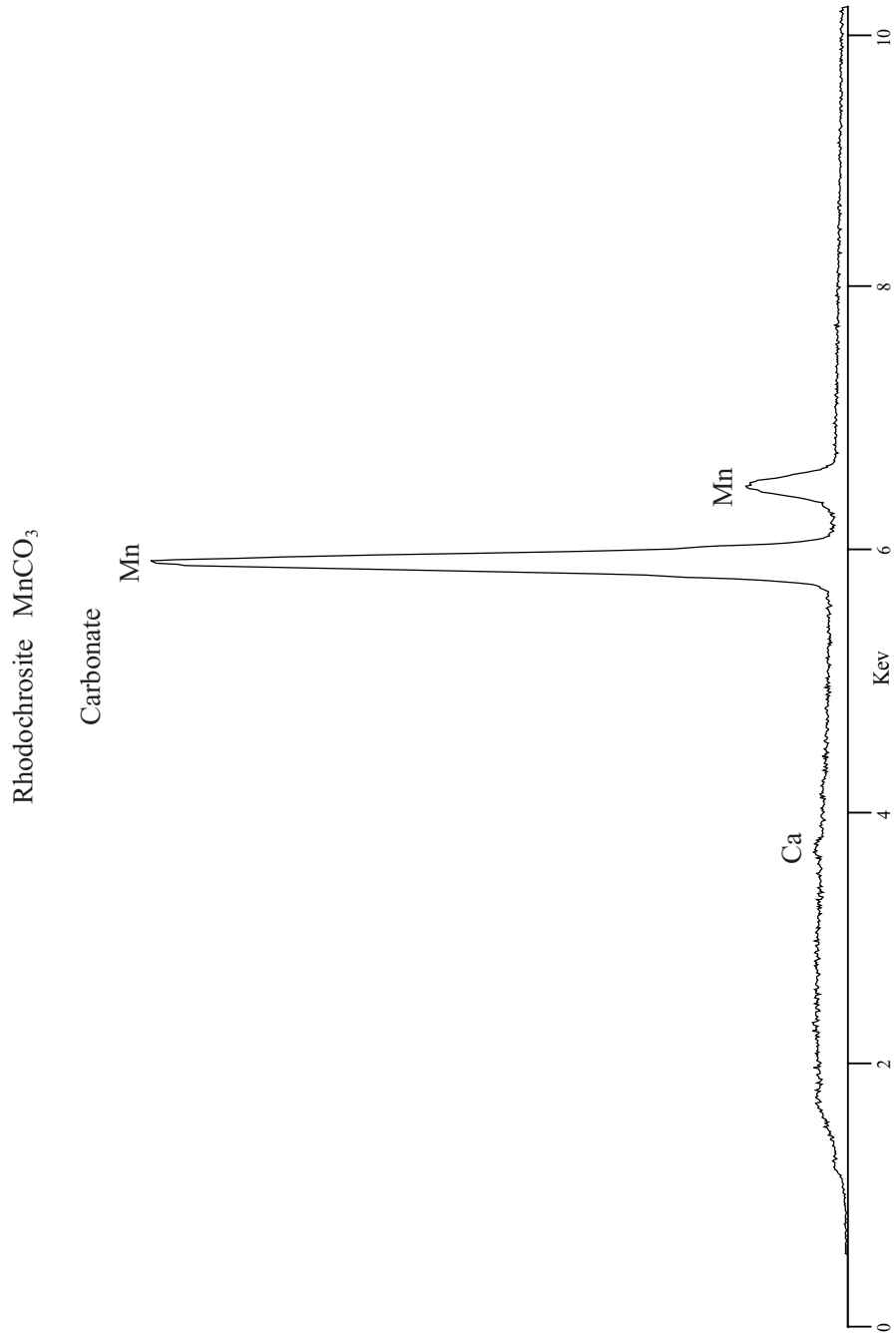
Carbonate

See also Periclase (MgO , pg. 160) and
Brucite ($Mg(OH)_2$, pg. 179)



Magnesite $MgCO_3$
Carbonate

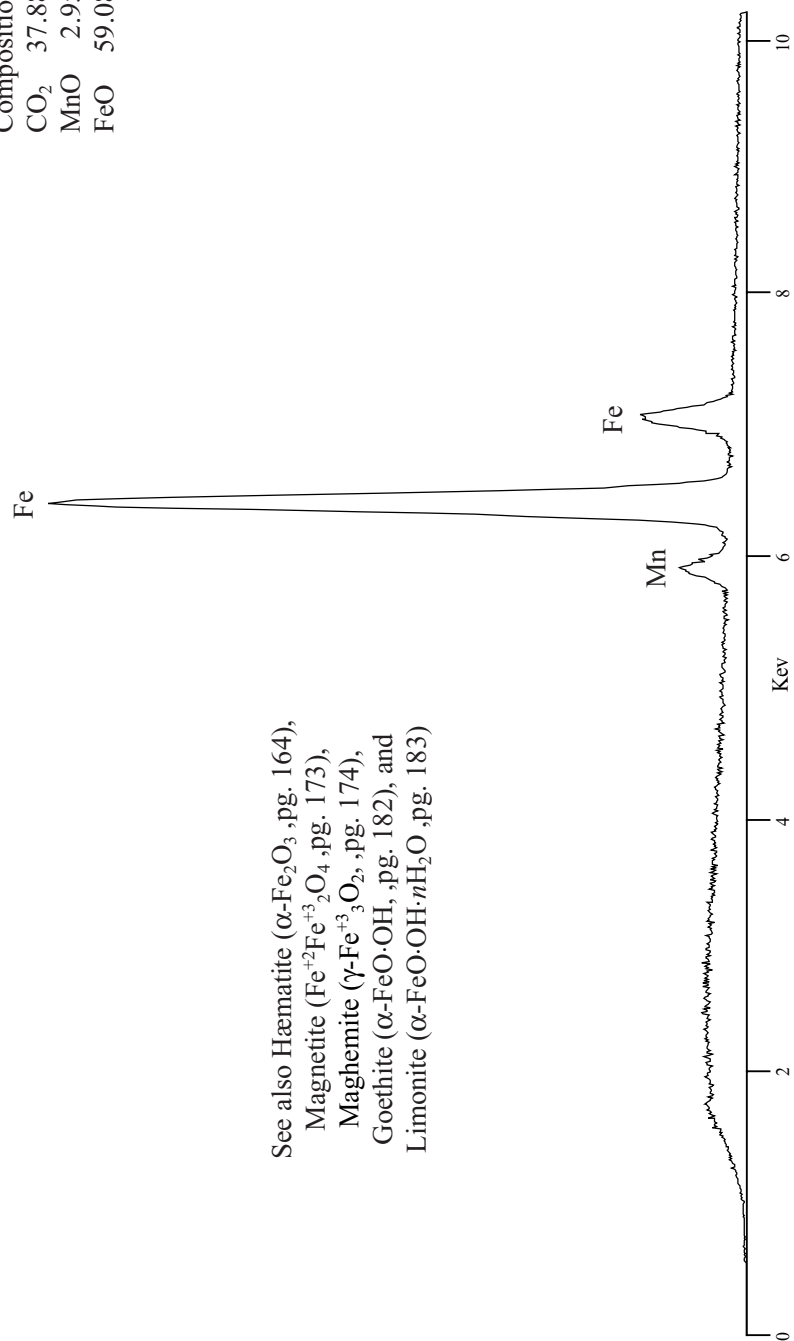




Siderite FeCO_3
 Carbonate

Smithsonian Standard
 USNM R2460

Composition
 CO_2 37.88
 MnO 2.95
 FeO 59.08



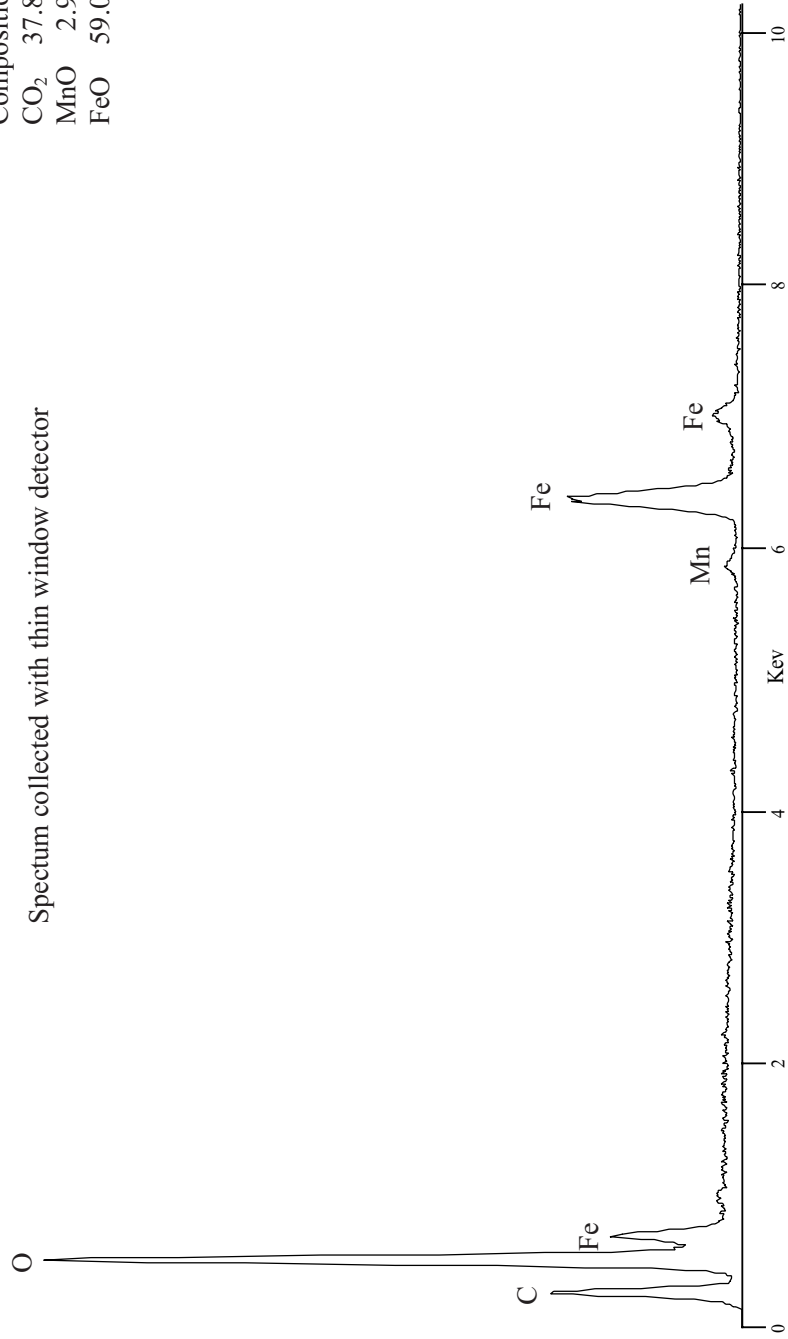
See also Hämatite ($\alpha\text{-Fe}_2\text{O}_3$, pg. 164),
 Magnetite ($\text{Fe}^{+2}\text{Fe}^{+3}_2\text{O}_4$, pg. 173),
 Maghemite ($\gamma\text{-Fe}^{+3}_3\text{O}_2$, pg. 174),
 Goethite ($\alpha\text{-FeO}\cdot\text{OH}$, pg. 182), and
 Limonite ($\alpha\text{-FeO}\cdot\text{OH}\cdot n\text{H}_2\text{O}$, pg. 183)

Siderite FeCO_3
Carbonate

Smithsonian Standard
USNM R2460

Composition
 CO_2 37.88
 MnO 2.95
 FeO 59.08

Spectrum collected with thin window detector

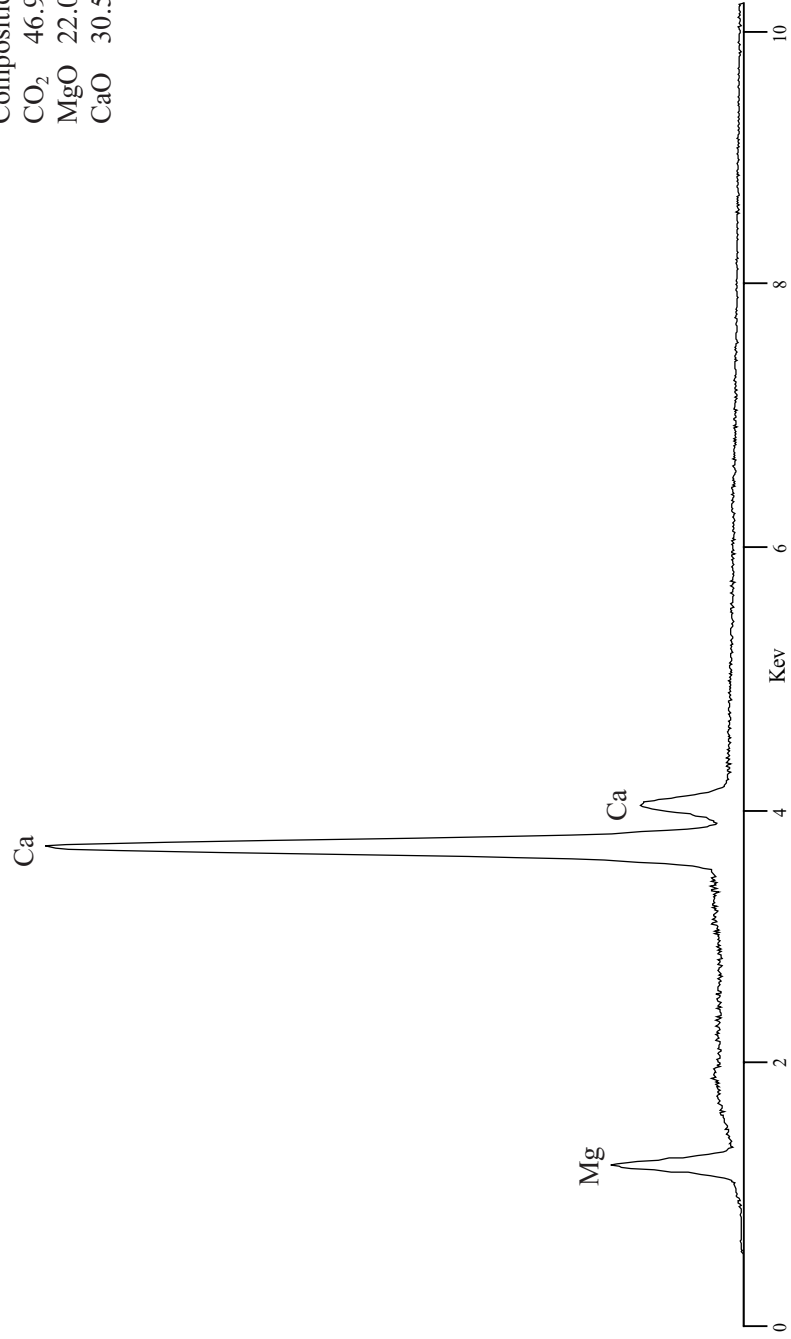


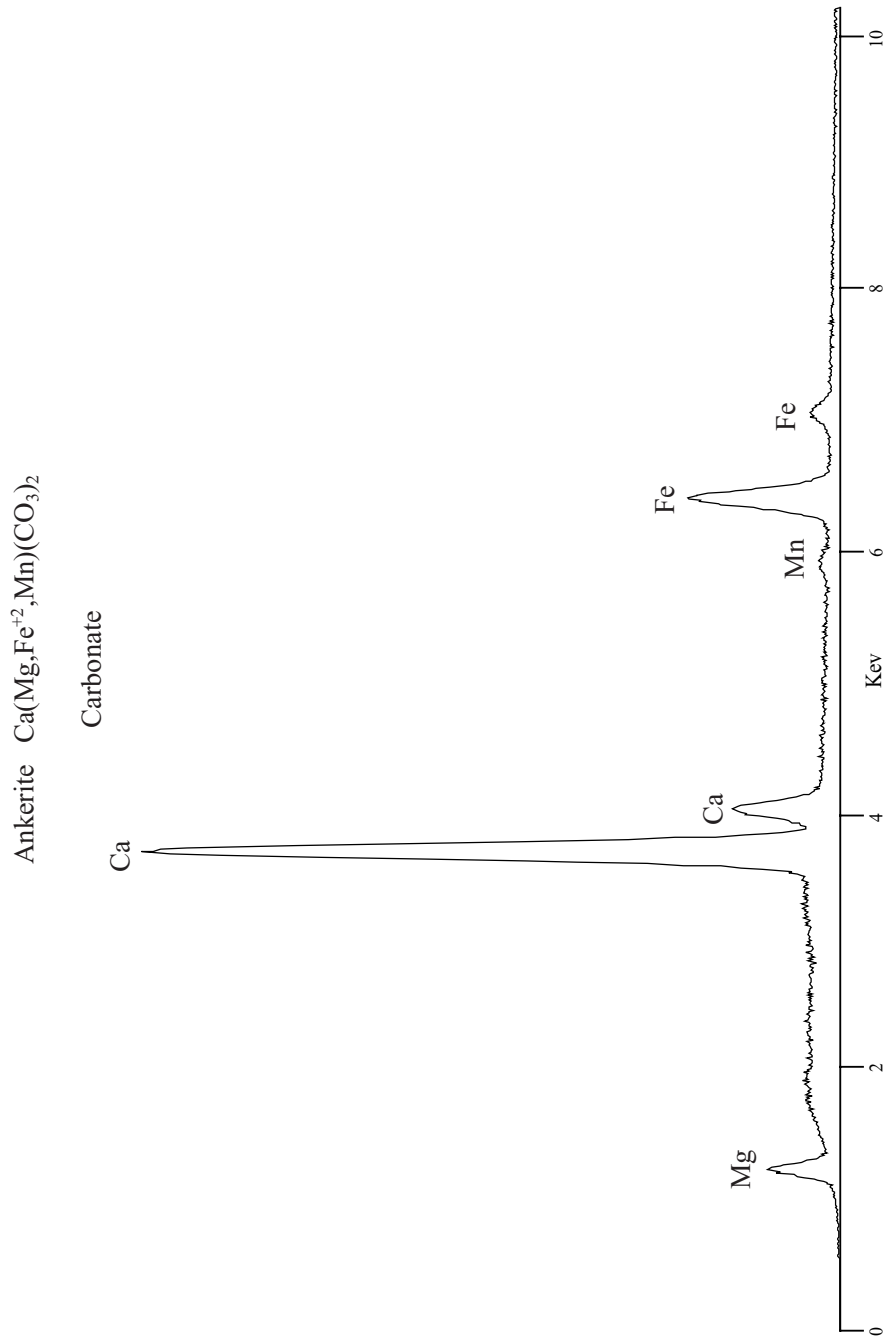
Smithsonian Standard
USNM 10057

Composition
CO₂ 46.93
MgO 22.04
CaO 30.56

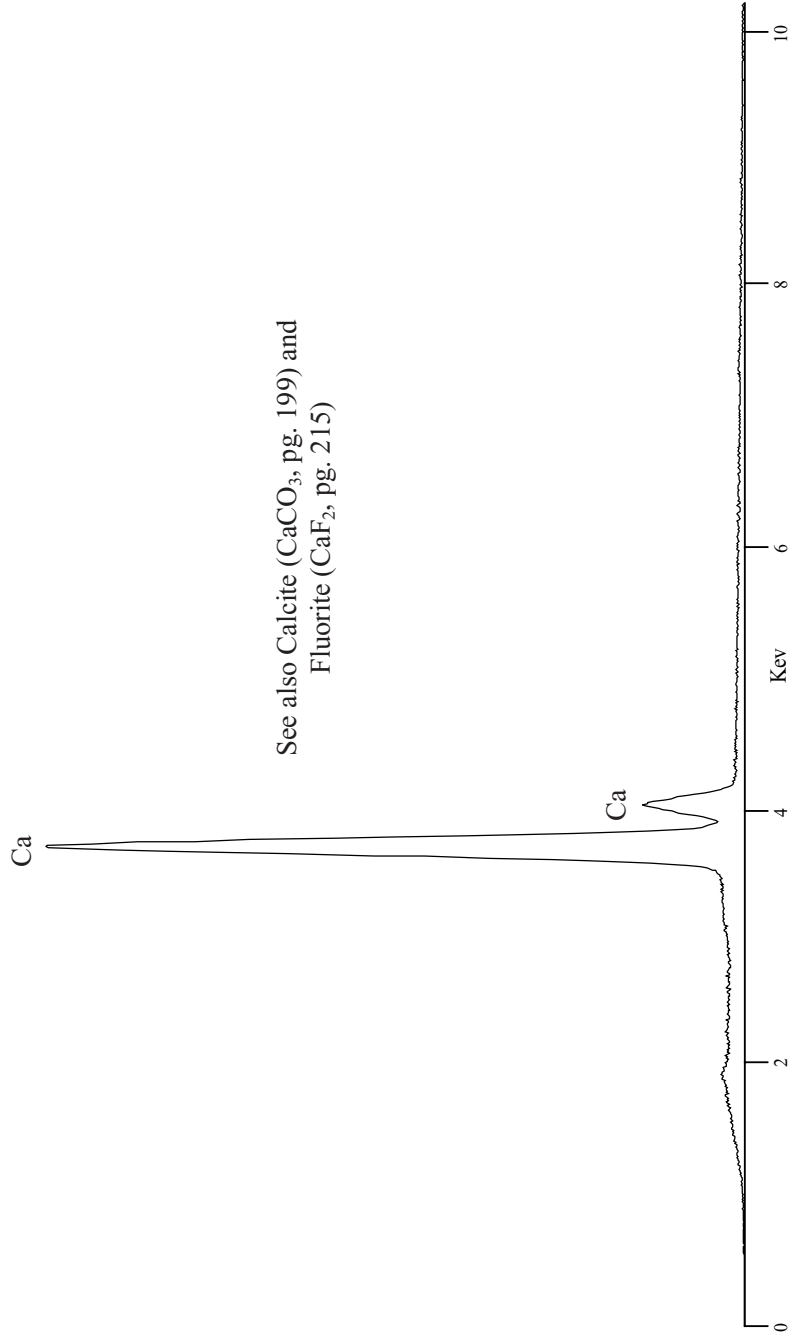
Dolomite CaMg(CO₃)₂

Carbonate





Aragonite CaCO_3
Carbonate

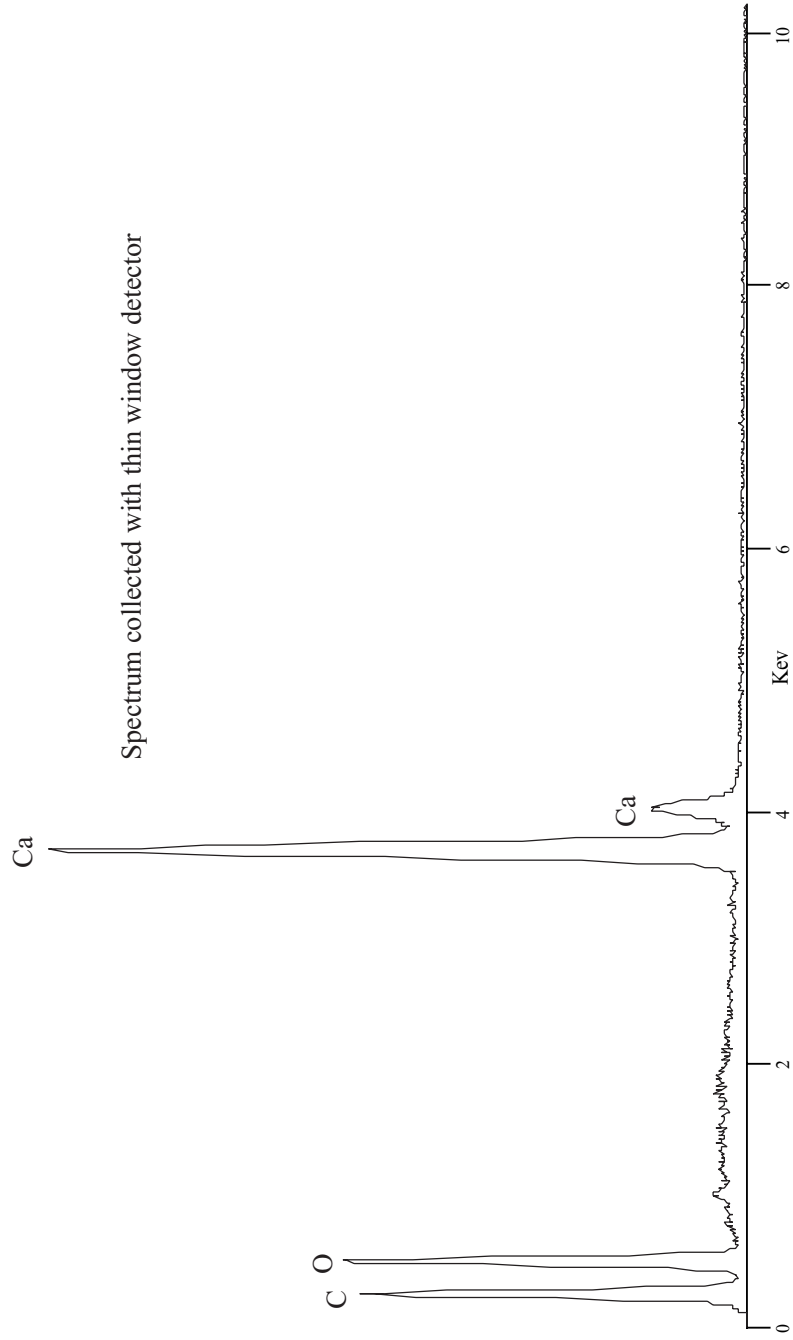


See also Calcite (CaCO_3 , pg. 199) and
Fluorite (CaF_2 , pg. 215)

Aragonite CaCO_3

Carbonate

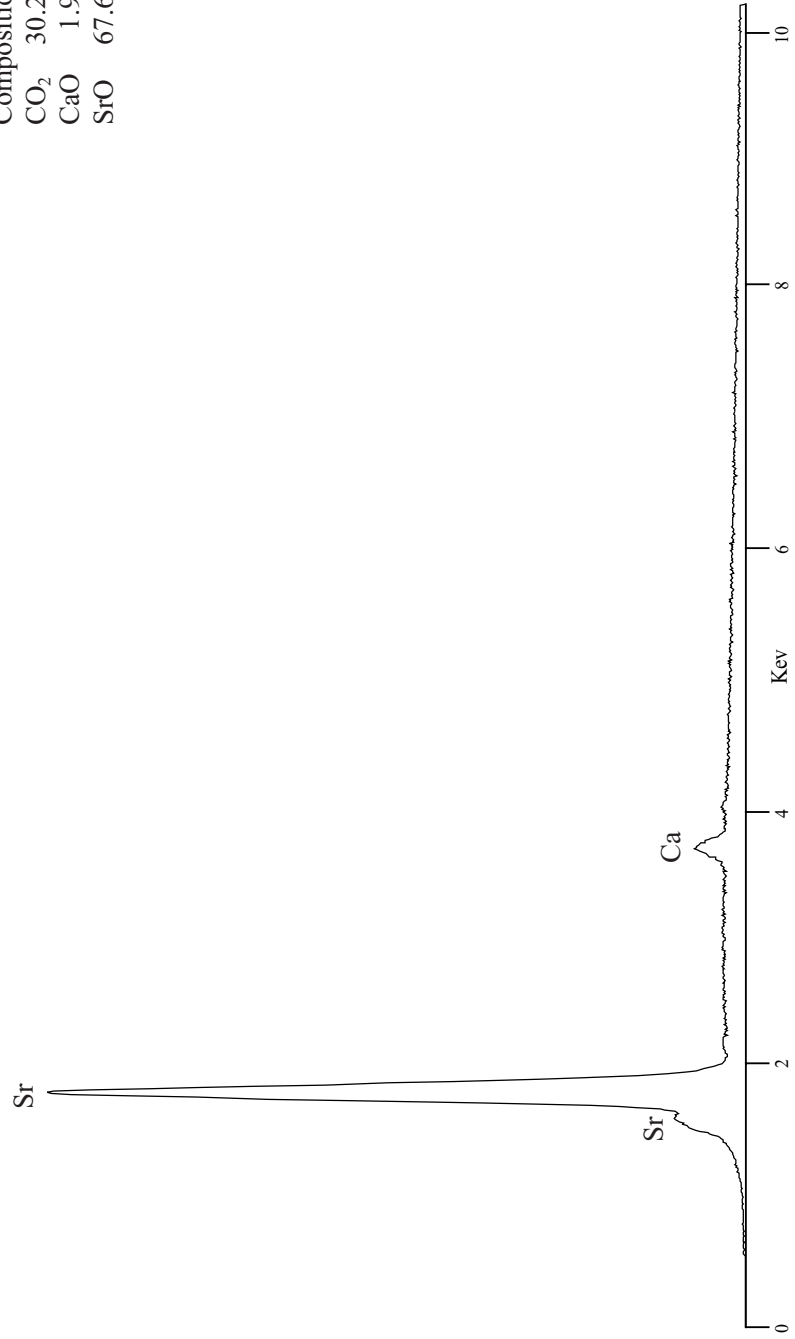
Spectrum collected with thin window detector



Strontianite SrCO_3
Carbonate

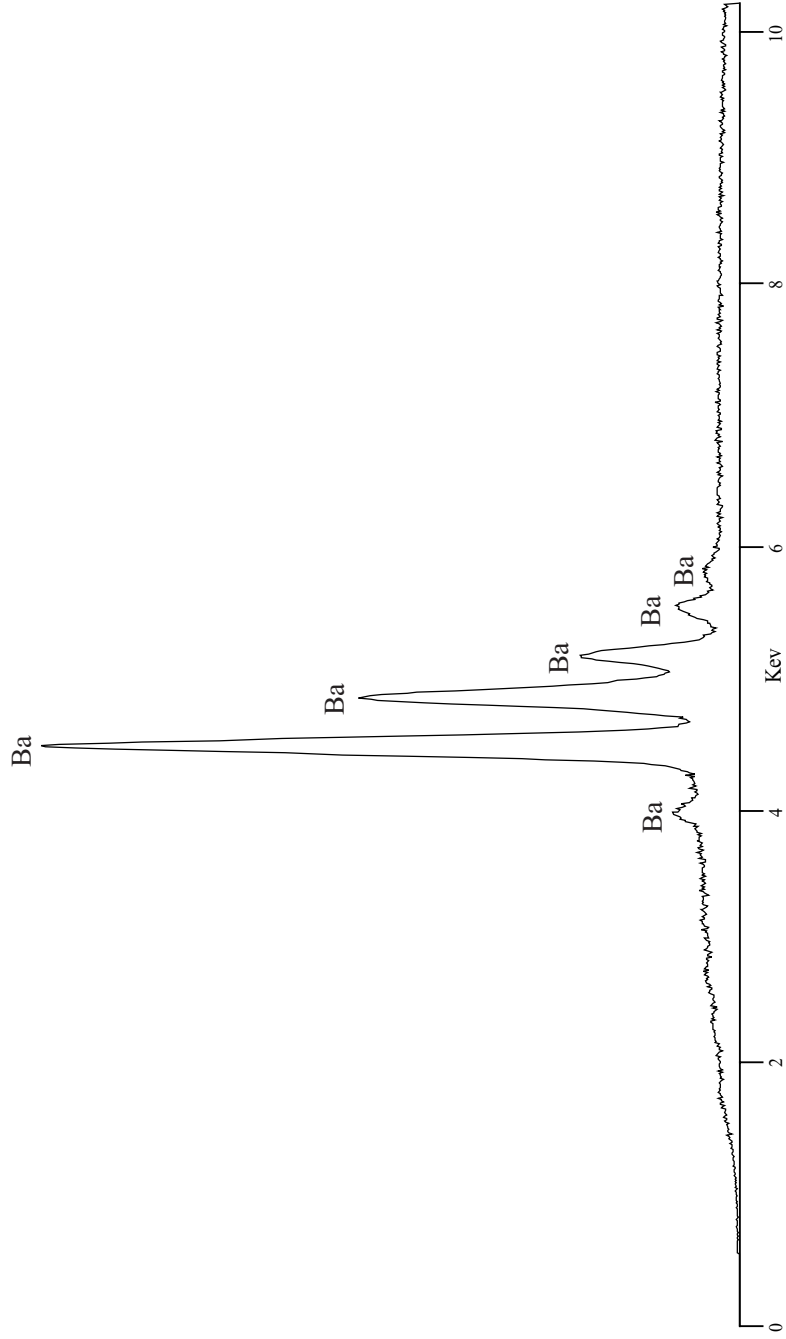
Smithsonian Standard
USNM R10065

Composition
 CO_2 30.23
 CaO 1.90
 SrO 67.67



Witherite BaCO_3

Carbonate

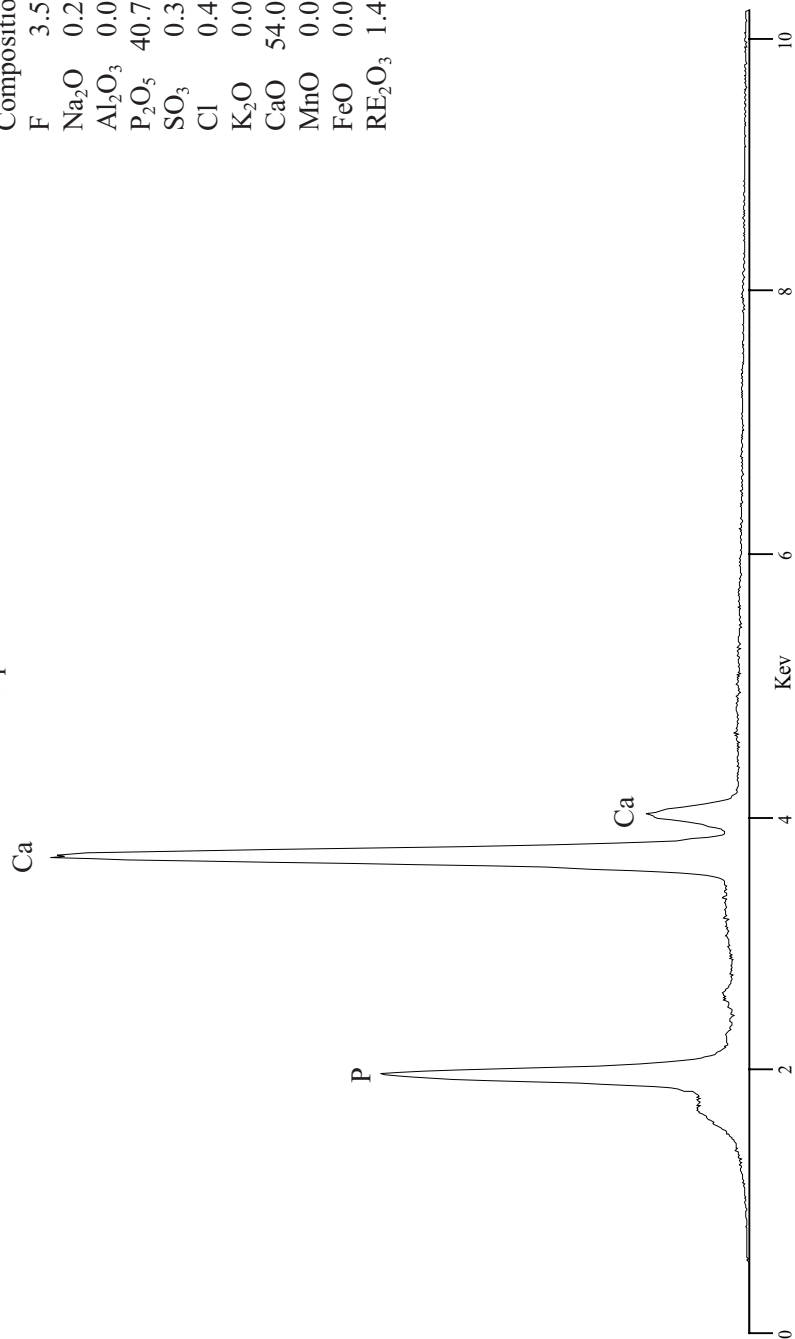


Smithsonian Standard
USNM 104021

Apatite $\text{Ca}_5(\text{PO}_4)_3(\text{OH},\text{F},\text{Cl})$

Phosphate

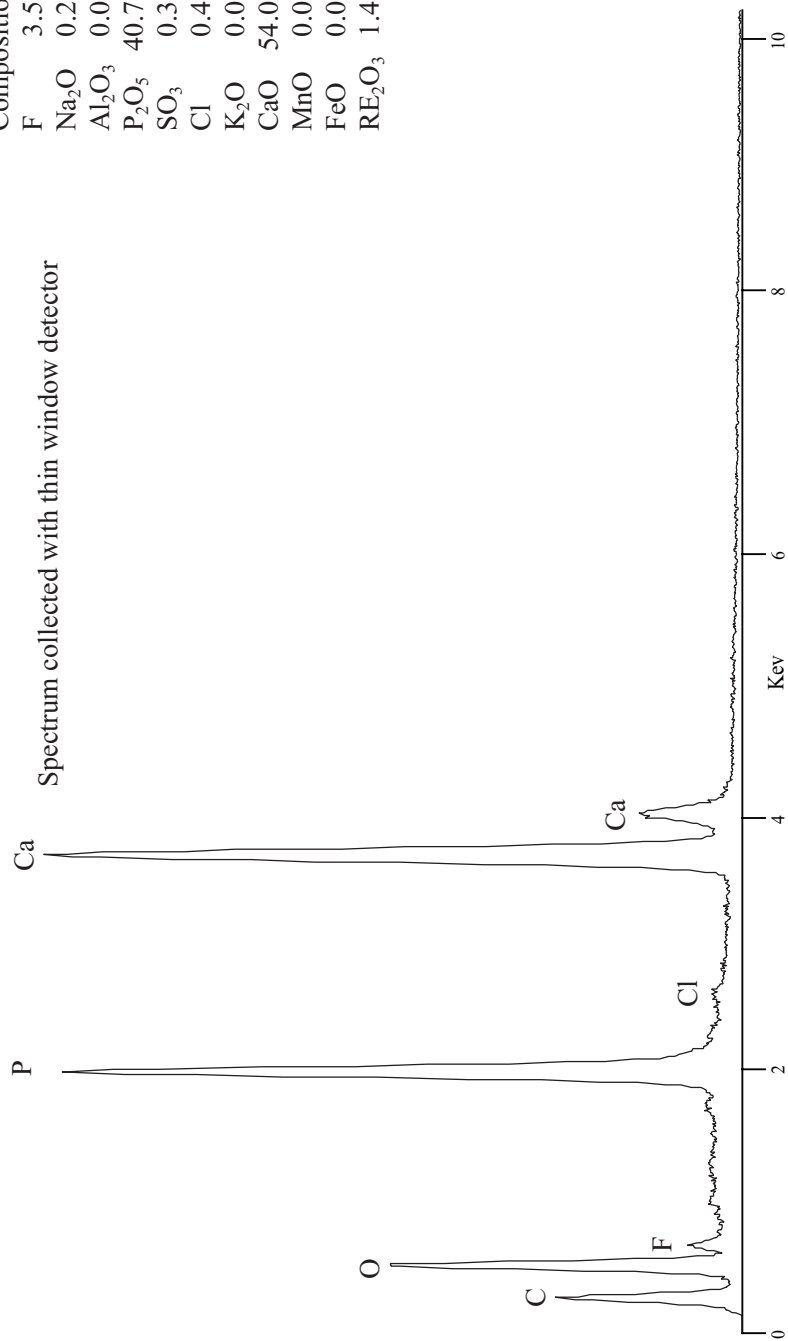
Composition	
F	3.53
Na_2O	0.23
Al_2O_3	0.07
P_2O_5	40.78
SO_3	0.37
Cl	0.41
K_2O	0.01
CaO	54.01
MnO	0.01
FeO	0.05
RE_2O_3	1.43



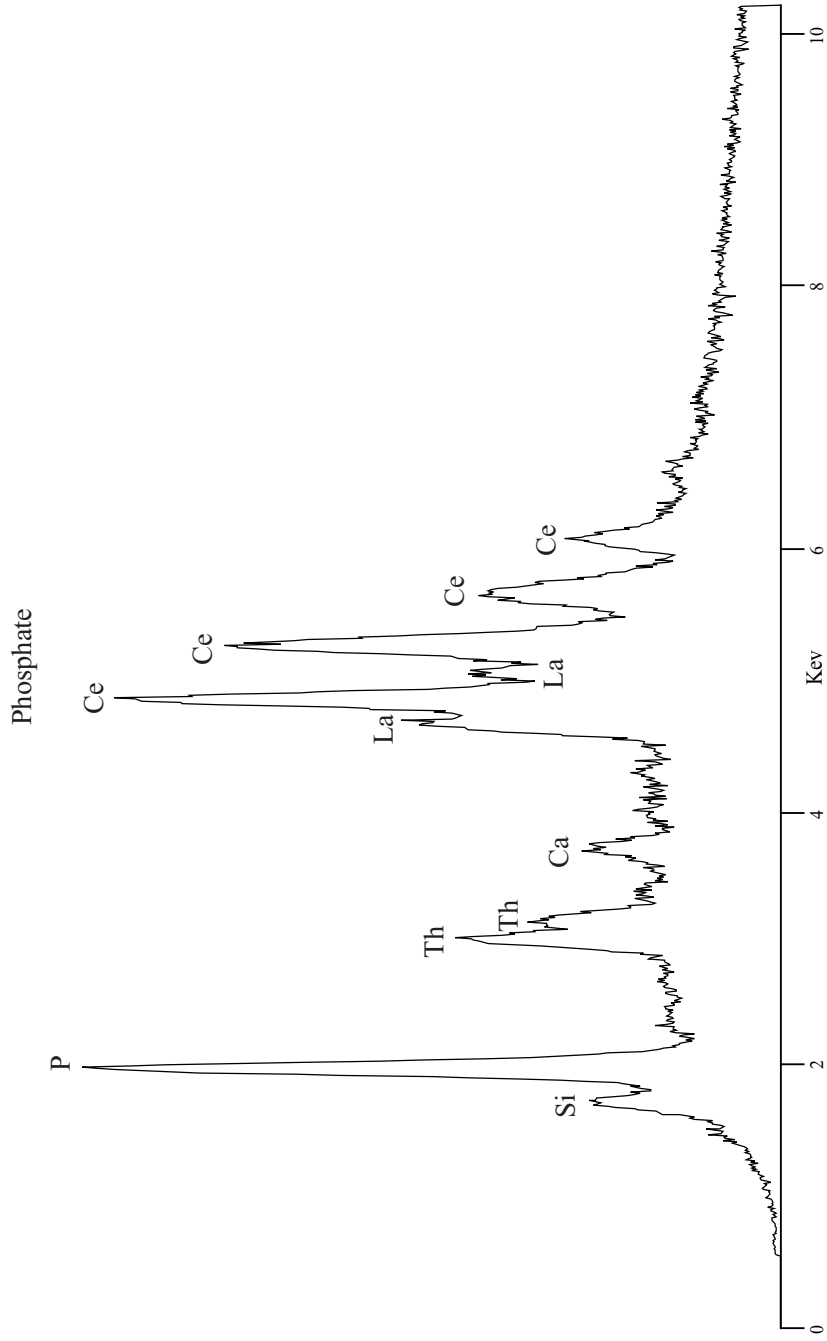
Apatite $\text{Ca}_5(\text{PO}_4)_3(\text{OH},\text{F},\text{Cl})$
 Smithsonian Standard
 USNM 104021

Composition	
F	3.53
Na_2O	0.23
Al_2O_3	0.07
P_2O_5	40.78
SO_3	0.37
Cl	0.41
K_2O	0.01
CaO	54.01
MnO	0.01
FeO	0.05
RE_2O_3	1.43

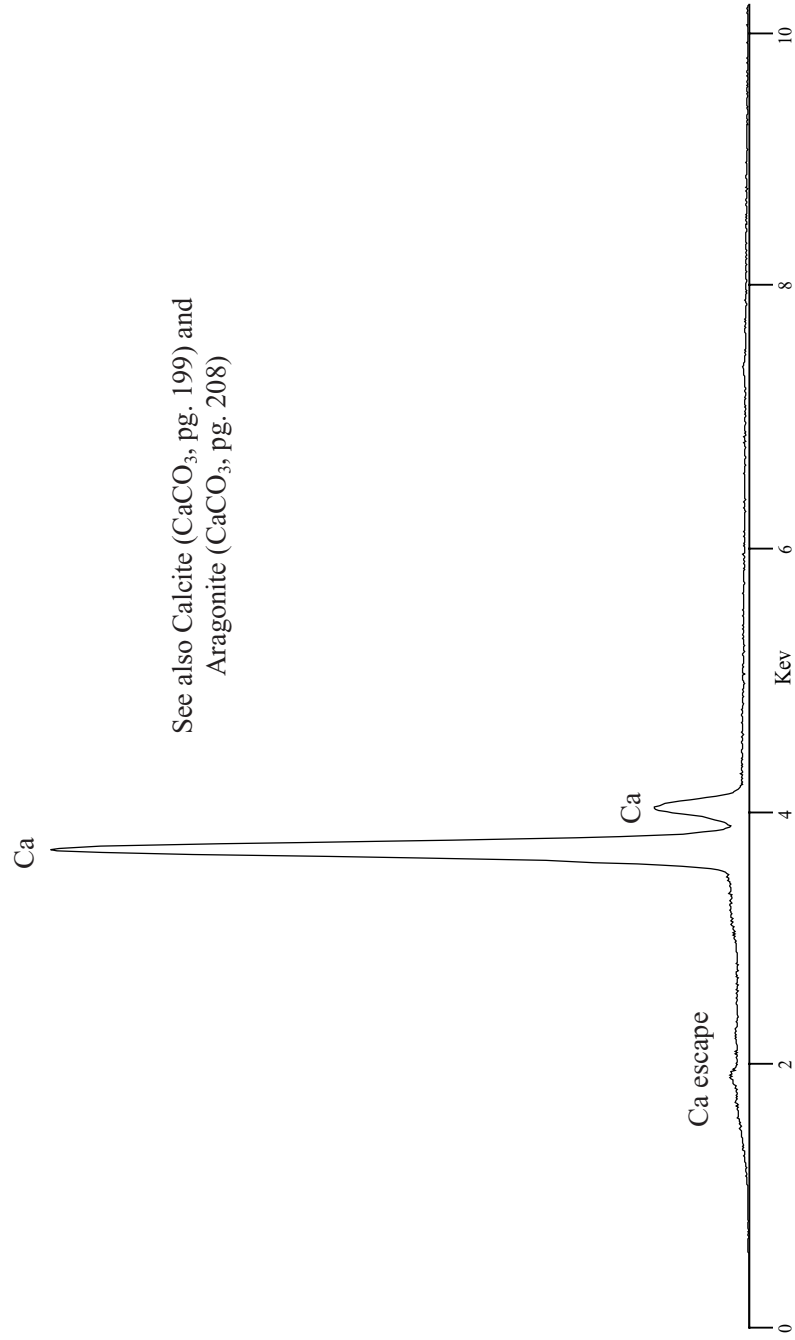
Phosphate
 Spectrum collected with thin window detector



Monazite (Ce,La,Th)PO₄



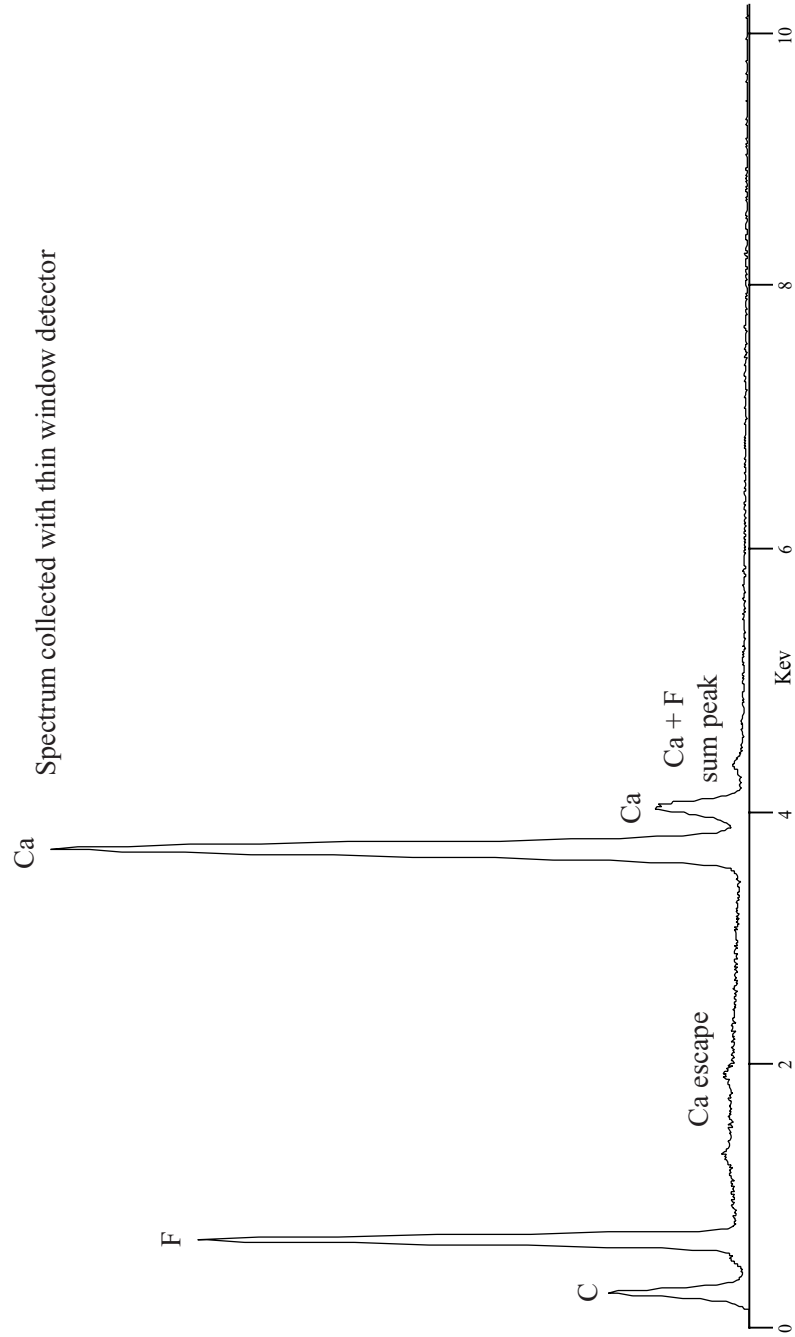
Fluorite CaF_2
Halide



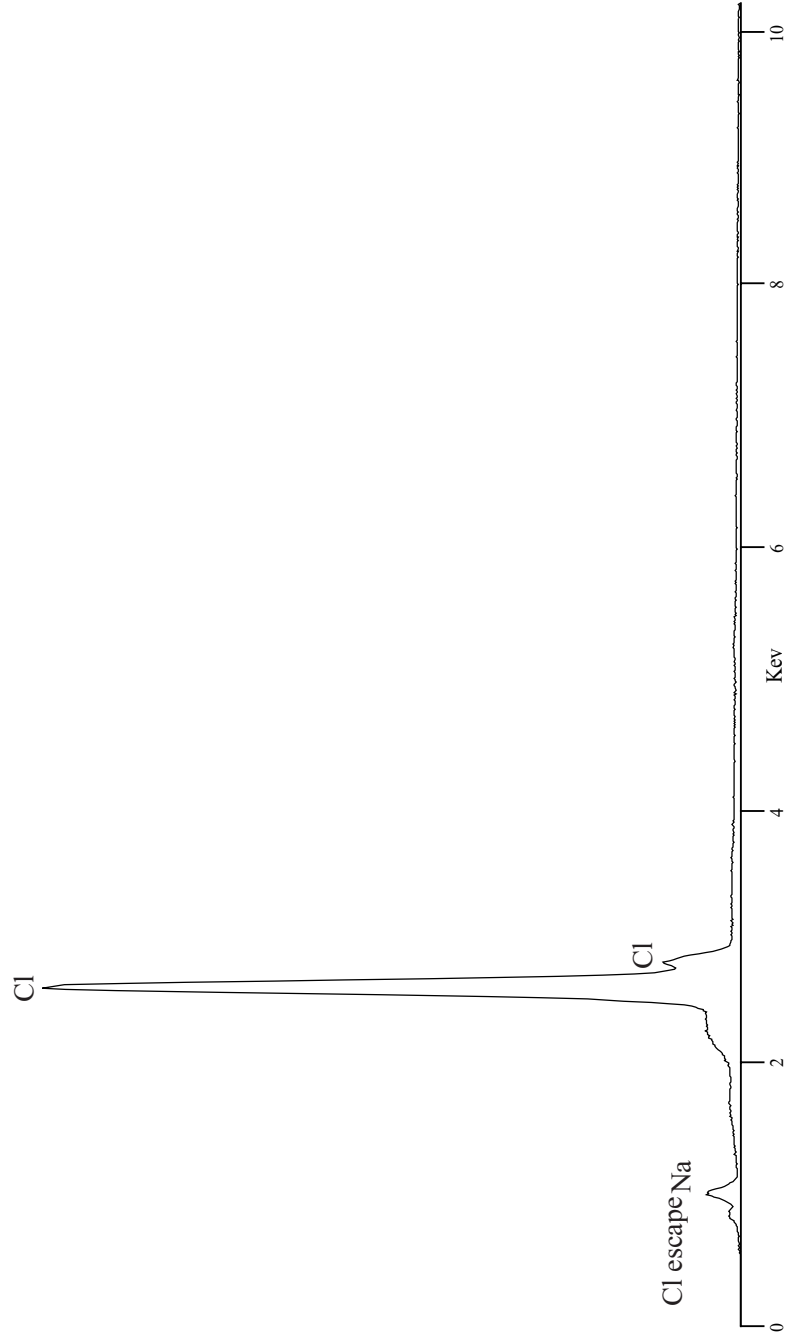
See also Calcite (CaCO_3 , pg. 199) and
Aragonite (CaCO_3 , pg. 208)

Fluorite CaF_2
Halide

Spectrum collected with thin window detector

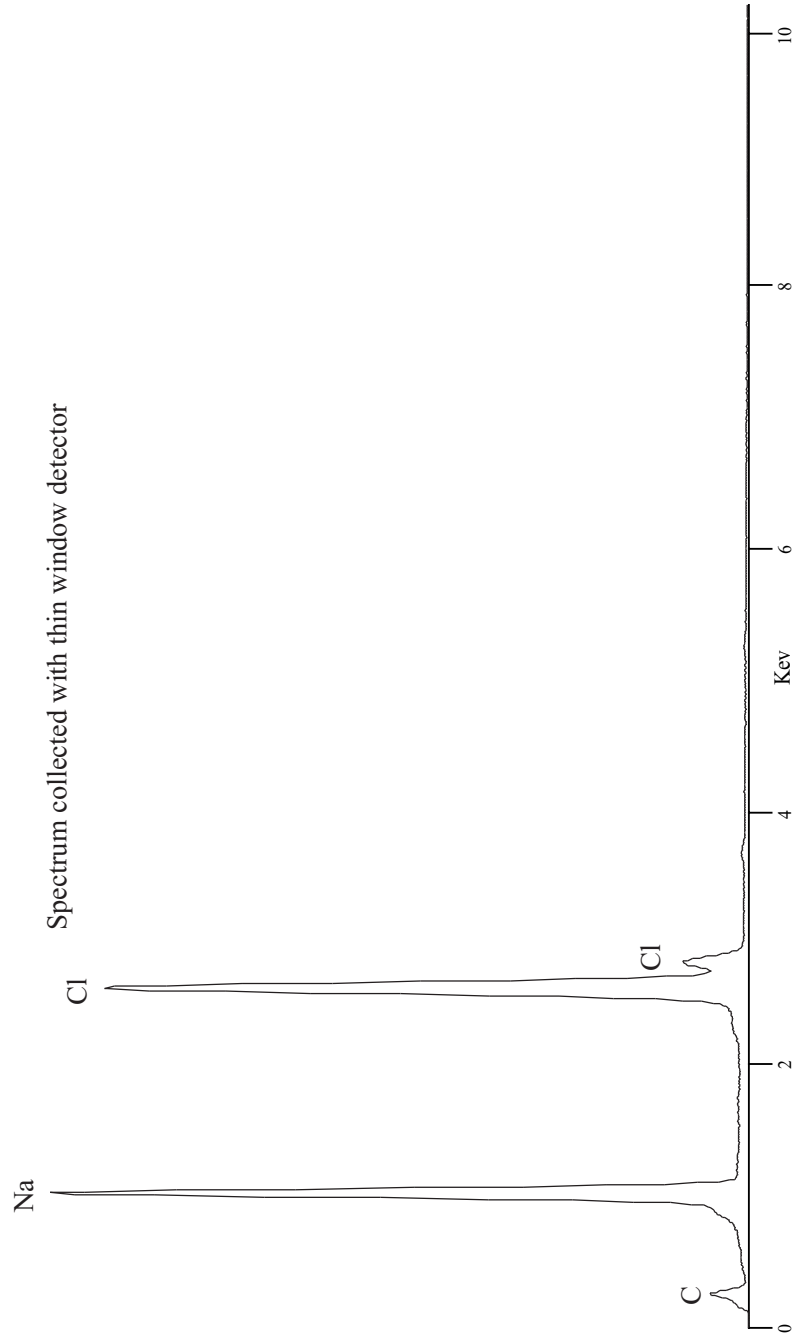


Halite NaCl
Halide

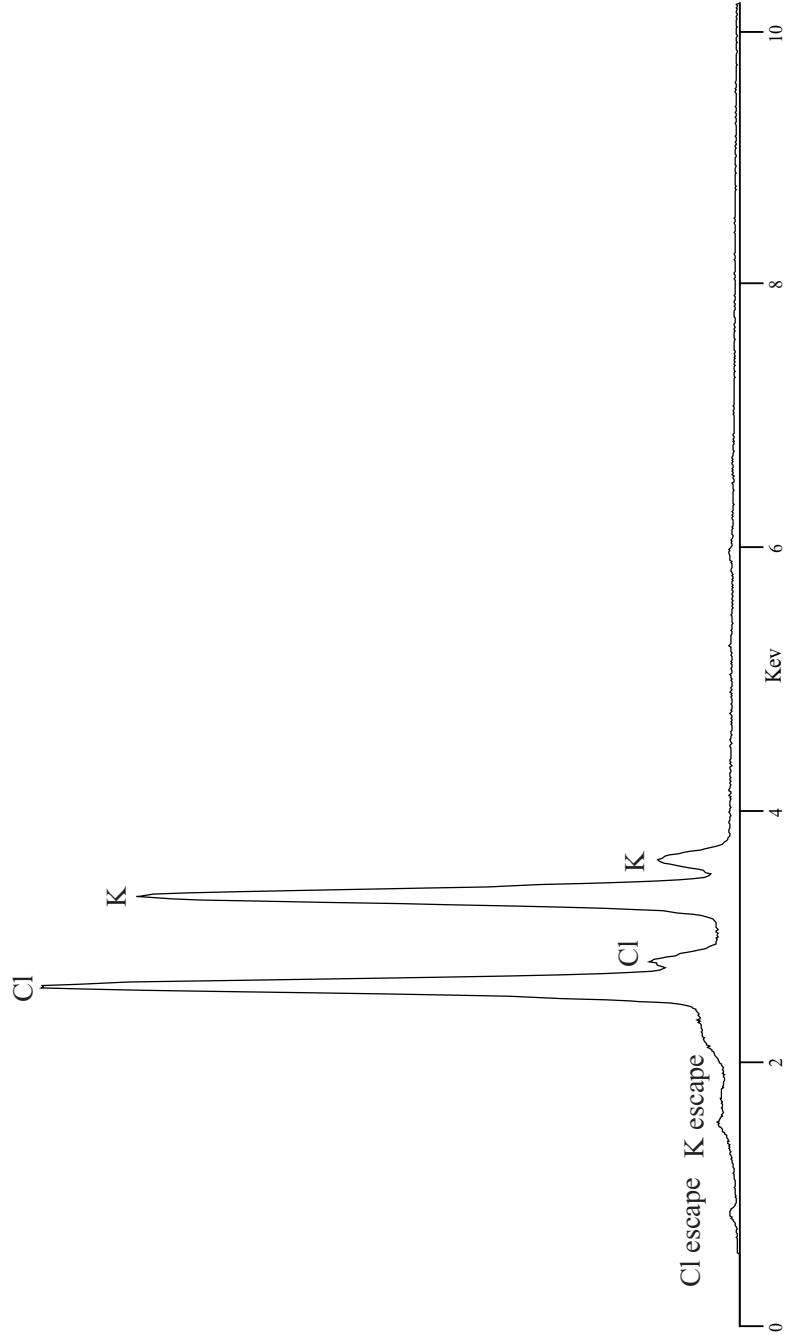


Halite NaCl

Halide



Sylvite KCl
Halide



References

- Bozzola, JJ, and Russell, LD. 1999. Electron microscopy: principles and techniques for biologists. Second Edition. Jones and Bartlett Publishers, Sudbury, Massachusetts. 670 pages.
- Goldstein, JI, Newbury, DE, Joy, DC, Lyman, Echlin, P, CE, Lifshin, E, Sawyer, L, and Michael, JR. 2003. Scanning electron microscopy and X-ray microanalysis. Third Edition, Kluwer Academic / Plenum Publishers, New York Boston, Dordrecht, London, Moscow. 689 pages.
- Kramers, HA. 1923. On the theory of X-Ray absorption and of the continuous X-Ray spectrum. Philosophical Magazine. 46:836-871.
- Moseley, HGJ. 1913. The high frequency spectra of the elements. Philosophical Magazine. 26:1024-1034
- Moseley, HGJ. 1914 The high frequency spectra of the elements II. Philosophical Magazine. 27:703-714.
- Potts PJ. 1987. A Handbook of Silicate Rock Analysis. Blackie. Glasgow, UK. 622 pages.
- Reed, SJB. 1993. Electron microprobe analysis. Second Edition. Cambridge University Press, Cambridge. 326 pages.
- Reed, SJB. 1996. Electron microprobe analysis and Scanning Electron Microscopy in Geology. Cambridge University Press, Cambridge. 201 pages.
- Welton, JE. 1984. S. E. M. Petrology Atlas. American Association of Petroleum Geologists, 237 pages.
- Williams, KL. 1987. An introduction to X-ray spectrometry : X-ray fluorescence and electron microprobe analysis. Allen and Unwin, London. 370 pages.

Index to Spectra, Minerals, and Mineral Groups

Mineral Groups:

Amphiboles	102-111	Micas	112-118
Brittle Micas	119-120	Olivines	38-42
Carbonates	199-211	Orthopyroxenes	86-87
Clays	126-130	Oxides	160-169
Clinopyroxenes	88-96	Phosphates	212-214
Epidotes	69-75	Sodalite Group	148-149
Feldspars	133-141	Spinel	170-178
Garnets	49-54	Sulfates	193-198
Halides	215-219	Sulfides	184-192
Hydroxides	179-183	Zeolites	153-159

Minerals and Spectra:

Note: SUTW – spectrum obtained using detector with Super Ultra Thin Window

Actinolite	106	Ankerite	207
Aegirine (Acmite)	93	Anorthite	139
Aegirine-augite	94	Anorthoclase	135
Albite	136	Anthophyllite	102
Allanite	74	Apatite	212
Allanite	75	Apatite - SUTW	213
Almandine (Garnet)	50	Apophyllite	131
Analcite	152	Aragonite	208
Anatase	167	Aragonite-SUTW	209
Andalusite	58	Arsenopyrite	187
Andradite (Garnet)	53	Augite	91
Anhydrite	198	Axinite	85

Barytes	193	Galena - 20 kv scale	191
Beryl	81	Galena - 25 kv	192
Biotite	116	Genthelvite	150
Boehmite	181	Gibbsite	180
Bronzite	86	Glauconite	114
Brookite	167	Glaucophanite	111
Brucite	179	Goethite	182
Bustamite	100	Grossular (Garnet)	52
Bytownite	138	Grunerite	104
Calcite	199	Gypsum	197
Calcite-SUTW	200	Haematite	164
Cassiterite	162	Haematite-SUTW	165
Celestine	194	Halite	217
Celestine - 20 kv scale	195	Halite - SUTW	218
Celestine - 25 kv	196	Haüyne	149
Celsian	140	Hedenbergite	89
Chabazite	155	Helvite	150
Chalcopyrite	186	Heulandite	156
Chlorite	124	Hornblende	108
Chloritoid	62	Hornblende	109
Chondrodite	45	Hyalophane	141
Chromite	178	Hypersthene	87
Clinozoisite	70	Illite	127
Cordierite	82	Ilmenite	166
Corundum	163	Jadeite	96
Cristobalite	142	Johansenite	90
Cummingtonite	103	Kaersutite	110
Danalite	150	Kalsilite	145
Datolite	63	Kaolinite	126
Diaspore	181	Knebelite	42
Diopside	88	Kyanite	59
Dolomite	206	Labradorite	137
Epidote	71	Laumontite	159
Eudialyte (Eucolite)	67	Lawsonite	76
Fayalite	39	Lepidocrocite	182
Ferroactinolite	107	Lepidolite	117
Fluorite	215	Leucite	147
Fluorite - SUTW	216	Limonite	183
Forsterite	40	Maghemite	174
Franklinite	175	Magnesiochromite	177
Gahnite	171	Magnesioferrite	172
Galena	190	Magnesite	201

Magnesite-SUTW	202	Scapolite	151
Magnetite	173	Scolecite	153
Margarite	119	Serpentine	125
Melilite	78	Siderite	204
Merwinite	65	Siderite-SUTW	205
Microcline	133	Sillimanite	56
Monazite	214	Smectite	128
Monticellite	43	Sodalite	148
Montmorillonite (Smectite)	128	Spessartine (Garnet)	51
Mullite	57	Sphalerite	188
Muscovite	112	Sphalerite - 25 kv	189
Nepheline	144	Sphene	48
Norbergite	44	Spinel	170
Nosean / Häüyne	149	Spodumene	95
Olivine	38	Spurrite (SUTW)	66
Orthoclase	134	Staurolite	61
Paragonite	113	Stilbite	157
Pectolite	98	Stilbite	158
Periclase	160	Stilpnomelane	121
Periclase-SUTW	161	Strontianite	210
Perovskite	169	Sylvite	219
Petalite	146	Talc	123
Phlogopite	115	Tephroite	41
Piemontite	72	Thomsonite	154
Piemontite	73	Tillyite	80
Pigeonite	92	Topaz	60
Prehnite	132	Tourmaline	83
Pumpellyite	77	Tourmaline	84
Pyrite	184	Tremolite	105
Pyrolusite	168	Trevorite	176
Pyrope (Garnet)	49	Tridymite	142
Pyrophyllite	122	Uvarovite (Garnet)	54
Pyroxmangite	101	Vermiculite	129
Pyrrhotite	185	Vermiculite	130
Quartz	142	Vesuvianite (Idocrase)	55
Quartz-SUTW	143	Witherite	211
Rankinite	79	Wollastonite	97
Rhodochrosite	203	Xanthophyllite	120
Rhodonite	99	Zinnwaldite	118
Rosenbuschite	68	Zircon	46
Rutile	167	Zircon 25 kev	47
Sapphirine	64	Zoisite	6